LIETUVOS SVEIKATOS MOKSLŲ UNIVERSITETAS

Povilas Daugėla

AUDINIŲ REGENERACIJA BIOAKTYVIAIS CELIULIOZĖS-HIDROKSIAPATITO TRANSPLANTANTAIS IR LEUKOCITŲ IR TROMBOCITŲ GAUSIU FIBRINU

Daktaro disertacija
Biomedicinos mokslai
odontologija (07B)

Kaunas, 2018

Disertacija rengta 2013–2018 metais Lietuvos sveikatos mokslų universiteto Medicinos akademijos Veido ir žandikaulių chirurgijos klinikoje.

Mokslinis vadovas

Prof. dr. Gintaras Juodžbalys (Lietuvos sveikatos mokslų universitetas, Medicinos akademija, biomedicinos mokslai, odontologija – 07B)

Disertacija ginama Lietuvos sveikatos mokslų universiteto Medicinos akademijos odontologijos mokslo krypties taryboje:

Pirmininkė

Prof. dr. Vita Mačiulskienė (Lietuvos sveikatos mokslų universitetas, Medicinos akademija, biomedicinos mokslai, odontologija – 07B)

Nariai:

Prof. dr. Jurgina Sakalauskienė (Lietuvos sveikatos mokslų universitetas, Medicinos akademija, biomedicinos mokslai, odontologija – 07B)

Prof. dr. Gediminas Žekonis (Lietuvos sveikatos mokslų universitetas, Medicinos akademija, biomedicinos mokslai, odontologija – 07B)

Doc. dr. Saulius Diliūnas (Kauno technologijos universitetas, technologijos mokslai, medžiagų inžinerija – 08T)

Prof. dr. David M. Dohan Ehrenfest (Mičigano universitetas (JAV), biomedicinos mokslai, odontologija – 07B)

Disertacija ginama viešame Lietuvos sveikatos mokslų universiteto Medicinos akademijos Odontologijos mokslo krypties tarybos posėdyje 2018 m. birželio 25 d. 14:00 val. Lietuvos sveikatos mokslų universiteto Lietuvos medicinos ir farmacijos istorijos muziejaus konferencijų salėje.

Disertacijos gynimo vietos adresas: Rotušės a. 28, LT-44279 Kaunas, Lietuva.

LITHUANIAN UNIVERSITY OF HEALTH SCIENCES

Povilas Daugėla

CELLULOSE-HYDROXYAPATITE BIOACTIVE SCAFFOLDS AND LEUKOCYTE- AND PLATELET-RICH FIBRIN FOR TISSUE REGENERATION

Doctoral Dissertation
Biomedical Sciences
Odontology (07B)

Kaunas, 2018

Dissertation has been prepared at the Department of Maxillofacial Surgery of Medical Academy of Lithuanian University of Health Sciences during the period of 2013–2018.

Scientific Supervisor

Prof. Dr. Gintaras Juodžbalys (Lithuanian University of Health Sciences, Medical Academy, Biomedical Sciences, Odontology – 07B)

Dissertation is defended at the Odontology Research Council of the Lithuanian University of Health Sciences.

Chairperson

Prof. Dr. Vita Mačiulskienė (Lithuanian University of Health Sciences, Medical Academy, Biomedical Sciences, Odontology – 07B)

Members:

Prof. Dr. Jurgina Sakalauskienė (Lithuanian University of Health Sciences, Medical Academy, Biomedical Sciences, Odontology – 07B)

Prof. Dr. Gediminas Žekonis (Lithuanian University of Health Sciences, Medical Academy, Biomedical Sciences, Odontology – 07B)

Assoc. Prof. Dr. Saulius Diliūnas (Kaunas University of Technology, Technological Sciences, Materials Engineering – 08T)

Prof. Dr. David M. Dohan Ehrenfest (University of Michigan, Biomedical Sciences, Odontology – 07B)

Dissertation will be defended at the open session of the Lithuanian University of Health Sciences on the 25th of June 2018 at 2:00 p.m. in the Conference Hall of the Museum of History of Lithuanian Medicine and Pharmacy of Lithuanian University of Health Sciences.

Address: Rotušės 28, LT-44279 Kaunas, Lithuania.

TURINYS

PAGRINDINĖS SANTRUMPOS

KPKT	– konusinio pluošto kompiuterinė tomografija
OPG	– ortopantomograma
µKT	– mikrokompiuterinė tomografija
L-PRF	– leukocitų ir trombocitų gausus fibrinas
PRP	– trombocitų gausi plazma
µHA	– mikrohidroksiapatitas
nHA	– nanohidroksiapatitas
Celiuliozė-µHA	– celiuliozės ir mikrohidroksiapatito kompozitas
Celiuliozė-nHA	– celiuliozės ir nanohidroksiapatito kompozitas
RAŽTKD	– retinuoti apatinio žandikaulio tretieji krūminiai dantys; retinuotas apatinio žandikaulio trečiasis krūminis dantis
RKR	– reguliuojamoji kaulo regeneracija
SEM	– skenuojantis elektroninis mikroskopas
MTT	– geltonojo tetrazolio druskų (3-(4,5-dimetiltiazol-2-il-)-2,5-difeniltetrazolio bromido) redukcijos metodas
ALP	– šarminė fosfatazė
AT-PGR	– atvirkštinės transkripcijos polimerazės grandininė reakcija
Col I	– I tipo kolagenas
BMP	– kaulo morfogenetinis baltymas
Runx-2	– slopinantis transkripcijos faktorius 2
RNR	– ribonukleino rūgštis
DNR	– deoksiribonukleino rūgštis
VOI	– tiriamasis tūris
BV	– kaulo tūris
TV	– bendrasis tūris
BV/TV	– kaulo tūrinė frakcija
HU	– Hounsfieldo vienetai
HI	– minkštųjų audinių gijimo indeksas
VAS	– vizualinė analoginė skausmo skalė
SN	– standartinis nuokrypis
V	– vidurkis
p	– reikšmingumo lygmuo

ĮVADAS

Viena aktualiausių šių dienų problemų odontologijoje bei veido ir žandikaulių chirurgijoje yra žandikaulių kaulinio audinio atrofija arba kaulo defektų susidarymas dėl dantų ligų ar onkologinių operacijų, traumų bei kitų etiologinių faktorių. Trūkstant kaulo, neįmanoma atkurti kramtymo funkcijos dantų implantais, pasikeičia paciento kalba, veido išvaizda. Literatūros duomenimis, papildomos kaulo rekonstrukcinės procedūros būtinos daugiau nei 50 proc. visų atliekamų dantų implantacijos operacijų, o implantuojant priekiniame viršutinio žandikaulio segmente papildomai regeneruoti kaulą prireikia iki 77 proc. atvejų [1, 2].

Žandikaulių kaulinių defektų rekonstrukcijos operacijose šiuo metu dažniausiai naudojama reguliuojamosios kaulo regeneracijos metodika, kurios esmę sudaro kaulo plastinės medžiagos įterpimas į defekto sritį ir jos uždengimas kolagenine ar kito tipo lėtai rezorbuojama membrana [3]. Kaulo defektų rekonstrukcijos operacijose naudojamos įvairios medžiagos: autogeniniai, ksenogeniniai, alogeniniai ir sintetiniai transplantantai. Kad kaulo defekto regeneracija vyktų sėkmingai, įsodinto transplantanto srityje taip pat būtina gera kraujotaka, osteoprogenitorinės ląstelės ir augimo faktoriai [4].

Autogeniniai kaulo transplantantai yra paimami iš paties paciento donorinės srities, dažniausiai apatinio žandikaulio šakos, smakro, klubakaulio, šeivikaulio ar blauzdikaulio. Autogeniniai transplantantai turi artimą donorinei sričiai mikrostruktūrą, osteoprogenitorinių ląstelių ir augimo faktorių. Nepaisant to, šių transplantantų naudojimą riboja sukuriama papildoma operacinė žaizda donorinėje srityje, didesnis paciento patiriamas pooperacinis diskomfortas, ilgesnis gijimo laikotarpis, ribotas osteoprogenitorinių ląstelių gyvybingumas, santykinai nedidelis galimo paimti transplantanto dydis, ribotas transplantanto ilgalaikis stabilumas ir santykinai didelė rezorbcija [5].

Ksenogeniniai kaulo transplantantai yra gyvūninės kilmės. Jie gali būti išgaunami iš perdirbto galvijų, kiaulių, arklių kaulinio audinio ar koralų skeleto. Ksenogeniniai tansplantantai gali būti liofilizuoti, demineralizuoti ir deproteinizuoti, siekiant išvengti autoimuninių reakcijų, zoonotinių ligų ir prionų infekcijų transmisijos [6]. Ksenogeniniai kaulo transplantantai atlieka osteokondukcinę funkciją, tačiau yra inertiški, jų klinikinį efektyvumą riboja lėtas transplantanto persimodeliavimas, ir santykinai maža naujo kaulo sintezė *in situ* [7, 8].

Alogeniniai kaulo transplantantai yra imami iš gyvų žmogaus donorų klubo sąnario endoprotezavimo operacijų metu arba mirusių donorų kaulų. Šie transplantantai taip pat liofilizuojami, deproteinizuojami ir (arba) demi-

neralizuojami, siekiant pagerinti biosuderinamumą su recipiento organizmu. Alogeninių transplantantų matricos mikrostruktūra yra artima recipiento kauliniam audiniui, tačiau jų naudojimą riboja lėta revaskuliarizacija, žymi rezorbcija ir ribotas ilgalaikis transplantanto stabilumas bei žmogaus infekcinių ligų transmisijos rizika [9].

Pastaruoju metu ypač padidėjo susidomėjimas sintetiniais kaulo transplantantais, gaminamais iš įvairių medžiagų ar jų derinių: beta trikalcio fosfato, hidroksiapatito, polikaprolaktono, chitosano, kolageno, celiuliozės. Sintetiniai kaulo transplantantai turi tam tikrų privalumų: santykinai neribotas transplantanto dydis ir prieinamumas, biosuderinamumas, minimali infekcijų transmisijos rizika [10]. Tačiau dauguma dabartinėje klinikinėje praktikoje galimų naudoti sintetinių (kaip ir alogeninių bei ksenogeninių) kaulo transplantantų yra inertiški. Tai riboja jų klinikinį efektyvumą. Jungtinėse Amerikos Valstijose (JAV) ir kai kuriose kitose pasaulio šalyse kaulo transplantanto inertiškumo problemai spręsti buvo pasiūlyta naudoti augimo faktorius – rekombinantinius žmogaus trombocitų augimo faktorius (rhPDGF) ir rekombinantinius kaulo morfogenetinius baltymus (rhBMP) [11, 77], tačiau jų naudojimas Europos Sąjungos šalyse nėra aprobuotas, taip pat aprašoma nemažai šalutinio poveikio atvejų [12, 13].

Kaip alternatyva sintetiniams augimo faktoriams kartu su kaulo transplantantais gali būti naudojamas leukocitų ir trombocitų gausus fibrinas (L-PRF). L-PRF yra natūralus autogeninis kraujo koncentratas, išgaunamas centrifuguojant paciento veninį kraują. L-PRF turi žaizdų gijimui ir kaulo regeneracijai svarbių augimo faktorių: trombocitų augimo faktorių (PDGF), kraujagyslių endotelio augimo faktorių (VEGF), transformuojančių augimo faktorių beta (TGF-β), fibroblastų augimo faktorių (FGF) [14, 15]. Nustatyta, kad L-PRF stimuliuoja žmogaus kaulų mezenchiminių kamieninių ląstelių diferenciaciją į osteoblastus [18], bei osteoblastų proliferaciją [16, 17] *in vitro*. L-PRF klinikinėje praktikoje galima naudoti kaip ir bet kurią kitą autogeninės kilmės medžiagą. L-PRF taip pat galima derinti su kitomis kaulo regeneracijai naudojamomis medžiagomis jų efektyvumui gerinti.

1. DARBO TIKSLAS IR UŽDAVINIAI

Darbo tikslas – sukurti naują celiuliozės-hidroksiapatito matricą, tinkamą kaulo defektų regeneracijai, ištirti jos efektyvumą *in vitro* ir *in vivo* modeliuose bei nustatyti L-PRF įtaką naujai sukurtos celiuliozės-hidroksiapatito matricos bioaktyvumui *in vivo* eksperimentuose ir poveikį minkštųjų audinių gijimui bei pacientų pooperaciniam diskomfortui, atliekant klinikinį tyrimą.

Darbo uždaviniai:

1. Susintetinti porėtas celiuliozės kompozitines matricas su mikrohidroksiapatito (μHA) ir nanohidroksiapatito (nHA) užpildais kaulo defektų regeneracijai, atitinkančias pagrindinius kaulinio audinio transplantantams keliamus struktūrinius, fizikocheminius ir biologinius reikalavimus.
2. Nustatyti celiuliozės-μHA ir celiuliozės-nHA matricų mikroporėtumą, cheminę sudėtį, kristališkumą, citotoksiškumą, įtaką osteoblastinių ląstelių kultūrų adhezijai, funkciniam ir metaboliniam aktyvumui *in vitro.*
3. Mikrokompiuterinės tomografijos (μKT) ir histologiniais tyrimais nustatyti celiuliozės μHA ir nHA matricų biosuderinamumą, bioskaidumą, naujo kaulo formavimąsi, ląstelių kompoziciją matricoje *in vivo* Naujosios Zelandijos triušių kaukolės skliauto defektų modelyje.
4. μKT ir histologiniais tyrimais nustatyti naujo kaulo formavimąsi, ląstelių kompoziciją, matricos bioskaidumą L-PRF rehidruotose ir L-PRF membranomis padengtose celiuliozės μHA ir nHA matricose *in vivo* Naujosios Zelandijos triušių kaukolės skliauto defektų modelyje.
5. Palyginti tarpusavyje ir su kontroliniu komerciniu alogeniniu kaulo transplantantu L-PRF rehidruotų, L-PRF membranomis padengtų celiuliozės μHA ir nHA matricų ir paprastų celiuliozės μHA ir nHA matricų efektyvumą regeneruojant kaulo defektus *in vivo* Naujosios Zelandijos triušių kaukolės skliauto defektų modelyje.
6. Sukurti ir validuoti žmogaus RAŽTKD šalinimo sudėtingumo klasifikaciją.
7. Įvertinti L-PRF įtaką minkštųjų audinių gijimui, alveolito pasireiškimui ir pooperaciniam pacientų diskomfortui žmogaus RAŽTKD šalinimo defektų modelyje, standartizuojant tyrimo grupes pagal RAŽTKD šalinimo sudėtingumo klasifikaciją.

2. MOKSLINIO DARBO NAUJUMAS IR PRAKTINĖ REIKŠMĖ

Žandikaulių kaulinių defektų sėkminga regeneracija yra vienas didžiausių iššūkių šiuolaikinėje odontologijoje bei veido ir žandikaulių chirurgijoje. Kasdienėje praktikoje naudojamos medžiagos – ksenogeniniai, alogeniniai, sintetiniai kaulo transplantantai yra inertiški, o autogeninio kaulo prieinamumas yra ribotas. Tai apsunkina žandikaulių kaulinių defektų regeneracijos galimybes, todėl mokslininkai siekia sukurti bioaktyvius kaulo transplantantus, kurie efektyviau galėtų regeneruoti kaulinius defektus. Šiame moksliniame darbe pasiūlyti nauji bioaktyvūs celiuliozės su hidroksiapatitu ir L-PRF kaulo transplantantai.

Sukurta osteokondukcinė celiuliozės matrica su µHA ir nHA užpildais turi trimatę porėtą struktūrą, palankią kraujagyslių įaugimui. Atliktais tyrimais patvirtintas šios matricos biosuderinamumas, bioskaidumas ir naujo kaulo formavimasis matricoje.

Celiuliozės matricų bioaktyvumui pagerinti pasirinktas L-PRF. Daugelis kaulinio audinio regeneracijai mokslinėje literatūroje aprašomų bioaktyvių medžiagų, tokių kaip rekombinantiniai kaulo morfogenetiniai baltymai, yra sintetinės kilmės, vis dar nepakanka turimų duomenų pagrįsti ir licencijuoti jų saugų naudojimą kasdienėje klinikinėje praktikoje. Todėl šiame darbe pasiūlyta celiuliozės ir komercinių kaulo transplantantų bioaktyvinimui naudoti laisvai kasdienėje chirurginėje praktikoje prieinamą autogeninį kraujo koncentratą – L-PRF, kuriame gausu kaulinių defektų regeneracijai svarbių autogeninių augimo faktorių, citokinų ir plazmos glikoproteinų. Atliktame moksliniame darbe L-PRF įtaka kaulinio audinio regeneracijai skatinti patvirtinta *in vivo* tyrimais, o efektyvumas minkštųjų audinių gijimui pagerinti, alveolito pasireiškimui ir pooperaciniam pacientų diskomfortui sumažinti – klinikiniu atsitiktinių imčių tyrimu RAŽTKD modelyje, kurio standartizavimui taip pat panaudota autorių pasiūlyta ir validuota RAŽTKD šalinimo sudėtingumo klasifikacija.

Šio mokslinio darbo rezultatai sudaro galimybės toliau tęsti sukurtų celiuliozės matricų su µHA ir nHA užpildais mokslinius tyrimus, siekiant jų aprobavimo klinikiniam naudojimui. Gydytojams praktikams šio darbo rezultatai padės kompleksiškai vertinti L-PRF panaudojimo galimybes kaulo ir minkštųjų audinių defektų regeneracijai pagerinti.

3. LITERATŪROS APŽVALGA

3.1. Kaulo defektų regeneracinės technikos

Kaulo defektų regeneracijai naudojamos įvairios technikos: reguliuojamoji kaulo regeneracija (RKR), suprapoziciniai ir intrapoziciniai kaulo blokų transplantantai, alveolinės ataugos skėlimas ir plėtimas, distrakcinė osteogenezė, ar šių metodų kombinacijos [1, 191]. RKR yra vienas dažniausiai šiuolaikinėje klinikinėje praktikoje taikomų žandikaulių kaulinių defektų regeneracijos metodų [3, 26, 27]. RKR esmę sudaro kaulinį audinį regeneruojančių mezenchiminių kamieninių ir osteogeninių ląstelių – osteoblastų migracija į kaulinį defektą ir (arba) kaulo transplantantą iš gretimo kaulinio audinio, kaulų čiulpų, antkaulio bei kaulinio audinio atsikūrimui trukdančių ląstelių – epiteliocitų ir fibroblastų eliminavimas iš regeneruojamo kaulinio defekto barjerinėmis membranomis [3, 26–28]. Epiteliocitai ir fibroblastai pasižymi iki 10 kartų greitesne migracija į kaulinį defektą nei osteogeninės ląstelės [29], todėl barjerų pagrindinė funkcija yra atskirti epitelines ir jungiamojo audinio ląsteles nuo kaulinio defekto ir sudaryti sąlygas jame vykti lėtesniam osteogenezės procesui. Kaulo defektų regeneracijai taip pat būtina osteoplastinė medžiaga, kuri išlaikytų defekto tūrį ir tarnautų kaip karkasas naujo kaulinio audinio susidarymui, bei augimo faktoriai, kurie regeneruojamoje srityje skatintų vaskuliarizaciją ir osteogenezę. Šio darbo autorius 2016 m. dalyvavo Baltijos osteointegracijos akademijos ir Lietuvos sveikatos mokslų universiteto tarptautinio konsensuso mokslininkų grupėje ir su bendraautoriais apžvelgė svarbiausius faktorius, turinčius įtakos kaulinių defektų regeneracijai, bei pasiūlė ir publikavo periimplantito chirurginio regeneracinio gydymo praktines rekomendacijas [222, 223].

Osteogenezės proceso pradžioje į kaulinį defektą implantuotas kaulo transplantantas užsipildo krauju, susiformuoja stabilizuotas kraujo krešulys, kuris atpalaiduoja augimo faktorius (trombocitų augimo faktorių) ir citokinus (interleukiną – 8), pritraukiančius į defekto sritį neutrofilus ir makrofagus. Kraujo krešulys ir kaulo transplantantas yra palaipsniui rezorbuojami ir užpildomi granuliaciniu audiniu, kuriame gausu kraujagyslių. Per naujai susiformavusias kraujagysles į regeneruojamą kaulinį defektą patenka audinių regeneracijai reikalingi substratai, migruoja mezenchiminės kamieninės ląstelės, galinčios formuoti naujus osteoidus. Mineralizuodami osteoidai formuoja akytąjį kaulą, kuris vėliau tarnauja kaip karkasas tankiojo kaulo apozicijai [30, 31]. Priklausomai nuo defekto dydžio ir kaulinio transplantanto rezorbcijos greičio, osteogenezės procesas trunka nuo 3 iki 9 mėnesių [32–

34]. Lėta osteogenezės eiga yra vienas pagrindinių RKR trūkumų [27]. Sudėtinga užtikrinti, kad kaulinį defektą dengianti membrana per visą gijimo laikotarpį tolygiai išlaikytų regeneruojamos srities tūrinį stabilumą, ribotų jungiamojo ir epitelinio audinių migraciją į defektą ir atlaikytų aplinkinių minkštųjų audinių spaudimą, tai lemia ribotą RKR efektyvumą, ypač regeneruojant vienasienius ir vertikalius kaulo defektus [35, 36]. RKR efektyvumui didinti literatūroje siūloma naudoti kaulo bioinžinerijos metodais kuriamus bioaktyvius kaulo transplantantus [9, 36, 37, 39–41].

3.2. Kaulinio audinio bioinžinerijos modelis

Kaulinio audinio bioinžinerija – tai metodika, skirta biomimetinio kaulo transplantanto sukūrimui, kurio matricoje sąveikaujančios kaulinį audinį formuojančios ląstelės ir augimo faktoriai galėtų sintezuoti kaulinį audinį *de novo* [38]. Išskiriami keturi pagrindiniai kaulinio audinio regeneracijai reikalingi komponentai [39, 40]:

1. Biosuderinama transplantanto matrica, kuo artimiau atkartojanti natūralaus kaulo ekstraląstelinę matricą.
2. Osteogeninės ląstelės, galinčios proliferuoti ir diferencijuoti į kaulinio audinio ląsteles transplantanto matricoje.
3. Augimo faktoriai, sąlygojantys morfogenetinius signalus ląstelių osteogeninei diferenciacijai.
4. Vaskuliarizacija, užtikrinanti regeneruojamo kaulinio audinio mitybą ir metabolitų apykaitą.

Sėkmingai kaulinio audinio regeneracijai būtina visų kaulo bioinžinerijos modelio komponentų sinergija, sudaranti tinkamas biochemines ir fizikochemines sąlygas osteogeninių ląstelių diferenciacijai, naujo kaulo formavimuisi ir integracijai kauliniame defekte [9, 41].

3.3. Kaulo transplantantų biologinis funkcionalumas

Pagal atliekamą biologinę funkciją kaulo transplantantai klasifikuojami į [43, 44]:

1. Osteogeninius.
2. Osteokondukcinius.
3. Osteoindukcinius.

Osteogeniniai kaulo transplantantai turi gyvybingų osteogeninių ląstelių, regeneruojamame kaulo defekte galinčių formuoti naują kaulinį audinį. Kaulinio transplantanto remodeliacijai ir naujo kaulo sintezei transplantante turi būti pakankamas kiekis osteogeninių ląstelių, kadangi didelė jų dalis

žūsta po kaulo transplantanto implantacijos į recipientinę ložę [45]. Nors osteogeninės ląstelės yra būtinos kaulinio audinio regeneracijai, išlikti ir funkcionuoti jos gali tik tinkamomis osteokondukcinėmis savybėmis pasižyminčiame kaulo transplantante [46].

Osteokondukcija – tai kaulo transplantantų savybė tarnauti kaip matrica, sudaranti tinkamas sąlygas endogeninių mezenchiminių ląstelių, osteoblastų ir osteoklastų migracijai, adhezijai, proliferacijai ir diferenciacijai. Osteokondukciniai kaulo transplantantai turi būti biosuderinami, mechaniškai tvirti, lėtai rezorbuojami ir turintys mikroporėtą, vaskuliarizacijai palankią mikrostruktūrą [47, 48]. Dauguma šiuo metu klinikinėje praktikoje naudojamų žmogaus, gyvūninės ar sintetinės kilmės kaulo transplantantų pasižymi tam tikro laipsnio osteokonduktyviškumu [49].

Osteoindukciniai kaulo transplantantai turi savybę skatinti ir indukuoti naujo kaulinio audinio formavimąsi siunčiant biocheminius signalus, kurie skatina mezenchiminių kamieninių ląstelių diferenciaciją į osteoblastus. Biocheminių signalų kaskada yra medijuojama augimo faktorių, kurie aktyvuoja tam tikrus ekstraląstelinius ir intraląstelinius receptorius. Osteoindukciniai kaulo transplantantai gali inicijuoti naujo kaulinio audinio formavimąsi *de novo* tiek ektopinėse, tiek ortotopinėse srityse [44]. Ši osteoindukcinių transplantantų savybė skiria juos nuo osteopromocinių medžiagų, kurios skatina kaulinio audinio regeneraciją, tačiau savarankiškai negali inicijuoti naujo kaulinio audinio formavimosi *de novo* [50].

3.4. Reikalavimai kaulo transplantantų matricai

Kaulo transplantantų matrica tarnauja kaip tridimensinis karkasas ląstelių migracijai, proliferacijai ir diferenciacijai. Kaulo transplantantai atlieka tiek ekstraląstelinės matricos, tiek mechaninę funkciją, išlaikydami regeneruojamo defekto tūrinį vientisumą.

Kaulo transplantantų matricos savybėms keliami šie reikalavimai [47, 48, 138]:

1. Tridimensinė ir gausiai porėta struktūra, kuri yra palanki kaulo ir kraujagyslių endotelio progenitorinių ląstelių migracijai, adhezijai, proangiogeninių augimo faktorių transportui ir kraujagyslių formavimuisi. Kaulo transplantanto matricos poros turėtų jungtis tarpusavyje, tai yra svarbu osteogeninėms ląstelėms reikalingų substratų transportui ir metabolitų apykaitai. Dauguma autorių rekomenduoja transplantanto matricos 200–600 μm porų diametrą [148–50]. Mažesnis porų dydis lemtų prastesnę transplantanto vaskuliarizaciją, didesnis – sumažintų akytųjų struktūrų paviršiaus plotą, tai lemtų mažesnę ląstelių adheziją bei prastesnes matricos mechanines savybes [151].

2. Matricos paviršiaus savybės turėtų būti palankios osteogeninių ląstelių adhezijai, migracijai, proliferacijai, diferenciacijai ir kaulinio audinio sintezei.

3. Biosuderinamumas, nesukeliantis citotoksiškumo, ryškios uždegiminės ir organizmo imuninių reakcijų.

4. Bioskaidumas – transplantanto matrica turėtų būti iš lėto rezorbuojama organizme, suteikiant pakankamai laiko kaulinio audinio sintezei ir regeneracijai.

5. Mechaninės matricos savybės turėtų būti artimos natūralaus recipientinės ložės kaulinio audinio mechaninėms savybėms ir pakankamai tvirtos regeneruojamo defekto tūrio išlaikymui.

6. Matrica turėtų būti lengvai apdirbama ir pritaikoma prie įvairių dydžių ir formų kaulo defektų.

3.5. Kaulo transplantantų tipai

Kaulo transplantantai pagal kilmę klasifikuojami į [47, 50–52]:

1. Natūralios kilmės kaulo transplantantai

Šiai grupei priskiriami tiek autogeninės kilmės transplantantai, paimti iš to paties organizmo donorinių sričių, tiek alogeniniai transplantantai, tokie kaip mineralizuota ir demineralizuota kaulo matrica ar šaldytas alogeninis kaulas, kurie imami iš gyvų ar mirusių tos pačios rūšies donorų kaulų (pavyzdžiui, klubo sąnario endoprotezavimo operacijų metu) [53]. Natūralios kilmės kaulo transplantantams taip pat priskiriami ksenogeninės (jaučių, arklių, kiaulių donoriniai kaulai) [54] ir fitogeninės (jūrinių dumblių, koralų) [55, 56] kilmės kaulo transplantantai.

2. Sintetiniai / aloplastiniai kaulo transplantantai

Šiai grupei priskiriamas bioaktyvus stiklas [57], trikalcio fosfatas [58], hidroksiapatitas [59], kalcio sulfatas [60]. Sintetiniams kaulo transplantantams taip pat priskiriami kai kurie metalai (titanas) [61], ir polimerinės medžiagos (polikaprolaktono, poliglikolio rūgšties, polilakto rūgšties, polilaktido-ko-glikolido junginiai, krakmolas, chitosanas, chitinas, kolagenas, želatina, celiuliozė) [62–68].

3. Kompozitiniai kaulo transplantantai

Kompozitiniams kaulo transplantantams priskiriami skirtingų medžiagų, pavyzdžiui, keramikos ir polimerų, junginiai [69–71]. Skirtingų medžiagų kombinacijos leidžia pagerinti struktūrines ir biochemines transplantantų savybes, įskaitant mechaninį atsparumą ir bioskaidumą [48, 72].

4. Kaulo transplantantai su augimo faktoriais

Kaulo transplantantų biologinio aktyvumo padidinimui, jie gali būti derinami su įvairiais natūraliais augimo faktorių koncentratais (trombocitų gausia plazma (PRP), augimo faktorių gausia plazma (PRGF), leukocitų ir trombocitų gausiu fibrinu (L-PRF)) [14–18, 79] ar rekombinantiniais augimo faktoriais (kaulo morfogenetiniais baltymais (BMP), trombocitų augimo faktoriumi (PDGF), transformuojančiu augimo faktoriumi beta (TGF-β), kraujagyslių endotelio augimo faktoriumi (VEGF), fibroblastų augimo faktoriumi (FGF), insulino augimo faktoriumi – 1 (IGF-1)) [73–75]. Augimo faktoriai gali veikti skirtingus regeneruojamos srities gijimo kaskados elementus, pagerindami vaskuliarizaciją, osteogeninių ląstelių migraciją, adheziją, proliferaciją, diferenciaciją, chemotaksį [73, 75], kas turi įtakos gaunamiems geresniems klinikiniams kaulo defektų regeneracijos rezultatams [11, 76, 77]. Tačiau rekombinantinių augimo faktorių naudojimas kaulo regeneracijai išlieka kontroversiškas dėl jų dozavimo, saugumo, pasireiškiančių komplikacijų ir aprobavimo klinikiniam naudojimui problemų [12, 13, 76, 78].

5. Ląsteliniai kaulo transplantantai

Kaulinio audinio bioinžinerijai naudojamos kaulų čiulpų, riebalinio audinio kamieninės ląstelės, antkaulio kamieninės ląstelės, kaulo ir antkaulio osteoblastai, embrioninės kamieninės ląstelės [80–84]. Parinkus tinkamas signalines molekules ir matricą – pernešėją, kurioje šios ląstelės galėtų proliferuoti ir diferencijuoti, galima kaulo sintezė *de novo* [85]. Ląsteliniai kaulo transplantantai literatūroje aprašomi tiek kaip duodantys gerus [86–88], tiek ir riboto efektyvumo [80, 89–91] klinikinius rezultatus žandikaulių kaulinių defektų regeneracijoje. Ląsteliniai transplantantai daugiausia vis dar tyrinėjami eksperimentinėse studijose, siekiant ištobulinti jų paruošimo metodologiją, išvengti genomo mutacijų, išlaikyti ląstelių fenotipą *in vitro* ir gyvybingumą *in situ*, išvengti autoimuninių reakcijų, užtikrinti ląstelinio transplantanto saugumą ir priartinti prie realaus klinikinio panaudojimo [92, 93].

Apibendrinti kaulo transplantantų tipai ir jų biologinis funkcionalumas pateikiami 3.5.1 lentelėje [324].

3.5.1 lentelė. *Kaulo transplantantų tipai*

Transplantantai	Aprašymas	Biologinis funkcionalumas
Autogeniniai	Naudojamas vienas arba su kitais kaulo transplantantais	Osteogeniškumas Osteoindukcija Osteokondukcija
Alogeniniai	Naudojamas vienas arba su kitais kaulo transplantantais ir (arba) augimo faktoriais	Osteokondukcija Silpna osteoindukcija
Ksenogeniniai	Naudojamas vienas arba su kitais kaulo transplantantais ir (arba) augimo faktoriais	Osteokondukcija
Sintetiniai neorganiniai	Naudojamos neorganinės medžiagos: kalcio fosfatas, kalcio sulfatas, bioaktyvus stiklas, hidroksiapatitas, titanas	Osteokondukcija
Sintetiniai organiniai	Naudojamos organinės polimerinės medžiagos: polikaprolaktonas, poliglikolidas, polilaktidas, polilaktido-ko-glikolidas, krakmolas, chitosanas, chitinas, kolagenas, želatina, celiuliozė	Osteokondukcija
Kompozitiniai	Sintetinių transplantantų junginiai	Osteokondukcija
Transplantantai su augimo faktoriais	Natūralūs ir rekombinantiniai augimo faktoriai, naudojami su transportine matrica	Osteoindukcija Osteokondukcija, jei naudojami su osteokondukcine matrica
Ląsteliniai	Osteogeninės ląstelės, naudojamos su transportine matrica	Osteogeniškumas Osteokondukcija, jei naudojami su osteokondukcine matrica

Pagal Samit K. Nandi ir kt. 2010 m. [324].

3.6. Sintetiniai ir kompozitiniai hidroksiapatito ir celiuliozės kaulo transplantantai

Sintetiniai kaulo transplantantai gali būti gaminami tiek iš įvairių neorganinių (beta trikalcio fosfato, hidroksiapatito, bioaktyvaus stiklo, kalcio silikato), tiek iš organinių (polikaprolaktono, poliglikolio rūgšties, polilakto rūgšties, polilaktido-ko-glikolido) medžiagų ar jų derinių [19, 20].

Viena dažniausiai kaulo transplantantų inžinerijoje naudojamų sintetinių neorganinės kilmės medžiagų yra hidroksiapatitas. Hidroksiapatitas pasižymi dideliu mechaniniu standumu (Jungo moduliu), mažu elastiškumu ir

kieta, tačiau biria struktūra [23, 32, 59, 79, 100, 139]. Sintetinis hidroksiapatitas $Ca_{10}(PO_4)_6(OH)_2$ – HA, savo chemine ir kristaline struktūra (kalcio – fosforo santykis 1,67) yra panašus į natūralaus kaulo hidroksiapatitą. Tai sudaro sąlygas lėtai sintetinio hidroksiapatito rezorbcijai ir nerezorbuotos dalies integracijai į kaulinį audinį kaulo remodeliacijos proceso metu [139]. Literatūros duomenimis, hidroksiapatito įtaka osteogenezei priklauso nuo jo dalelių dydžio – nustatytas nHA dalelių didesnis funkcinis aktyvumas osteoblastų ir mezenchiminių kamieninių ląstelių adhezijai, proliferacijai ir diferenciacijai, palyginti su μHA dalelėmis [146, 147]. Nepaisant gero biosuderinamumo, hidroksiapatito transplantantų panaudojimą kaulo regeneracijai apsunkina jų trapumas, sudėtingas apdirbimas ir pritaikymas prie esamos defekto konfigūracijos, prastesnės sintetinį hidroksiapatitą inkorporavusio kaulinio audinio mechaninės savybės [140].

Literatūros duomenimis, sintetinių kaulo transplantantų sintezei naudojami natūralūs polimerai (krakmolas, chitosanas, chitinas, kolagenas, želatina) gali pagerinti transplantanto biosuderinamumą, hidrofiliškumą, tačiau žmogaus organizmo fermentai padidina šių polimerų bioskaidumą *in situ*, kas sumažina transplantanto dimensinį stabilumą [21–23]. Pastaruoju aspektu ypač įdomus natūralus polimeras – celiuliozė. Žmogaus organizmas neturi celiuliozę skaldančių fermentų – celiulazių, kurios atakuoja β-1,4-gliukozidines jungtis [24], todėl celiuliozės bioskaidumo procesas yra lėtesnis, daugiausia vykstantis dėl mechaninės erozijos ir rūgštinės hidrolizės procesų [25]. Todėl, priešingai nei kitų gamtinių polimerų – baltymų ar kitų polisacharidų atveju, celiuliozės pagrindu sukurti kaulo transplantantai žmogaus organizme gali išlaikyti savo formą, kol vyksta kaulo regeneracijos procesas. Celiuliozė pasižymi biosuderinamumu, hidrofiliškumu, karkasų porėtumu, atsparumu tempimui ir lengvu apdirbimu [68, 141]. Iš kitos pusės, celiuliozės polimerai neturi struktūrinių panašumų į kaulinio audinio organį matriksą, tai turi įtakos silpnesnei ląstelių adhezijai ir proliferacijai bei silpnesnėms osteokondukcinėms ir mechaninėms celiuliozės savybėms [142, 143]. Siekiant priartinti celiuliozės karkasų struktūrinį panašumą kaulinio audinio struktūrai, pagerinti osteokondukcines savybes ir integraciją kaule, galimas celiuliozės ir hidroksiapatito karkasų jungimas ir jų kompozitų bioinžinerinė sintezė [144, 145]. Šio darbo autorius kartu su bendraautoriais yra pasiūlęs, aprašęs ir straipsniuose publikavęs keletą kompozitinių celiuliozės karkasų modifikacijų [219, 220].

3.7. Kaulo transplantantų bioaktyvavimas ląstelėmis

Sėkmingai kaulinio audinio regeneracijai kartu su osteokondukcine matrica būtini augimo faktoriai ir mezenchiminės kamieninės arba osteoprogenitorinės ląstelės. Mezenchiminės kamieninės ląstelės yra polipotentinės ląstelės, randamos kaulo čiulpuose, riebaliniame ir kituose audiniuose. XX a. pabaigoje atliktuose prof. Arnoldo Kaplano grupės [94, 95] darbuose buvo nustatyta, kad žiurkių kaulų čiulpų mezenchiminės kamieninės ląstelės gali būti kultivuojamos ir multiplikuojamos *in vitro*, o osteogeninėje terpėje diferencijuojamos į osteoblastus. Kaulinio audinio regeneracijai mezenchiminės kamieninės ląstelės dažniausiai išskiriamos iš kaulo čiulpų arba riebalinio audinio. Kaulų čiulpuose šių ląstelių skaičius, priklausomai nuo paciento amžiaus ir individualių organizmo ypatybių, varijuoja nuo 0,001 iki 0,01 proc., riebaliniame audinyje – nuo 1 iki 5 proc. visų ląstelių [96, 97, 98]. Tokia koncentracija yra per maža tiesioginiam jų panaudojimui be papildomo kultivavimo, todėl išskyrus šias ląsteles iš kaulų čiulpų ar riebalinio audinio aspirato, jos multiplikuojamos daugiausiai iki 50 populiacijų *in vitro* [99]. Studijos su gyvūnais parodė daug žadančius pirminius mezenchiminių kamieninių ląstelių panaudojimo kaulinio audinio defektų regeneracijai rezultatus. Nustatytas didesnis regeneruojamo kaulo agiogeninis potencialas, mineralizacija ir osifikacija [42, 81, 100, 101]. Tačiau gaunami klinikiniai rezultatai yra prieštaringi. Nors pavieniuose klinikiniuose tyrimuose aprašomas teigiamas mezenchiminių kamieninių ląstelių poveikis kaulo regeneracijai [86–88], taip pat gaunama nemažai ir neigiamų kamieninių ląstelių panaudojimo rezultatų [80, 89–91]. *In vitro* terpėje norint pagausinti kamieninių ląstelių, būtina papildoma chirurginė intervencija – kaulų čiulpų arba riebalų aspirato paėmimas, tai lemia papildomą operacinę žaizdą, didesnę komplikacijų riziką ir padidėjusį paciento diskomfortą [102]. Kita problema, susijusi su kamienių ląstelių panaudojimu, – jų kultivavimui būtinos laboratorinės sąlygos, reikalaujančios daug technologinių, laiko ir finansinių resursų. Taip pat iki šiol vis dar išlieka iki galo neišspręsta tolygaus kamieninių ląstelių pasiskirstymo kaulinėje matricoje ir vaskuliarizacijos problema. Ląstelių išlikimui recipientinėje ložėje būtina iš karto užtikrinti gerą kraujotaką, tą sunku pasiekti didesnio tūrio kauliniuose transplantantuose [103]. Taip pat aktualios išlieka ir ląstelių genomo mutacijų bei panaudojimo saugumo problemos, ribojančios ląstelinių kaulo transplantantų panaudojimą klinikinėje praktikoje [103, 104, 105].

3.8. Kaulo transplantantų bioaktyvavimas augimo faktoriais

Dėl esamų ląstelinių kaulo transplantantų trūkumų ir ribotų klinikinio panaudojimo galimybių, pastaruoju metu aktyviai kuriami ir tyrinėjami kaulo transplantantai su augimo faktoriais. Iš klinikinės pusės transplantantai su augimo faktoriais turi tam tikrų privalumų: geresnė sterilumo kontrolė, paprastesnės laikymo sąlygos ir ilgesnis galiojimo laikas, lengviau užtikrinamas geras augimo faktorių pasiskirstymas didelio tūrio transplantantuose, rekombinantiniai augimo faktoriai gali būti naudojami skirtingiems pacientams, nesukeliant papildomų imuninių reakcijų [93, 105].

Augimo faktoriai – tai signaliniai polipeptidai, prisijungiantys prie ląstelių specifinių transmembraninių receptorių ar ekstraląstelinio matrikso ir reguliuojantys ląstelių proliferaciją, diferenciaciją, chemotaksį, migraciją, funkcinį ir biologinį aktyvumą [106]. Augimo faktorius išskiria įvairios organizmo ląstelės: fibroblastai, epitelinės ląstelės, hemopoetinės kamieninės ląstelės, osteoblastai, leukocitai, trombocitai [107]. Kaulinio audinio regeneracijai stiprią įtaką daro ląstelių ir ekstraląstelinio matrikso biologiniai ir biocheminiai signalai, todėl svarbu, kad kaulo transplantantai atliktų ne tik osteokondukcinę funkciją, tačiau galėtų pernešti osteogenezei svarbius augimo faktorius, adhezinius baltymus ir citokinus, kurie skatintų osteoindukciją [108, 109]. Su osteokondukcinėmis ar transportinėmis matricomis naudojami autogeniniai ir rekombinantiniai augimo faktoriai. Autogeniniai augimo faktoriai išgaunami iš paciento organizmo, dažniausiai koncentruojant kraujyje cirkuliuojančias ląsteles – trombocitus ir leukocitus [14–18]. Rekombinantiniai augimo faktoriai yra sintezuojami molekulinės bioinžinerijos metodais, į produkcines ląsteles įterpiant tam tikrą augimo faktorių koduojančias genų sekas ir vėliau filtruojant ir koncentruojant jų produkuojamus rekombinantinius augimo faktorius [110].

Osteoindukciniai augimo faktoriai yra būtini osteoblastinių progenitorinių ląstelių proliferacijai, diferenciacijai ir kaulinio audinio formavimui. Literatūroje aprašoma daug kaulo regeneraciją tiesiogiai ir netiesiogiai skatinančių augimo faktorių: transformuojantis augimo faktorius beta (TGF-β), kraujagyslių endotelio augimo faktorius (VEGF), fibroblastų augimo faktorius (FGF), insulino augimo faktorius – 1 (IGF-1), trombocitų augimo faktorius (PDGF), kaulo morfogenetiniai baltymai (BMP) [14, 15, 73–75, 162] (3.8.1 lentelė).

TGF-β1 ir TGF-β2 izoformos yra svarbūs augimo faktoriai jungiamojo audinio ir kaulo regeneracijai. TGF-β gali inhibuoti osteoklastus ir proteazes, taip sulėtindamas kaulo rezorbcinius procesus ir netiesiogiai skatindamas kaulo regeneraciją [126]. Nustatyta, kad TGF-β taip pat tiesiogiai skatina osteoblastų proliferaciją, diferenciaciją ir osteoido sintezę [127].

VEGF yra svarbiausias vaskulogenezės, angiogenezės ir limfangiogenezės, kurios būtinos kaulinio, kaip ir kiekvieno kito, audinio regeneracijai, augimo faktorius [128]. VEGF skatina kraujagyslių endotelinių ląstelių migraciją, proliferaciją bei kraujagyslių fenestraciją ir pralaidumą [129, 130].

FGF taip pat svarbus angiogenezės, kolageno sintezės, žaizdų gijimo ir kaulo regeneracijos augimo faktorius. Literatūroje plačiausiai aprašoma FGF-2 izoforma [131]. FGF-2 per heparino kofaktorius gali prisijungti prie daugelio ląstelių receptorių ir pasižymi plačiu angiogeniniu ir mitogenininiu poveikiu, įskaitant ir osteoprogenitorinių ląstelių proliferacijos ir diferenciacijos skatinimą [132].

IGF-1 dalyvauja daugelio ląstelių, įskaitant kamienines ląsteles ir osteoblastus, proliferacijoje ir diferenciacijoje, yra svarbus žaizdų gijimo uždegiminės fazės mediatorius [133]. IGF-1 reguliuoja ląstelių energijos apykaitą ir mitochondrijų funkcinį aktyvumą, kuris ypač svarbus veiksnys kamieninių ląstelių osteogeninei diferenciacijai ir diferencijuotų osteoblastų matrikso formavimui [134, 135].

Nors rekombinantiniai TGF-β, VEGF, FGF ir IGF-1 yra plačiai tyrinėjami kaulo inžinerijoje, eksperimentiniuose *in vitro* ir *in vivo* tyrimuose [136, 137], jų klinikinis panaudojimas nėra aprobuotas.

PDGF yra vienas svarbiausių žaizdų gijime dalyvaujančių augimo faktorių, stimuliuojančių mezoderminės kilmės ląstelių mitogeninį aktyvumą [106]. PDGF yra svarbus kolageno sintezei, angiogenezei ir makrofagų aktyvacijai [124]. Nustatyta, kad PDGF didina ir osteoblastų chemotaksį bei mitogeninį aktyvumą [106, 125]. Rekombinantinė PDGF augimo faktoriaus izoforma – rhPDGF-BB kartu su β-TCP transportine matrica (Gem 21S, Shirley, Niujorkas, JAV) JAV Maisto ir vaistų administracijos (FDA) yra aprobuota panaudojimui periodonto intrakaulinių defektų, furkacijų defektų ir dantenų recesijų operacijose [118]. Pirminiuose klinikiniuose tyrimuose su rhPDGF-BB gauti geri rezultatai regeneruojant periodonto intrakaulinius defektus ir gerinant minkštųjų audinių gijimą [118–120], tačiau nustatytas ir ribotas rhPDGF-BB efektyvumas regeneruojant žandikaulių atrofuotos alveolinės ataugos defektus [121–123].

BMP, priskiriami TGF-β šeimai, yra vieni svarbiausių osteoindukcinių augimo faktorių [11, 63, 78, 110]. BMP prisijungia prie kamieninių ląstelių specifinių receptorių ir skatina jų chemotaksį ir osteoblastinę diferenciaciją per Smad baltymų signalinę sistemą [111]. Rekombinantiniai BMP-2 ir BMP-7 yra plačiausiai klinikiniuose tyrimuose aprašyti morfogenetiniai baltymai [11, 63, 78, 110]. JAV FDA yra davusi leidimą naudoti rhBMP-2 (INFUSE Bone Graft, Medtronic, Mineapolis, Minesota, JAV) ortopedinėje chirurgijoje (stuburo priekinės juosmens srities slankstelių kūnų sujungimo,

blauzdikaulio diafizės lūžių operacijose) bei veido ir žandikaulių chirurgijoje (viršutinio žandikaulio sinuso dugno pakėlimo, pavienių poekstrakcinių defektų augmentacijos operacijose) [112]. rhBMP-7 (OP-1 Putty, Stryker Corporation, Kalamazu, Mičiganas, JAV) naudojimą JAV FDA yra reglamentavusi tik stuburo užpakalinės šoninės juosmens srities slankstelių lūžių recidyvų operacijose. Europos Sąjungoje ir Lietuvoje BMP ir kitų rekombinantinių augimo faktorių klinikinis naudojimas kol kas nėra licencijuotas. Nors literatūroje aprašoma sėkmingo BMP panaudojimo žandikaulių kaulinių defektų regeneracijai atvejų [11, 113–116], taip pat keliamas klausimas ir dėl rekombinantinių augimo faktorių nelicencijuoto naudojimo, sukeliamos ryškios edemos, saugios koncentracijos parinkimo, nekontroliuojamo ektopinio kaulo formavimosi ir išaugusios vėžinių susirgimų rizikos [13, 78, 117].

3.8.1 lentelė. *Kaulinio audinio bioinžinerijoje naudojami osteoindukciniai augimo faktoriai ir jų įtaka osteogenezei bei vaskulogenezei.*

Augimo faktorius	**Osteoblastų diferenciacija**	**Osteoblastų proliferacija**	**Vaskulogenezė**
TGF-β	Skatina	Skatina	Skatina
VEGF	–	–	Indukuoja / Skatina
FGF-2	Skatina	Skatina	Indukuoja / Skatina
IGF-1	Skatina	Skatina	Skatina
PDGF-BB	Skatina	Skatina	Skatina
BMP-2	Indukuoja	Skatina ankstyvąją; Inhibuoja vėlyvąją	–
BMP-4	Indukuoja	Skatina ankstyvąją; Inhibuoja vėlyvąją	–
BMP-6	Indukuoja	Skatina ankstyvąją; Inhibuoja vėlyvąją	–
BMP-7	Indukuoja	Skatina ankstyvąją; Inhibuoja vėlyvąją	–
BMP-9	Indukuoja	Skatina ankstyvąją; Inhibuoja vėlyvąją	–

Pagal Viktor Tollemar ir kt. 2016 m. [162]; TGF-β – transformuojantis augimo faktorius beta; VEGF – kraujagyslių endotelio augimo faktorius; FGF-2 – fibroblastų augimo faktorius – 2; IGF-1 – insulino augimo faktorius – 1; PDGF-BB – trombocitų augimo faktorius BB; BMP – kaulo morfogenetinis baltymas.

3.9. Kraujo koncentratų panaudojimas kaulo defektų regeneracijai

Dėl esamų rekombinantinių augimo faktorių trūkumų ir klinikinio panaudojimo apribojimų, literatūroje plačiai tyrinėjamos autogeninių augimo faktorių panaudojimo galimybės, kaip autogeninių augimo faktorių šaltinį naudojant kraujo koncentratus [14–18, 59, 79]. Kraujo koncentratuose koncentruojamos kraujyje cirkuliuojančios ląstelės – trombocitai (su arba be leukocitų), o jų išskiriami autogeniniai augimo faktoriai naudojami kaulo bei minkštųjų audinių gijimo ir regeneracijos aktyvinimui [136, 171].

Kraujyje cirkuliuojančios ląstelės – trombocitai ir leukocitai – turi įvairių intraląstelinių augimo faktorių ir baltymų, svarbių žaizdų gijimui ir kaulo regeneracijai. Trombocitai savo alfa, tankiosiose granulėse ir lizosomose kaupia PDGF, TGF-β, VEGF, FGF, IGF-1, epidermio augimo faktorių (EGF), įvairius bioaktyvius baltymus ir citokinus (angiopoietiną-1, RANTES, jungiamojo audinio aktyvuojantį baltymą – 3, trombocitų bazinį baltymą, timoziną β-4, fibrinopeptidus A ir B, interleukinus 1β ir 8 (IL-1β ir IL-8), neutrofilų chemoatraktinį baltymą) [152, 153]. Trombocitai kraujyje cirkuliuoja neaktyvuotos formos ir gali būti aktyvuojami natūraliai organizme esančiais aktyvavimo faktoriais (kolagenu, tromboksanu A2 (TXA2), adenozino difosfatu (ADP), trombinu, epinefrinu, serotoninu) arba dirbtiniais faktoriais (kalcio chloridu, ksenogeniniu arba alogeniniu trombinu) [154, 155]. Aktyvuoti trombocitai pakeičia savo formą ir iš intraląstelinių granulių išskiria bioaktyvias medžiagas. Trombocitų išskiriami PDGF ir TGF-β dalyvauja mezenchiminių kamieninių ląstelių ir osteoblastų proliferacijoje, chemotaksyje, ekstraląstelinio matrikso sintezėje ir angiogenezėje [156, 157]. FGF, VEGF ir angiopoietinas-1indukuoja ir skatina angiogenezę, yra svarbūs homeostazės procesams ir proliferacinės bei reparacinės žaizdos gijimo fazės užtikrinimui [158–161]. Kiti trombocitų išskiriami citokinai ir bioaktyvūs baltymai, tokie kaip RANTES, IL-1β, IL-8 ir neutrofilų chemoatraktinis baltymas moduliuoja žaizdos gijimo procesą [153]. Tuo tarpu RANTES, jungiamojo audinio aktyvuojantis baltymas 3, trombocitų bazinis baltymas, timozinas β-4 ir fibrinopeptidai A ir B pasižymi mikrobicidiniu poveikiu [152, 163, 164].

Literatūros duomenys apie leukocitų išskiriamų bioaktyvių medžiagų įtaką kaulinio audinio regeneracijai yra skirtingi. Vieni autoriai laikosi nuomonės, kad leukocitai atlieka žalingą poveikį kaulo gijimui, išskirdami uždegiminius interleukinus (IL-1β, IL-6, IL-16) ir laisvuosius radikalus [165–167]. Kitų autorių nuomone, leukocitai ir jų išskiriami augimo faktoriai (VEGF, TGF-β, IGF), uždegimą slopinantys citokinai (IL-4, IL-10, IL-13), opioidiniai peptidai (β-endorfinas, metenkefalinas, dinorfinas-A) ir antimikrobiniai peptidai (katelicidinai, defensinai) yra būtini kaulo defekto

gijimui, kaulinio audinio gijimo uždegiminės, proliferacinės ir remodeliacinės stadijų moduliacijai ir ekstraląstelinio matrikso sintezei [163, 168–170].

Literatūroje aprašoma įvairių technikų kraujo koncentratų paruošimui [168, 174]. Trombocitų gausi plazma (PRP) yra pirmasis prof. Roberto E. Markso ir kt. 1998 m. [172] aprašytas kraujo koncentratas. PRP išgauti į mėgintuvėlį su antikoaguliantais imama veninio paciento kraujo, kuris centrifuguojamas vienu arba dviem etapais, atskiriant bei pašalinant eritrocitus, dalį kraujo plazmos ir nedideliame tūryje plazmos koncentruojant trombocitus. Priklausomai nuo PRP paruošimo metodikos variacijų, kartu su trombocitais gali būti koncentruojami ir leukocitai [173]. Koncentruotieji trombocitai yra aktyvinami kalcio chloridu ir (arba) trombinu. Cheminė PRP aktyvacija lemia greitą trombocitų degranuliaciją ir augimo faktorių atpalaidavimą. Plazmoje esantis fibrinogenas polimerizuojamas į tetramolekulinėmis jungtimis sujungtą, plokštuminės konfigūracijos, mažo tankio fibrino tinklą, kuris silpnai inkorporuoja ląsteles ir augimo faktorius [174]. Dėl cheminių aktyvatorių sukeliamos greitos trombocitų aktyvacijos ir degranuliacijos, dauguma jų augimo faktorių iš PRP atpalaiduojami per pirmąsias keletą valandų po PRP paruošimo, o silpnas fibrino tinklas ištirpsta audinių terpėje 3 dienų laikotarpiu [169]. Literatūroje aprašoma įvairių PRP paruošimo modifikacijų, viena dažniausiai naudojamų klinikinėje praktikoje – augimo faktorių gausi plazma (PRGF), pirmą kartą aprašyta Eduardo Anitua ir kt. 1999 m. [175]. PRGF išskyrimui paciento kraujas taip pat imamas į mėgintuvėlį su antikoaguliantais (natrio citratu) ir centrifuguojamas 8 minutes 580 g ištcentrine jėga, mėgintuvėlio viršutinėje dalyje koncentruojant plazmos, trombocitų ir leukocitų sluoksnį. Po centrifugavimo pipete yra paimama dalis apatinio plazmos sluoksnio, kuriame gausu trombocitų, tačiau nėra leukocitų. Plazmoje koncentruoti trombocitai aktyvuojami kalcio chloridu [176]. PRGF biologinės, fizikocheminės ir klinikinės savybės yra panašios į kitų naudojamų PRP produktų [192].

Literatūroje yra plačiai aprašytas teigiamas PRP poveikis minkštųjų audinių gijimui [177–180], tačiau daugelis autorių abejoja PRP efektyvumu regeneruojant kaulinio audinio defektus [181–184]. Literatūroje nurodomos pagrindinės silpno PRP poveikio kaulinio audinio regeneracijai priežastys: greitas augimo faktorių išskyrimas ir pašalinimas iš reneneruojamos srities, silpna PRP fibrino matrica ir negalėjimas užtikrinti ilgalaikio osteopromocinio poveikio [154, 168, 174].

Siekiant supaprastinti kraujo koncentratų paruošimą ir pagerinti klinikines savybes, kurių trūko PRP, 2001 m. Joseph Choukroun ir kt. [185] pristatytas leukocitų ir trombocitų gausus fibrinas (L-PRF), literatūroje dažnai vadinamas antrosios kartos kraujo koncentratu. Priešingai nei PRP ar jos

variacijoms (PRGF), L-PRF paruošimui nereikia naudoti antikoaguliantų ir cheminių aktyvatorių. Paciento veninis kraujas imamas į stiklinį arba silicio dioksidu padengtą mėgintuvėlį ir centrifuguojamas 400 g ištcentrine jėga 12 minučių [14]. Centrifugavimo proceso metu mėgintuvėlyje prasideda natūrali kraujo krešėjimo mechanizmo kaskada ir kraujo ėminyje esantis fibrinogenas yra polimerizuojamas į plastiškos konsistencijos fibrino matriksą, kuriame inkorporuojama didžioji dalis trombocitų, apie 65 proc. kraujo ėminio leukocitų, jų augimo faktorių, citokinų ir plazmos glikoproteinų. Stiprios trimolekulinės jungtys sudaro santykinai tvirtą erdvinę L-PRF fibrino matricos struktūrą, palankią ląstelių ir augimo faktorių inkorporacijai. Priešingai nei PRP, L-PRF augimo faktorius atpalaiduoja palaipsniui – nustatyta, kad L-PRF išskiria TGF β-1, PDGF, FGF ir VEGF iki 28 dienų laikotarpiu po paruošimo [15, 169]. Ilgesnis augimo faktorių atpalaidavimo periodas leidžia tikėtis ir geresnio nei PRP atveju L-PRF poveikio tiek minkštųjų audinių gijimui [186, 187], tiek kaulinio audinio regeneracijai [188–190]. Šio darbo autorius kartu su bendraautoriais yra pasiūlęs ir publikavęs klinikinį L-PRF panaudojimo protokolą periimplantito kaulinių defektų regeneraciniam gydymui [221].

3.10. L-PRF panaudojimas retinuotų apatinio žandikaulio trečiųjų krūminių dantų šalinimo operacijose

Literatūroje retinuoti apatinio žandikaulio tretieji krūminiai dantys (RAŽTKD) traktuojami kaip patologinės vystymosi deformacijos, kurios dažnai pasireiškia šiuolaikinėje žmonių civilizacijoje [207–209]. Neišdygusių trečiųjų krūminių dantų turi apie 73 proc. jaunų suaugusių žmonių populiacijos [207]. Todėl RAŽTKD šalinimo operacijos tapo vienos dažniausiai atliekamų procedūrų burnos bei veido ir žandikaulių chirurgijos praktikoje [208, 209]. Nepaisant kai kurių autorių aprašomos nuomonės dėl abejotinos būtinybės šalinti RAŽTKD [210], literatūroje yra aprašyta nemažai pagrįstų indikacijų RAŽTKD šalinimui. Tarp jų yra ortodontinės ir susijusios su dantų protezavimu indikacijos, dantų kariesas, skausmas, infekcijos, RAŽTKD, susiję su cistomis arba augliais, RAŽTKD sukelti gretimų dantų pažeidimai, retinuotų dantų artumas prie apatinio žandikaulio lūžio linijos arba ortognatinės chirurgijos srities, infekcijos židinių profilaktika dėl širdies operacijų ir endokardito [209, 211]. RAŽTKD šalinimo operacijos dažnai siejamos su pacientų patiriamu pooperaciniu diskomfortu, įskaitant skausmą, tinimą, kramtymo funkcijos sutrikimą ir žymų burnos ertmės sveikatos pablogėjimą, kuris turi įtakos gyvenimo kokybei ankstyvo pooperacinio periodo metu, bei gana dažnas alveolito pasireiškimas [212, 213]. Pagrindinė chirurginė užduotis RAŽTKD šalinimo operacijų metu yra

minimaliai invazyviai pašalinti retinuotą dantį, išvengti komplikacijų, palengvinti pooperacinį periodą ir sumažinti paciento diskomfortą iki žemiausio įmanomo lygio. RAŽTKD operacijos planavimui pasiūlyta nemažai klasifikacijų. Populiariausios iš jų yra Winter [197], Pell ir Gregory [198], Pedersono [201] klasifikacijos, aprašančios danties padėtį žandikaulyje bei leidžiančios vertinti RAŽTKD šalinimo sudėtingumą ir galimų komplikacijų riziką. Tačiau nė viena iš šiuo metu siūlomų RAŽTKD klasifikacijų neatsižvelgia į gretimų svarbių anatominių struktūrų – apatinio alveolinio nervo ir liežuvinio nervo pažeidimo riziką, šalinant RAŽTKD [215]. Taip pat literatūroje aprašomas abejotinas populiarių Pell ir Gregory ir Pedersono klasifikacijų patikimumas [216–218]. Juodžbalys ir Daugėla 2013 m. [199] pasiūlė RAŽTKD šalinimo sudėtingumo klasifikaciją, vertinančią progonzuojamą RAŽTKD šalinimo sudėtingumą bei galimą apatinio alveolinio nervo ir liežuvinio nervo pažeidimo riziką. Ši klasifikacija naudinga tiek klinikine prasme, planuojant RAŽTKD šalinimo operacijos eigą ir siekiant išvengti komplikacijų, tiek moksliniuose tyrimuose tiriamųjų grupių standartizavimui RAŽTKD šalinimo tiriamuosiuose modeliuose.

RAŽTKD šalinimo operacijų išeičių pagerinimui siūlomi įvairūs preparatai ir operacinės technikos, tarp jų: kortikosteroidai ir nesteroidiniai vaistai nuo uždegimo, krioterapija, kompresija, gydymas lazeriu, pjezo chirurgija ir kraujo koncentratai [214].

Pastaraisiais metais labai padidėjo susidomėjimas įvairiais autogeniniais kraujo koncentratais (PRP, L-PRF) ir jų naudojimu žaizdų gijimui pagerinti. Per pastaruosius du dešimtmečius buvo publikuota daug literatūros, kurioje teigiamai atsiliepiama apie kraujo koncentratų panaudojimo burnos chirurgijoje perspektyvas, kurios ypač išaugo chirurginėje praktikoje pradėjus naudoti L-PRF [154, 163, 169, 323].

L-PRF yra autogeninė fibrino biomedžiaga, kurios fibrino tinkle yra trombocitų, leukocitų ir citokinų. Nustatyta, kad L-PRF stimuliuoja tokias biologines funkcijas kaip chemotaksis, angiogenezė, ląstelių proliferacija bei diferenciacija [16, 18] ir taip gali pagerinti žaizdų gijimą. Kitaip nei PRP, L-PRF paruošimui nereikia trombocitų aktyvavimo cheminiais priedais ir L-PRF yra autogeninė, priedų neturinti biomedžiaga. L-PRF yra plastiškos konsistencijos biomedžiaga, kuri po naudojimo greitai nesuyra. Buvo nustatyta, kad L-PRF fibrino matrica stipriai prisijungia trombocitų ir leukocitų augimo faktorius, tai prailgina citokinų gyvavimo laiką [15]. L-PRF taip pat stimuliuoja žmogaus osteoblastų ir fibroblastų proliferaciją [16, 17] bei žmogaus kaulų mezenchiminių kamieninių ląstelių diferenciaciją [18]. L-PRF gali skatinti tiek minkštųjų audinių, tiek kaulinio audinio regeneraciją, todėl turi potencialo būti naudojamas ir RAŽTKD šalinimo operacijose.

3.11. Literatūros apžvalgos apibendrinimas

Klinikinėje praktikoje žandikaulių kaulinių defektų regeneracijai naudojamos įvairios medžiagos: autogeniniai, ksenogeniniai, alogeniniai ir sintetiniai transplantantai. Idealus kaulo transplantantas turi pasižymėti osteogeninėmis, osteoindukcinėmis ir osteokondukcinėmis savybėmis. Autogeninis kaulas iš dalies atitinka idealiam transplantantui keliamus reikalavimus, tačiau autogeninio donorinio kaulo prieinamumas yra ribotas, imant transplantantą sukuriama papildoma operacinė žaizda, didėja komplikacijų rizika. Dauguma šių dienų klinikinėje praktikoje naudojamų ksenogeninių, alogeninių ir sintetinių transplantantų pasižymi tik osteokondukcinėmis savybėmis, tai riboja jų klinikinį efektyvumą. Šiai problemai spręsti literatūroje siūloma įvairių eksperimentinių kaulo bioinžinerijos modelių, naudojančių įvairių tipų osteokondukcinius karkasus, augimo faktorius ir (arba) osteoprogenitorines ląsteles. Tačiau šių modelių klinikinis naudojimas nėra aprobuotas, trūksta duomenų jų efektyvumui ir saugumui pagrįsti.

L-PRF yra autogeninės kilmės augimo faktorių koncentratas. L-PRF yra aprobuotas klinikiniam naudojimui ir gali būti naudojamas kaulo ir minkštųjų audinių regeneracijai gerinti kaip alternatyva rekombinantiniams augimo faktoriams.

4. TYRIMO MEDŽIAGA IR METODAI

Mokslinis darbas atliktas Lietuvos sveikatos mokslų universiteto (LSMU) Medicinos akademijos Odontologijos fakulteto Veido ir žandikaulių chirurgijos klinikoje, bendradarbiaujant su Kauno technologijos universiteto Polimerų chemijos ir technologijos katedra, Valstybiniu mokslinių tyrimų instituto Inovatyvios medicinos centru, Vilniaus universiteto Biochemijos instituto Gyvybės mokslų centru, Porto universitetu (angl. *University of Porto*, Portas, Portugalija) ir Triesto universitetu (angl. *University of Trieste*, Triestas, Italija). Moksliniams tyrimams gauti Valstybinės maisto ir veterinarijos tarnybos leidimai (Nr. G2-18; Nr. G2-55), Kauno regioninio biomedicininių tyrimų komiteto ir LSMU Bioetikos centro leidimai (Nr. BE-2-12 Nr. BEC-MF-01; Nr. BEC-OF-367) ir Valstybinės duomenų apsaugos inspekcijos (ADA) leidimas (Nr. 2R-2338).

Mokslinį darbą sudaro eksperimentinė ir klinikinė dalys.

A. Eksperimentinės tyrimo dalies schema:

1. Kompozitinių celiuliozės karkasų su nHA ir µHA užpildais sintezė, *in vitro* tyrimai.
2. Kompozitinių celiuliozės karkasų su nHA ir µHA užpildais µKT ir histologiniai *in vivo* tyrimai Naujosios Zelandijos triušių kaukolės skliauto defektų modelyje.
3. L-PRF bioaktyvuotų kompozitinių celiuliozės karkasų su nHA ir µHA užpildais µKT ir histologiniai *in vivo* tyrimai Naujosios Zelandijos triušių kaukolės skliauto defektų modelyje.
4. Neaktyvuotų ir L-PRF bioaktyvuotų kompozitinių celiuliozės karkasų su nHA ir µHA užpildais efektyvumo *in vivo* kaulo defektų regeneracijai palyginimas tarpusavyje ir su komerciniu alogeniniu kaulo transplantantu.
5. Statistinė analizė.

B. Klinikinės tyrimo dalies schema:

1. Žmogaus retinuotų apatinio žandikaulio trečiųjų krūminių dantų (RAŽTKD) šalinimo sudėtingumo klasifikacijos sukūrimas ir publikavimas.
2. RAŽTKD šalinimo sudėtingumo klasifikacijos validacija, statistinė analizė.
3. L-PRF įtakos minkštųjų audinių gijimui, alveolito pasireiškimui ir pooperaciniam pacientų diskomfortui įvertinimas žmogaus RAŽTKD šalinimo defektų modelyje, tyrimo grupes standartizuojant pagal RAŽTKD šalinimo sudėtingumo klasifikaciją.
4. Statistinė analizė.

4.1. Eksperimentiniai *in vitro* ir *in vivo* tyrimai

4.1.1. Kompozitinių celiuliozės karkasų su nHA ir µHA užpildais sintezė

Celiuliozės gelis gautas regeneruojant acetilceliuliozę (Sigma-Aldrich, Sent Luisas, Misūris, JAV) acetono tirpale pagal metodiką, aprašytą Jolantos Bryjak ir kt. 2007 m. [193]. Celiuliozės su nano- ar mikrodydžio hidroksiapatito dalelėmis kompozitai buvo gauti, celiuliozės gelio formavimo metu įterpiant atitinkamo dydžio sferines HA daleles pagal metodiką, aprašytą Odetos Petrauskaitės ir kt. 2008 m. [68]. Įterpiamų nHA (Sigma-Aldrich, Sent Luisas, Misūris, JAV) vidutinis dalelių dydis – 100 nm, µHA (Sigma-Aldrich, Sent Luisas, Misūris, JAV) vidutinis dalelių dydis – 20 µm. Atitinkamai buvo suformuotos celiuliozės-nHA ir celiuliozės-µHA kompozitinės matricos, kuriose HA masės dalis sudarė 50 proc. Siekiant gauti norimos morfologijos kompozitus, šie buvo inkliuduoti 20 proc. etilo alkoholiu, šaldyti –25 °C temperatūroje ir liofilizuoti ALPHA 2-4 LSC (Martin Christ Gefriertrocknungsanlagen GmbH, Osterode am Harz, Vokietija) liofilizatoriuje (kondensatoriaus temperatūra –85 °C) 24 valandas (4.1.1.1 pav.).

4.1.1.1 pav. *Eksperimentiniai celiuliozės (kairėje) bei kompozitiniai celiuliozės-µHA (viduryje) ir celiuliozės-nHA (dešinėje) karkasai.*
Celiuliozė-µHA – celiuliozės ir mikrohidroksiapatito kompozitinis transplantantas; celiuliozė-nHA – celiuliozės ir nanohidroksiapatito kompozitinis transplantantas.

4.1.2. Celiuliozės-nHA ir celiuliozės-µHA karkasų *in vitro* struktūrinė analizė

Celiuliozės-nHA ir celiuliozės-µHA karkasų morfologiniai parametrai buvo vertinami µKT analizatoriumi µCT40 (Scanco Medical AG, Bruttisellen, Šveicarija). Analizei naudoti kiekvieno tipo karkasų (n = 4) cilindriniai 10 mm skersmens ir 8 mm aukščio mėginiai. µKT skenavimui nustatyti šie parametrai: rentgeno įtampa 45 kVp; integracijos laikas 600 ms; 2× kadrų triukšmo mažinimas, nominali raiška 10 µm. Mikrotomogramų triukšmui sumažinti naudotas 3D Gauso filtras (σ = 0,8; palaikymas = 1). Dvimačių ir trimačių mikrotomogramų vaizdų kiekybiniai ir struktūriniai parametrai vertinti Scanco 6.0 programine įranga (Scanco Medical AG, Bruttisellen, Šveicarija).

Celiuliozės-nHA ir celiuliozės-µHA kompozitai tirti Furjė transformacijos infraraudonųjų spindulių spektrofotometru (Perkin-Elmer, Waltham, Masačusetsas, JAV) infraraudonojo spektro pagrindiniame diapazone nuo 4000 iki 400 cm^{-1}. Spektrometrijos mėginiai paruošti sumaišant po keturis miligramus kiekvieno tipo matricos (n = 4) su 200 mg kalio bromido.

Kiekvieno karkasų tipo (n = 4) elementinė sudėtis analizuota skenuojančio elektroninio dispersinio spektroskopo (SEM-EDS) Quantax EDS (Bruker AXS Microanalysis GmbH, Karlsrūhė, Vokietija) sistema.

Celiuliozės kristališkumo laipsnis analizuotas rentgeno difraktometru DRON-6 (Bourevestnik, Sankt Peterburgas, Rusija), taikant 30 kV ir 20 mA Cu-Kα spinduliuotę.

4.1.3. Celiuliozės-nHA ir celiuliozės-µHA karkasų *in vitro* citotoksiškumo analizė

Kompozitinių karkasų *in vitro* citotoksiškumo analizei naudotos 27 persėjimų žmogaus osteoblastų tipo ląstelės (Mg-63, ATCC Nr. CRL-1427). Ląstelės augintos α-MEM ląstelių kultūros auginimo terpėje su 10 proc. jaučio embriono serumo, 50 µg/ml askorbo rūgšties, 50 µg/ml gentamicino ir 2,5 µg/ml fungizono, inkubuojant 37 °C temperatūroje 5 proc. CO_2 atmosferoje. Terpėje esant apie 75 proc. ląstelių susiliejimui, ląstelės atskirtos į suspensiją, naudojant 0,05 proc. tripsiną, 0,25 proc. EDTA ir 5 minutes inkubuojant 37 °C temperatūroje.

Celiuliozės-nHA ir celiuliozės-µHA karkasai padengti 2×10^4 ląstelių/cm^2 tankiu ir inkubuoti 7 dienų laikotarpiui. Skenuojančiu elektroniniu mikroskopu (SEM) vertinta ląstelių morfologija (n = 4), geltonojo tetrazolio druskų redukcijos metodu (MTT) analizuotas ląstelių metabolinis aktyvu-

mas (n = 6), genų ekspresija (n = 3) ir šarminės fosfatazės (ALP) aktyvumas (n = 6).

4.1.3.1. Analizė skenuojančiu elektroniniu mikroskopu (SEM)

Celiuliozės-nHA ir celiuliozės-µHA karkasai buvo fiksuoti laikant 1,5 proc. gliutaraldehido 0,14 M natrio kakodilato buferyje, pH = 7,3, 10 min., praėjus 24 valandoms po kultivavimo terpėje. Mėginiai buvo laipsniškai dehidruoti alkoholiuose, išdžiovinti iki ribinio taško bei padengti Au/Pd plėvele mėginių dengimo aparate SPI Module Sputter Coater equipment (Structure Probe Inc, West Chester, Pensilvanija, JAV). Paruošti mėginiai analizuoti Quanta 400 FEG (FEI Company, Hilsboras, Oregonas, JAV) skenuojančiu elektroniniu mikroskopu.

4.1.3.2. Geltonojo tetrazolio druskų redukcijos (MTT) analizė

Ląstelių kultūrų metabolinis aktyvumas vertintas MTT analize, kurioje stebimas geltonos spalvos geltonojo tetrazolio druskos (3-(4,5-dimetiltiazol-2-il-)-2,5-difeniltetrazolio bromido) redukavimas į tamsiai mėlynos spalvos formazino kristalus gyvų ląstelių mitochondrijose. Gyvų ląstelių skaičius yra tiesiogiai proporcingas susidariusio produkto – formazano kiekiui, kuris spektrofotometriškai vertintas 3 valandų laikotarpiu Synergy HT skaitytuvu (Biotek Instruments, Winooski, Vermontas, JAV) 550 nm bangos ilgyje, gautus netirpius produktus ištirpinus dimetilsulfokside.

4.1.3.3. Genų raiškos vertinimas atvirkštinės transkripcijos polimerazės grandinine reakcija (AT-PGR)

Praėjus 7 dienų inkubaciniam periodui, vertinta ląstelių kultūrų bendrinio GAPDH (gliceraldehido-3-fosfato-dehidrogenazės) geno, ir osteoblastinių genų (slopinančio transkripcijos faktoriaus 2 (Runx-2), ALP, BMP-2 bei I tipo kolageno (Col I) genų) raiška. Ribonukleino rūgštys (RNR) buvo išgautos RNeasy® Mini Kit (QIAGEN, Hildenas, Vokietija) ekstrakcine sistema. RNR išeiga ir grynumas vertinti spektrofotometriškai prie 260 ir 280 nm bangos ilgių, kokybė vertinta elektroforeze 2 proc. agarozės gelyje. 0,5 µg RNR atvirkštinė transkripcija ir amplifikacija atlikti Titan One Tube AT-PGR sistema (Roche Diagnostics, Manheimas, Vokietija) 55 ºC temperatūroje. AT-PGR analizei naudotos pradmenų sekos pateikiamos 4.1.3.3.1 lentelėje.

4.1.3.3.1 lentelė. *AT-PRG analizėje vertinti genai ir jų pradmenų sekos.*

Genas	Tiesioginis pradmuo	Atvirkštinis pradmuo
GAPDH	CAGGACCAGGTTCACCAACAAGT	GTGGCAGTGATGGCATGGACTGT
Runx-2	CAGTTCCCAAGCATTTCATCC	TCAATATGGTCGCCAAACAG
ALP	ACGTGGCTAAGAATGTCATC	CTGGTAGGCGATGTCCTTA
BMP-2	GACGAGGTCCTGAGCGAGTT	GCAATGGCCTTATCTGTGAC
Col I	TCCGGCTCCTGCTCCTCTTA	ACCAGCAGGACCAGCATCTC

AT-PGR – atvirkštinės transkripcijos polimerazės grandininė reakcija; GAPDH – gliceraldehido-3-fosfato-dehidrogenazės genas; Runx-2 – slopinantis transkripcijos faktorius 2; ALP – šarminė fosfatazė; BMP-2 – kaulo morfogenetinis baltymas 2; Col I – I tipo kolagenas.

Genų densitometrinė analizė atlikta ImageJ 1.41 (National Institutes of Health, Bethesda, Marilandas, JAV) programine įranga.

4.1.3.4. ALP aktyvumo analizė

ALP aktyvumas vertintas atliekant ląstelių lizatų (su 0,1 Triton X-100 (Sigma-Aldrich, Sent Luisas, Misūris, JAV), 5 min.) hidrolizę p-nitrofenilfosfatu (pH = 10,3; 30 min., 37 °C temperatūroje) ir spektrofotometriškai Synergy HT skaitytuvu (Biotek Instruments, Winooski, Vermontas, JAV) 400 nm bangos ilgyje vertinant p-nitrofenolio susidarymą. ALP aktyvumas normalizuotas ir kiekybiškai nustatytas Bradfordo metodu, kiekybinę išraišką pateikiant nmol/min/mg vienetais.

4.1.4. *In vivo* tyrimų grupės

In vivo tyrimai atlikti naudojant Naujosios Zelandijos triušių kaukolės skliauto defektų modelį. Tyrimams paruošti celiuliozės-nHA ir celiuliozės-µHA karkasų 8,0 mm skersmens ir 2,0 mm storio cilindro formos mėginiai. Kaip kontrolinė medžiaga naudotas paruoštas tų pačių matmenų ir formos komercinis alogeninis akytojo kaulo transplantantas Maxgraft (Botiss Biomaterials GmbH, Zossen, Vokietija). Mėginiai prieš chirurginę procedūrą buvo rehidruoti arba fiziologiniu tirpalu, arba L-PRF eksudatu, pagal tai sudarant tiriamąsias grupes: celiuliozė-nHA, celiuliozė-µHA, kontrolė (alogeninis transplantantas), celiuliozė-nHA + L-PRF, celiuliozė-µHA+ L-PRF, kontrolė (alogeninis transplantantas) + L-PRF (4.1.4.1 pav.).

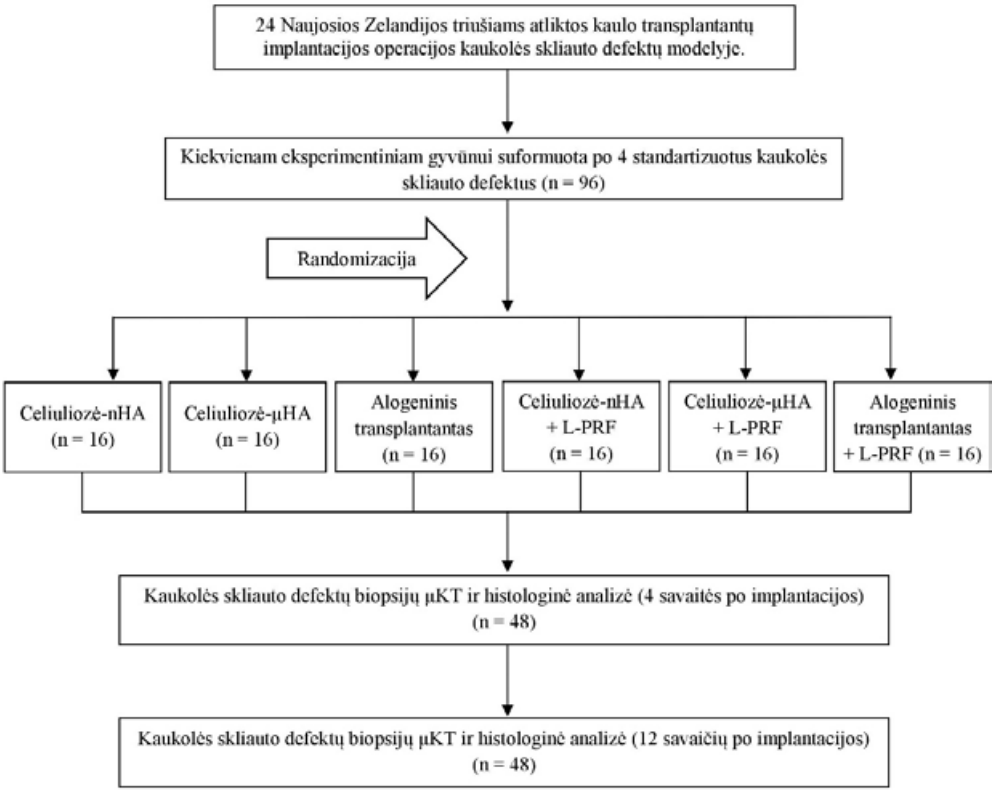

4.1.4.1 pav. *In vivo tyrimo eigos schema.*
Celiuliozė-nHA – celiuliozės ir nanohidroksiapatito kompozitinis transplantantas; celiuliozė-µHA – celiuliozės ir mikrohidroksiapatito kompozitinis transplantantas; L-PRF – leukocitų ir trombocitų gausus fibrinas; µKT – mikrokompiuterinė tomografija.

4.1.5. L-PRF paruošimas

L-PRF buvo paruoštas pagal Choukroun ir kt. 2001 m. aprašytą protokolą [185]. Prieš chirurginę procedūrą Naujosios Zelandijos triušiams iš šoninės ausies venos į du 9 ml talpos silicio dioksidu dengtus mėgintuvėlius (Intra-Lock International, Boca Raton, Florida, JAV) paimta veninio kraujo. Mėgintuvėliai centrifuguoti EBA 20 centrifugoje (Andreas Hettich GmbH & Co.KG, Tuttlingen, Vokietija) 12 min. 2800 apsukų per minutę režimu. Po centrifugavimo L-PRF buvo atskirtas nuo raudonųjų kraujo kūnelių bazės (4.1.5.1 pav.) ir perkeltas į paruošimo dėžutę PRF & growth factor-rich fibrin (GRF) box (Osung Mnd Company, Gimpo, Pietų Korėja). Dėžutėje pagal Dohan Ehrenfest 2010 m. aprašytą metodiką [194] išskirtas L-PRF eksudatas ir paruoštos L-PRF membranos.

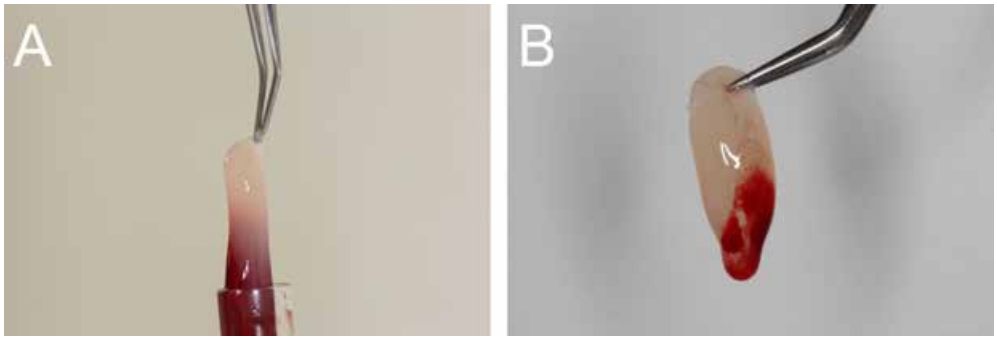

4.1.5.1 pav. *A – triušio L-PRF, po centrifugavimo sukibęs su raudonaisiais kraujo kūneliais;*
B – nuo raudonųjų kraujo kūnelių bazės atskirtas triušio L-PRF.

4.1.6. *In vivo* chirurginės procedūros

Chirurginėms operacijoms pasirinkti 24 vyriškos lyties, 30–35 savaičių amžiaus, 3,5–4,0 kilogramų svorio laboratoriniai Naujosios Zelandijos triušiai. Visos chirurginės manipuliacijos atliktos laikantis Lietuvos valstybinės maisto ir veterinarijos tarnybos reikalavimų bei Europos Parlamento ir Europos Tarybos direktyvos 2010/63 ES dėl mokslo tikslais naudojamų gyvūnų apsaugos.

Prieš chirurginę procedūrą gyvūnai buvo premedikuoti acepromazino (0,5 mg/kg) injekcija į raumenis bei poodine buprenorfino (0,03 mg/kg) injekcija analgezijos kontrolei. Bendrinė anestezija atlikta į raumenis suleidžiant ketamino hidrochlorido (35 mg/kg) ir ksilazino hidrochlorido (5 mg/kg). Triušių kaukolės skliauto srityje nuskustas kailis, oda dezinfekuota oktenidino dihidrochlorido tirpalu. Papildomai vietinei anestezijai ir kraujavimo kontrolei kaukolės skliauto srityje suleista 1,4 ml 4 proc. artikaino hidrochlorido su 1:100 000 epinefrino.

Triušių kaukolės skliauto vidurio linijoje sagitaliai atlikta incizija, atkeltas odos ir antkaulio lopas. Kiekvienoje kaukolės skliauto pusėje trepano grąžteliu, gausiai aušinant fiziologiniu tirpalu, suformuormuota po du standartizuotus 8,0 mm skersmens, 2,0 mm gylio apskritus defektus. Iš viso kiekvieno gyvūno kaukolės skliaute paruošta po 4 defektus (4.1.6.1 A pav.). Formuojant defektus, ypatingas dėmesys skirtas išsaugoti intaktišką *dura mater*. Kaulo defektai atsitiktine tvarka buvo užpildomi celiuliozės-nHA, celiuliozės-µHA arba kontroliniu (alogeniniu transplantantu) paruoštais mėginiais, kurie, priklausomai nuo tiriamosios grupės, buvo rehidruojami

fiziologiniame tirpale arba L-PRF eksudate (4.1.6.1 B pav.). Adaptuoti kaulo defekte L-PRF eksudatu rehidruoti mėginiai papildomai buvo uždengiami paruoštomis L-PRF membranomis. Fiziologiniame tirpale rehidruotų mėginių uždengimui papildomų membranų nenaudota (4.1.6.2 pav). Transplantantų atsitiktinės atrankos randomizacija atlikta tam skirta kompiuterine programa, prieinama internete http://www.randomization.com.

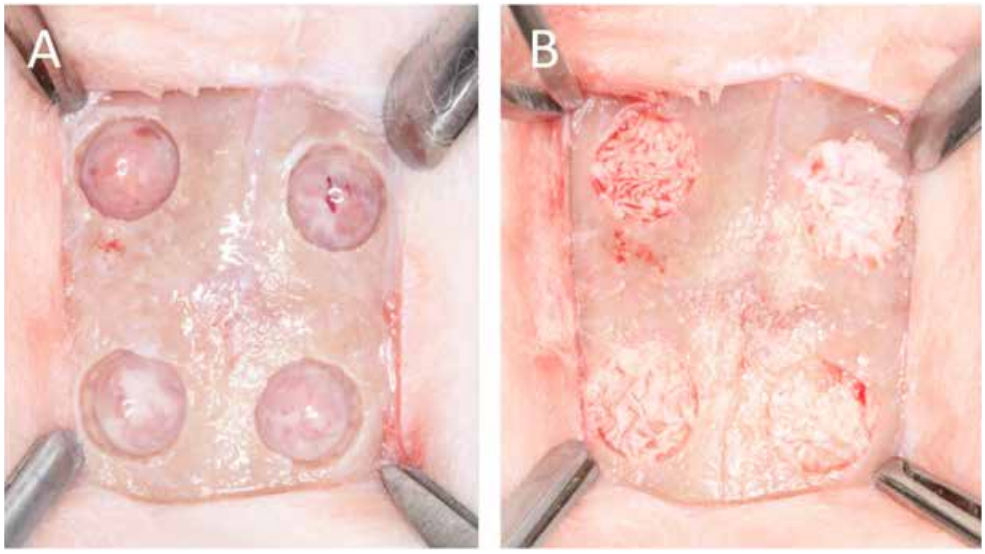

4.1.6.1 pav. *A – Paruošti standartizuoti triušio kaukolės skliauto kauliniai defektai; B – kauliniai defektai užpildyti fiziologiniame tirpale rehidruotais celiuliozės-µHA (kairėje) ir celiuliozės-nHA (dešinėje) kompozitiniais transplantantais.*

Transplantantų pozicionavimo kontrolei po operacijos atliktos kontrolinės gyvūnų kaukolės skliautų rentgenogramos. Pooperaciniu periodu gyvūnai laikyti laboratoriniuose narveliuose, kontroliuojant aplinkos temperatūrą bei dienos šviesos ir nakties ciklus. Gyvūnams maistas ir vanduo užtikrinti *ad libitum*. Skausmo kontrolei pirmąją savaitę kasdien tęstos buprenorfino injekcijos. Gyvūnams antibiotikų neskirta.

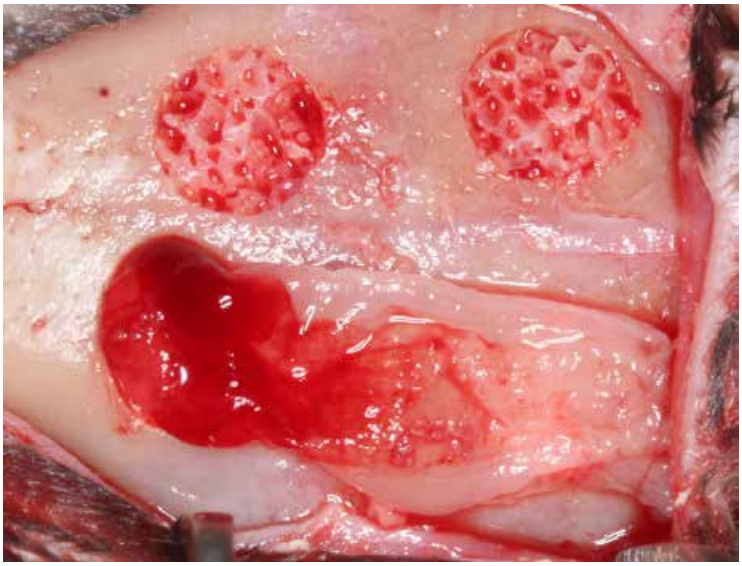

4.1.6.2 pav. *Viršuje – standartizuoti triušio kaukolės skliauto kauliniai defektai užpildyti fiziologiniu tirpalu rehidruotu kontroliniu alogeniniu transplantantu; apačioje – kauliniai defektai užpildyti L-PRF rehidruotais celiuliozės-nHA kompozitiniais transplantantais, uždengtais L-PRF membrana.*

Praėjus 4 ir 12 savaičių nuo transplantantų implantacijos, gyvūnams atlikta eutanazija, pradžioje į raumenis suleidžiant ketamino hidrochlorido (20 mg/kg) su ksilazino hidrochloridu (50 mg/kg) ir po 20 minučių į šoninę ausies veną suleidžiant 25 mg/kg natrio tiopentalio. Sisteminių toksinių efektų vertinimui atlikta kepenų ir inkstų histopatologinė analizė. Gausiai aušinant fiziologiniu tirpalu, kaulo pjūklu ekscizuoti kaukolės skliauto transplantantų ir aplinkinio kaulo bioptatai. Kaulo biopsijos analizuotos histologiškai ir µKT, vertinant transplantantų bioskaidumą ir naujo kaulo formavimąsi.

4.1.7. *In vivo* biopsijų µKT analizė

Kaulo bioptatų µKT analizė atlikta mikrokompiuteriniu analizatoriumi µCT 35 (Scanco Medical AG, Bruttisellen, Šveicarija). Naudoti šie skenavimo parametrai: tūrinis vaizdo elemento dydis 15 µm, apžvalgos laukas 30,72 mm, rentgeno įtampa 70 kVp, intensyvumas 114 µA, integracijos laikas 800 ms. Struktūrinė naujai susiformavusių audinių analizė atlikta Scanco 6.0 programine įranga (Scanco Medical AG, Bruttisellen, Šveicarija).

Naujai susiformavusio kaulo ir likutinio transplantanto vertinimui nustatytas tiriamasis tūris (VOI), atsižvelgiant į cilindro defektų formą ir skersmenį (8,0 mm) bei per transplantanto storį išplečiant vertikalioje plokštumoje. Visų mėginių analizei naudotas vienodas standartizuotas VOI. µKT vertinti šie mikrostruktūriniai bioptatų parametrai: kaulo tūris (BV), bendrasis tūris (TV), kaulo tūrinė frakcija (BV/TV). Šių parametrų skaičiavimai atlikti pagal metodiką, aprašytą Silva ir kt. 2015 m. [195]. Mineralizuotų struktūrų (kaulo ir transplantanto) išskyrimui naudotas automatinės multislenkstinės segmentacijos metodas. Slenkstis susiformavusiam naujam kaului nustatytas prie 3044 Hounsfieldo vienetų (HU), slenkstis naujai susiformavusiam kauliui kartu su transplantantu – 2033 HU, taip segmentuojant ir išskiriant bioptato mineralizuotas struktūras, kaip aprašyta Calvo-Guirado ir kt. 2015 m. [196].

4.1.8. *In vivo* biopsijų histologinė analizė

Kaulo bioptatai fiksuoti 10 proc. formaldehido tirpale, laipsniškai dehidruoti alkoholiuose ir įlieti į metilmetakrilato dervas. Mėginiai supjauti iki 50–60 µm storio preparatų ir nudažyti solochromo cianino R dažais. Histologinė analizė atlikta šviesiniu Eclipse E600 mikroskopu (Nikon, Tokijas, Japonija) su skaitmeniniu kalibruotu foto moduliu Nikon DS-5 M-L1 Digital Sight Camera System (Nikon, Tokijas, Japonija).

4.1.9. Eksperimentinių *in vitro* ir *in vivo* tyrimų statistinė analizė

In vitro tyrimuose atlikti 3 nepriklausomi eksperimentai, *in vivo* tyrimų µKT analizėje kiekvienoje grupėje vertinti 8 bandiniai. Rezultatai pateikti kaip vidurkis ± SN. Imties dydis nustatytas galios analizės metodu G*Power 3 (Heinrich-Heine universitetas, Diuseldorfas, Vokietija) programiniu paketu, pasirinkus 90 proc. galią ir $\alpha = 0,05$. *In vitro* tyrimų imties dydžio nustatymui naudoti pilotinių tyrimų, vertinančių 3 dienų ląstelių kultūrų metabolinį aktyvumą, rezultatai, *in vivo* tyrimams imtis nustatyta vertinant pilotinių tyrimų 12 savaičių biopsijų kaulo tūrinės frakcijos (BV/TV) rezultatus.

Vienos krypties dispersine analize *in vitro* grupių viduje statistiškai reikšmingų skirtumų nenustatyta. Statistinė eksperimentinių *in vitro* tyrimų grupių analizė atlikta Bonferonio metodu.

Statistinė *in vivo* tyrimų analizė atlikta, remiantis Stjudento t-testu ir vienfaktorine dispersine Student–Newman–Keuls analize.

Tiek *in vitro,* tiek *in vivo* studijoms taikytas $p \leq 0,05$ reikšmingumo lygmuo.

4.2. Klinikiniai tyrimai

4.2.1. Retinuotų apatinio žandikaulio trečiųjų krūminių dantų šalinimo sudėtingumo klasifikacija

RAŽTKD šalinimo sudėtingumo klasifikacija pasiūlyta pagal literatūroje aprašomus svarbiausius RAŽTKD chirurginės operacijos eigą ir pooperacines išeitis įtakojančius faktorius, apimančius RAŽTKD etiologiją, klinikinę anatomiją, diagnostinius metodus, RAŽTKD šalinimo indikacijas, chirurgines technikas, komplikacijas ir jų rizikos faktorius. Literatūros apžvalga ir autorių pasiūlyta RAŽTKD šalinimo sudėtingumo klasifikacija aprašyta Juodžbalio ir Daugėlos 2013 m. publikuotame straipsnyje [199].

4.2.2. Retinuotų apatinio žandikaulio trečiųjų krūminių dantų šalinimo sudėtingumo klasifikacijos validacija

Tyrimas atliktas siekiant validuoti pasiūlytą Juodžbalio ir Daugėlos RAŽTKD šalinimo sudėtingumo klasifikaciją [199]. RAŽTKD šalinimo sudėtingumo klasifikacijos validacijos tyrimas atliktas trijuose tyrimo centruose:

1. Triesto universiteto (angl. *University of Trieste*, Triestas, Italija) Medicinos, chirurgijos ir sveikatos mokslų klinikoje (1 centras).
2. Lietuvos sveikatos mokslų universiteto (LSMU) Medicinos akademijos Odontologijos fakulteto Veido ir žandikaulių chirurgijos klinikoje (2 centras).
3. Hesire klinikoje (Cassano allo Ionio, Italija) (3 centras).

Šio darbo autorius dalyvavo ruošiant tyrimo protokolą ir koordinavo tyrimo vykdymą tyrimo centruose.

Tyrimas registruotas ClinicalTrials.gov klinikinių tyrimų duomenų bazėje (identifikacinis nr. NCT02519426). Visi tyrime dalyvaujantys pacientai pasirašė asmens informuoto susitikimo formą.

Pacientai atrinkti, taikant šiuos įtraukimo į tyrimą kriterijus:

1. Pacientų amžius ≥ 18 metų.
2. Sveiki pacientai, kurių sveikatos indeksas pagal Amerikos anesteziologų draugijos (angl. *American Society of Anesthesiologists*) priešoperacinės fizinės būklės klasifikaciją (ASA) ≤ 2.

3. Pacientų KPKT ir (arba) OPG atlikta ne anksčiau nei 12 mėnesių iki operacijos.

4. KPKT ir (arba) OPG stebimas visiškas 38 arba 48 danties šaknų susiformavimas.

5. Paciento sutikimas dalyvauti tyrime ir pasirašyta asmens informuoto sutikimo forma.

Taikyti šie atrankos atmetimo kriterijai:

1. Daugiau nei 10 cigarečių per dieną surūkantys pacientai.

2. Rentgenologiškai stebimas didesnis nei 1 cm skersmens lėtinio uždegimo židinys RAŽTKD ar gretimų dantų srityje.

3. Ūmus uždegimas ir (ar) infekcija RAŽTKD ar gretimų dantų srityje.

4. Kliniškai ar (ir) rentgenologiškai stebimi gerybiniai, piktybiniai ir nepatikslintos kilmės navikiniai dariniai RAŽTKD ar gretimų dantų srityje.

5. Antrųjų apatinio žandikaulio krūminių dantų adentija.

6. Pacientai, turintys sklaidos anomalijų, paveldimų ar sisteminių ligų.

7. Pacientai, vartojantys vaistus, turinčius įtakos burnos mikrobiologinei pusiausvyrai, imuninei sistemai arba uždegiminiam atsakui (pvz., kortikosteroidus).

8. Pacientai, kuriems, 24 mėnesių laikotarpiu iki operacijos taikytas chemoterapinis arba spindulinis gydymas.

9. Pacientai, kuriems tyrime jau yra pašalintas priešingos pusės RAŽTKD.

Vienas kalibruotas tyrėjas aklai vertino visų tirtųjų pacientų OPG ir / ar KPKT bei priskyrė kiekvieną planuojamą šalinti RAŽTKD tam tikrai grupei pagal Winter [197], Pell ir Gregory [198] klasifikacijas bei Juodžbalio ir Daugėlos RAŽTKD šalinimo sudėtingumo klasifikaciją [199].

Atrinktiems pacientams pagal standartizuotą chirurginį protokolą, aprašytą Farish ir Bouloux 2007 m. [200], atliktos vienpusės RAŽTKD šalinimo operacijos. Kiekviename tyrimo centre operacijas atliko po vieną patyrusį burnos chirurgą, turintį ne mažiau nei 5 metų klinikinę patirtį. 1 val. prieš operaciją pacientams buvo skirta antibiotikų (2000 mg amoksicilino arba 500 mg klaritromicino, pacientams alergiškiems amoksicilinui) *per os*. Prieš pradedant chirurginę procedūrą, pacientai 1 minutę skalavo burną 0,2 proc. chlorheksidino digliukonato tirpalu.

Operacijos trukmė skaičiuota nuo minkštųjų audinių incizijos momento iki visiško RAŽTKD pašalinimo ir operacinės žaizdos susiuvimo. Taip pat vertintos atliktos chirurginės manipuliacijos (lopo dizainas, osteotomija, koronektomija, šaknų sekcionavimas) ir galimos intraoperacinės komplikacijos (šaknies viršūnės lūžis, kraujavimas, *c. mandibularis* vientisumo pažeidi-

mas, gretimų dantų pažeidimas, danties ar jo fragmentų migracija į minkštuosius audinius, apatinio žandikaulio ar jo fragmentų lūžiai).

Pooperaciniu laikotarpiu skausmo kontrolei pagal poreikį skirta 600 mg ibuprofeno, taip pat 2 savaitėms 2 kartus per dieną skirti antiseptiniai burnos skalavimai 0,2 proc. chlorheksidino digliukonato tirpalu, skalaujant po 1 minutę. Siūlai pašalinti po 7 dienų, kartu įvertinant gijimą ir per pirmąją savaitę pasireiškusias pooperacines komplikacijas (alveolitą, operacinės srities infekcijas, hematomas, parestezijas).

4.2.2.1. Statistinė analizė

Statistinė analizė atlikta SPSS 22.0 programiniu paketu (International Business Machines Corp., Armonk, North Castle, Niujorko valstija, JAV). RAŽTKD šalinimo procedūros trukmė pasirinkta pagrindiniu parametru vertinant RAŽTKD šalinimo sudėtingumą ir nustatant tyrimo imties dydį. Atlikus pilotinį tyrimą su 25 pacientais, išskirtos 2 grupės:

- I grupė – Juodžbalio ir Daugėlos RAŽTKD šalinimo sudėtingumo klasifikacijos suminis balas ≤ 9;
- II grupė – Juodžbalio ir Daugėlos RAŽTKD šalinimo sudėtingumo klasifikacijos suminis balas > 9.

Pasirinkus 80 proc. galią ir $\alpha = 0,05$, kiekvienai grupei apskaičiuotas 52 pacientų imties dydis, tarp grupių esant 10 minučių su 18 minučių SN chirurginės procedūros trukmės skirtumui.

Demografiniai ir klinikiniai duomenys aprašyti vidurkiu arba mediana ± SN. Kategoriniai duomenys pateikti dažnio lentelėse ir procentine išraiška. Statistinė tyrimo grupių analizė atlikta Kruskal-Wallis metodu, esant reikšmingumo lygmeniui $p \leq 0,05$.

4.2.3. L-PRF įtakos gijimui vertinimas retinuotų apatinio žandikaulio trečiųjų krūminių dantų šalinimo operacijose

Šis tyrimas atliktas siekiant įvertinti L-PRF poveikį RAŽTKD alveolių gijimui, pooperaciniam paciento diskomfortui ir alveolito pasireiškimui po RAŽTKD šalinimo operacijų. Tyrimas suplanuotas kaip prospektyvinis burnos padalijimo (angl. *split-mouth*) metodu atliktas atsitiktinės imties klinikinis tyrimas su pacientais, kuriems reikalingas abipusis RAŽTKD šalinimas. Tyrimas buvo atliktas Lietuvos sveikatos mokslų universiteto (LSMU) Medicinos akademijos Odontologijos fakulteto Veido ir žandikaulių chirurgijos klinikoje. Tyrimas registruotas ClinicalTrials.gov klinikinių tyrimų duomenų bazėje (identifikacinis nr. NCT03357484). Visi tyrime dalyvaujantys pacientai pasirašė asmens informuoto susitikimo formą.

4.2.3.1. Pacientų atranka

Atlikus pilotinius tyrimus, Statistica 6.0 (Dell Software, Round Rock, Teksasas, JAV) programiniu paketu buvo atlikta imties dydžio nustatymo analizė. Skaičiavimai parodė, kad minimalus imties dydis yra n = 30, esant 90 proc. galiai ir $\alpha = 5$ proc.

Pacientai atrinkti, taikant šiuos įtraukimo į tyrimą kriterijus:

1. Nuo 18 iki 60 metų amžiaus, vyriškos ir moteriškos lyties pacientai.
2. Sveiki pacientai, kurių sveikatos indeksas pagal Amerikos anesteziologų draugijos (angl. *American Society of Anesthesiologists*) priešoperacinės fizinės būklės klasifikaciją (ASA) ≤ 2.
3. Vienos operacijos metu abiejose pusėse šalinami tik 38, 48 dantys.
4. Rengenologiškai stebimas visiškas 38 ir 48 dantų šaknų susiformavimas.
5. Ūmaus uždegimo ir (arba) infekcijos nebuvimas RAŽTKD srityje.
6. Pacientai, 4 savaičių laikotarpiu iki operacijos nenaudoję nesteroidinių vaistų nuo uždegimo ar kitų vaistų, galinčių turėti įtakos skausmo jutimui.
7. Tokio pat sudėtingumo dvipusis RAŽTKD šalinimas pagal Pedersono klasifikaciją [201] bei Juodžbalio ir Daugėlos RAŽTKD šalinimo sudėtingumo klasifikaciją [199].
8. Paciento sutikimas dalyvauti tyrime ir pasirašyta asmens informuoto sutikimo forma.

Taikyti šie atrankos atmetimo kriterijai:

1. Rūkantys pacientai.
2. Didesnis nei 10 minučių RAŽTKD operacijos trukmės skirtumas to paties paciento skirtingose apatinio žandikaulio pusėse.
3. To paties paciento skirtingų pusių RAŽTKD šalinimui naudotos skirtingos chirurginės manipuliacijos.
4. Kliniškai ar (ir) rentgenologiškai stebimi gerybiniai, piktybiniai ir nepatikslintos kilmės navikiniai dariniai RAŽTKD ar gretimų dantų srityje.
5. Rentgenologiškai stebimas didesnis nei 1 cm skersmens lėtinio uždegimo židinys RAŽTKD ar gretimų dantų srityje.
6. Antrųjų apatinio žandikaulio krūminių dantų adentija.
7. Pacientai, turintys sklaidos anomalijų, paveldimų ar sisteminių ligų.
8. Pacientai, vartojantys vaistus, turinčius įtakos burnos mikrobiologinei pusiausvyrai, imuninei sistemai arba uždegiminiam atsakui (pvz., kortikosteroidus).
9. Piktnaudžiavimas alkoholiu arba narkotikais.
10. Nėščios arba krūtimi maitinančios moterys.

11. Nepakankamai bendradarbiaujantys arba tyrimo protokolo nesilaikantys pacientai.

Prieš operaciją du kalibruoti tyrėjai aklai vertino visų tirtųjų pacientų OPG ir / ar KPKT bei priskyrė kiekvieną planuojamą šalinti RAŽTKD tam tikrai grupei pagal Pedersono [201] klasifikaciją bei Juodžbalio ir Daugėlos RAŽTKD šalinimo sudėtingumo klasifikaciją [199]. Į tyrimą įtraukti tik vienodo sudėtingumo šalinamus 38, 48 dantis, vertinant pagal abi klasifikacijas, turintys pacientai. Diagnostinis atitikimas tarp tyrėjų ir tyrėjų viduje vertintas taikant svertinį Kappa indeksą. Nustatytas bendras svertinis Kappa indeksas tarp tyrėjų buvo 0,93, tyrėjų viduje – 0,95 (pirmam tyrėjui) ir 0,97 (antram tyrėjui).

Tyrimui atrinkti 34 pacientai, kuriems vienos procedūros metu atliktos abipusės RAŽTKD šalinimo operacijos. Pooperaciniu periodu 4 pacientai neatvyko į numatytas apžiūras. Galutiniam vertinimui analizuoti 30 pacientų duomenys (4.2.3.1.1 pav.).

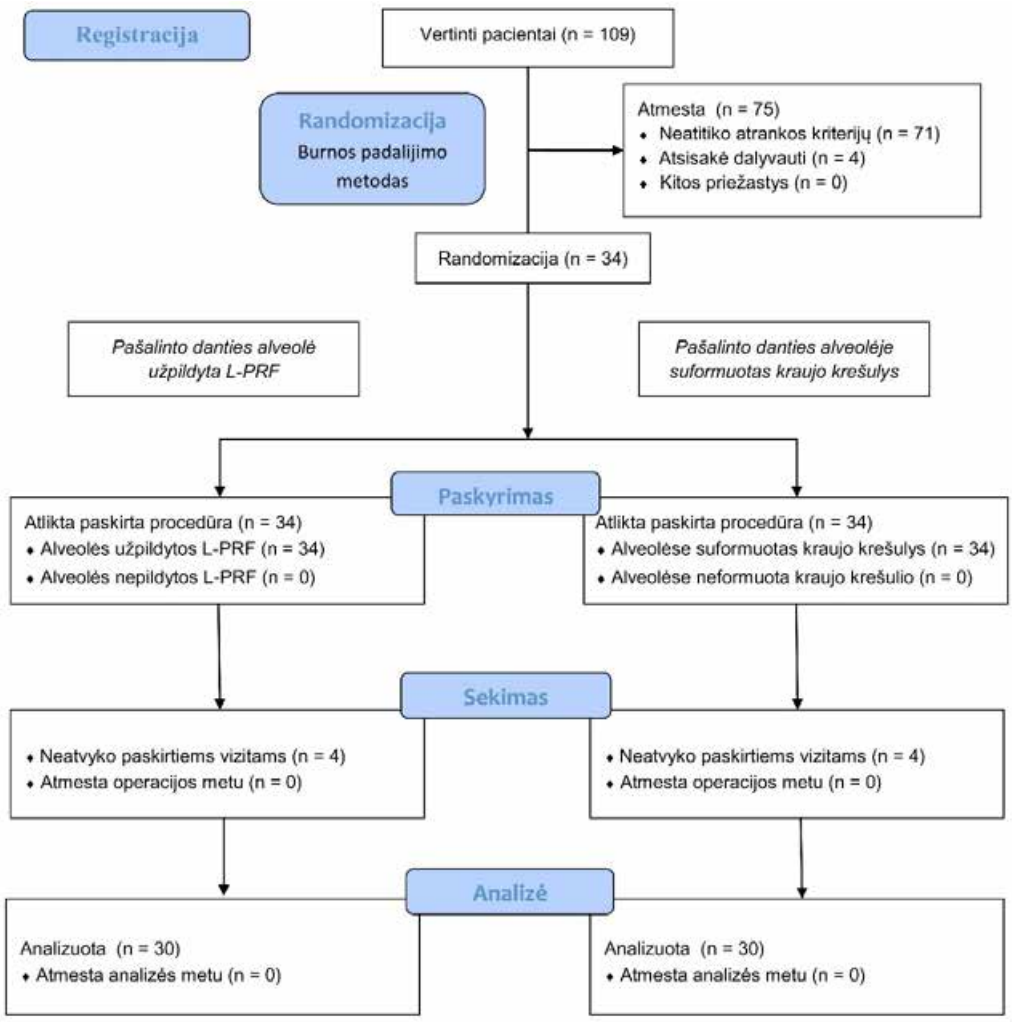

4.2.3.1.1 pav. *Tyrimo pacientų atrankos schema.*

4.2.3.2. L-PRF paruošimas

L-PRF buvo paruoštas pagal Choukroun ir kt. 2001 m. aprašytą protokolą [185]. Prieš chirurginę procedūrą, laikantis aseptikos ir antiseptikos reikalavimų, pacientams iš vidurinės alkūnės venos į du 9 ml talpos silicio dioksidu dengtus mėgintuvėlius (Intra-Lock International, Boca Raton, Florida, JAV) paimta veninio kraujo. Mėgintuvėliai centrifuguoti EBA 20 centrifugoje (Andreas Hettich GmbH & Co.KG, Tuttlingen, Vokietija) 12 min. 2800 apsukų per minutę režimu. Po centrifugavimo L-PRF buvo atskirtas nuo raudonųjų kraujo kūnelių bazės (4.2.3.2.1 pav.) ir perkeltas saugoti į paruošimo dėžutę PRF & growth factor-rich fibrin (GRF) box (Osung Mnd Company, Gimpo, Pietų Korėja), nespaudžiant į membranas ar cilindrus [194].

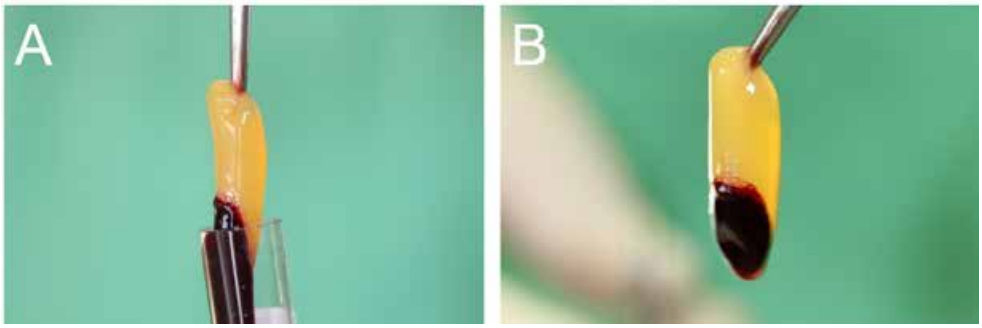

4.2.3.2.1 pav. *A – žmogaus L-PRF, po centrifugavimo sukibęs su raudonaisiais kraujo kūneliais; B – nuo raudonųjų kraujo kūnelių bazės atskirtas žmogaus L-PRF.*

4.2.3.3. Chirurginės procedūros

Abipusės RAŽTKD šalinimo operacijos (4.2.3.3.1 pav.) atliktos vieno patyrusio burnos chirurgo, turinčio daugiau nei 5 metų klinikinę patirtį, pagal standartizuotą chirurginį protokolą, aprašytą Farish ir Bouloux 2007 m. [200]. 1 val. prieš operaciją ir 6 val. po jos pacientams buvo skirta antibiotikų (600 mg klindamicino) *per os*. Prieš pradedant chirurginę procedūrą, pacientai 1 minutę skalavo burną 0,2 proc. chlorheksidino digliukonato tirpalu.

Dantų šalinimui naudotos šios chirurginės manipuliacijos: paprasta danties mobilizacija elevatoriais ir (arba) replėmis, koronektomija, šaknų sekcionavimas, incizija ir gleivinės – antkaulio lopo atkėlimas, osteotomija. Pašalinus RAŽTKD ir revizavus alveolę (4.2.3.3.1 B pav.), vienos pusės

alveolė užpildyta dviem L-PRF krešuliais (L-PRF grupė; 4.2.3.3.1 C pav.), tam pačiam pacientui atlikus priešingos pusės RAŽTKD šalinimą, alveolėje leista susiformuoti natūraliam kraujo krešuliui (kontrolinė grupė). L-PRF priskyrimas tam tikrai alveolei pasirinktas atsitiktinės atrankos užklijuotų nepermatomų vokų metodu. Operacinės žaizdos susiūtos Atramat 5–0 poliglaktino (Internacional Farmacéutica, Meksikas, Meksika) siūlais (4.2.3.3.1 D pav.). Pacientai nežinojo, kuri pusė buvo priskirta L-PRF, o kuri – kontrolinei grupei.

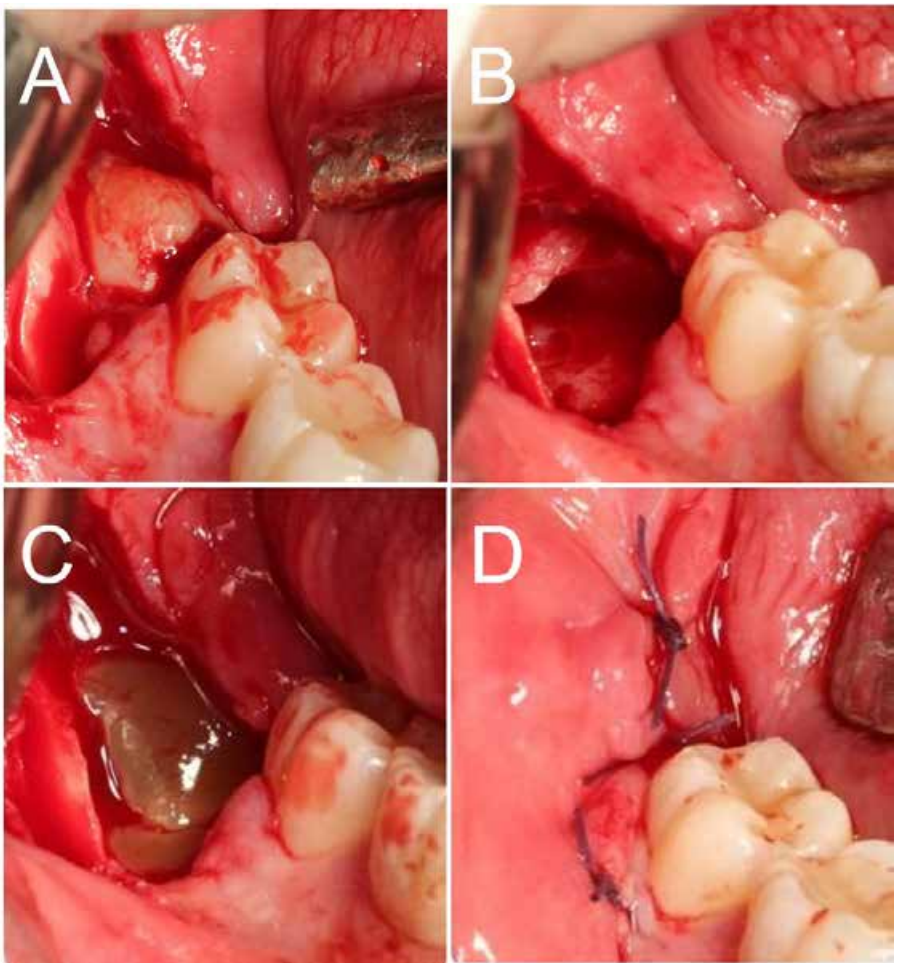

4.2.3.3.1 pav. *A – atkeltas gleivinės ir antkaulio lopas retinuoto 48 danties srityje; B – po danties pašalinimo atlikta alveolės revizija; C – alveolė užpildyta dviem L-PRF krešuliais; D – operacinės žaizdos susiuvimas 5–0 poliglaktino siūlais.*

38 ir 48 dantų šalinimo operacijos trukmė skaičiuota kiekvienam dančiui atskirai nuo minkštųjų audinių incizijos momento iki visiško RAŽTKD pašalinimo ir operacinės žaizdos susiuvimo. Tyrime dalyvavo tik tie pacientai, kurių RAŽTKD operacijos trukmė, šalinant to paties paciento skirtingų pusių RAŽTKD, skyrėsi mažiau nei 10 minučių. To paties paciento skirtingų pusių RAŽTKD šalinimui taip pat turėjo būti naudojamos vienodos chirurginės manipuliacijos.

Pooperaciniu laikotarpiu skausmo kontrolei pagal poreikį skirta 8 mg lornoksikamo, taip pat 3 kartus per dieną skirti antiseptiniai burnos skalavimai 0,2 proc. chlorheksidino digliukonato tirpalu, skalaujant po 1 minutę ir skalavimus tęsiant 2 savaites. Pacientams žodžiu ir raštu paruoštose specialiose atmintinėse buvo paaiškintas pooperacinis režimas. Siūlai pašalinti praėjus 7 dienoms po operacijos.

Pooperaciniu laikotarpiu vertintas minkštųjų audinių gijimas, alveolito pasireiškimas, skausmas ir veido tinimas.

4.2.3.4. Minkštųjų audinių gijimo vertinimas

Operacinės žaizdos minkštųjų audinių gijimas vertintas modifikuotu minkštųjų audinių gijimo indeksu (HI) [202]. HI susideda iš 4 vertinamų parametrų: kraujavimo, pūliavimo, gyjančių audinių spalvos ir konsistencijos. Kiekvienas parametras vertintas balais nuo 1 iki 3, taip HI bendroms vertėms varijuojant nuo 4 balų, rodančių puikų gijimą, iki 12 balų, rodančių labai blogą gijimą. HI vertintas aklai vieno operacijoje nedalyvavusio tyrėjo 1-ą, 3-ą, 7-ą ir 14-ą dienomis po operacijos.

Likus vienai savaitei iki tyrimo pradžios, HI vertinęs tyrėjas atliko kalibraciją penkiems pilotiniams pacientams, neįtrauktiems į tiriamųjų grupę, du kartus atlikdamas HI vertinimą. Diagnostinis atitikimas tyrėjo viduje vertintas taikant svertinį Kappa indeksą ir sudarė 0,87.

4.2.3.5. Alveolitas

Alveolitas nustatytas, ankstyvuoju pooperaciniu laikotarpiu pasireiškiant alveolės kraštų paraudimui ir pasikartojančiam, didėjančio intensyvumo tvinksinčiam skausmui pašalinto danties srityje, kurio nepalengvina vartojami analgetikai. Skausmas pasireiškia su arba be halitozės, pašalinto danties alveolėje iš dalies arba visiškai netekus kraujo krešulio [203, 204].

4.2.3.6. Skausmo vertinimas

Skausmas vertintas vizualinėje analoginėje skausmo skalėje (VAS) [205] pacientams išdalytose anketose. Kiekvieną pirmos pooperacinės savaitės dieną pacientai grafinėje VAS skalėje žymėjo tos dienos skausmo intensyvumą balais nuo 0 iki 10. Kairėje grafinės skalės pusėje esantis 0 žymėjo visišką skausmo nebuvimą, o dešinėje pusėje esantis balas 10 – didžiausią, nepakeliamą, kankinantį skausmą. Pacientai kiekvienos apatinio žandikaulio pusės skausmo intensyvumą vertino atskirai, nežinodami, kurios pusės RAŽTKD šalintas L-PRF, o kurios – kontrolinėje grupėje.

4.2.3.7. Veido tinimo vertinimas

Veido tinimas vertintas aklai vieno operacijoje nedalyvavusio tyrėjo 1-ą, 3-ą ir 7-ą dienomis po operacijos, apytiksliai tuo pačiu dienos metu. Pacientai buvo sodinami atpalaiduotoje padėtyje, apatinio žandikaulio kūną pozicionuojant lygiagrečiai grindims. Veido tinimas vertintas atliekant dviejų krypčių veido matavimus netampria, kas 0,5 mm graduota matavimo juosta, kaip aprašyta Rakprasitkul ir Pairuchvej 1997 m. [206]:

- Vertikalioje plokštumoje matuotas atstumas nuo akies vokų šoninės komisūros iki labiausiai atsikišusio apatinio žandikaulio kampo taško (lot. *gonion*);
- Horizontalioje plokštumoje matuotas atstumas nuo distaliausio ausies kramslio taško iki tos pačios veido pusės lūpų komisūros.

Veido tinimo skaitinė reikšmė apskaičiuota kaip šių dviejų matavimų vidurkis milimetrais (4.2.3.7.1 pav.). Kiekvienos pusės priešoperacinių matmenų vidurkiai laikyti pradinėmis tinimo skaitinėmis reikšmėmis.

Likus vienai savaitei iki tyrimo pradžios, veido tinimą vertinęs tyrėjas atliko kalibraciją penkiems pilotiniams pacientams, neįtrauktiems į tiriamųjų grupę, du kartus atlikdamas veido tinimo vertinimą. Diagnostinis atitikimas tyrėjo viduje vertintas taikant svertinį Kappa indeksą ir sudarė 0,82.

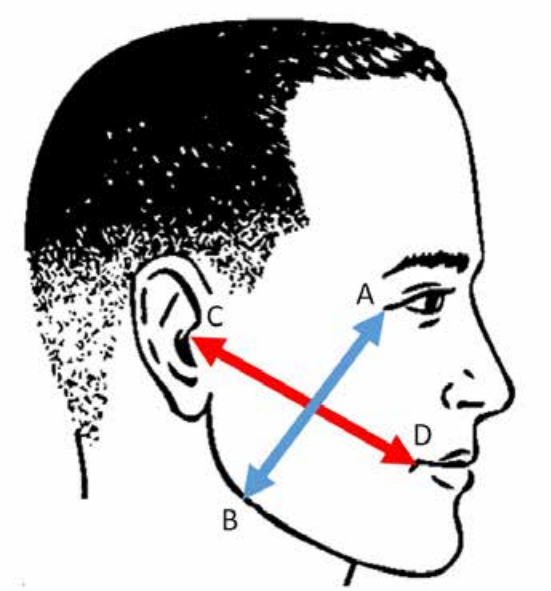

4.2.3.7.1 pav. *Veido tinimas apskaičiuotas, išmatavus atstumus A–B ir C–D milimetrais, pagal formulę (AB+CD)/2.*

4.2.3.8. Statistinė analizė

Statistinė analizė atlikta SPSS 22.0 programiniu paketu (International Business Machines Corp., Armonk, North Castle, Niujorko valstija, JAV). Demografiniai ir klinikiniai duomenys aprašyti vidurkiu arba mediana ± SN. Duomenų pasiskirstymas vertintas Kolmogorovo ir Smirnovo testu. Kiekybinių dydžių pasiskirstymas neatitiko normaliojo skirstinio, todėl p reikšmės apskaičiuotos neparametriniais testais. Skirtumai tarp dviejų nepriklausomų grupių vidurkių vertinti Mann-Whitney U testu. Priklausomi kintamieji vertinti Wicoxon testu. Skirtumai laikyti statistiškai reikšmingais, esant reikšmingumo lygmeniui $p \leq 0,05$.

5. REZULTATAI

5.1. *In vitro* ir *in vivo* tyrimų rezultatai

5.1.1. Kompozitinių celiuliozės karkasų su nHA ir µHA užpildais struktūrinė analizė

Celiuliozės-HA kompozitiniai karkasai paruošti regeneruojant acetil-celiuliozę (Sigma-Aldrich, Sent Luisas, Misūris, JAV) acetono tirpale ir paruošimo metu į celiuliozės gelį mechaniškai įterpiant nHA arba µHA užpildų daleles. Didelio porėtumo celiuliozės-nHA ir celiuliozės-µHA karkasų paruošimui naudota liofilizacijos metodika, aprašyta Petrauskaitės ir kt. 2008 m. [68].

Celiuliozės, nHA, µHA bei celiuliozės-nHA ir celiuliozės-µHA kompozitų infraraudonųjų spindulių (IR) sugerties analizės duomenys pateikiami 5.1.1.1 pav. IR spektruose aptikta plati absorbcijos juosta 3500–3200 cm^{-1} srityje leidžia identifikuoti hidroksilo (OH) grupes grynoje celiuliozėje (5.1.1.1 A-e pav.) ir celiuliozės-HA kompozitiniuose karkasuose (5.1.1.1 A-e ir 5.1.1.1 A-d pav.). Stebima absorbcijos smailė ties 2893 cm^{-1}, kuri priskiriama CH_2 grupėms, o asimetrinė virpesių smailė ties 1159 cm^{-1} – C-O-C grupėms. 1024 cm^{-1} ir 1069 cm^{-1} virpesių smailės priskiriamos C-O grupėms. Vertinti nHA ir µHA spektrai atitiko hidroksiapatitui būdingas absorbcijos smailes. Absorbcijos smailės ties 3571 cm^{-1} ir 633 cm^{-1} nustatytos dėl OH grupės virpesių. 1092 cm^{-1}, 1044 cm^{-1} ir 962 cm^{-1} smailės priskiriamos P-O virpesiams, o 603 cm^{-1}, 568 cm^{-1} ir 474 cm^{-1} smailės – O-P-O virpesiams. Nustatyti panašūs tiek µHA (5.1.1.1 A-a pav.), tiek nHA (5.1.1.1 A-b pav.) IR sugerties spektrai. HA dalelėms būdingos absorbcijos smailės stebimos ir tirtuose celiuliozės-µHA (5.1.1.1 A-c pav.) bei celiuliozės-nHA (5.1.1.1 A-d pav.) kompozitiniuose karkasuose.

Skenuojančiu elektroniniu dispersiniu spektroskopu (SEM-EDS) atlikta karkasų paviršiaus elementinė analizė parodė pagrindinių HA elementų (kalcio (Ca) ir fosforo (P)) bei pagrindinio celiuliozės elemento (anglies (C)) pasiskirstymą karkasų paviršiuje (5.1.1.1 B, C pav.). Abiejų tipų kompozitiniuose karkasuose nustatytas tolygus HA dalelių pasiskirstymas celiuliozės matricoje bei skirtingo laipsnio HA dalelių aglomeracija. HA dalelės buvo linkusios labiau aglomeruoti celiuliozės-µHA nei celiuliozės-nHA karkasuose.

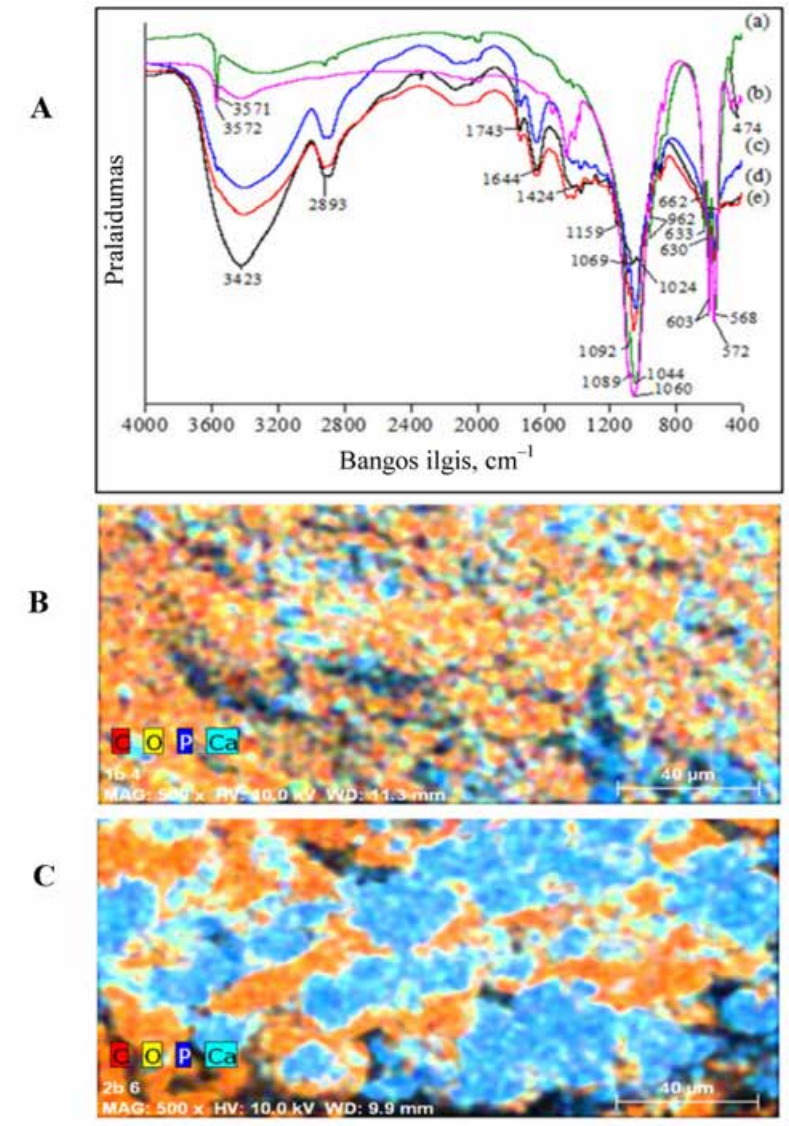

5.1.1.1 pav. *Infraraudonosios sugerties spektrometrinė analizė. A – IR sugerties spektrai: (a) µHA, (b) nHA, (c) celiuliozė-µHA, (d) celiuliozė-nHA, (e) celiuliozė. Apačioje pateikiami SEM-EDS elementinės analizės vaizdai: B – celiuliozė-nHA, C – celiuliozė-µHA.*

IR – infraraudonieji spinduliai; SEM-EDS – skenuojamoji elektroninė dispersinė spektroskopija; celiuliozė-nHA – celiuliozės ir nanohidroksiapatito kompozitinis karkasas; celiuliozė-µHA – celiuliozės ir mikrohidroksiapatito kompozitinis karkasas; celiuliozė – celiuliozės karkasas.

Rentgeno difrakcinė analizė tirtiesiems kompozitiniams karkasams parodė amorfinei celiuliozei būdingus difrakcinius maksimumus prie 12,4°, 20,7°, 21,1° ir 34,9° (5.1.1.2 a pav.), ir hidroksiapatitui būdingus difrakcinius maksimumus prie 25,9°, 31,8°, 32,2°, 34,1°, 46,7° ir 49,6°, esant 2 Θ laipsnių difrakcijos kampui (5.1.1.2 b, c pav.).

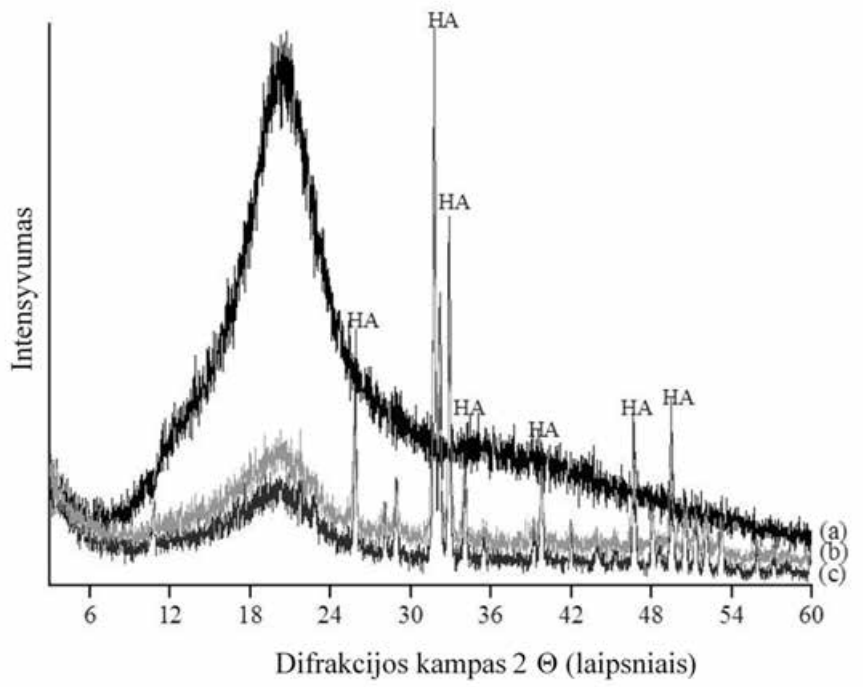

5.1.1.2 pav. *Rentgeno difrakcinės analizės kreivės: (a) celiuliozė, (b) celiuliozė-nHA; (c) celiuliozė-µHA.*

Celiuliozė – celiuliozės karkasas; celiuliozė-nHA – celiuliozės ir nanohidroksiapatito kompozitinis karkasas; celiuliozė-µHA – celiuliozės ir mikrohidroksiapatito kompozitinis karkasas.

Kompozitinių celiuliozės-nHA ir celiuliozės-µHA karkasų µKT analizės dvimatės ir trimatės mikrotomogramos bei trimatės analizės struktūriniai parametrai pateikiami (5.1.1.3 pav.). µKT analizėje nustatyta struktūrinių skirtumų tarp celiuliozės-nHA ir celiuliozės-µHA karkasų. Celiuliozės-nHA karkasuose rastas mažesnis karkasų medžiagos tūris, didesnis porėtumas ir didesnis savitasis paviršiaus plotas, palyginti su celiuliozės-µHA karkasais. Visi šie skirtumai buvo statistiškai reikšmingi. Abiejuose karkasuose nustatyta porėta vidinė struktūra su susisiekiančiomis vidinėmis poromis. Vidutinis porų skersmuo celiuliozės-nHA karkasuose buvo 490 ± 94 µm, o celiuliozės-µHA karkasuose – 540 ± 132 µm.

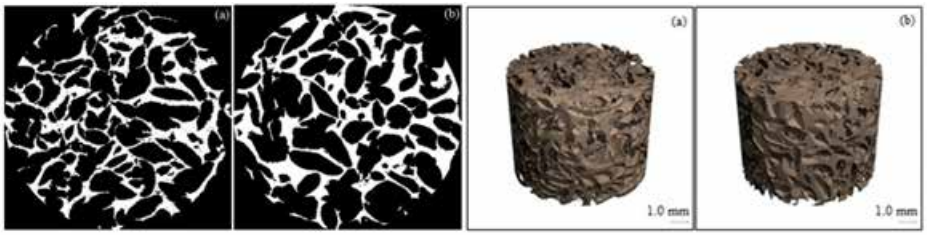

Karkasas	Struktūriniai parametrai			
	$X_{V,\%}$	P, %	SS, mm^{-1}	L, mm
Celiuliozė-nHA	28,09 (0,94)*	72,04 (1,72)*	19,06 (0,25)*	0,12 (0,01)*
Celiuliozė-µHA	34,03 (1,11)	66,12 (2,09)	13,01 (0,50)	0,21 (0,01)

5.1.1.3 pav. *Celiuliozės-nHA (a) ir celiuliozės-µHA (b) kompozitų mikrokompiuterinės tomografijos analizė. Pateikiamas abiejų kompozitų procentinis karkaso medžiagos tūris (X_V), porėtumas (P), savitasis paviršiaus plotas (SS) ir vidutinis karkaso elementų storis (L).*
*Statistiškai reikšmingas skirtumas, palyginti su celiuliozės-µHA kompozitu; skliausteliuose pateikiamas standartinis nuokrypis.

5.1.2. Karkasų *in vitro* citotoksiškumo analizė

Eksperimentinių celiuliozės-µHA ir celiuliozės-nHA kompozitinių karkasų citotoksiškumas vertintas ant karkasų užsėjant žmogaus osteoblastinių ląstelių kultūras (Mg-63, ATCC numeris CRL-1427). 7 dienų laikotarpiu numatytais laiko periodais vertinta ląstelių adhezija, proliferacija ir funkcinis aktyvumas.

Ląstelių adhezija ir pasiskirstymas vertintas SEM, praėjus 24 valandoms po užsėjimo (5.1.2.1 viršutinis pav.). Celiuliozės-µHA karkasuose ląstelių pasiskirstymas daugiausia koncentravosi ties µHA dalelių aglomeratais (5.1.2.1 A, B pav.). Didelio didinimo vaizduose stebėtos µHA dalelių link formuojamos trumpos ląstelių citoplazmos išaugos (5.1.2.1 C pav.). Prikibusių ląstelių forma – apvali ir sferinė, su nedideliu citoplazmos plitimu. Celiuliozės-nHA karkasų paviršiuje stebėtas tolygesnis ląstelių pasiskirstymas (5.1.2.1 D pav.). Taip pat stebėtas aktyvesnis ląstelių plitimas, atitinkamai vyraujant apvalios ir labiau elonguotos formos ląstelėms. Nors, kaip ir celiuliozės-µHA atveju, nustatyta apvalios formos ląstelių, dauguma celiuliozės-nHA karkasuose stebėtų ląstelių buvo plokštesnės ir daugiakampės morfologijos su didesniu citoplazmos plitimu (5.1.2.1 E pav.). Didelio didinimo vaizduose stebėtos gausios, storesnės ir ilgesnės ląstelių filopodijos (5.1.2.1 F pav.).

MTT analizės metodu nuo 1 iki 7 dienos po užsėjimo nustatyta aktyvi ląstelių proliferacija tiek abiejuose eksperimentiniuose, tiek kontroliniame transplantante. Celiuliozės-µHA karkasų MTT redukcija buvo mažesnė nei kontrolinės medžiagos. Tačiau celiuliozės-nHA karkasai pasižymėjo didesniu metaboliniu aktyvumu ir statistiškai reikšmingai didesnėmis MTT reikšmėmis, palyginti su kontroliniais ir celiuliozės-µHA karkasais, 3-ą ir 7-ą dienomis po užsėjimo (5.1.2.1 apatinis pav.).

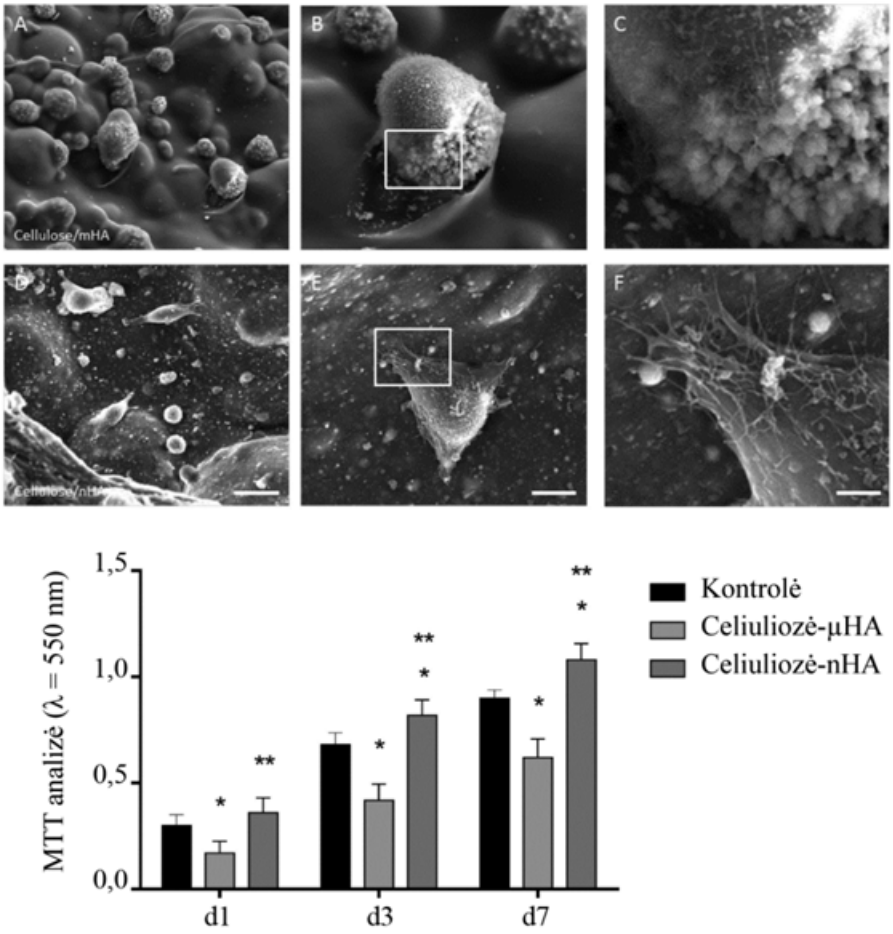

5.1.2.1 pav. *Viršuje – SEM mikrografijos: A–C celiuliozės-µHA, D–F celiuliozės-nHA karkasai, užsėti žmogaus osteoblastinėmis ląstelėmis, 24-ą valandą po kultivavimo. Skalė atitinka: 25 µm (A ir D), 10 µm (B ir E), 4 µm (C ir F). Apačioje – žmogaus osteoblastinių ląstelių gyvybingumo ir proliferacijos vertinimo geltonojo tetrazolio druskų redukcijos (MTT) metodu grafikas 1-ą, 3-ą ir 7-ą kultivavimo dienomis.*

*Statistiškai reikšmingas skirtumas, palyginti su kontrole.

**Statistiškai reikšmingas skirtumas, palyginti su celiuliozės-µHA karkasais.

Ląstelių funkcinis aktyvumas buvo analizuojamas 7-ą dieną po užsėjimo vertinant ALP aktyvumą ir tam tikrų už osteoblastų funkciją atsakingų genų raišką: Runx-2, ALP, BMP-2 ir Col I (5.1.2.2 pav.). Ant celiuliozės-nHA karkasų kultivuotos ląstelės pasižymėjo statistiškai reikšmingai didesne Runx-2, ALP ir BMP-2 genų raiška, palyginti su ant celiuliozės-µHA ir kontrolinių karkasų kultivuotomis ląstelėmis. 7-ą kultivavimo dieną celiuliozės-nHA karkasų ląstelėms taip pat nustatytas statistiškai reikšmingai didesnis ALP aktyvumas. Vertinant celiuliozės-µHA ir kontrolinių karkasų ląstelių genų raišką ir ALP aktyvumą, statistiškai reikšmingų skirtumų negauta.

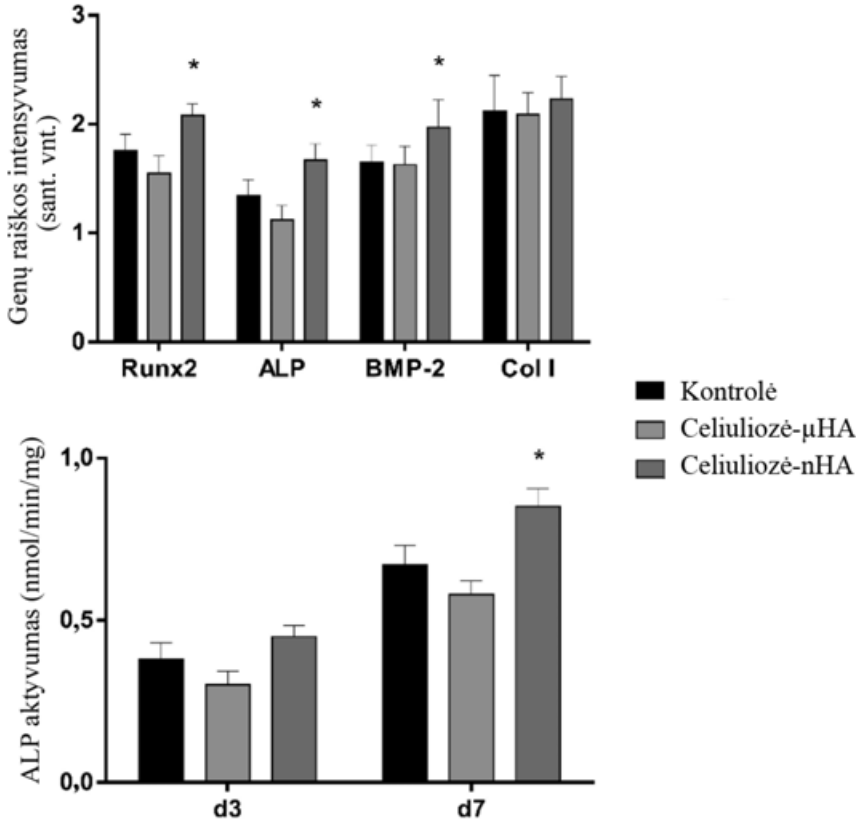

5.1.2.2 pav. *Viršuje – ant eksperimentinių ir kontrolinių karkasų kultivuotų žmogaus osteoblastinių ląstelių genų raiška 7-ą dieną po užsėjimo. Apačioje – šarminės fosfatazės (ALP) aktyvumas ant eksperimentinių ir kontrolinių karkasų kultivuotų žmogaus osteoblastinių ląstelių kultūrose 3-ą ir 7-ą dieną po užsėjimo.*

*Statistiškai reikšmingas skirtumas, palyginti su kontrole.

5.1.3. *In vivo* tyrimų rezultatai

Pooperaciniu laikotarpiu eksperimentiniams gyvūnams nerimo ar streso simptomų nestebėta. Visi operuoti gyvūnai išgyveno, operacinės žaizdos gijo be komplikacijų. Numatytais laiko intervalais gyvūnams atlikus eutanaziją, atlikta sisteminė nekropsija. Nenustatyta jokių tirtųjų transplantantų sukeltų lokalių ar sisteminių patologinių pažeidimų.

Naujai susiformavusio kaulo tiriamajame tūryje (VOI) vertinimui, atlikta triušių kaukolės skliauto biopsijų mikrotomografinė segmentinė analizė (5.1.3.1 ir 5.1.3.2 pav.). Naujai susiformavusio kaulo (tamsiai geltona spalva) ir likutinio karkaso (šviesiai geltona spalva) išskyrimui naudoti segmentiniai slenksčiai. Kontrolinės grupės 4 savaičių biopsijų mikrotomografiniuose vaizduose (5.1.3.1 pav.) nustatytas minimalus naujų plonų kaulo trabekulių formavimasis defekto kraštuose su aiškiai išskiriamomis defekto ribomis. Dvimatėse ir trimatėse mikrotomogramose naujo kaulo formavimosi sritys buvo netolygios ir nutrūkstančios ties savo kaulo ir kontrolinės grupės karkasų riba. Celiuliozės-µHA ir celiuliozės-nHA karkasų grupės pasižymėjo didesne kaulo formavimosi indukcija ir geresne karkaso integracija į savą kaulinį audinį, aplink karkasą tolygiai formuojantis mineralizuotam audiniui. Celiuliozės-nHA karkasų mikrotomogramų dvimačių vaizdų rekonstrukcijose stebėta osteokondukcija – nuo defekto ribos centrinės karkaso dalies link vykstantis naujo kaulo formavimasis. 4 savaičių biopsijų L-PRF grupėse visų tipų karkasams nustatytas didesnis naujo kaulo formavimasis. L-PRF rehidruotų ir L-PRF membranomis padengtų karkasų grupėse stebėtas didesnis mineralizuoto audinio formavimasis karkasų ir defekto riboje. Tarp visų tirtųjų 4 savaičių biopsijų, celiuliozės-µHA + L-PRF ir celiuliozės-nHA + L-PRF grupėse stebėtas nuo defekto kraštų transplantantų centro link plintantis ir labiausiai subrendęs trabekulinio kaulo tinklas, susiliejantis su likutine karkasų matrica.

12 savaičių biopsijų mikrotomogramose stebėta visų tirtųjų karkasų padidėjusi integracija į savą kaulą, palyginti su 4 savaičių biopsijomis. Kontroliniai karkasai buvo visiškai integruoti į savą kaulą, tačiau, priešingai nei eksperimentiniuose celiuliozės kompozitiniuose karkasuose, kontrolinėje grupėje nestebėta ryškesnio naujo kaulo įaugimo į kontrolinių karkasų vidų. 12 savaičių visų tipų transplantantuose su L-PRF stebėtas didesnis naujo kaulo formavimasis. 12 savaičių kontrolinėje + L-PRF grupėje nustatytas dalinis naujo kaulo įaugimas transplantanto viduje. Palyginti su kontrole + L-PRF, celiuliozės-µHA + L-PRF grupėje naujo kaulo įaugimas į karkaso vidų buvo didesnis, o celiuliozės-nHA + L-PRF grupės biopsijose stebėtas viso karkaso peraugimas savu kaulu.

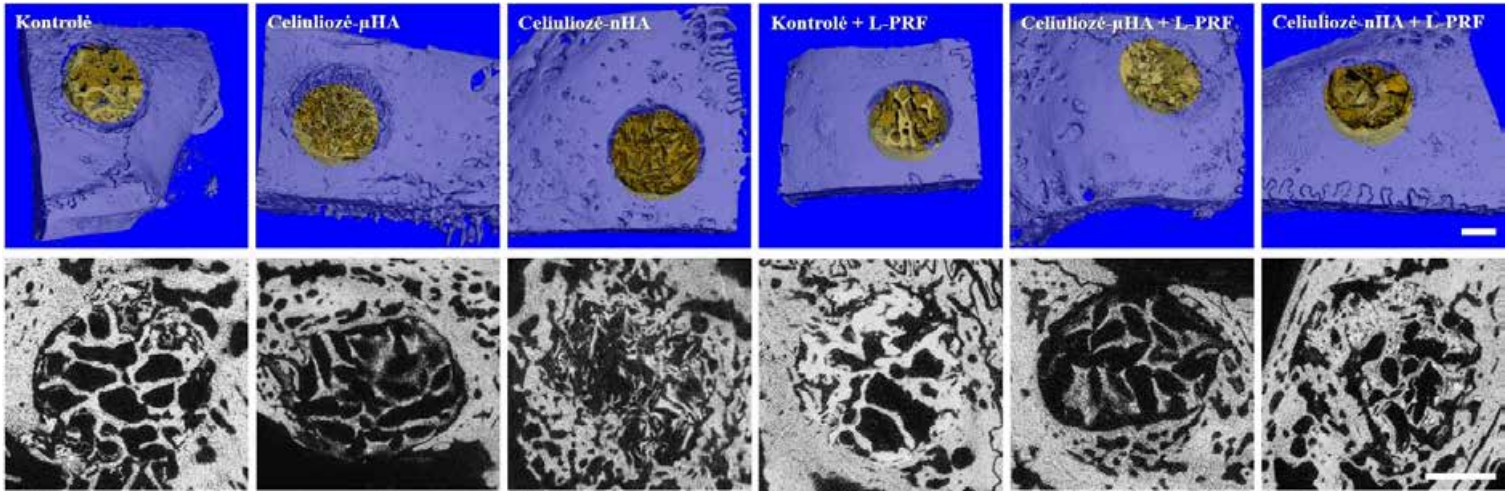

5.1.3.1 pav. *Triušių kaukolės skliauto 4 savaičių biopsijų mikrokompiuterinės tomografijos trimatės (viršutinėje eilėje) ir dvimatės (apatinėje eilėje) mikrotomogramos. Trimatėse mikrotomogramose tamsiai geltona spalva pažymėtas naujai susiformavęs kaulas, šviesiai geltona spalva – likutinis karkasas. Matavimo skalė atitinka 3 mm.*

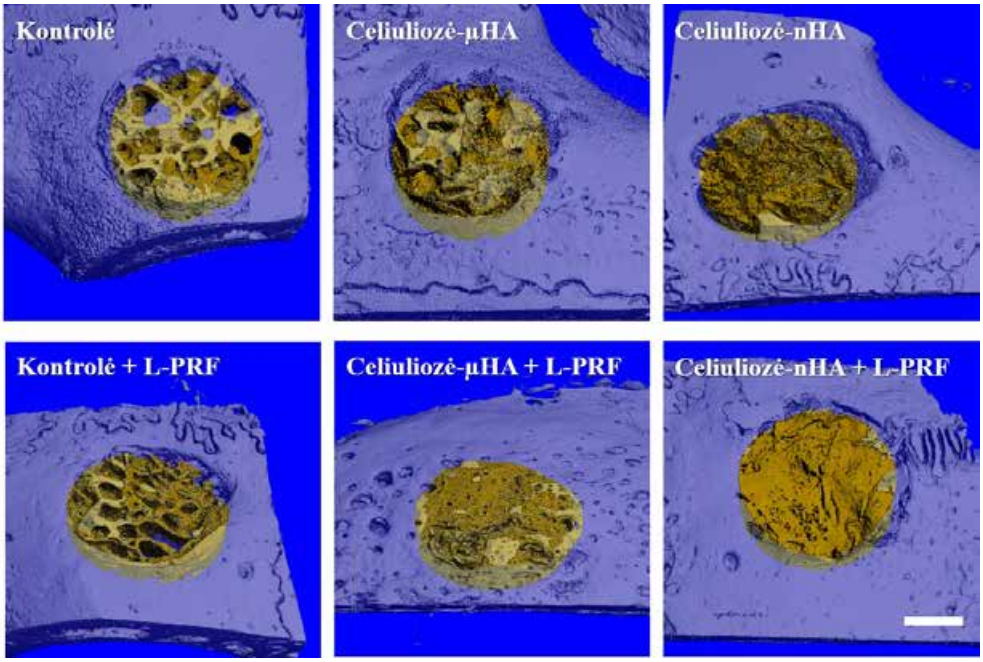

5.1.3.2 pav. *Triušių kaukolės skliauto 12 savaičių biopsijų mikrokompiuterinės tomografijos trimatės mikrotomogramos. Tamsiai geltona spalva pažymėtas naujai susiformavęs kaulas, šviesiai geltona spalva – likutinis karkasas. Matavimo skalė atitinka 3 mm.*

Patvirtindama rastus kokybinius mikrotomografinius duomenis, kiekybinė kaulo tūrinės frakcijos (BV/TV) analizė (5.1.3.3 pav.) visiems tirtiesiems karkasams parodė didesnį 12 savaičių BV/TV santykį, palyginti su 4 savaičių biopsijomis ($p = 0{,}001$). Abiejų tipų celiuliozės kompoziciniams karkasams nustatytas didesnis BV/TV santykis nei kontrolinės grupės karkasams abiem tirtais laiko intervalais ($p = 0{,}001$). Tiek 4, tiek 12 savaičių biopsijose visų tipų karkasų su L-PRF biopsijose nustatyta statistiškai reikšmingai didesnė kaulo tūrinė frakcija nei tų pačių tipų karkasams rehidruotiems fiziologiniu tirpalu ($p < 0{,}05$). 12 savaičių biopsijose celiuliozės-nHA + L-PRF grupėje nustatytas didžiausias BV/TV santykis, kuris statistiškai reikšmingai skyrėsi nuo celiuliozės-µHA + L-PRF ir kitų eksperimentinių grupių kaulo tūrinės frakcijos ($p = 0{,}001$).

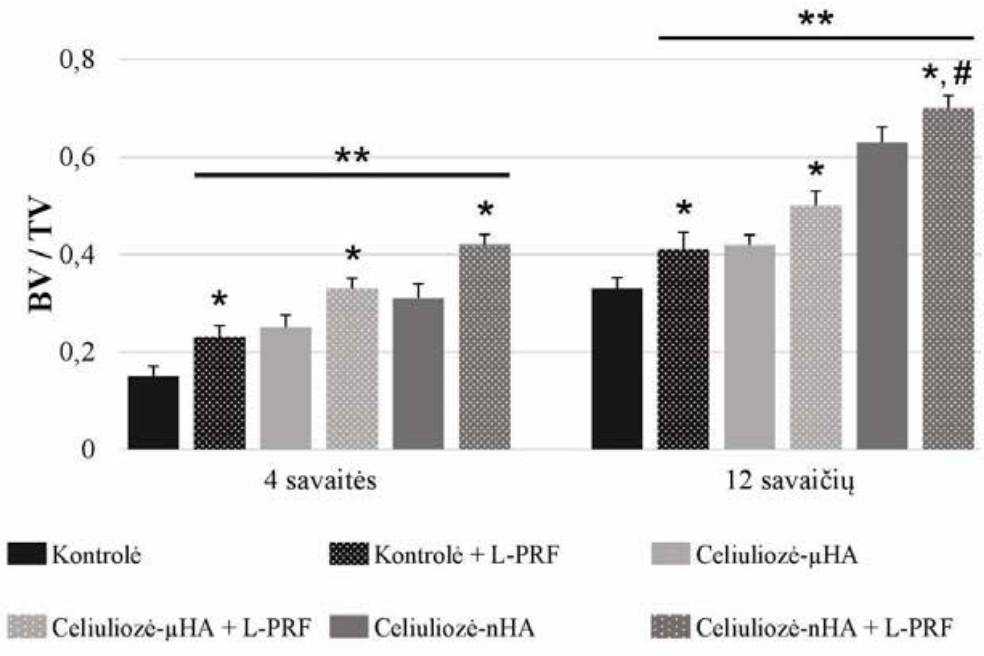

5.1.3.3 pav. *Triušių kaukolės skliauto 4 ir 12 savaičių biopsijų tiriamojo tūrio kaulo tūrinės frakcijos (BV/TV) analizė.*

*Statistiškai reikšmingas skirtumas tarp to paties tipo transplantanto su L-PRF.
**Statistiškai reikšmingas skirtumas, palyginti su kontrole.
#Statistiškai reikšmingas skirtumas, palyginti su 12 savaičių celiuliozės-µHA + L-PRF grupe.

Kaulo biopsijų histologinėje analizėje vertintas transplantantų – savo kaulo ribos histologinis vaizdas bei kaulo įaugimas į karkasų vidų. 4 savaičių biopsijose (5.1.3.4 pav.) kontrolinės medžiagos karkasų ir savo kaulo riboje stebėta fibrozinio audinio jungtis su vos matomu naujai mineralizuoto audinio formavimusi kontrolinių transplantantų kraštuose. Abiejų tipų tirti celiuliozės kompozitiniai karkasai 4 savaičių biopsijose turėjo geresnę integraciją, su defekto kraštais sudarydami kaulinę jungtį. Stebėtas trabekulinio kaulo įaugimas į celiuliozės kompozitinių karkasų poras. 4 savaičių biopsijose visų tipų karkasams su L-PRF stebėta geresnė integracija su savu kaulu nei tų pačių tipų karkasams, rehidruotiems fiziologiniu tirpalu. Kontrolinėje grupėje L-PRF padidino kaulo apoziciją karkaso – defekto krašto riboje, o celiuliozės-µHA + L-PRF ir celiuliozės-nHA + L-PRF grupėse stebėtas susiformavęs tankesnis kaulo trabekulių tinklas.

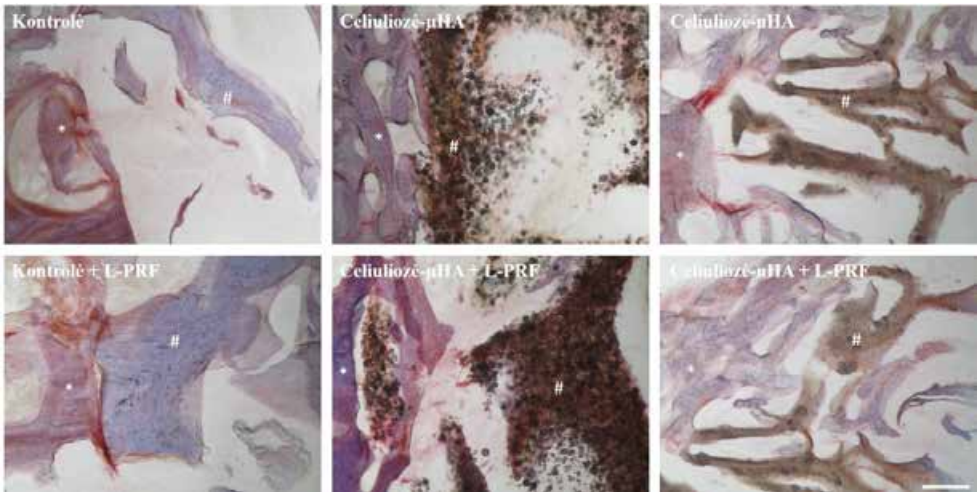

5.1.3.4 pav. *Triušių kaukolės skliauto 4 savaičių biopsijų histologinė analizė. Matavimo skalė atitinka 150 µm.*
*Kaulinis audinys. #Karkasas.

Histologiškai analizuojant 12 savaičių biopsijas (5.1.3.5 pav.), visose tirtose grupėse stebėtas didesnis kaulo formavimasis, palyginti su 4 savaičių biopsijomis. 12 savaičių kontrolinės grupės biopsijose patvirtintas mikrotomogramose matytas tęstinis naujo mineralizuoto audinio formavimasis karkaso – savo kaulo riboje ir osteokondukcijos požymiai, naujam kaului įaugant transplantanto kraštuose. Abiejų tipų celiuliozės kompozitiniuose karkasuose patvirtintas naujo kaulo formavimasis karkasų porose ir kartu vykstantis karkasų irimas. Palyginti su fiziologiniame tirpale rehidruotais kontroliniu ir abiejų tipų celiuliozės kompozitiniais karkasais, 12 savaičių tų pačių tipų transplantantų L-PRF grupėse stebėtas didesnis kaulo įaugimas ir geresnė trabekulinė kaulo struktūrinė organizacija. Didžiausias naujo kaulo formavimasis ir tankiausias kaulo trabekulių tinklas stebėtas celiuliozės-nHA + L-PRF grupėje.

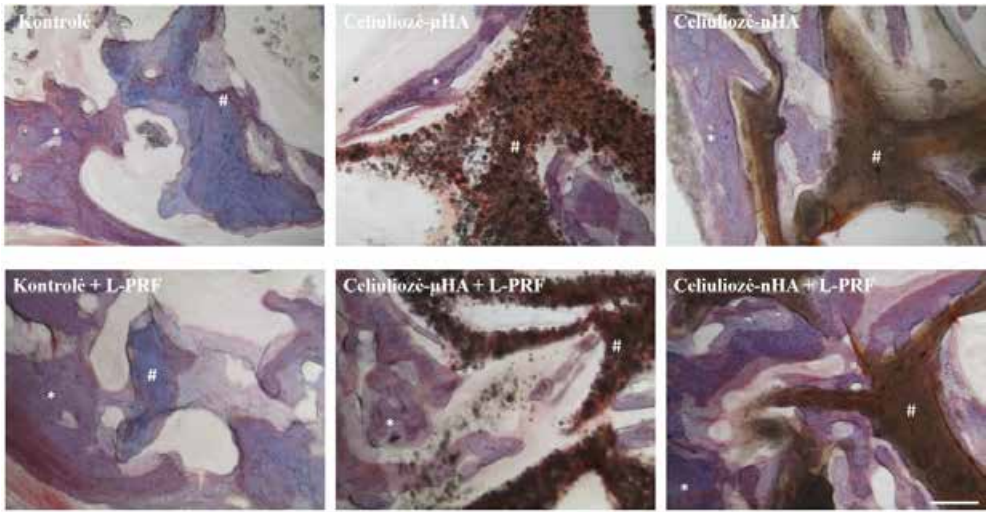

5.1.3.5 pav. *Triušių kaukolės skliauto 12 savaičių biopsijų histologinė analizė. Matavimo skalė atitinka 150 μm.*
*Kaulinis audinys. #Karkasas.

5.2. Klinikinių tyrimų rezultatai

5.2.1. Retinuotų apatinio žandikaulio trečiųjų krūminių dantų šalinimo sudėtingumo klasifikacija

RAŽTKD šalinimo sudėtingumo klasifikacija, sudaryta atsižvelgiant į literatūroje aprašomus svarbiausius anatominius ir diagnostinius kriterijus, turinčius įtakos RAŽTKD šalinimo operacijos planavimui, eigai ir pooperacinėms išeitims. Klasifikacija, aprašyta Juodžbalio ir Daugėlos 2013 m. [199] publikuotame straipsnyje, pateikiama 5.2.1.1 lentelėje.

Pasiūlyta RAŽTKD šalinimo sudėtingumo klasifikacija aprašo RAŽTKD santykį su gretimomis anatominėmis struktūromis: apatinio žandikaulio šaka, antruoju apatiniu krūminiu dantimi, alveolės ketera, apatinio žandikaulio kanalu ir RAŽTKD erdvinę padėtį žandikaulyje. RAŽTKD vertinimas atliekamas kliniškai bei vertinant OPG ir (arba) KPKT duomenis. Klasifikacijoje nurodoma:

- RAŽTKD mediodistalinė padėtis antrojo krūminio danties (M) ir apatinio žandikaulio šakos (R) atžvilgiu.
- RAŽTKD vainikinė – šaknies padėtis alveolinės keteros (A) ir apatinio žandikaulio kanalo (C) atžvilgiu.

5.2.1.1 lentelė. *Apatinio žandikaulio trečiųjų krūminių dantų šalinimo sudėtingumo klasifikacija.*

Apatinio trečiojo krūminio danties pozicija	**Galimas intervencijos rizikos laipsnis (balas)**			
	Įprastas (0)	**Nesudėtingas (1)**	**Vidutinis (2)**	**Sudėtingas (3)**
Mediodistalinė padėtis antrojo krūminio danties (M) ir apatinio žandikaulio šakos (R) atžvilgiu				
Padėtis antrojo krūminio danties atžvilgiu (M)	Vainiko pozicija ties arba aukščiau antrojo krūminio danties ekvatoriaus	Vainiko pozicija tarp antrojo krūminio danties ekvatoriaus ir šaknies vainikinio trečdalio	Vainiko / šaknų pozicija ties viduriniu antrojo krūminio danties šaknų trečdaliu	Vainiko / šaknų pozicija ties viršūniniu antrojo krūminio danties šaknų trečdaliu
Padėtis apatinio žandikaulio šakos atžvilgiu (R)	Pakankamai vietos dantų lanke	Dalinė retencija apatinio žandikaulio šakoje	Visiška retencija apatinio žandikaulio šakoje	Visiška retencija apatinio žandikaulio šakoje distoanguliarinėje arba horizontalioje pozicijoje
Vainikinė – šaknies padėtis alveolinės keteros (A) ir apatinio žandikaulio kanalo (C) atžvilgiu				
Padėtis alveolinės keteros (nuo aukščiausio taško iki danties) atžvilgiu (A)	Visiškai išdygęs dantis	Dalinė retencija, tačiau danties vainiko ekvatorius yra virš alveolinės keteros	Dalinė retencija, tačiau danties vainiko ekvatorius yra žemiau alveolinės keteros	Visiška retencija
Padėtis apatinio žandikaulio kanalo (nuo žemiausio danties taško) atžvilgiu (C)	$\geq$ 3 mm nuo apatinio žandikaulio kanalo	< 3 mm nuo apatinio žandikaulio kanalo, kontaktas ar išsikišimas į kanalą, stebima intaktiška kanalo siena	Kontaktas ar išsikišimas į apatinio žandikaulio kanalą, intaktiškos kanalo sienos nestebima	Šaknys apsupa apatinio žandikaulio kanalą
Skruosto – liežuvinė padėtis apatinio žandikaulio skruostinės ir liežuvinės sienelių (B) atžvilgiu				
Padėtis apatinio žandikaulio skruostinės ir liežuvinės sienelių atžvilgiu (B)	Arčiau skruostinės sienelės	Viduryje tarp skruostinės ir liežuvinės sienelių	Arčiau liežuvinės sienelės	Arčiau liežuvinės sienelės ir dantis dalinai arba visiškai retinuotas kaule (A_2 ir A_3)
Erdvinė pozicija (S)				
Erdvinė pozicija (S)	Vertikali (90°)	Medioanguliarinė $\leq$ 60°	Distoanguliarinė $\geq$ 120°	Horizontali (0°) arba inversinė (270°)

- RAŽTKD skruosto – liežuvinė padėtis apatinio žandikaulio skruostinės ir liežuvinės sienelių (B) atžvilgiu.
- RAŽTKD danties erdvinė pozicija (S).

Kiekvienas iš klasifikacijos (M), (R), (A), (C), (B), (S) kriterijų vertinamas balais, priskiriant įprastam (0 balų), nesudėtingam (1 balas), vidutiniam (2 balai) arba sudėtingam (3 balai) prognozuojamam šalinimo sudėtingumui. Klasifikacijoje balais įvertinami visi keturi RAŽTKD kriterijai. RAŽTKD šalinimo sudėtingumas prognozuojamas pagal kriterijuose priskirtą aukščiausią balą:

- Visų kriterijų reikšmei esant 0 (t. y. $M_0R_0A_0C_0B_0S_0$), tikėtinas įprastinis RAŽTKD šalinimas.
- Bent vienam kriterijui turint 1 balą (pvz., $M_1R_0A_0C_0B_0S_0$), prognozuojamas nesudėtingas RAŽTKD šalinimas.
- Bent vienam kriterijui turint 2 balus (pvz., $M_0R_2A_0C_0B_0S_1$), prognozuojamas vidutinio sudėtingumo RAŽTKD šalinimas.
- Bent vienam kriterijui turint 3 balus (pvz., $M_0R_2A_3C_0B_0S_1$), prognozuojamas sudėtingas RAŽTKD šalinimas.

Prognostinė RAŽTKD šalinimo sudėtingumo klasifikacija gydytojams suteikia galimybę įvertinti tikėtiną RAŽTKD šalinimo sudėtingumą, planuoti operacijos eigą ir išvengti galimų komplikacijų. Moksliniuose tyrimuose klasifikacija gali būti naudojama tiriamųjų grupių standartizavimui RAŽTKD šalinimo tiriamuosiuose modeliuose.

5.2.2. Retinuotų apatinio žandikaulio trečiųjų krūminių dantų šalinimo sudėtingumo klasifikacijos validacija

RAŽTKD šalinimo sudėtingumo klasifikacijos validacijos tyrime trijuose tyrimo centruose dalyvavo 124 pacientai: 61 vyras (amžiaus vidurkis – 30,5 ± 10,7 metų) ir 63 moterys (amžiaus vidurkis – 27,5 ± 11,3 metų). Pirmajame centre tyrime dalyvavo 51 pacientas, antrajame – 50, trečiajame – 23 pacientai. Dantų šalinimo indikacijos ir pooperacinių komplikacijų pasiskirstymas tarp centrų pateikiami 5.2.2.1 ir 5.2.2.2 lentelėse.

5.2.2.1 lentelė. *Indikacijos tyrime dalyvavusių pacientų RAŽTKD šalinimui.*

Indikacija	Pacientų skaičius
Profilaktinė	61
Ortodontinė	7
Lėtinė infekcija	38
Periodontologinė	12
Endodontologinė	6
Iš viso	124

RAŽTKD – retinuoti apatinio žandikaulio tretieji krūminiai dantys.

5.2.2.2 lentelė. *RAŽTKD šalinimo komplikacijų pasiskirstymas tarp centrų.*

Centras	Pacientų skaičius	Komplikacijų skaičius
1	51	5
2	50	0
3	23	2
Iš viso	124	7

RAŽTKD – retinuoti apatinio žandikaulio tretieji krūminiai dantys.

Vidutinės RAŽTKD šalinimo operacijos trukmės reikšmės tyrimo centruose pateikiamos 5.2.2.3 lentelėje. Bendra visuose tyrimo centruose fiksuota operacijos vidutinė trukmė buvo 24,1 ± 22,2 min. (intervalas – nuo 1,0 iki 120,0 min.) ir statistiškai reikšmingai skyrėsi tarp centrų (p = 0,001).

5.2.2.3 lentelė. *Vidutinė RAŽTKD šalinimo operacijos trukmė tyrimo centruose.*

Centras	Pacientų skaičius	Operacijos trukmė (minutėmis)	
		Vidurkis ± SN	Laiko intervalas
1	51	18,7 ± 20,7*	1,0–120,0
2	50	28,6 ± 20,6*	2,0–120,0
3	23	26,4 ± 26,9	1,0–98,0
Iš viso	124	24,1 ± 22,2	1,0–120,0

RAŽTKD – retinuoti apatinio žandikaulio tretieji krūminiai dantys;
SN – standartinis nuokrypis.
*Statistiškai reikšmingas skirtumas tarp centrų pagal Mann-Whitney testą.

RAŽTKD vertinant pagal Winter klasifikaciją [197], 48 RAŽTKD nustatyta vertikali, 54 dantims – medioanguliarinė, 9 dantims – horizontali, 4 dantims – skruosto – liežuvinė ir 9 dantims – distoanguliarinė padėtis. Chirurginės operacijos trukmė tarp skirtingų Winter klasifikacijos grupių statistiškai reikšmingai nesiskyrė (p > 0,05).

Vertinant pagal Pell ir Gregory klasifikaciją [198], 37 RAŽTKD priskirti I klasei, 63 dantys – II klasei ir 24 dantys – III klasei, RAŽTKD esant įvairiose padėtyse (A, B ir C) okliuzinės plokštumos atžvilgiu. Chirurginės operacijos trukmė tarp skirtingų Pell ir Gregory klasifikacijos grupių statistiškai reikšmingai nesiskyrė (p > 0,05).

Vertinant pagal Juodžbalio ir Daugėlos RAŽTKD šalinimo sudėtingumo klasifikaciją [199], 3 RAŽTKD priskirti prognozuojamam įprastinio sudėtingumo šalinimui (visų kriterijų balas 0), 30 dantų – nesudėtingam šalinimui (aukščiausias bent vieno iš kriterijų balas – 1), 66 dantys – vidutinio sudėtingumo šalinimui (aukščiausias bent vieno iš kriterijų balas – 2) ir 25 dantys – sudėtingam šalinimui (aukščiausias bent vieno iš kriterijų balas – 3). Chirurginės operacijos trukmė tarp skirtingų Juodžbalio ir Daugėlos RAŽTKD šalinimo sudėtingumo klasifikacijos grupių skyrėsi statistiškai reikšmingai (p = 0,002) (5.2.2.4 lentelė).

5.2.2.4 lentelė. *Operacijos trukmės pasiskirstymas Juodžbalio ir Daugėlos RAŽTKD šalinimo sudėtingumo klasifikacijos grupėse.*

	Klasifikacijos grupė								**p reikšmė**
	0		**1**		**2**		**3**		
	n	**Vidurkis ± SN**	**n**	**Vidurkis ± SN**	**n**	**Vidurkis ± SN**	**n**	**Vidurkis ± SN**	
Trukmė (minutės)	3	20,0 ± 8,7	30	13,1 ± 11,1	66	26,0 ± 23,4	25	32,8 ± 25,5	0,002*

RAŽTKD – retinuoti apatinio žandikaulio tretieji krūminiai dantys; n – tiriamųjų skaičius; SN – standartinis nuokrypis; p – reikšmingumo lygmuo.
*Statistiškai reikšmingas skirtumas pagal Kruskal-Wallis testą.

5.2.3. L-PRF įtakos gijimui vertinimas retinuotų apatinio žandikaulio trečiųjų krūminių dantų šalinimo operacijose

Tyrimas atliktas siekiant įvertinti L-PRF įtaką RAŽTKD alveolių gijimui, pooperaciniam paciento diskomfortui ir alveolito pasireiškimui po RAŽTKD šalinimo operacijų. Tyrimui atrinkti 34 pacientai, kuriems vienos procedūros metu atliktos abipusės RAŽTKD šalinimo operacijos (5.2.3.1 lentelė). Tyrimo populiacijoje tarp tiriamųjų demografinių duomenų statistiškai reikšmingų skirtumų nenustatyta (p > 0,05). Pooperaciniu periodu 4 pacientai neatvyko į numatytas apžiūras, tyrimą baigė 30 pacientų.

5.2.3.1 lentelė. *Tyrime dalyvavusių pacientų demografiniai duomenys.*

	Vyrai	**Moterys**	**Iš viso**	**p reikšmė**
Pacientų skaičius, n (proc.)	14 (41,18)	20 (58,82)	34 (100)	0,303*
Pacientų amžius (V ± SN)	23,35 ± 1,73	22,35 ± 2,13	22,76 ± 2,02	0,08**

V – vidurkis; SN – standartinis nuokrypis; p – reikšmingumo lygmuo.
*Statistiškai nereikšmingas skirtumas pagal Chi kvadrato testą.
**Statistiškai nereikšmingas skirtumas pagal Mann-Whitney testą.

Pooperaciniu laikotarpiu RAŽTKD alveolės L-PRF grupėje gijo gerai, be ryškesnių komplikacijų. Kontrolinėje grupėje pirmąją pooperacinę savaitę 4 alveolėse išsivystė alveolitas, tai sudarė 13,3 proc. kontrolinės grupės atvejų ir statistiškai reikšmingai skyrėsi palyginti su L-PRF grupe (p = 0,001). Alveolitas gydytas revizuojant alveoles ir suformuojant naują kraujo krešulį. Vienoje kontrolinėje alveolėje pasireiškė pooperacinis kraujavimas, kuris sustabdytas pacientui duodant pakartotinai sukąsti sterilų spaudžiamąjį tvarstelį. Dviejose L-PRF ir trijose kontrolinėse pusėse pooperaciniu periodu atsirado veido hematomos, kurios išsiskirstė savaime per pirmąsias 2 pooperacines savaites ir nereikalavo papildomo gydymo. Šalutinių reiškinių, susijusių su veninio kraujo paėmimo procedūra, anestezija ar skirtais medikamentais, operaciniu ir pooperaciniu periodu nestebėta.

Vertinant bendrą pirmųjų dviejų savaičių minkštųjų audinių gijimo indeksą (HI), Wilcoxon Rank Sum testu nustatytos statistiškai reikšmingai mažesnės HI reikšmės ir geresnis minkštųjų audinių gijimas L-PRF grupėje, palyginti su kontroline grupe (p = 0,001). L-PRF ir kontrolinėje grupėse pasirinktais laiko intervalais nustatytos HI reikšmės pateikiamos 5.2.3.2 lentelėje. L-PRF grupėje nustatytas statistiškai reikšmingai mažesnis HI ir greitesnis pooperacinės žaizdos gijimas, palyginti su kontrole visais tirtais laiko intervalais – 1-ą, 3-ą, 7-ą ir 14-ą pooperacinėmis dienomis.

5.2.3.2 lentelė. *Minkštųjų audinių gijimo indekso (HI) reikšmės.*

Diena	**1**	**3**	**7**	**14**
HI vidurkis ± SN				
L-PFR grupė	5,10 ± 1,30	4,83 ± 0,95	4,33 ± 0,61	4,10 ± 0,40
Kontrolinė grupė	6,47 ± 1,36	6,33 ± 1,27	4,97 ± 0,85	4,37 ± 0,62
p reikšmė	0,001*	0,001*	0,002*	0,023*

SN – standartinis nuokrypis; p – reikšmingumo lygmuo.
*Statistiškai reikšmingas skirtumas pagal Mann-Whitney testą.

Vertinant bendrą pirmosios savaitės skausmo intensyvumą VAS balais, Wilcoxon Rank Sum testu nustatytos statistiškai reikšmingai mažesnės VAS reikšmės L-PRF grupėje, palyginti su kontroline grupe (p = 0,001). VAS

balų pasiskirstymas tarp grupių kiekvieną pirmosios pooperacinės savaitės dieną pateikiamas 5.2.3.3 lentelėje. L-PRF užpildytoms alveolėms pacientai nurodė mažesnį VAS skausmo intensyvumą, palyginti su kontrole. Šis skirtumas buvo statistiškai reikšmingas kiekvieną pirmosios pooperacinės savaitės dieną ($p \leq 0,004$).

5.2.3.3 lentelė. *Vizualinės analoginės skausmo skalės (VAS) balų reikšmės.*

Diena	**1**	**2**	**3**	**4**	**5**	**6**	**7**
VAS balas (vidurkis ± SN)							
L-PFR grupė	2,87 ± 0,97	2,67 ± 1,03	1,67 ± 0,88	1,37 ± 0,72	1,13 ± 0,82	0,67 ± 0,76	0,07 ± 0,25
Kontrolinė grupė	4,20 ± 1,35	3,53 ± 1,28	3,13 ± 1,28	2,97 ± 1,13	2,57 ± 1,10	1,97 ± 0,85	1,53 ± 0,82
p reikšmė	0,001*	0,004*	0,001*	0,001*	0,001*	0,001*	0,001*

SN – standartinis nuokrypis; p – reikšmingumo lygmuo.
*Statistiškai reikšmingas skirtumas pagal Mann-Whitney testą.

Veido tinimo priešoperaciniuose matmenyse tarp pacientų skirtingų veido pusių statistiškai reikšmingo skirtumo nenustatyta ($p = 0,594$). Veido tinimo matavimo reikšmių dinamika pirmąją savaitę pateikiama 5.2.3.4 lentelėje. 1-ą ($p = 0,035$) ir 3-ą ($p = 0,023$) pooperacinėmis dienomis L-PRF grupėje nustatytas statistiškai reikšmingai mažesnis veido tinimas, palyginti su kontroline grupe. 7-ą pooperacinę dieną tinimo reikšmės tarp grupių statistiškai reikšmingai nesiskyrė ($p = 0,224$). Tačiau palyginus 7-os pooperacinės dienos tinimo reikšmes su priešoperaciniais matmenimis, tinimas buvo visiškai atslūgęs tik L-PRF grupėje ($p = 0,593$), tuo tarpu kontrolinėje grupėje išliko statistiškai reikšmingas veido patinimas ($p = 0,001$).

5.2.3.4 lentelė. *Veido tinimo reikšmės pirmąją pooperacinę savaitę.*

Diena	**Prieš operaciją**	**1**	**3**	**7**
Veido tinimo reikšmės (vidurkis ± SN)				
L-PRF grupė	84,20 ± 7,98	87,67 ± 7,21	87,27 ± 7,16	84,23 ± 7,91
Kontrolinė grupė	84,70 ± 7,03	91,47 ± 6,88	91,07 ± 7,51	86,53 ± 6,99
p reikšmė	0,594	0,035*	0,023*	0,224

SN – standartinis nuokrypis; p – reikšmingumo lygmuo.
*Statistiškai reikšmingas skirtumas pagal Mann-Whitney testą.

6. REZULTATŲ APTARIMAS

6.1. *In vitro* tyrimų rezultatų aptarimas

Šiame darbe susintetinti celiuliozės su mikrohidroksiapatitu (celiuliozės-μHA) ir celiuliozės su nanohidroksiapatitu (celiuliozės-nHA) kompozitiniai kaulo transplantantai, aprašytos jų fizikocheminės ir biologinės savybės. Biologinių transplantantų savybių vertinimas atliktas *in vitro* su žmogaus osteoblastinėmis ląstelėmis, atliekant SEM, MTT, osteogeninių genų (Runx-2, ALP, BMP-2, Col I) raiškos ir ALP aktyvumo tyrimus.

Mikrohidroksiapatito (μHA) ir nanohidroksiapatito (nHA) dalelės į celiuliozės karkasus įterptos siekiant pagerinti celiuliozės karkasų biologinį aktyvumą. Gryna celiuliozė literatūroje aprašoma kaip labai hidrofiliška medžiaga [224]. Tai lemia grynos celiuliozės karkasams būdingą gana mažą baltymų adsorbciją, kuri riboja ląstelių adheziją ir proliferaciją karkaso paviršiuje [225–227]. Transplantanto kolonizacija ląstelėmis labai priklauso nuo karkaso fizikocheminių savybių ir gebėjimo adsorbuoti bioaktyvias molekules ir baltymus, su kuriais sąveikaudamos ląstelės gali prisitvirtinti prie karkaso paviršiaus. μHA ir nHA dalelės modifikuoja celiuliozės karkasų struktūrines savybes ir tarnauja kaip ligandai, su kuriais gali sąveikauti osteogeninės ląstelės [138]. Literatūros duomenimis, hidroksiapatitas (HA) ant karkasų paviršiaus pritraukia osteogeninių ląstelių adhezijai būtinus specifinius baltymus ir adhezinius integrinus, taip pagerindamas ankstyvą transplantanto kolonizaciją ląstelėmis [228–229]. HA pasižymi vidutiniu paviršiaus hidrofiliškumu, kuris yra palankus specifinių baltymų ir molekulių depozicijai bei jų įtakojamai ląstelių migracijai, adhezijai ir proliferacijai [230]. Tai patvirtina ir šio darbo *in vitro* tyrimų duomenys, rodantys, kad kompozitiniuose celiuliozės-HA karkasuose osteoblastinių ląstelių adhezija ir pasiskirstymas daugiausia koncentravosi ties μHA ir nHA dalelių sankaupomis.

Šiame darbe eksperimentinių celiuliozės-μHA ir celiuliozės-nHA karkasų mikrokompiuterinės tomografijos analizės duomenys parodė didelį abiejų tipų karkasų porėtumą su susisiekiančiomis vidinėmis poromis, būtinomis ląstelių metabolizmo užtikrinimui ir šalutinių produktų šalinimui [231]. Karkaso gausus vidinis porų tinklas palengvina kraujagyslių įaugimą, sudaro galimybes naujo kaulo formavimuisi, kuris yra labai priklausomas nuo regeneracijoje dalyvaujančiose ląstelėse vykstančių anabolinių procesų ir jų aprūpinimo šiems procesams būtinomis medžiagomis [232]. Gausus porėtumas taip pat svarbus deguonies tiekimo užtikrinimui, kadangi hipoksinė aplinka yra nepalanki osteoblastų diferenciacijai [233]. Nustatytas

celiuliozės-µHA ir celiuliozės-nHA eksperimentinių karkasų bendras porėtumas buvo gerokai didesnis nei daugelio autorių rekomenduojamas minimalus 50 proc. porėtumas, būtinas karkaso vaskuliarizacijai ir osteogenezei [234, 235]. Didelis porėtumas taip pat palengvina karkasų mechaninę integraciją su gretimais audiniais, gerindamas transplantanto integralumą su defekto kraštais, kuris būtinas kraujagyslių įaugimui ir naujo kaulo formavimuisi [150]. Su karkasų porėtumu labai susijęs ir karkasų savitasis paviršiaus plotas. Didėjant porėtumui, didėja ir savitasis karkasų paviršiaus plotas. Didesnis savitasis paviršiaus plotas lemia didesnį paviršiaus reaktyvumą, vykstant ląstelių adhezijai, proliferacijai ir diferenciacijai. Didelis savitasis paviršiaus plotas kartu su dideliu karkasų porėtumu susisiekiančiomis vidinėmis poromis yra būtini gerai ląstelių adhezijai ir pasiskirstymui karkase bei kraujagyslių įaugimui į karkaso vidų [231]. Tirtųjų celiuliozės-nHA eksperimentinių karkasų savitasis paviršiaus plotas, nors ir nežymiai, bet statistiškai reikšmingai, buvo didesnis nei celiuliozės-µHA transplantantų ($p = 0,001$).

Kitas svarbus faktorius, turintis įtakos osteogenezei transplantanto viduje, yra karkaso porų dydis. Abiejų šio tyrimo eksperimentinių karkasų vidutinis porų skersmuo buvo panašus – apie 500 µm. Schek ir kt. 2004 m. [236] publikuotame tyrime nustatyta, kad mažesnės nei 100 µm karkasų poros neužtikrina pakankamos karkaso vaskuliarizacijos. Tai lemia hipoksinę aplinką karkaso viduje, trikdo ląstelių proliferacijos ir diferenciacijos procesus. Didesnis porų diametras yra palankus ląstelių migracijai į karkaso vidų, kadangi išvengiama ląstelių agregacijos transplantanto paviršiuje [236]. Tačiau didesnis nei 1000 µm porų skersmuo siejamas su prastesnėmis transplantanto mechaninėmis savybėmis ir sumažėjančiu savituoju paviršiaus plotu, tai lemia mažesnę ląstelių adheziją prie karkaso paviršiaus [151]. Dauguma autorių kaulo transplantantų matricoms rekomenduoja 200–600 µm porų diametrą, kaip palankiausią angiogenezės ir osteogenezės procesams [148–150, 237].

Šiame darbe tirtųjų celiuliozės-µHA ir celiuliozės-nHA kompozitinių karkasų fizikocheminės savybės buvo panašios. Nepaisant to, *in vitro* biologinis ląstelių atsakas į skirtingo dydžio HA dalelių užpildus turinčius celiuliozės kompozitinius karkasus buvo skirtingas. Skenuojančiu elektroniniu mikroskopu vertinant celiuliozės-µHA paviršių, stebėtos prie µHA dalelių sankaupų koncentruotos apvalios formos, trumpomis filopodijomis ląstelės, o ant celiuliozės-nHA karkasų kultivuojamų ląstelių pasiskirstymas karkaso paviršiuje buvo tolygesnis, vyravo daugiakampės formos, elonguotos ląstelės su gausesnėmis ir labiau išreikštomis filopodijomis. Geltonojo tetrazolio druskų (3-(4,5-dimetiltiazol-2-il-)-2,5-difeniltetrazolio bromido) redukcijos metodu (MTT) nustatytas didesnis ant celiuliozės-nHA karkasų

kultivuojamų ląstelių metabolinis aktyvumas. Filovos ir kt. 2014 m. [238] atlikto tyrimo duomenimis, kompozitiniai karkasai su nHA dalelėmis pasižymi gausesne ląstelių adhezija, palyginti su µHA kompozitiniais karkasais. Mažesnis nHA dalelių dydis ir didesnis paviršiaus plotas skatina selektyvių adhezinių baltymų adsorbciją ir ląstelių adheziją, karkaso paviršiuje greičiau susiformuojant ląstelių tarpusavio sąveikai būtinam tarpląsteliniam matriksui [239]. Dėl savo struktūrinių ir cheminių ypatybių nHA dalelės yra labiau linkę adsorbuoti vitronektiną – glikoproteiną, kuris dalyvauja ląstelių adhezijos ir pasiskirstymo transplantanto paviršiuje procesuose [240]. Nustatyta, kad prie nHA dalelių adhezavusios ląstelės išskiria didesnius kiekius beta-aktinino ir talino baltymų, kurie taip pat dalyvauja ląstelių citoskeleto formavime ir pasiskirstyme karkaso paviršiuje [238]. Tai patvirtino ir šiame darbe nustatytas gausesnis ląstelių pasiskirstymas ant celiuliozės-nHA kompozitų.

Tyrimo MTT analizės duomenys parodė didesnę ląstelių proliferaciją celiuliozės-nHA kompozitų paviršiuje, palyginti su celiuliozės-µHA ir kontroline grupėmis. SEM nustatyti ląstelių morfologijos skirtumai gali turėti didelės įtakos jų proliferaciniams procesams. Celiuliozės-nHA paviršiuje stebėtos daugiakampės, elonguotos formos osteoblastinės ląstelės yra linkusios aktyviai formuoti tarpląstelinius ryšius, proliferuoti ir kolonizuoti transplantanto matricą [241, 242]. Nustatyta, kad nHA dalelės osteoblastų kultūroms turi didesnį tiesioginį proliferacinį poveikį, palyginti su µHA dalelėmis [243, 244]. Osteoblastinės ląstelės gali endocituoti nHA daleles, ląstelės citoplazmoje susiformuojant endosomoms, kuriose nHA dalelės iš dalies ištirpsta, į citoplazmą atpalaiduodamos kalcio jonus [245]. Tinkama kalcio jonų koncentracija ląstelės citoplazmoje yra būtina tiek osteoblastų proliferacijos, tiek osteoblastų diferenciacijos procesams užtikrinti [246]. Literatūros duomenimis, nHA dalelės gali skatinti tam tikrų osteoblastinę diferenciaciją lemiančių grandininių signalų ekspresiją [247, 248]. nHA skatinamasis poveikis osteoblastų diferenciacijai buvo patvirtintas ir nHA turinčiuose kompozitiniuose karkasuose [238, 249], o poveikio stiprumas kai kurių autorių lygintas netgi su osteoindukcinių augimo faktorių poveikiu [250].

Šio tyrimo celiuliozės-nHA kompozitų grupėje nustatyta statistiškai reikšmingai didesnė osteogeninių genų (Runx-2, ALP ir BMP-2) raiška ($p = 0,001$) ir ALP aktyvumas ($p = 0,001$), palyginti su celiuliozės-µHA kompozitais, tačiau tarp grupių negauta statistiškai reikšmingo skirtumo vertinant Col I geno raišką ($p > 0,05$). Runx-2 yra pagrindinis transkripcijos faktorius, kuris reguliuoja daugelio osteogeninei diferenciacijai svarbių genų ekspresiją, turinčią įtakos osteopontino, osteokalcino ir BMP-2 aktyvumui [251]. ALP yra ląstelių membranų glikoproteinas, dalyvaujantis ekstraląstelinio

matrikso mineralizacijoje ir laikomas ankstyvosios osteogenezės žymeniu [252]. BMP-2 yra signalinis baltymas, priskiriamas TGF-β augimo faktorių šeimai. BMP-2 yra literatūroje plačiai aprašytas osteoindukcinis augimo faktorius [63, 78, 110, 112]. Rekombinantinis BMP-2 kai kuriose šalyse yra aprobuotas ir klinikiniam naudojimui, kaip osteoindukcinė medžiaga žandikaulių kaulinių defektų regeneracijai [11, 113, 114, 116]. Col I geno raiška ypač suaktyvėja osteogeninių ląstelių proliferacijos metu [251, 252]. Col I svarbus užtikrinant pagrindinę osteoblastų funkciją – kolageno sintezę ir ekstraląstelinio matrikso formavimą [253].

6.2. Eksperimentinių *in vivo* tyrimų rezultatų aptarimas

Šiame darbe tirta eksperimentinių celiuliozės-nHA ir celiuliozės-μHA kompozitinių karkasų įtaka naujo kaulo formavimuisi *in vivo* Naujosios Zelandijos triušių kaukolės skliauto defektų modelyje. Karkasų bioaktyvavimui naudotas L-PRF.

L-PRF yra antrosios kartos trombocitų koncentratas, sudarytas iš fibrino matricos su joje įsiterpusiais trombocitais, leukocitais ir jų atpalaiduojamais augimo faktoriais [185]. L-PRF išskiriamas iš veninio kraujo, jį centrifuguojant stikliniuose ar silicio dioksidu dengtuose mėgintuvėliuose 400 g išcentrine jėga be antikoaguliantų ar papildomų cheminių aktyvatorių [277]. L-PRF paruošimo metu fibrino polimerizacija yra paremta natūraliu kraujo koaguliacijos procesu. Hagemano (XII) faktoriui kontaktuojant su neigiamą krūvį turinčiomis mėgintuvėlio sienelėmis, yra aktyvuojami trombocitai ir prasideda vidinė koaguliacijos kaskada [273]. Tuo pačiu metu veikiant išcentrinei jėgai, mėgintuvėlio viršutinėje dalyje yra koncentruojama kraujo plazma, trombocitai, leukocitai. Kraujo plazmoje esantis tirpus fibrinogenas, veikiant trombinui, yra polimerizuojamas į netirpią fibrino matricą, kartu joje įterpiant plazmos baltymus, trombocitus ir leukocitus. Pasibaigus centrifugavimui, fibrino matrica nusistovi viršutiniame mėgintuvėlio trečdalyje tarp aukščiau liekančios beląstelinės plazmos ir apačioje esančių raudonųjų kraujo kūnelių bazės [14]. Priešingai nei skystos konsistencijos PRP, iš karto po aplikavimo L-PRF audinių terpėje neištirpsta, ir 4 savaičių laikotarpiu yra palaipsniui reorganizuojamas, panašiai kaip ir natūralus kraujo krešulys [15]. Stiprios trimolekulinės jungtys sudaro santykinai tvirtą erdvinę L-PRF fibrino matricos struktūrą, kuri apsaugo inkorporuotas ląsteles ir augimo faktorius nuo proteolitinių fermentų. Kaulo regeneracijai svarbūs augimo faktoriai (TGF β-1, PDGF, FGF, VEGF, BMP-2) yra palaipsniui atpalaiduojami iš L-PRF matricos iki 28 dienų laikotarpiu po paruošimo [15, 169, 278]. Svarbu pažymėti, kad L-PRF turėtų būti laikomas ne tik augimo faktorių koncentratu. L-PRF yra fibrino pagrindo bioaktyvi medžiaga,

turinti gyvų ląstelių, matrikso proteinų (trombospondino-1, fibronektino, vitronektino), glikozaminoglikanų (heparino, hialurono rūgšties) ir kompleksinių reguliacinių citokinų, įskaitant interleukinus (IL-1β, IL-4, IL-6) ir tumoro nekrozės faktorių alfa (TNF-α). L-PRF skatina pirminę hemostazę, ląstelių chemotaksį, mitogenezę ir regeneruojamoje srityje veikia kaip bioaktyvi medžiaga, reguliuojanti žaizdos gijimo kaskados ląstelinį atsaką [14, 154, 274, 277, 296].

Literatūroje aprašomas geras celiuliozės transplantantų biosuderinamumas [68, 141]. Celiuliozės transplantantai neprovokuoja išreikštų organizmo uždegiminių ar svetimkūnio atmetimo reakcijų, o jų matrica yra palanki terpė kraujagyslių įaugimui [254, 255]. Kaip parodė šio tyrimo *in vitro* dalies rezultatai ir literatūroje pateikiami duomenys, skirtingo dydžio HA dalelių įterpimas į celiuliozės matricą turi įtakos kompozitinio transplantanto bioaktyvumui [256, 257]. Šio tyrimo *in vivo* dalyje tiek celiuliozės-µHA, tiek celiuliozės-nHA transplantantai standartizuotuose kaulo defektuose pasižymėjo statistiškai reikšmingai didesniu naujo mineralizuoto audinio formavimu, palyginti su kontroliniu komerciniu alogeniniu transplantantu ($p = 0,001$). Ilgesniu (12 savaičių) gijimo periodu celiuliozės kompozitinių karkasų bioaktyvumas taip pat priklausė nuo HA dalelių tipo – celiuliozės-nHA kompozitams nustatytas labiau išreikštas naujo kaulo formavimasis, palyginti su celiuliozės-µHA kompozitais, tiek L-PRF, tiek fiziologiniu tirpalu rehidruotose grupėse ($p = 0,001$).

Šiame tyrime nustatyta, kad papildomas transplantantų bioaktyvavimas L-PRF taip pat turi įtakos naujo kaulinio audinio formavimuisi *in vivo*. L-PRF yra silpnomis osteokondukcinėmis savybėmis pasižyminti biomedžiaga. Pašalinus eksudatą, L-PRF netenka nuo 84 iki 98 proc. savo svorio [284], todėl vienas L-PRF nerekomenduojamas naudoti kaip osteokondukcinis karkasas. Iš kitos pusės, lėtos rezobcijos osteokondukcinės medžiagos, naudojamos kaulo regeneracijai (ksenogeniniai, alogeniniai, sintetiniai kaulo transplantantai), atlikdamos osteokondukcinę funkciją, kartu gali lėtinti kaulo regeneracijos procesą [285, 286]. Literatūros duomenimis, transplantantų bioaktyvinimas L-PRF osteokondukcinei matricai suteikia osteopromocinių savybių [258–260]. Šiuo atveju savo osteopromocinėmis savybėmis L-PRF gali pagerinti transplantanto biologinį aktyvumą, regeneruojamoje srityje paskatindamas angiogenezę, ląstelių chemotaksio, proliferacijos ir diferenciacijos procesus [287], tai netiesiogiai patvirtina ir šio darbo *in vivo* dalies rezultatai, parodę, kad visose tirtosiose grupėse transplantantų bioaktyvavimas L-PRF statistiškai reikšmingai padidino BV/TV santykį ($p = 0,001$) abiem tirtaisiais (4 ir 12 savaičių) laiko intervalais.

Tyrime vertinant ilgesnį kaulo gijimo periodą (12 savaičių), tarp visų tirtųjų transplantantų, L-PRF bioaktyvuotų celiuliozės-nHA transplantantų grupėje nustatytas statistiškai reikšmingai didžiausias naujo kaulo formavimasis ($p = 0,001$). nHA ir L-PRF aktyvumas pagrįstas tam tikrų kaulo gijimo proceso fazių moduliacija. Kaulo defekto regeneracijos procesas turi kiekvienos žaizdos gijimui būdingas išreikštas 4 gijimo fazes: hemostazės, uždegimo, regeneracijos, remodeliacijos [261]. Gijimo proceso pradžioje į kaulinį defektą implantuotas neaktyvuotas kaulo transplantantas užsipildo krauju, susiformuoja stabilizuotas kraujo krešulys, moduliuojantis tolimesnę gijimo proceso eigą. Transplantantus bioaktyvavus L-PRF, kaulo defekte suformuojamas optimizuotas kraujo krešulys [154, 274], turintis 4–7 kartus didesnę trombocitų ir leukocitų [173, 297, 322], bei 2–5 kartus didesnę augimo faktorių koncentraciją, palyginti su natūraliu kraujo krešuliu [270–273]. L-PRF palaipsniui atpalaiduoja augimo faktorius, aktyvuojančius molekulinį ir ląstelinį atsaką, ir moduliuojančius balansą tarp uždegiminės ir regeneracinės gijimo fazių [275, 276]. Tam tikri uždegiminiai mediatoriai ir saikingai išreikštas uždegimas yra būtini kaulo gijimo procesui, tačiau per stipriai išreikštas uždegiminis atsakas gali neigiamai veikti kaulinio audinio formavimąsi ar netgi sukelti jo destrukciją [262]. L-PRF eksudate ir matrikse koncentruoti citokinai, adheziniai baltymai, leukocitų ir trombocitų augimo faktoriai skatina ląstelių chemotaksį, neovaskuliarizaciją, osteogeninių ląstelių migraciją, adheziją, proliferaciją ir diferenciaciją [16–18], taip sutrumpinant žaizdos gijimo kaskados uždegiminę ir skatinant regeneracinę fazes [263, 264]. HA dalelės taip pat turi įtakos žaizdos gijimo uždegiminės fazės eigai. Nustatyta, kad nHA dalelės sukelia mažesnę organizmo imuninę-uždegiminę reakciją nei µHA dalelės [265]. Už uždegiminį atsaką atsakingos imunokompetentinės ląstelės lengvai fagocituoja mažas nHA daleles, o µHA dalelės linkę jungtis prie šių ląstelių membranų paviršiaus ir provokuoti labiau išreikštą uždegiminę reakciją [266]. Nanohidroksiapatito dalelės taip pat gali turėti tiesioginės įtakos kaulo formavimosi proceso moduliacijai. Aksakal ir kt. 2014 m. [267] publikuotoje studijoje nustatė geresnę titano lydinio implantų, padengtų nHA dalelėmis fiksaciją, stabilizaciją, didesnį kaulo įaugimą ir osteointegraciją nei µHA dalelėmis dengtų implantų. Tiesioginė nHA transplantantų implantacija į eksperimentinius kaulo defektus taip pat labiau paskatina naujo kaulinio audinio formavimąsi nei į defektus implantuotų µHA karkasų atveju [248, 268]. Chung ir kt. 2011 m. [269] taip pat nustatė didesnį trabekulinio kaulo formavimąsi bioskaidžiuose kompozitiniuose karkasuose su įterptomis nHA dalelėmis nei karkasuose su µHA dalelėmis. Tai patvirtina ir šio darbo *in vivo* dalyje su celiuliozės-nHA kompozitiniais transplantantais gauti geresni naujo kaulo formavimosi rezultatai.

6.3. Klinikinių tyrimų rezultatų aptarimas

Šio darbo klinikinėje dalyje vertintas Juodžbalio ir Daugėlos pasiūlytos RAŽTKD šalinimo sudėtingumo klasifikacijos [199] patikimumas bei L-PRF įtaką alveolito pasireiškimui, minkštųjų audinių gijimui ir pooperaciniam pacientų diskomfortui. Nustatyta statistiškai reikšminga priklausomybė tarp RAŽTKD šalinimo sudėtingumo klasifikacijoje prognozuoto danties šalinimo sudėtingumo ir vykusios operacijos trukmės ($p = 0,002$). Tai leido standartizuoti RAŽTKD šalinimo operacijų modelį, vertinant L-PRF įtaką pooperaciniam gijimui.

Literatūroje yra plačiai aprašytas L-PRF klinikinis panaudojimas burnos chirurgijoje [154, 274]. Suttapreyasri ir Leepong 2013 m. [279] tyrė L-PRF įtaką poekstrakcinių alveolės žaizdų gijimui ir kaulo rezorbcijai po prieškrūminių dantų šalinimo. Autoriai nenustatė L-PRF įtakos poekstrakcinei kaulo rezorbcijai, tačiau L-PRF reikšmingai pagerino minkštųjų audinių gijimą. Marenzi ir kt. 2015 m. [280], Singh ir kt. 2012 m. [281] ir Varghese ir kt. 2017 m. [282] taip pat nustatė geresnį prieškrūminių dantų poekstrakcinių defektų minkštųjų audinių gijimą bei mažesnį pooperacinį skausmo pasireiškimą pacientams, kuriems pašalintų dantų alveolės buvo užpildytos L-PRF. Yelamali ir Saikrishna 2015 m. [283] lygino PRP ir L-PRF efektyvumą RAŽTKD šalinimo operacijose ir nustatė geresnį minkštųjų audinių gijimą L-PRF grupėje. Literatūroje aprašomi duomenys sutampa ir su šio tyrimo rezultatais bei L-PRF grupėje nustatytu statistiškai reikšmingai mažesniu ($p = 0,001$) gijimo indeksu (geresniu minkštųjų audinių gijimu).

Šio darbo klinikinėje dalyje taip pat nustatytas statistiškai reikšmingai mažesnis alveolito pasireiškimas L-PRF užpildytose RAŽTKD alveolėse, palyginti su kontrole ($p = 0,001$). Alveolitas yra viena dažniausių po RAŽTKD šalinimo pasireiškiančių pooperacinių komplikacijų. Literatūroje aprašomas nuo 4,1 iki 32,6 proc. alveolito pasireiškimas po RAŽTKD šalinimo operacijų [288, 289]. Alveolitas yra multifaktorinė komplikacija, pirmiausia siejama su padidėjusiu vietiniu fibrinolitiniu aktyvumu ir kraujo krešulio suirimu pašalinto danties alveolėje [203, 290]. Pakankamai dideliam alveolito pasireiškimui po RAŽTKD šalinimo operacijų turi įtakos RAŽTKD anatominės srities didelis kaulo tankis, retas kraujagyslių tinklas ir mažas granuliacinio audinio formavimosi potencialas [291]. Hoaglin ir Lines 2013 m. [292] atliktas retrospektyvinis tyrimas su 100 pacientų, kuriems šalinti RAŽTKD, nustatė 1 proc. alveolito pasireiškimą L-PRF užpildytose alveolėse ir 9,5 proc. – alveolėse su natūraliu kraujo krešuliu. Panašūs rezultatai gauti ir kituose dviejuose tyrimuose [293, 294] bei šio darbo klinikinėje dalyje, kur taip pat nustatytas statistiškai reikšmingai mažesnis alveolito dažnis L-PRF grupėje ($p = 0,001$). L-PRF turi tvirtos struktūros

fibrino matricą [169, 278], kuri alveolėje pagerina hemostazę, padidina krešulio stabilizaciją [295] ir sudaro tinkamas sąlygas vykti kaulo ir minkštųjų audinių regeneracijos procesui [296]. Naudojant L-PRF pašalintų dantų alveolių užpildymui, iš gijimo kaskados taip pat eliminuojami eritrocitai ir jų irimo produktai, kas taip pat gali pagerinti gijimo proceso eigą [292]. L-PRF matricoje inkorporuoti trombocitai, leukocitai ir jų atpalaiduojami augimo faktoriai gyjančioje alveolėje atlieka imunomoduliacinį vaidmenį.

Trombocitai yra bebranduolės ląstelės, kurios savo citoplazmoje esančiose alfa, tankiosiose granulėse ir lizosomose kaupia įvairius bioaktyvius baltymus, citokinus ir augimo faktorius (PDGF, TGF-β, VEGF, FGF, IGF-1, EGF) [152, 153]. Aktyvuotų trombocitų atpalaiduojami augimo faktoriai skatina gijimą, veikdami įvairius ląstelinius receptorius, stimuliuodami chemotaksį, ląstelių migraciją, adheziją, proliferaciją ir diferenciaciją. Eksperimentinių studijų duomenys rodo, kad trombocitų išskiriami augimo faktoriai, tokie kaip FGF ir TGF-β1, skatina osteogenezę [312, 313]. FGF kartu su VEGF taip pat yra svarbūs angiogenezės ir vaskulogenezės induktoriai [128, 129, 132], tai užtikrina mitybinių substratų ir deguonies apykaitą regeneruojamame defekte [314]. PDGF stimuliuoja mezenchiminių kamieninių ląstelių migraciją ir proliferaciją bei prisideda prie kaulo, endotelio ir kitų mezoderminės kilmės audinių gijimo procesų [106, 277, 296, 315]. Tang ir kt. 2002 m. [152] nustatė, kad aktyvuoti trombocitai atpalaiduoja antimikrobinius baltymus (RANTES, trombocitų faktorių 4, jungiamojo audinio aktyvuojantį baltymą 3, trombocitų bazinį baltymą, timoziną β-4 ir fibrinopeptidus A ir B). Nustatyta, kad šios bioaktyvios medžiagos gali inhibuoti *Escherichia coli* ir *Staphylococcus aureus* augimą *in vitro* [152]. Trombocitų antimikrobiniai peptidai, sinergistiškai veikdami su fibrinogeno skilimo produktais, atlieka imunomoduliacinį vaidmenį, į gijimo sritį pritraukdami leukocitus ir skatindami jų antimikrobinį atsaką [152, 297, 298].

L-PRF matricoje inkorporuotų leukocitų populiaciją gausiausiai sudaro limfocitai ir neutrofilai, mažiau randama monocitų, eozinofilinių ir bazofilinių granuliocitų [297, 299]. Nors literatūroje aprašoma prieštaringų nuomonių dėl leukocitų reikšmės žaizdų gijimo ir kaulo regeneracijos procesuose [165, 192], gijimo srityje leukocitai yra nepakeičiama imunomoduliacinio proceso dalis ir yra atsakingi už specifinį ir nespecifinį imuninį atsaką [163, 300]. Limfocitai yra pagrindinės specifinio imuninio atsako ląstelės bei išskiria IGF-1 [320], kuris yra vienas svarbiausių faktorių ląstelės ciklo reguliacijai, ląstelių augimui ir diferenciacijai [321]. L-PRF fibrino matricoje inkorporuoti neutrofilai yra pirmosios ląstelės, pasirodančios gijimo srityje uždegiminės žaizdos gijimo stadijos pradžioje. Neutrofilai pasižymi

antimikrobiniu veikimu bei dalyvauja specifiniame ir nespecifiniame imuniniame atsake [301], gyjančioje žaizdoje atlikdami apsauginę funkciją. Monocitai, patekę į audinius, diferencijuoja į makrofagus. Makrofagai atlieka fagocitinę funkciją ir atpalaiduoja fermentus (kolagenazę, elastazę, plazminogeno aktyvatorių), palengvinančius negyvybingų audinių pašalinimą ir žaizdos gijimą [303]. Leukocitai yra ne tik imuninės ląstelės, jie taip pat išskiria audinių regeneracijai svarbius augimo faktorius. Makrofagai yra vieni pagrindinių kaulo gijimo mediatorių, lemiančių kaulinės žaizdos gijimo perėjimą iš uždegiminės į regeneracinę fazę ir osteogenezę [302, 303]. Makrofagų išskiriami TGF-β stimuliuoja keratinocitus [302]. Makrofagų sekretuojami IL-1, FGF, ir TNF-α skatina kolageno sintezę fibroblastuose ir stimuliuoja angiogenezę [126, 127, 302], o onkostatinas M, BMP-2 ir BMP-4 skatina osteogenezę [316–318]. Nustatyta, kad PDGF, kuris ilgą laiką buvo priskiriamas tik trombocituose randamiems augimo faktoriams, taip pat išskiriamas makrofagų [319].

Leukocitai taip pat išskiria įvairius chemokinus, uždegimą slopinančius interleukinus (IL-4, IL-10, IL-13) ir opioidinius baltymus (β-endorfiną, metenkefaliną, dinorfiną-A). Šie citokinai gali sutrumpinti žaizdos gijimo uždegiminę fazę, nuslopindami organizme produkuojamus uždegiminius faktorius, taip pat turi antinociceptinių savybių, galinčių sumažinti pooperacinio skausmo jutimą. [168]. Šio darbo klinikinėje dalyje pirmąją pooperacinę savaitę nustatytas statistiškai reikšmingai sumažėjęs pacientų skausminis diskomfortas, RAŽTKD šalinimo operacijose naudojant L-PRF ($p = 0,001$). 1-ą ($p = 0,035$) ir 3-ą ($p = 0,023$) pooperacinėmis dienomis taip pat nustatytas mažesnis veido tinimas L-PRF grupės pusėse, palyginti su kontrole. Pooperacinio skausmo ir tinimo sumažinimas turi didelės reikšmės RAŽTKD šalinimo operacijos sėkmingumui. Klinikinėje praktikoje efektyvus pacientų patiriamo pooperacinio diskomforto sumažinimas, reikalauja mažesnio skaičiaus neplanuotų pooperacinių vizitų ir pagerina bendrą paciento savijautą gijimo periodu [213, 311]. Literatūroje aprašoma nemažai tyrimų, analizavusių pooperacinį skausmą [281, 294, 304–309] ir tinimą [303–309] po RAŽTKD šalinimo operacijų. Nurodomi prieštaringi duomenys apie L-PRF įtaką pooperaciniam pacientų diskomfortui po RAŽTKD šalinimo operacijų. Kai kurie autoriai nenustatė statistiškai reikšmingos L-PRF įtakos pooperacinio skausmo [281, 306, 308] ir tinimo [303, 308, 309] sumažinimui. Kituose tyrimuose rastas statistiškai reikšmingas L-PRF poveikis sumažinant pooperacinį skausmą [294, 304, 305, 307, 309] ir tinimą [306, 307] po RAŽTKD šalinimo. Su pastarųjų studijų duomenimis sutampa ir šio darbo klinikinėje dalyje nustatytas teigiamas L-PRF poveikis tiek pacientų pooperacinio skausmo, tiek pooperacinio veido tinimo sumažinimui. Svarbu pažymėti, kad 7-ą pooperacinę dieną skausmo intensyvumo

VAS skalės balų vidurkis, tiek L-PRF ($p = 0,001$), tiek kontrolinėje grupėje ($p = 0,001$) statistiškai reikšmingai skyrėsi nuo nulinių priešoperacinių VAS reikšmių. Pirmosios pooperacinės savaitės pabaigoje veido tinimas statistiškai nesiskyrė nuo pradinių verčių tik L-PRF grupėje ($p = 0,593$). Kontrolinėje grupėje, praėjus savaitei po operacijos, išliko statistiškai reikšmingas veido patinimas ($p = 0,001$), palyginti su priešoperacinėmis vertėmis. Šie rezultatai atitinka ir kitų literatūros šaltinių duomenis [292, 294, 304, 307, 310], kuriuose pooperacinės komplikacijos po RAŽTKD šalinimo operacijų nustatomos ir vėliau nei per pirmąją pooperacinę savaitę. Atsižvelgiant į vėlyvųjų komplikacijų pasireiškimą, šio darbo autoriai po RAŽTKD šalinimo operacijų rekomenduoja bent 2 savaičių pooperacinio stebėjimo periodą.

IŠVADOS

1. Susintetinti eksperimentiniai celiuliozės-nHA ir celiuliozės-µHA karkasai atitinka pagrindinius kaulinio audinio transplantantams keliamus struktūrinius, fizikocheminius ir biologinius reikalavimus.

2. Hidroksiapatito užpildo dalelių dydis turi įtakos celiuliozės-HA kompozitinių karkasų *in vitro* biologinėms savybėms. Celiuliozės-nHA karkasai pasižymi geresne ląstelių adhezija, didesniu osteoblastinių ląstelių metaboliniu aktyvumu ir didesne osteoblastinių genų raiška, palyginti su celiuliozės-µHA karkasais, *in vitro*.

3. µKT ir histologiškai tiriant celiuliozės-µHA ir celiuliozės-nHA matricų biosuderinamumą, bioskaidumą ir naujo kaulo formavimąsi, nustatyta, kad hidroksiapatito užpildo dalelių dydis turi įtakos celiuliozės-HA kompozitinių karkasų *in vivo* biologinėms savybėms. Celiuliozės-nHA karkasai 12-os savaičių laikotarpiu pasižymi didesniu naujo kaulo formavimusi *in vivo*, palyginti su celiuliozės-µHA karkasais ir kontroliniu alogeniniu transplantantu.

4. µKT ir histologiniais tyrimais nustatyta, kad celiuliozės-µHA ir celiuliozės-nHA karkasų bioaktyvinimas L-PRF didina naujo kaulo susiformavimą *in vivo*.

5. Didžiausiu naujo kaulo formavimusi 12-os savaičių laikotarpiu tarp visų tirtųjų transplantantų *in vivo* pasižymėjo L-PRF bioaktyvuoti celiuliozės-nHA transplantantai.

6. Juodžbalio ir Daugėlos pasiūlyta ir su bendraautoriais validuota RAŽTKD šalinimo sudėtingumo klasifikacija leidžia patikimai prognozuoti RAŽTKD šalinimo operacijos trukmę.

7. L-PRF gali sumažinti alveolito pasireiškimą, pacientų patiriamą pooperacinį skausmo diskomfortą veido tinimą bei pagerinti ankstyvąjį minkštųjų audinių gijimą po RAŽTKD šalinimo operacijų.

MOKSLINĖS IR PRAKTINĖS REKOMENDACIJOS

Remiantis gautais šio darbo rezultatais, rekomenduojama:

1. Tęsti sukurtų eksperimentinių celiuliozės matricų su µHA ir nHA užpildais mokslinius tyrimus, siekiant jų aprobavimo klinikiniam naudojimui.

2. L-PRF gali būti naudojama kaip autogeninė osteopromocinė medžiaga kartu su osteokondukciniais karkasais žandikaulių kaulinių defektų regeneracijai.

3. Gydytojams praktikams rekomenduojama naudoti pasiūlytą RAŽTKD šalinimo sudėtingumo klasifikaciją operacijos planavimui, operacijos rizikos veiksnių įvertinimui, RAŽTKD šalinimo sudėtingumo ir operacijos trukmės prognozei.

4. Moksliniuose tyrimuose, naudojančiuose RAŽTKD modelį, rekomenduojama pasiūlytą RAŽTKD šalinimo sudėtingumo klasifikaciją naudoti tiriamųjų grupių standartizavimui.

5. Klinikinėje praktikoje L-PRF gali būti naudojamas kaip profilaktinė priemonė alveolito prevencijai, minkštųjų audinių gijimo pagerinimui ir pacientų pooperacinio diskomforto (skausmo, tinimo) sumažinimui ankstyvuoju gijimo periodu po RAŽTKD šalinimo operacijų.

BIBLIOGRAFIJOS SĄRAŠAS

1. Cha HS, Kim JW, Hwang JH, Ahn KM. Frequency of bone graft in implant surgery. Maxillofac Plast Reconstr Surg. 2016 Mar 31;38(1):19.
2. Schiegnitz E, Al-Nawas B, Tegner A, Sagheb K, Berres M, Kämmerer PW, Wagner W. Clinical and Radiological Long-Term Outcome of a Tapered Implant System with Special Emphasis on the Influence of Augmentation Procedures. Clin Implant Dent Relat Res. 2016 Aug;18(4):810–20.
3. Retzepi M, Donos N. Guided Bone Regeneration: biological principle and therapeutic applications. Clin Oral Implants Res. 2010 Jun;21(6):567–76.
4. Bruder SP, Fox BS. Tissue engineering of bone. Cell based strategies. Clin Orthop Relat Res. 1999 Oct;(367 Suppl):S68-83.
5. Ebraheim NA, Elgafy H, Xu R. Bone-graft harvesting from iliac and fibular donor sites: techniques and complications. J Am Acad Orthop Surg. 2001 May-Jun;9(3):210–8.
6. Kim Y, Nowzari H, Rich SK. Risk of prion disease transmission through bovine-derived bone substitutes: a systematic review. Clin Implant Dent Relat Res. 2013 Oct;15(5):645–53.
7. Artzi Z, Tal H, Dayan D. Porous bovine bone mineral in healing of human extraction sockets. Part 1: histomorphometric evaluations at 9 months. J Periodontol. 2000 Jun;71(6):1015–23.
8. Ramírez-Fernández MP, Calvo-Guirado JL, Maté-Sánchez Del Val JE, Delgado-Ruiz RA, Negri B, Barona-Dorado C. Ultrastructural study by backscattered electron imaging and elemental microanalysis of bone-to-biomaterial interface and mineral degradation of porcine xenografts used in maxillary sinus floor elevation. Clin Oral Implants Res. 2013 May;24(5): 523–30.
9. Oryan A, Alidadi S, Moshiri A, Maffulli N. Bone regenerative medicine: classic options, novel strategies, and future directions. J Orthop Surg Res. 2014 Mar 17;9(1):18.
10. Tayton E, Purcell M, Aarvold A, Smith JO, Kalra S, Briscoe A, Shakesheff K, Howdle SM, Dunlop DG, Oreffo RO. Supercritical CO2 fluid-foaming of polymers to increase porosity: a method to improve the mechanical and biocompatibility characteristics for use as a potential alternative to allografts in impaction bone grafting? Acta Biomater. 2012 May;8(5):1918–27.
11. Herford AS, Tandon R, Stevens TW, Stoffella E, Cicciu M. Immediate distraction osteogenesis: the sandwich technique in combination with rhBMP-2 for anterior maxillary and mandibular defects. J Craniofac Surg. 2013 Jul;24(4):1383–7.
12. Woo EJ. Adverse events reported after the use of recombinant human bone morphogenetic protein 2. J Oral Maxillofac Surg. 2012 Apr;70(4):765–7.
13. Kim MJ, Kim KM, Kim J, Kim KN. BMP-2 promotes oral squamous carcinoma cell invasion by inducing CCL5 release. PLoS One. 2014 Oct 1;9(10):e108170.

14. Dohan DM, Choukroun J, Diss A, Dohan SL, Dohan AJ, Mouhyi J, Gogly B. Platelet-rich fibrin (PRF): a second-generation platelet concentrate. Part I: technological concepts and evolution. Oral Surg Oral Med Oral Pathol Oral Radiol Endod. 2006 Mar;101(3):e37–44.
15. He L, Lin Y, Hu X, Zhang Y, Wu H. A comparative study of platelet-rich fibrin (PRF) and platelet-rich plasma (PRP) on the effect of proliferation and differentiation of rat osteoblasts in vitro. Oral Surg Oral Med Oral Pathol Oral Radiol Endod. 2009 Nov;108(5):707–713.
16. Dohan Ehrenfest DM, Diss A, Odin G, Doglioli P, Hippolyte MP, Charrier JB. In vitro effects of Choukroun's PRF (platelet-rich fibrin) on human gingival fibroblasts, dermal prekeratinocytes, preadipocytes, and maxillofacial osteoblasts in primary cultures. Oral Surg Oral Med Oral Pathol Oral Radiol Endod. 2009 Sep;108(3):341–352.
17. Chang IC, Tsai CH, Chang YC. Platelet-rich fibrin modulates the expression of extracellular signal-regulated protein kinase and osteoprotegerin in human osteoblasts. J Biomed Mater Res A. 2010 Oct;95(1):327–332.
18. Dohan Ehrenfest DM, Doglioli P, de Peppo GM, Del Corso M, Charrier JB. Choukroun's platelet-rich fibrin (PRF) stimulates in vitro proliferation and differentiation of human oral bone mesenchymal stem cell in a dose-dependent way. Arch Oral Biol. 2010 Mar;55(3):185–194.
19. Gao C, Deng Y, Feng P, Mao Z, Li P, Yang B, Deng J, Cao Y, Shuai C, Peng S. Current progress in bioactive ceramic scaffolds for bone repair and regeneration. Int J Mol Sci. 2014 Mar 18;15(3):4714–32.
20. BaoLin G, Ma PX. Synthetic biodegradable functional polymers for tissue engineering: a brief review. Sci China Chem. 2014 Apr 1;57(4):490–500.
21. Qiu K, Netravali AN. A review of fabrication and applications of bacterial cellulose based nanocomposites. Polym Rev. 2014 54:598–626.
22. Salgado AJ, Coutinho OP, Reis RL. Novel starch-based scaffolds for bone tissue engineering: cytotoxicity, cell culture, and protein expression. Tissue Eng. 2004 Mar-Apr;10(3–4):465–74.
23. Wang X, Wang X, Tan Y, Zhang B, Gu Z, Li X. Synthesis and evaluation of collagen-chitosan-hydroxyapatite nanocomposites for bone grafting. J Biomed Mater Res A. 2009 Jun 15;89(4):1079–87.
24. Wilson DB. Three microbial strategies for plant cell wall degradation. Ann N Y Acad Sci. 2008 Mar;1125:289–97.
25. Märtson M, Viljanto J, Hurme T, Laippala P, Saukko P. Is cellulose sponge degradable or stable as implantation material? An in vivo subcutaneous study in the rat. Biomaterials. 1999 Nov;20(21):1989–95.
26. Hämmerle CH, Jung RE. Bone augmentation by means of barrier membranes. Periodontol 2000. 2003;33:36–53.
27. Liu J, Kerns DG. Mechanisms of guided bone regeneration: a review. Open Dent J. 2014 May 16;8:56–65.
28. Dahlin C, Linde A, Gottlow J, Nyman S. Healing of bone defects by guided tissue regeneration. Plast Reconstr Surg. 1988 May;81(5):672–6.

29. Engler WO, Ramfjord SP, Hiniker JJ. Healing following simple gingivectomy. A tritiated thymidine radioautographic study. I. Epithelialization. J Periodontol. 1966 Jul-Aug;37(4):298–308.
30. Schenk RK, Buser D, Hardwick WR, Dahlin C. Healing pattern of bone regeneration in membrane-protected defects: a histologic study in the canine mandible. Int J Oral Maxillofac Implants. 1994 Jan-Feb;9(1):13–29.
31. Javed A, Chen H, Ghori FY. Genetic and transcriptional control of bone formation. Oral Maxillofac Surg Clin North Am. 2010 Aug;22(3):283–93.
32. Byun SH, Lim HK, Kim SM, Lee SM, Kim HE, Lee JH. The Bioresorption and Guided Bone Regeneration of Absorbable Hydroxyapatite-Coated Magnesium Mesh. J Craniofac Surg. 2017 Mar;28(2):518–523.
33. Ersanli S, Olgac V, Leblebicioglu B. Histologic analysis of alveolar bone following guided bone regeneration. J Periodontol. 2004 May;75(5):750–6.
34. Artzi Z, Tal H, Dayan D. Porous bovine bone mineral in healing of human extraction sockets: 2. Histochemical observations at 9 months. J Periodontol. 2001 Feb;72(2):152–9.
35. Hermann JS, Buser D. Guided bone regeneration for dental implants. Curr Opin Periodontol. 1996;3:168–77.
36. Sanz-Martin I, Ferrantino L, Vignoletti F, Nuñez J, Baldini N, Duvina M, Alcaraz J, Sanz M. Contour changes after guided bone regeneration of large non-contained mandibular buccal bone defects using deproteinized bovine bone mineral and a porcine-derived collagen membrane: an experimental in vivo investigation. Clin Oral Investig. 2018 Apr;22(3):1273–1283.
37. Li G, Zhou T, Lin S, Shi S, Lin Y. Nanomaterials for Craniofacial and Dental Tissue Engineering. J Dent Res. 2017 Jul;96(7):725–732.
38. Langer R, Vacanti JP. Tissue engineering. Science. 1993 May 14;260(5110): 920–6.
39. Amini AR, Laurencin CT, Nukavarapu SP. Bone tissue engineering: recent advances and challenges. Crit Rev Biomed Eng. 2012;40(5):363–408.
40. Hosseinpour S, Ghazizadeh Ahsaie M, Rezai Rad M, Baghani MT, Motamedian SR, Khojasteh A. Application of selected scaffolds for bone tissue engineering: a systematic review. Oral Maxillofac Surg. 2017 Jun;21(2):109–129.
41. Fu Y, Deng S, Wang J, Chen Z, Zhang S, Wu S, Jiang Y, Ye L, Peng Q, Lin Y. Potential replication of induced pluripotent stem cells for craniofacial reconstruction. Curr Stem Cell Res Ther. 2014 May;9(3):205–14.
42. Bruder SP, Kraus KH, Goldberg VM, Kadiyala S. The effect of implants loaded with autologous mesenchymal stem cells on the healing of canine segmental bone defects. J Bone Joint Surg Am. 1998 Jul; 80(7):985–96.
43. Giannoudis PV, Dinopoulos H, Tsiridis E. Bone substitutes: an update. Injury. 2005 Nov;36 Suppl 3:S20–7.
44. Albrektsson T, Johansson C. Osteoinduction, osteoconduction and osseointegration. Eur Spine J. 2001 Oct;10 Suppl 2:S96–101.

45. Acocella A, Bertolai R, Colafranceschi M, Sacco R. Clinical, histological and histomorphometric evaluation of the healing of mandibular ramus bone block grafts for alveolar ridge augmentation before implant placement. J Craniomaxillofac Surg. 2010 Apr;38(3):222–30.
46. El-Ghannam A. Bone reconstruction: from bioceramics to tissue engineering. Expert Rev Med Devices. 2005 Jan;2(1):87–101.
47. Henkel J, Woodruff MA, Epari DR, Steck R, Glatt V, Dickinson IC, Choong PF, Schuetz MA, Hutmacher DW. Bone Regeneration Based on Tissue Engineering Conceptions - A 21st Century Perspective. Bone Res. 2013 Sep 25;1(3):216–48.
48. Hutmacher DW. Scaffolds in tissue engineering bone and cartilage. Biomaterials. 2000 Dec;21(24):2529–43.
49. Fillingham Y, Jacobs J. Bone grafts and their substitutes. Bone Joint J. 2016 Jan;98-B(1 Suppl A):6–9.
50. Kumar P, Vinitha B, Fathima G. Bone grafts in dentistry. J Pharm Bioallied Sci. 2013 Jun;5(Suppl 1):S125–7.
51. Kolk A, Handschel J, Drescher W, Rothamel D, Kloss F, Blessmann M, Heiland M, Wolff KD, Smeets R. Current trends and future perspectives of bone substitute materials - from space holders to innovative biomaterials. J Craniomaxillofac Surg. 2012 Dec;40(8):706–18.
52. Laurencin C, Khan Y, El-Amin SF. Bone graft substitutes. Expert Rev Med Devices. 2006 Jan;3(1):49–57.
53. Reddy BR, Sudhakar J, Rajesh N, Sandeep V, Reddy YM, Gnana Sagar WR. Comparative clinical and radiographic evaluation of mineralized cancellous bone allograft (puros®) and autogenous bone in the treatment of human periodontal intraosseous defects: 6-months follow-up study. J Int Soc Prev Community Dent. 2016 Dec;6(Suppl 3):S248–S253.
54. Moest T, Wehrhan F, Lutz R, Schmitt CM, Neukam FW, Schlegel KA.Extra-oral defect augmentation using autologous, bovine and equine bone blocks: A preclinical histomorphometrical comparative study. J Craniomaxillofac Surg. 2015 May;43(4):559–66.
55. Lee CY, Prasad HS, Suzuki JB, Stover JD, Rohrer MD. The correlation of bone mineral density and histologic data in the early grafted maxillary sinus: a preliminary report. Implant Dent. 2011 Jun;20(3):202–14.
56. Pountos I, Giannoudis PV.Injury. Is there a role of coral bone substitutes in bone repair? 2016 Dec;47(12):2606–2613.
57. Pereira RS, Menezes JD, Bonardi JP, Griza GL, Okamoto R, Hochuli-Vieira E. Comparative study of volumetric changes and trabecular microarchitecture in human maxillary sinus bone augmentation with bioactive glass and autogenous bone graft: a prospective and randomized assessment. Int J Oral Maxillofac Surg. 2018 May;47(5):665–671.
58. Knabe C, Adel-Khattab D, Kluk, Struck R, Stiller M. Effect of a Particulate and a Putty-Like Tricalcium Phosphate-Based Bone-grafting Material on Bone Formation, Volume Stability and Osteogenic Marker Expression after

Bilateral Sinus Floor Augmentation in Humans. J Funct Biomater. 2017 Jul 29;8(3).
59. Pradeep AR, Bajaj P, Rao NS, Agarwal E, Naik SB. Platelet-Rich Fibrin Combined With a Porous Hydroxyapatite Graft for the Treatment of 3-Wall Intrabony Defects in Chronic Periodontitis: A Randomized Controlled Clinical Trial. J Periodontol. 2017 Dec;88(12):1288–1296.
60. Pandit N, Sharma A, Jain A, Bali D, Malik R, Gugnani S. The use of nanocrystalline and two other forms of calcium sulfate in the treatment of infrabony defects: A clinical and radiographic study. J Indian Soc Periodontol. 2015 Sep–Oct;19(5):545–53.
61. Dursun CK, Dursun E, Eratalay K, Orhan K, Tatar I, Baris E, Tözüm TF. Effect of Porous Titanium Granules on Bone Regeneration and Primary Stability in Maxillary Sinus: A Human Clinical, Histomorphometric, and Microcomputed Tomography Analyses. J Craniofac Surg. 2016 Mar;27(2): 391–7.
62. Brown A, Zaky S, Ray H Jr, Sfeir C. Porous magnesium/PLGA composite scaffolds for enhanced bone regeneration following tooth extraction. Acta Biomater. 2015 Jan;11:543–53.
63. Bae JC, Lee JJ, Shim JH, Park KH, Lee JS, Bae EB, Choi JW, Huh JB. Development and Assessment of a 3D-Printed Scaffold with rhBMP-2 for an Implant Surgical Guide Stent and Bone Graft Material: A Pilot Animal Study. Materials (Basel). 2017 Dec 16;10(12).
64. Akita D, Morokuma M, Saito Y, Yamanaka K, Akiyama Y, Sato M, Mashimo T, Toriumi T, Arai Y, Kaneko T, Tsukimura N, Isokawa K, Ishigami T, Honda MJ. Periodontal tissue regeneration by transplantation of rat adipose-derived stromal cells in combination with PLGA-based solid scaffolds. Biomed Res. 2014;35(2):91–103.
65. Requicha JF, Viegas CA, Muñoz F, Azevedo JM, Leonor IB, Reis RL, Gomes ME. A tissue engineering approach for periodontal regeneration based on a biodegradable double-layer scaffold and adipose-derived stem cells. Tissue Eng Part A. 2014 Sep;20(17–18):2483–92.
66. Ahsan SM, Thomas M, Reddy KK, Sooraparaju SG, Asthana A, Bhatnagar I. Chitosan as biomaterial in drug delivery and tissue engineering. Int J Biol Macromol. 2018 Apr 15;110:97–109.
67. Nakajima D, Tabata Y, Sato S. Periodontal tissue regeneration with PRP incorporated gelatin hydrogel sponges. Biomed Mater. 2015 Oct 20;10(5): 055016.
68. Petrauskaitė O, Gomes Pde S, Fernandes MH, Juodzbalys G, Stumbras A, Maminskas J, Liesiene J, Cicciù M. Biomimetic mineralization on a macroporous cellulose-based matrix for bone regeneration. Biomed Res Int. 2013;2013:452750.
69. Chen X, Zhao Y, Geng S, Miron RJ, Zhang Q, Wu C, Zhang Y. In vivo experimental study on bone regeneration in critical bone defects using PIB

nanogels/boron-containing mesoporous bioactive glass composite scaffold. Int J Nanomedicine. 2015 Jan 22;10:839–46.
70. Iviglia G, Cassinelli C, Torre E, Baino F, Morra M, Vitale-Brovarone C. Novel bioceramic-reinforced hydrogel for alveolar bone regeneration. Acta Biomater. 2016 Oct 15;44:97–109.
71. Baheiraei N, Nourani MR, Mortazavi SMJ, Movahedin M, Eyni H, Bagheri F, Norahan MH. Development of a bioactive porous collagen/β-tricalcium phosphate bone graft assisting rapid vascularization for bone tissue engineering applications. J Biomed Mater Res A. 2018 Jan;106(1):73–85.
72. Ma Y, Zhang W, Wang Z, Wang Z, Xie Q, Niu H, Guo H, Yuan Y, Liu C. PEGylated poly(glycerol sebacate)-modified calcium phosphate scaffolds with desirable mechanical behavior and enhanced osteogenic capacity. Acta Biomater. 2016 Oct 15;44:110–24.
73. Dimitriou R, Tsiridis E, Giannoudis PV. Current concepts of molecular aspects of bone healing. Injury. 2005 Dec;36(12):1392–404.
74. Lu J, Hao Y, Zhao W, Lyu C, Zou D. Molecular, Cellular and Pharmaceutical Aspects of Autologous Grafts for Peri-implant Hard and Soft Tissue Defects. Curr Pharm Biotechnol. 2017;18(1):85–94.
75. Herford AS, Miller M, Signorino F. Maxillofacial Defects and the Use of Growth Factors. Oral Maxillofac Surg Clin North Am. 2017 Feb;29(1):75–88.
76. Misch CM. The Lazarus Bone Graft: Revitalizing Allogenic Bone Blocks. Dent Today. 2016 Nov;35(11):114, 116, 118–9.
77. Kubota A, Sarmiento H, Alqahtani MS, Llobell A, Fiorellini JP. The Use of Recombinant Human Platelet-Derived Growth Factor for Maxillary Sinus Augmentation. Int J Periodontics Restorative Dent. 2017 Mar/Apr; 37(2):219–225.
78. Poon B, Kha T, Tran S, Dass CR. Bone morphogenetic protein-2 and bone therapy: successes and pitfalls. J Pharm Pharmacol. 2016 Feb;68(2):139–47.
79. Rodriguez IA, Sell SA, McCool JM, Saxena G, Spence AJ, Bowlin GL. A preliminary evaluation of lyophilized gelatin sponges, enhanced with platelet-rich plasma, hydroxyapatite and chitin whiskers for bone regeneration. Cells. 2013 Apr 26;2(2):244–65.
80. Bajestan MN, Rajan A, Edwards SP, Aronovich S, Cevidanes LHS, Polymeri A, Travan S, Kaigler D. Stem cell therapy for reconstruction of alveolar cleft and trauma defects in adults: A randomized controlled, clinical trial. Clin Implant Dent Relat Res. 2017 Oct;19(5):793–801.
81. Frasca S, Norol F, Le Visage C, Collombet JM, Letourneur D, Holy X, Sari Ali E. Calcium-phosphate ceramics and polysaccharide-based hydrogel scaffolds combined with mesenchymal stem cell differently support bone repair in rats. J Mater Sci Mater Med. 2017 Feb;28(2):35.
82. Nuntanaranont T, Promboot T, Sutapreyasri S. Effect of expanded bone marrow-derived osteoprogenitor cells seeded into polycaprolactone/ trical-

cium phosphate scaffolds in new bone regeneration of rabbit mandibular defects. J Mater Sci Mater Med. 2018 Feb 9;29(3):24.
83. Adel-Khattab D, Giacomini F, Gildenhaar R, Berger G, Gomes C, Linow U, Hardt M, Peleska B, Günster J, Stiller M, Houshmand A, Ghaffar KA, Gamal A, El-Mofty M, Knabe C. Development of a synthetic tissue engineered three-dimensional printed bioceramic-based bone graft with homogenously distributed osteoblasts and mineralizing bone matrix in vitro. J Tissue Eng Regen Med. 2018 Jan;12(1):44–58.
84. van Gastel N, Torrekens S, Roberts SJ, Moermans K, Schrooten J, Carmeliet P, Luttun A, Luyten FP, Carmeliet G. Engineering vascularized bone: osteogenic and proangiogenic potential of murine periosteal cells. Stem Cells. 2012 Nov;30(11):2460–71.
85. Fröhlich M, Grayson WL, Wan LQ, Marolt D, Drobnic M, Vunjak-Novakovic G. Tissue engineered bone grafts: biological requirements, tissue culture and clinical relevance. Curr Stem Cell Res Ther. 2008 Dec;3(4):254–64.
86. Kaigler D, Pagni G, Park CH, Braun TM, Holman LA, Yi E, Tarle SA, Bartel RL, Giannobile WV. Stem cell therapy for craniofacial bone regeneration: a randomized, controlled feasibility trial. Cell Transplant. 2013;22(5): 767–77.
87. Gonshor A, McAllister BS, Wallace SS, Prasad H. Histologic and histomorphometric evaluation of an allograft stem cell-based matrix sinus augmentation procedure. Int J Oral Maxillofac Implants. 2011 Jan-Feb;26(1): 123–31.
88. Kaigler D, Avila-Ortiz G, Travan S, Taut AD, Padial-Molina M, Rudek I, Wang F, Lanis A, Giannobile WV. Bone Engineering of Maxillary Sinus Bone Deficiencies Using Enriched CD90+ Stem Cell Therapy: A Randomized Clinical Trial. J Bone Miner Res. 2015 Jul;30(7):1206–16.
89. Wildburger A, Payer M, Jakse N, Strunk D, Etchard-Liechtenstein N, Sauerbier S. Impact of autogenous concentrated bone marrow aspirate on bone regeneration after sinus floor augmentation with a bovine bone substitute-a split-mouth pilot study. Clin Oral Implants Res. 2014 Oct;25(10):1175–81.
90. Rickert D, Vissink A, Slot WJ, Sauerbier S, Meijer HJ, Raghoebar GM. Maxillary sinus floor elevation surgery with BioOss® mixed with a bone marrow concentrate or autogenous bone: test of principle on implant survival and clinical performance. Int J Oral Maxillofac Surg. 2014 Feb;43(2):243–7.
91. Chen FM, Gao LN, Tian BM, Zhang XY, Zhang YJ, Dong GY, Lu H, Chu Q, Xu J, Yu Y, Wu RX, Yin Y, Shi S, Jin Y. Treatment of periodontal intrabony defects using autologous periodontal ligament stem cells: a randomized clinical trial. Stem Cell Res Ther. 2016 Feb 19;7:33.
92. Walmsley GG, Ransom RC, Zielins ER, Leavitt T, Flacco JS, Hu MS, Lee AS, Longaker MT, Wan DC. Stem Cells in Bone Regeneration. Stem Cell Rev. 2016 Oct;12(5):524–529.

93. Fisher JN, Peretti GM, Scotti C. Stem Cells for Bone Regeneration: From Cell-Based Therapies to Decellularised Engineered Extracellular Matrices. Stem Cells Int. 2016;2016:9352598.
94. Caplan AI. Mesenchymal stem cells. J Orthop Res. 1991 Sep; 9(5):641–50.
95. Goshima J, Goldberg VM, Caplan AI. The osteogenic potential of culture-expanded rat marrow mesenchymal cells assayed in vivo in calcium phosphate ceramic blocks. Clin Orthop Relat Res. 1991 Jan; (262):298–311.
96. Pittenger MF, Mackay AM, Beck SC, Jaiswal RK, Douglas R, Mosca JD, Moorman MA, Simonetti DW, Craig S, Marshak DR. Multilineage potential of adult human mesenchymal stem cells. Science. 1999 Apr 2;284(5411): 143–7.
97. Bieback K, Kern S, Kocaömer A, Ferlik K, Bugert P. Comparing mesenchymal stromal cells from different human tissues: bone marrow, adipose tissue and umbilical cord blood. Biomed Mater Eng. 2008; 18(1 Suppl):S71–6.
98. Jurgens WJ, Oedayrajsingh-Varma MJ, Helder MN, Zandiehdoulabi B, Schouten TE, Kuik DJ, Ritt MJ, van Milligen FJ. Effect of tissue-harvesting site on yield of stem cells derived from adipose tissue: implications for cell-based therapies. Cell Tissue Res. 2008 Jun; 332(3):415–26.
99. Bianco P, Riminucci M, Gronthos S, Robey PG. Bone marrow stromal stem cells: nature, biology, and potential applications. Stem Cells. 2001; 19(3):180–92.
100. Kon E, Muraglia A, Corsi A, Bianco P, Marcacci M, Martin I, Boyde A, Ruspantini I, Chistolini P, Rocca M, Giardino R, Cancedda R, Quarto R. Autologous bone marrow stromal cells loaded onto porous hydroxyapatite ceramic accelerate bone repair in critical-size defects of sheep long bones. J Biomed Mater Res. 2000 Mar 5; 49(3):328–37.
101. Coelho de Faria AB, Chiantia FB, Teixeira ML, Aloise AC, Pelegrine AA. Comparative Study Between Mesenchymal Stem Cells Derived from Bone Marrow and from Adipose Tissue, Associated with Xenograft, in Appositional Reconstructions: Histomorphometric Study in Rabbit Calvaria. Int J Oral Maxillofac Implants. 2016 Nov/Dec;31(6):e155–e161.
102. Zahid MF. Methods of reducing pain during bone marrow biopsy: a narrative review. Ann Palliat Med. 2015 Oct;4(4):184–93.
103. Marolt D, Knezevic M, Novakovic GV. Bone tissue engineering with human stem cells. Stem Cell Res Ther. 2010 May 4;1(2):10.
104. Pan Q, Fouraschen SM, de Ruiter PE, Dinjens WN, Kwekkeboom J, Tilanus HW, van der Laan LJ. Detection of spontaneous tumorigenic transformation during culture expansion of human mesenchymal stromal cells. Exp Biol Med (Maywood). 2014 Jan;239(1):105–15.
105. Pearl JI, Kean LS, Davis MM, Wu JC. Pluripotent stem cells: immune to the immune system? Sci Transl Med. 2012 Dec 12;4(164):164ps25.

106. Civinini R, Macera A, Nistri L, Redl B, Innocenti M. The use of autologous blood-derived growth factors in bone regeneration. Clin Cases Miner Bone Metab. 2011 Jan;8(1):25–31.
107. Gonchar IV, Lipunov AR, Afanasov IM, Larina V, Faller AP, Kibardin AV. Platelet rich plasma and growth factors cocktails for diabetic foot ulcers treatment: State of art developments and future prospects. Diabetes Metab Syndr. 2017 Sep 21. pii: S1871–4021(17)30294–1.
108. Place ES, Evans ND, Stevens MM. Complexity in biomaterials for tissue engineering. Nat Mater. 2009 Jun;8(6):457–70.
109. Tayalia P, Mooney DJ. Controlled growth factor delivery for tissue engineering. Adv Mater. 2009 Sep 4;21(32–33):3269–85.
110. Yano K, Hoshino M, Ohta Y, Manaka T, Naka Y, Imai Y, Sebald W, Takaoka K. Osteoinductive capacity and heat stability of recombinant human bone morphogenetic protein-2 produced by Escherichia coli and dimerized by biochemical processing. J Bone Miner Metab. 2009;27(3):355–63.
111. Fishero BA, Kohli N, Das A, Christophel JJ, Cui Q. Current concepts of bone tissue engineering for craniofacial bone defect repair. Craniomaxillofac Trauma Reconstr. 2015 Mar;8(1):23–30.
112. Díaz-Sánchez RM, Yáñez-Vico RM, Fernández-Olavarría A, Mosquera-Pérez R, Iglesias-Linares A, Torres-Lagares D. Current Approaches of Bone Morphogenetic Proteins in Dentistry. J Oral Implantol. 2015 Jun;41(3):337–42.
113. Marx RE, Armentano L, Olavarria A, Samaniego J. rhBMP-2/ACS grafts versus autogenous cancellous marrow grafts in large vertical defects of the maxilla: an unsponsored randomized open-label clinical trial. Int J Oral Maxillofac Implants. 2013 Sep-Oct;28(5):e243–51.
114. de Freitas RM, Susin C, Spin-Neto R, Marcantonio C, Wikesjö UM, Pereira LA, Marcantonio E Jr. Horizontal ridge augmentation of the atrophic anterior maxilla using rhBMP-2/ACS or autogenous bone grafts: a proof-of-concept randomized clinical trial. J Clin Periodontol. 2013 Oct;40(10):968–75.
115. Ayoub A, Roshan CP, Gillgrass T, Naudi K, Ray A. The clinical application of rhBMP-7 for the reconstruction of alveolar cleft. J Plast Reconstr Aesthet Surg. 2016 Jan;69(1):101–7.
116. Coomes AM, Mealey BL, Huynh-Ba G, Barboza-Arguello C, Moore WS, Cochran DL. Buccal bone formation after flapless extraction: a randomized, controlled clinical trial comparing recombinant human bone morphogenetic protein 2/absorbable collagen carrier and collagen sponge alone. J Periodontol. 2014 Apr;85(4):525–35.
117. Carragee EJ, Chu G, Rohatgi R, Hurwitz EL, Weiner BK, Yoon ST, Comer G, Kopjar B. Cancer risk after use of recombinant bone morphogenetic protein-2 for spinal arthrodesis. J Bone Joint Surg Am. 2013 Sep 4;95(17): 1537–45.

118. Nevins M, Kao RT, McGuire MK, McClain PK, Hinrichs JE, McAllister BS, Reddy MS, Nevins ML, Genco RJ, Lynch SE, Giannobile WV. Platelet-derived growth factor promotes periodontal regeneration in localized osseous defects: 36-month extension results from a randomized, controlled, double-masked clinical trial. J Periodontol. 2013 Apr;84(4):456–64.
119. Maroo S, Murthy KR. Treatment of periodontal intrabony defects using β-TCP alone or in combination with rhPDGF-BB: a randomized controlled clinical and radiographic study. Int J Periodontics Restorative Dent. 2014 Nov-Dec;34(6):841–7.
120. McGuire MK, Scheyer ET, Schupbach P. Growth factor-mediated treatment of recession defects: a randomized controlled trial and histologic and microcomputed tomography examination. J Periodontol. 2009 Apr;80(4): 550–64.
121. Amorfini L, Migliorati M, Signori A, Silvestrini-Biavati A, Benedicenti S. Block allograft technique versus standard guided bone regeneration: a randomized clinical trial. Clin Implant Dent Relat Res. 2014 Oct;16(5):655–67.
122. Froum SJ, Wallace S, Cho SC, Rosenburg E, Froum S, Schoor R, Mascarenhas P, Tarnow DP, Corby P, Elian N, Fickl S, Ricci J, Hu B, Bromage T, Khouly I. A histomorphometric comparison of Bio-Oss alone versus Bio-Oss and platelet-derived growth factor for sinus augmentation: a postsurgical assessment. Int J Periodontics Restorative Dent. 2013 May-Jun;33(3):269–79.
123. Santana RB, Santana CM. A clinical comparison of guided bone regeneration with platelet-derived growth factor-enhanced bone ceramic versus autogenous bone block grafting. Int J Oral Maxillofac Implants. 2015 May-Jun;30(3):700–6.
124. Alvarez RH, Kantarjian HM, Cortes JE. Biology of platelet-derived growth factor and its involvement in disease. Mayo Clin Proc. 2006 Sep; 81(9): 1241–57.
125. Kim SJ, Kim SY, Kwon CH, Kim YK. Differential effect of FGF and PDGF on cell proliferation and migration in osteoblastic cells. Growth Factors. 2007 Apr;25(2):77–86.
126. Houde N, Chamoux E, Bisson M, Roux S. Transforming growth factor-beta1 (TGF-beta1) induces human osteoclast apoptosis by up-regulating Bim. J Biol Chem. 2009 Aug 28;284(35):23397–404.
127. Ripamonti U, Parak R, Klar RM, Dickens C, Dix-Peek T, Duarte R. The synergistic induction of bone formation by the osteogenic proteins of the TGF-β supergene family. Biomaterials. 2016 Oct;104:279–96.
128. Coultas L, Chawengsaksophak K, Rossant J. Endothelial cells and VEGF in vascular development. Nature. 2005 Dec 15; 438(7070):937–45.
129. Ferrara N, Gerber HP, LeCouter J. The biology of VEGF and its receptors. Nat Med. 2003 Jun; 9(6):669–76.

130. Hu K, Olsen BR. The roles of vascular endothelial growth factor in bone repair and regeneration. Bone. 2016 Oct;91:30–8.
131. Murakami S. Periodontal tissue regeneration by signaling molecule(s): what role does basic fibroblast growth factor (FGF-2) have in periodontal therapy? Periodontol 2000. 2011 Jun; 56(1):188–208.
132. Kao RT, Murakami S, Beirne OR. The use of biologic mediators and tissue engineering in dentistry. Periodontol 2000. 2009; 50():127–53.
133. Sheng MH, Lau KH, Baylink DJ. Role of Osteocyte-derived Insulin-Like Growth Factor I in Developmental Growth, Modeling, Remodeling, and Regeneration of the Bone. J Bone Metab. 2014 Feb;21(1):41–54.
134. Myers TJ, Yan Y, Granero-Molto F, Weis JA, Longobardi L, Li T, Li Y, Contaldo C, Ozkan H, Spagnoli A. Systemically delivered insulin-like growth factor-I enhances mesenchymal stem cell-dependent fracture healing. Growth Factors. 2012 Aug;30(4):230–41.
135. Guntur AR, Rosen CJ. IGF-1 regulation of key signaling pathways in bone. Bonekey Rep. 2013 Oct 2;2:437.
136. Peres JA, Lamano T. Strategies for stimulation of new bone formation: a critical review. Braz Dent J. 2011;22(6):443–8.
137. Thrivikraman G, Athirasala A, Twohig C, Boda SK, Bertassoni LE. Biomaterials for Craniofacial Bone Regeneration. Dent Clin North Am. 2017 Oct;61(4):835–856.
138. O'Brien FJ. Biomaterials & scaffolds for tissue engineering. Mater Today 2011; 14(3): 88–95.
139. Draenert M, Draenert A, Draenert K. Osseointegration of hydroxyapatite and remodeling-resorption of tricalciumphosphate ceramics. Microsc Res Tech. 2013 Apr;76(4):370–80.
140. Wang M. Developing bioactive composite materials for tissue replacement. Biomaterials. 2003 Jun;24(13):2133–51.
141. Ko HF, Sfeir C, Kumta PN. Novel synthesis strategies for natural polymer and composite biomaterials as potential scaffolds for tissue engineering. Philos Trans A Math Phys Eng Sci. 2010 Apr 28;368(1917):1981–97.
142. Atila D, Keskin D, Tezcaner A. Crosslinked pullulan/cellulose acetate fibrous scaffolds for bone tissue engineering. Mater Sci Eng C Mater Biol Appl. 2016 Dec 1;69:1103–15.
143. Pei B, Wang W, Fan Y, Wang X, Watari F, Li X. Fiber-reinforced scaffolds in soft tissue engineering. Regen Biomater. 2017 Aug;4(4):257–268.
144. Kumbhar JV, Jadhav SH, Bodas DS, Barhanpurkar-Naik A, Wani MR, Paknikar KM, Rajwade JM. In vitro and in vivo studies of a novel bacterial cellulose-based acellular bilayer nanocomposite scaffold for the repair of osteochondral defects. Int J Nanomedicine. 2017 Sep 1;12:6437–6459.
145. Ao C, Niu Y, Zhang X, He X, Zhang W, Lu C. Fabrication and characterization of electrospun cellulose/nano-hydroxyapatite nanofibers for bone tissue engineering. Int J Biol Macromol. 2017 Apr;97:568–573.

146. Domingos M, Gloria A, Coelho J, Bartolo P, Ciurana J. Three-dimensional printed bone scaffolds: The role of nano/micro-hydroxyapatite particles on the adhesion and differentiation of human mesenchymal stem cells. Proc Inst Mech Eng H. 2017 Jun;231(6):555–564.
147. Tetteh G, Khan AS, Delaine-Smith RM, Reilly GC, Rehman IU. Electrospun polyurethane/hydroxyapatite bioactive scaffolds for bone tissue engineering: the role of solvent and hydroxyapatite particles. J Mech Behav Biomed Mater. 2014 Nov;39:95–110.
148. Muschler GF, Nakamoto C, Griffith LG. Engineering principles of clinical cell-based tissue engineering. J Bone Joint Surg Am. 2004 Jul;86–A(7): 1541–58.
149. Bose S, Vahabzadeh S, Bandyopadhyay A. Bone tissue engineering using 3D printing. Mater Today. 2013;16:496–504.
150. Karageorgiou V, Kaplan D. Porosity of 3D biomaterial scaffolds and osteogenesis. Biomaterials. 2005 Sep;26(27):5474–91.
151. Kim K, Yeatts A, Dean D, Fisher JP. Stereolithographic bone scaffold design parameters: osteogenic differentiation and signal expression. Tissue Eng Part B Rev. 2010 Oct;16(5):523–39.
152. Tang YQ, Yeaman MR, Selsted ME. Antimicrobial peptides from human platelets. Infect Immun. 2002 Dec;70(12):6524–33.
153. Rozman P, Bolta Z. Use of platelet growth factors in treating wounds and soft-tissue injuries. Acta Dermatovenerol Alp Pannonica Adriat. 2007 Dec; 16(4):156–65.
154. Del Corso M, Vervelle A, Simonpieri A, Jimbo R, Inchingolo F, Sammartino G, Dohan Ehrenfest DM. Current knowledge and perspectives for the use of platelet-rich plasma (PRP) and platelet-rich fibrin (PRF) in oral and maxillofacial surgery part 1: Periodontal and dentoalveolar surgery. Curr Pharm Biotechnol. 2012 Jun;13(7):1207–30.
155. Zhou L, Schmaier AH. Platelet aggregation testing in platelet-rich plasma: description of procedures with the aim to develop standards in the field. Am J Clin Pathol. 2005 Feb;123(2):172–83.
156. Burnouf T, Goubran HA, Chen TM, Ou KL, El-Ekiaby M, Radosevic M. Blood-derived biomaterials and platelet growth factors in regenerative medicine. Blood Rev 2013;27(2):77–89.
157. Lubkowska A, Dolegowska B, Banfi G. Growth factor content in PRP and their applicability in medicine. J Biol Regul Homeost Agents 2012;26:3S–22S.
158. Scarano A, Ceccarelli M, Marchetti M, Piattelli A, Mortellaro C. Soft tissue augmentation with autologous platelet gel and β-TCP: a histologic and histometric study in mice. Biomed Res Int 2016;12:2016:2078104.
159. Demidova-Rice TN, Wolf L, Deckenback J, Hamblin MR, Herman IM. Human platelet-rich plasma- and extracellular matrix-derived peptides promote impaired cutaneous wound healing in vivo. Plos One 2012;7:e32146.

160. Intini G. The use of platelet-rich plasma in bone reconstruction therapy. Biomaterials 2009;30(28):4956–4966.
161. Lacci KM, Dardik A. Platelet-rich plasma: support for its use in wound-healing. Yale J Biol Med 2010;83(1):1–9.
162. Tollemar V, Collier ZJ, Mohammed MK, Lee MJ, Ameer GA, Reid RR. Stem cells, growth factors and scaffolds in craniofacial regenerative medicine. Genes Dis. 2016 Mar;3(1):56–71.
163. Cieslik-Bielecka A, Dohan Ehrenfest DM, Lubkowska A, Bielecki T. Microbicidal properties of Leukocyte- and Platelet-Rich Plasma/Fibrin (L-PRP/L-PRF): new perspectives. J Biol Regul Homeost Agents. 2012 Apr–Jun;26(2 Suppl 1):43S–52S.
164. Yeaman MR. The role of platelets in antimicrobial host defense. Clin Infect Dis. 1997 Nov;25(5):951–68; 969–70.
165. Anitua E, Zalduendo MM, Prado R, Alkhraisat MH, Orive G. Morphogen and proinflammatory cytokine release kinetics from PRGF-Endoret fibrin scaffolds: Evaluation of the effect of leukocyte inclusion. J Biomed Mater Res A. 2015 Mar;103(3):1011–20.
166. Mountziaris PM, Spicer PP, Kasper FK, Mikos AG. Harnessing and modulating inflammation in strategies for bone regeneration. Tissue Eng Part B Rev. 2011 Dec;17(6):393–402.
167. Anitua E, Zalduendo M, Troya M, Padilla S, Orive G. Leukocyte inclusion within a platelet rich plasma-derived fibrin scaffold stimulates a more pro-inflammatory environment and alters fibrin properties. PLoS One. 2015 Mar 30;10(3):e0121713.
168. Dohan Ehrenfest DM, Andia I, Zumstein MA, Zhang CQ, Pinto NR, Bielecki T. Classification of platelet concentrates (Platelet-Rich Plasma-PRP, Platelet-Rich Fibrin-PRF) for topical and infiltrative use in orthopedic and sports medicine: current consensus, clinical implications and perspectives. Muscles Ligaments Tendons J. 2014 May 8;4(1):3–9.
169. Dohan Ehrenfest DM, Bielecki T, Jimbo R, Barbé G, Del Corso M, Inchingolo F, Sammartino G. Do the fibrin architecture and leukocyte content influence the growth factor release of platelet concentrates? An evidence-based answer comparing a pure platelet-rich plasma (P-PRP) gel and a leukocyte- and platelet-rich fibrin (L-PRF). Curr Pharm Biotechnol. 2012 Jun;13(7):1145–52.
170. Bielecki T, Dohan Ehrenfest DM, Everts PA, Wiczkowski A. The role of leukocytes from L-PRP/L-PRF in wound healing and immune defense: new perspectives. Curr Pharm Biotechnol. 2012 Jun;13(7):1153–62.
171. Mendes BB, Gómez-Florit M, Babo PS, Domingues RM, Reis RL, Gomes ME. Blood derivatives awaken in regenerative medicine strategies to modulate wound healing. Adv Drug Deliv Rev. 2017 Dec 28. pii: S0169–409X(17)30321–6.

172. Marx RE, Carlson ER, Eichstaedt RM, Schimmele SR, Strauss JE, Georgeff KR. Platelet-rich plasma: Growth factor enhancement for bone grafts. Oral Surg Oral Med Oral Pathol Oral Radiol Endod. 1998 Jun;85(6):638–646.
173. Dhurat R, Sukesh M. Principles and Methods of Preparation of Platelet-Rich Plasma: A Review and Author's Perspective. J Cutan Aesthet Surg. 2014 Oct-Dec;7(4):189–97.
174. Dohan Ehrenfest DM, Rasmusson L, Albrektsson T. Classification of platelet concentrates: from pure platelet-rich plasma (P-PRP) to leucocyte- and platelet-rich fibrin (L-PRF). Trends Biotechnol. 2009 Mar;27(3):158–67.
175. Anitua E. Plasma rich in growth factors: preliminary results of use in the preparation of future sites for implants. Int J Oral Maxillofac Implants. 1999 Jul-Aug;14(4):529–35.
176. Giannini S, Cielo A, Bonanome L, Rastelli C, Derla C, Corpaci F, Falisi G. Comparison between PRP, PRGF and PRF: lights and shadows in three similar but different protocols. Eur Rev Med Pharmacol Sci. 2015;19(6): 927–30.
177. Taschieri S, Lolato A, Ofer M, Testori T, Francetti L, Del Fabbro M. Immediate post-extraction implants with or without pure platelet-rich plasma: a 5-year follow-up study. Oral Maxillofac Surg. 2017 Jun;21(2): 147–157.
178. Haraji A, Lassemi E, Motamedi MH, Alavi M, Adibnejad S. Effect of plasma rich in growth factors on alveolar osteitis. Natl J Maxillofac Surg. 2012 Jan;3(1):38–41.
179. Alissa R, Esposito M, Horner K, Oliver R. The influence of platelet-rich plasma on the healing of extraction sockets: an explorative randomised clinical trial. Eur J Oral Implantol. 2010 Summer;3(2):121–34.
180. Torres J, Tamimi F, Alkhraisat MH, Manchón A, Linares R, Prados-Frutos JC, Hernández G, López Cabarcos E. Platelet-rich plasma may prevent titanium-mesh exposure in alveolar ridge augmentation with anorganic bovine bone. J Clin Periodontol. 2010 Oct;37(10):943–51.
181. Sakio R, Sakamoto Y, Ogata H, Sakamoto T, Ishii T, Kishi K.Effect of Platelet-Rich Plasma on Bone Grafting of Alveolar Clefts. J Craniofac Surg. 2017 Mar;28(2):486–488.
182. Shukla S, Chug A, Mahesh L, Grover HS. Effect of Addition of Platelet-rich Plasma to Calcium Phosphosilicate Putty on Healing at 9 Months in Periodontal Intrabony Defects. J Contemp Dent Pract. 2016 Mar 1;17(3): 230–4.
183. Badr M, Coulthard P, Alissa R, Oliver R. The efficacy of platelet-rich plasma in grafted maxillae. A randomised clinical trial. Eur J Oral Implantol. 2010 Autumn;3(3):233–44.
184. Gürbüzer B, Pikdöken L, Urhan M, Süer BT, Narin Y. Scintigraphic evaluation of early osteoblastic activity in extraction sockets treated with platelet-rich plasma. J Oral Maxillofac Surg. 2008 Dec;66(12):2454–60.

185. Choukroun J, Adda F, Schoeffler C, Vervelle A. Une opportunite en paro-implantologie: le PRF. Implantodontie 2001;42:55–62.
186. Ajwani H, Shetty S, Gopalakrishnan D, Kathariya R, Kulloli A, Dolas RS, Pradeep AR. Comparative evaluation of platelet-rich fibrin biomaterial and open flap debridement in the treatment of two and three wall intrabony defects. J Int Oral Health. 2015 Apr;7(4):32–7.
187. Ozcan M, Ucak O, Alkaya B, Keceli S, Seydaoglu G, Haytac MC. Effects of Platelet-Rich Fibrin on Palatal Wound Healing After Free Gingival Graft Harvesting: A Comparative Randomized Controlled Clinical Trial. Int J Periodontics Restorative Dent. 2017 Sep/Oct;37(5):e270–e278.
188. Agarwal A, Gupta ND, Jain A. Platelet rich fibrin combined with decalcified freeze-dried bone allograft for the treatment of human intrabony periodontal defects: a randomized split mouth clinical trail. Acta Odontol Scand. 2016;74(1):36–43.
189. Xuan F, Lee CU, Son JS, Jeong SM, Choi BH. A comparative study of the regenerative effect of sinus bone grafting with platelet-rich fibrin-mixed Bio-Oss® and commercial fibrin-mixed Bio-Oss®: an experimental study. J Craniomaxillofac Surg. 2014 Jun;42(4):e47–50.
190. Lekovic V, Milinkovic I, Aleksic Z, Jankovic S, Stankovic P, Kenney EB, Camargo PM. Platelet-rich fibrin and bovine porous bone mineral vs. platelet-rich fibrin in the treatment of intrabony periodontal defects. J Periodontal Res. 2012 Aug;47(4):409–17.
191. Chiapasco M, Zaniboni M, Boisco M. Augmentation procedures for the rehabilitation of deficient edentulous ridges with oral implants. Clin Oral Implants Res. 2006 Oct;17 Suppl 2:136–59.
192. Dohan Ehrenfest DM, Zhang CQ, Pinto NR, Bielecki T. Merchants shall be expelled from the Temple: the PRGF(®) (Plasma-Preparation Rich in Growth Factors)-Endoret(®) case. Muscles Ligaments Tendons J. 2015 Feb 5;4(4):473–7.
193. Bryjak J, Aniulyte J, Liesiene J. Evaluation of man-tailored cellulose-based carriers in glucoamylase immobilization. Carbohydr Res. 2007 Jun 11; 342(8):1105–9.
194. Dohan Ehrenfest DM. How to optimize the preparation of leukocyte- and platelet-rich fibrin (L-PRF, Choukroun's technique) clots and membranes: introducing the PRF Box. Oral Surg Oral Med Oral Pathol Oral Radiol Endod. 2010 Sep;110(3):275–8; author reply 278–80.
195. Silva JC, Sampaio P, Fernandes MH, Gomes PS. The Osteogenic Priming of Mesenchymal Stem Cells is Impaired in Experimental Diabetes. J Cell Biochem. 2015 Aug;116(8):1658–67.
196. Calvo-Guirado JL, Garces M, Delgado-Ruiz RA, Ramirez Fernandez MP, Ferres-Amat E, Romanos GE. Biphasic β-TCP mixed with silicon increases bone formation in critical site defects in rabbit calvaria. Clin Oral Implants Res. 2015 Aug;26(8):891–7.

197. Winter GB. Impacted mandibular third molars. St. Louis: American Medical Book, 1926.
198. Pell GJ, Gregory BT. Impacted mandibular third molars: classification and modified techniques for removal. Dent Digest 1933;39:330–338.
199. Juodzbalys G, Daugela P. Mandibular third molar impaction: review of literature and a proposal of a classification. J Oral Maxillofac Res. 2013 Jul 1;4(2):e1.
200. Farish SE, Bouloux GF. General technique of third molar removal. Oral Maxillofacial Surg Clin N Am 2007;19:23–43.
201. Pederson GW. Surgical removal of tooth. In: Pederson GW, editor. Oral surgery. Philadelphia: WB Saunders; 1988.
202. Mozzati M, Gallesio G, di Romana S, Bergamasco L, Pol R. Efficacy of plasma-rich growth factor in the healing of postextraction sockets in patients affected by insulin-dependent diabetes mellitus. J Oral Maxillofac Surg. 2014 Mar;72(3):456–462.
203. Cardoso CL, Rodrigues MT, Ferreira Júnior O, Garlet GP, de Carvalho PS. Clinical concepts of dry socket. J Oral Maxillofac Surg. 2010 Aug;68(8): 1922–1932.
204. Cheung LK, Chow LK, Tsang MH, Tung LK. An evaluation of complications following dental extractions using either sterile or clean gloves. Int J Oral Maxillofac Surg. 2001 Dec;30(6):550–554.
205. Campbell WI, Lewis S. Visual analogue measurement of pain. Ulster Med J. 1990 Oct; 59(2): 149–154.
206. Rakprasitkul S, Pairuchvej V. Mandibular third molar surgery with primary closure and tube drain. Int J Oral Maxillofac Surg. 1997 Jun;26(3):187–190.
207. Hugoson A, Kugelberg CF. The prevalence of third molars in a Swedish population. An epidemiological study. Community Dent Health. 1988 Jun;5(2):121–138.
208. Eklund SA, Pittman JL. Third-molar removal patterns in an insured population. J Am Dent Assoc. 2001 Apr;132(4):469–475.
209. Costa MG, Pazzini CA, Pantuzo MC, Jorge ML, Marques LS. Is there justification for prophylactic extraction of third molars? A systematic review. Braz Oral Res. 2013 Mar-Apr;27(2):183–188.
210. Normando D. Third molars: To extract or not to extract? Dental Press J Orthod. 2015 Jul-Aug;20(4):17–8.
211. Guerrouani A, Zeinoun T, Vervaet C, Legrand W. A Four-Year Monocentric Study of the Complications of Third Molars Extractions under General Anesthesia: About 2112 Patients. Int J Dent. 2013;2013:763837.
212. Mantovani E, Arduino PG, Schierano G, Ferrero L, Gallesio G, Mozzati M, Russo A, Scully C, Carossa S. A split-mouth randomized clinical trial to evaluate the performance of piezosurgery compared with traditional technique in lower wisdom tooth removal. J Oral Maxillofac Surg. 2014 Oct; 72(10):1890–1897.

213. Lee CT, Zhang S, Leung YY, Li SK, Tsang CC, Chu CH. Patients' satisfaction and prevalence of complications on surgical extraction of third molar. Patient Prefer Adherence. 2015 Feb 10;9:257–263.
214. Barone A, Marconcini S, Giacomelli L, Rispoli L, Calvo JL, Covani U. A randomized clinical evaluation of ultrasound bone surgery versus traditional rotary instruments in lower third molar extraction. J Oral Maxillofac Surg. 2010 Feb;68(2):330–336.
215. Chen Y, Liu J, Pei J, Liu Y, Pan J. The Risk Factors that Can Increase Possibility of Mandibular Canal Wall Damage in Adult: A Cone-Beam Computed Tomography (CBCT) Study in a Chinese Population. Med Sci Monit. 2018 Jan 2;24:26–36.
216. Akadiri OA, Fasola AO, Arotiba JT. Evaluation of Pederson index as an instrument for predicting difficulty of third molar surgical extraction. Niger Postgrad Med J. 2009 Jun;16(2):105–8.
217. Lima CJ, Silva LC, Melo MR, Santos JA, Santos TS. Evaluation of the agreement by examiners according to classifications of third molars. Med Oral Patol Oral Cir Bucal. 2012 Mar 1;17(2):e281–6.
218. Almendros-Marqués N, Berini-Aytés L, Gay-Escoda C. Evaluation of intraexaminer and interexaminer agreement on classifying lower third molars according to the systems of Pell and Gregory and of Winter. J Oral Maxillofac Surg. 2008 May;66(5):893–9.
219. Palaveniene A, Harkavenko V, Kharchenko V, Daugela P, Pranskunas M, Juodzbalys G, Babenko N, Liesiene J. Cuttlebone as a Marine-Derived Material for Preparing Bone Grafts. Mar Biotechnol (NY). 2018 Apr 3. doi: 10.1007/s10126-018-9816-6. [Epub ahead of print].
220. Daugela P, Pranskunas M, Juodzbalys G, Liesiene J, Baniukaitiene O, Afonso A, Sousa Gomes P. Novel cellulose/hydroxyapatite scaffolds for bone tissue regeneration: In vitro and in vivo study. J Tissue Eng Regen Med. 2018 May;12(5):1195–1208.
221. Ramanauskaite A, Daugela P, Juodzbalys G. Treatment of peri-implantitis: Meta-analysis of findings in a systematic literature review and novel protocol proposal. Quintessence Int. 2016;47(5):379–93.
222. Daugela P, Cicciù M, Saulacic N. Surgical Regenerative Treatments for Peri-Implantitis: Meta-analysis of Recent Findings in a Systematic Literature Review. J Oral Maxillofac Res. 2016 Sep 9;7(3):e15. eCollection 2016 Jul–Sep.
223. Suárez-López Del Amo F, Faria E Almeida R, Cicciù M, Daugela P, Ramanauskaite A, Saulacic N, Tervonen T, Wang HL, Yu SH. The 1st Baltic Osseointegration Academy and Lithuanian University of Health Sciences Consensus Conference 2016. Summary and Consensus Statements: Group III - Peri-Implantitis Treatment. J Oral Maxillofac Res. 2016 Sep 9;7(3):e16. eCollection 2016 Jul–Sep.

224. Sheng L, Jiang R, Zhu Y, Ji Y: Electrospun Cellulose Nanocrystals/ Polycaprolactone Nanocomposite Fiber Mats. J Macromol Sci, Part B. 2013;53:820–828.
225. Bäckdahl H, Helenius G, Bodin A, Nannmark U, Johansson BR, Risberg B, Gatenholm P. Mechanical properties of bacterial cellulose and interactions with smooth muscle cells. Biomaterials. 2006 Mar;27(9):2141–9.
226. Novotna K., Havelka P., Sopuch T., Kolarova K., Vosmanska V., Lisa V., Svorcik V., Bacakova L. Cellulose-based materials as scaffolds for tissue engineering. Cellulose. 2013;20:2263–2278.
227. Wu CY, Suen SY, Chen SC, Tzeng JH. Analysis of protein adsorption on regenerated cellulose-based immobilized copper ion affinity membranes. J Chromatogr A. 2003 May 9;996(1-2):53–70.
228. Kilpadi KL, Chang PL, Bellis SL. Hydroxylapatite binds more serum proteins, purified integrins, and osteoblast precursor cells than titanium or steel. J Biomed Mater Res. 2001 Nov;57(2):258–67.
229. Sawyer AA, Hennessy KM, Bellis SL. The effect of adsorbed serum proteins, RGD and proteoglycan-binding peptides on the adhesion of mesenchymal stem cells to hydroxyapatite. Biomaterials. 2007 Jan;28(3):383–92.
230. Wilson CJ, Clegg RE, Leavesley DI, Pearcy MJ.Mediation of biomaterial-cell interactions by adsorbed proteins: a review. Tissue Eng. 2005 Jan-Feb;11(1–2):1–18.
231. Polo-Corrales L, Latorre-Esteves M, Ramirez-Vick JE. Scaffold design for bone regeneration. J Nanosci Nanotechnol. 2014 Jan;14(1):15–56.
232. Causa F, Netti PA, Ambrosio L. A multi-functional scaffold for tissue regeneration: the need to engineer a tissue analogue. Biomaterials. 2007 Dec;28(34):5093–9.
233. He J, Genetos DC, Yellowley CE, Leach JK. Oxygen tension differentially influences osteogenic differentiation of human adipose stem cells in 2D and 3D cultures. J Cell Biochem. 2010 May;110(1):87–96.
234. Kim HJ, Kim UJ, Vunjak-Novakovic G, Min BH, Kaplan DL. Influence of macroporous protein scaffolds on bone tissue engineering from bone marrow stem cells. Biomaterials. 2005 Jul;26(21):4442–52.
235. Murphy CM, Haugh MG, O'Brien FJ. The effect of mean pore size on cell attachment, proliferation and migration in collagen-glycosaminoglycan scaffolds for bone tissue engineering. Biomaterials. 2010 Jan;31(3):461–6.
236. Schek RM, Taboas JM, Segvich SJ, Hollister SJ, Krebsbach PH. Engineered osteochondral grafts using biphasic composite solid free-form fabricated scaffolds. Tissue Eng. 2004 Sep-Oct;10(9–10):1376–85.
237. Loh QL, Choong C. Three-dimensional scaffolds for tissue engineering applications: role of porosity and pore size. Tissue Eng Part B Rev. 2013 Dec;19(6):485–502.
238. Filova E, Suchy T, Sucharda Z, Supova M, Zaloudkova M, Balik K, Lisa V, Slouf M, Bacakova L. Support for the initial attachment, growth and differentiation of MG-63 cells: a comparison between nano-size hydro-

xyapatite and micro-size hydroxyapatite in composites. Int J Nanomedicine. 2014 Aug 6;9:3687–706.
239. Webster TJ, Ergun C, Doremus RH, Siegel RW, Bizios R. Enhanced functions of osteoblasts on nanophase ceramics. Biomaterials. 2000 Sep;21(17): 1803–10.
240. Lord MS, Foss M, Besenbacher F. Influence of nanoscale surface topography on protein adsorption and cellular response. Nano Today 2010;5:66–78.
241. Lee LC, Gadegaard N, de Andrés MC, Turner LA, Burgess KV, Yarwood SJ, Wells J, Salmeron-Sanchez M, Meek D, Oreffo RO, Dalby MJ. Nanotopography controls cell cycle changes involved with skeletal stem cell self-renewal and multipotency. Biomaterials. 2017 Feb;116:10–20.
242. Bacakova L, Filova E, Parizek M, Ruml T, Svorcik V. Modulation of cell adhesion, proliferation and differentiation on materials designed for body implants. Biotechnol Adv. 2011 Nov-Dec;29(6):739–67.
243. Guo X, Gough JE, Xiao P, Liu J, Shen Z. Fabrication of nanostructured hydroxyapatite and analysis of human osteoblastic cellular response. J Biomed Mater Res A. 2007 Sep 15;82(4):1022–32.
244. Shi Z, Huang X, Cai Y, Tang R, Yang D. Size effect of hydroxyapatite nanoparticles on proliferation and apoptosis of osteoblast-like cells. Acta Biomater. 2009 Jan;5(1):338–45.
245. Chen L, Mccrate JM, Lee JC, Li H. The role of surface charge on the uptake and biocompatibility of hydroxyapatite nanoparticles with osteoblast cells. Nanotechnology. 2011 Mar 11;22(10):105708.
246. Maeno S, Niki Y, Matsumoto H, Morioka H, Yatabe T, Funayama A, Toyama Y, Taguchi T, Tanaka J. The effect of calcium ion concentration on osteoblast viability, proliferation and differentiation in monolayer and 3D culture. Biomaterials. 2005 Aug;26(23):4847–55.
247. Huang Y, Zhou G, Zheng L, Liu H, Niu X, Fan Y. Micro-/nano- sized hydroxyapatite directs differentiation of rat bone marrow derived mesenchymal stem cells towards an osteoblast lineage. Nanoscale. 2012 Apr 7;4(7):2484–90.
248. Liu Y, Wang G, Cai Y, Ji H, Zhou G, Zhao X, Tang R, Zhang M. In vitro effects of nanophase hydroxyapatite particles on proliferation and osteogenic differentiation of bone marrow-derived mesenchymal stem cells. J Biomed Mater Res A. 2009 Sep 15;90(4):1083–91.
249. Li J, Dou Y, Yang J, Yin Y, Zhang H, Yao F, Wang H, Yao K. Surface characterization and biocompatibility of micro- and nano-hydroxyapatite/ chitosan-gelatin network films. Mater. Sci. Eng. C. 2009;29:1207–1215.
250. Polini A, Pisignano D, Parodi M, Quarto R, Scaglione S. Osteoinduction of human mesenchymal stem cells by bioactive composite scaffolds without supplemental osteogenic growth factors. PLoS One. 2011;6(10):e26211.

251. Lin GL, Hankenson KD. Integration of BMP, Wnt, and notch signaling pathways in osteoblast differentiation. J Cell Biochem. 2011 Dec;112(12): 3491–501.
252. Czekanska EM, Stoddart MJ, Richards RG, Hayes JS.In search of an osteoblast cell model for in vitro research. Eur Cell Mater. 2012 Jul 9;24:1–17.
253. Jafary F, Hanachi P, Gorjipour K. Osteoblast Differentiation on Collagen Scaffold with Immobilized Alkaline Phosphatase. Int J Organ Transplant Med. 2017;8(4):195–202.
254. Helenius G, Bäckdahl H, Bodin A, Nannmark U, Gatenholm P, Risberg B. In vivo biocompatibility of bacterial cellulose. J Biomed Mater Res A. 2006 Feb;76(2):431–8.
255. Luo LH, Zhang YF, Wang XM, Wan Y, Chang PR, Anderson DP, Chen Y. Preparation, characterization, and in vitro and in vivo evaluation of cellulose/soy protein isolate composite sponges. J Biomater Appl. 2010 Feb; 24(6):503–26.
256. Gleeson JP, Plunkett NA, O'Brien FJ. Addition of hydroxyapatite improves stiffness, interconnectivity and osteogenic potential of a highly porous collagen-based scaffold for bone tissue regeneration. Eur Cell Mater. 2010 Oct 4;20:218–30.
257. Swetha M, Sahithi K, Moorthi A, Srinivasan N, Ramasamy K, Selvamurugan N. Biocomposites containing natural polymers and hydroxyapatite for bone tissue engineering. Int J Biol Macromol. 2010 Jul 1;47(1):1–4.
258. Anitua E, Tejero R, Alkhraisat MH, Orive G. Platelet-rich plasma to improve the bio-functionality of biomaterials. BioDrugs. 2013 Apr;27(2):97–111.
259. Shimojo AAM, Perez AGM, Galdames SEM, Brissac ICS, Santana MHA. Stabilization of porous chitosan improves the performance of its association with platelet-rich plasma as a composite scaffold. Mater Sci Eng C Mater Biol Appl. 2016 Mar;60:538–546.
260. Gassling V, Hedderich J, Açil Y, Purcz N, Wiltfang J, Douglas T. Comparison of platelet rich fibrin and collagen as osteoblast-seeded scaffolds for bone tissue engineering applications. Clin Oral Implants Res. 2013 Mar; 24(3):320–8.
261. Reinke JM, Sorg H. Wound repair and regeneration. Eur Surg Res. 2012; 49(1):35–43.
262. Thomas MV, Puleo DA. Infection, inflammation, and bone regeneration: a paradoxical relationship. J Dent Res. 2011 Sep;90(9):1052–61.
263. Dohan DM, Choukroun J, Diss A, Dohan SL, Dohan AJ, Mouhyi J, Gogly B. Platelet-rich fibrin (PRF): a second-generation platelet concentrate. Part III: leukocyte activation: a new feature for platelet concentrates? Oral Surg Oral Med Oral Pathol Oral Radiol Endod. 2006 Mar;101(3):e51–5.
264. De Pascale MR, Sommese L, Casamassimi A, Napoli C. Platelet derivatives in regenerative medicine: an update. Transfus Med Rev. 2015 Jan;29(1):52–61.

265. Bota PC, Collie AM, Puolakkainen P, Vernon RB, Sage EH, Ratner BD, Stayton PS. Biomaterial topography alters healing in vivo and monocyte/ macrophage activation in vitro. J Biomed Mater Res A. 2010 Nov;95(2): 649–57.
266. Nicolete R, dos Santos DF, Faccioli LH. The uptake of PLGA micro or nanoparticles by macrophages provokes distinct in vitro inflammatory response. Int Immunopharmacol. 2011 Oct;11(10):1557–63.
267. Aksakal B, Kom M, Tosun HB, Demirel M. Influence of micro- and nano-hydroxyapatite coatings on the osteointegration of metallic (Ti6Al4 V) and bioabsorbable interference screws: an in vivo study. Eur J Orthop Surg Traumatol. 2014 Jul;24(5):813–9.
268. Appleford MR, Oh S, Oh N, Ong JL. In vivo study on hydroxyapatite scaffolds with trabecular architecture for bone repair. J Biomed Mater Res A. 2009 Jun 15;89(4):1019–27.
269. Chung EJ, Qiu H, Kodali P, Yang S, Sprague SM, Hwong J, Koh J, Ameer GA. Early tissue response to citric acid-based micro- and nanocomposites. J Biomed Mater Res A. 2011 Jan;96(1):29–37.
270. Agren MS, Rasmussen K, Pakkenberg B, Jørgensen B. Growth factor and proteinase profile of Vivostat® platelet-rich fibrin linked to tissue repair. Vox Sang. 2014 Jul;107(1):37–43.
271. Arora S, Kotwal U, Dogra M, Doda V. Growth Factor Variation in Two Types of Autologous Platelet Biomaterials: PRP Versus PRF. Indian J Hematol Blood Transfus. 2017 Jun;33(2):288–292.
272. Bai MY, Wang CW, Wang JY, Lin MF, Chan WP. Three-dimensional structure and cytokine distribution of platelet-rich fibrin. Clinics (Sao Paulo). 2017 Feb 1;72(2):116–124.
273. Nishimoto S, Fujita K, Sotsuka Y, Kinoshita M, Fujiwara T, Kawai K, Kakibuchi M. Growth Factor Measurement and Histological Analysis in Platelet Rich Fibrin: A Pilot Study. J Maxillofac Oral Surg. 2015 Dec;14(4): 907–13.
274. Simonpieri A, Del Corso M, Vervelle A, Jimbo R, Inchingolo F, Sammartino G, Dohan Ehrenfest DM. Current knowledge and perspectives for the use of platelet-rich plasma (PRP) and platelet-rich fibrin (PRF) in oral and maxillofacial surgery part 2: Bone graft, implant and reconstructive surgery. Curr Pharm Biotechnol. 2012 Jun;13(7):1231–56.
275. Naik B, Karunakar P, Jayadev M, Marshal VR. Role of Platelet rich fibrin in wound healing: A critical review. J Conserv Dent. 2013 Jul;16(4):284–93.
276. Agrawal M, Agrawal V. Platelet rich fibrin and its applications in dentistry - A review article. Natl J Med Dent Res 2014;2:51–8.
277. Dohan DM, Choukroun J, Diss A, Dohan SL, Dohan AJ, Mouhyi J, Gogly B. Platelet-rich fibrin (PRF): a second-generation platelet concentrate. Part II: platelet-related biologic features. Oral Surg Oral Med Oral Pathol Oral Radiol Endod. 2006 Mar;101(3):e45–50.

278. Dohan Ehrenfest DM, Pinto NR, Pereda A, Jiménez P, Corso MD, Kang BS, Nally M, Lanata N, Wang HL, Quirynen M. The impact of the centrifuge characteristics and centrifugation protocols on the cells, growth factors, and fibrin architecture of a leukocyte- and platelet-rich fibrin (L-PRF) clot and membrane. Platelets. 2018 Mar;29(2):171–184.
279. Suttapreyasri S, Leepong NJ. Influence of platelet-rich fibrin on alveolar ridge preservation. Craniofac Surg. 2013 Jul;24(4):1088–94.
280. Marenzi G, Riccitiello F, Tia M, di Lauro A, Sammartino G. Influence of Leukocyte- and Platelet-Rich Fibrin (L-PRF) in the Healing of Simple Postextraction Sockets: A Split-Mouth Study. Biomed Res Int. 2015;2015: 369273.
281. Singh A, Kohli M, Gupta N. Platelet rich fibrin: a novel approach for osseous regeneration. J Maxillofac Oral Surg. 2012 Dec;11(4):430–434.
282. Varghese MP, Manuel S, Kumar LKS. Potential for Osseous Regeneration of Platelet-Rich Fibrin – A Comparative Study in Mandibular Third Molar Impaction Sockets. J Oral Maxillofac Surg. 2017 Feb 4. pii: S0278–2391(17)30120–30129.
283. Yelamali T, Saikrishna D. Role of platelet rich fibrin and platelet rich plasma in wound healing of extracted third molar sockets: a comparative study. J Maxillofac Oral Surg. 2015 Jun;14(2):410–6.
284. Kobayashi M, Kawase T, Horimizu M, Okuda K, Wolff LF, Yoshie H. A proposed protocol for the standardized preparation of PRF membranes for clinical use. Biologicals. 2012 Sep;40(5):323–329.
285. Iasella JM, Greenwell H, Miller RL, Hill M, Drisko C, Bohra AA, Scheetz JP. Ridge preservation with freeze-dried bone allograft and a collagen membrane compared to extraction alone for implant site development: a clinical and histologic study in humans. J Periodontol. 2003 Jul;74(7):990–999.
286. Araújo MG, Lindhe J. Ridge preservation with the use of Bio-Oss collagen: A 6-month study in the dog. Clin Oral Implants Res. 2009 May;20(5):433–440.
287. Jain V, Triveni MG, Kumar AB, Mehta DS. Role of platelet-rich-fibrin in enhancing palatal wound healing after free graft. Contemp Clin Dent. 2012 Sep;3(Suppl 2):S240–243.
288. Sigron GR, Pourmand PP, Mache B, Stadlinger B, Locher MC. The most common complications after wisdom-tooth removal: part 1: a retrospective study of 1,199 cases in the mandible. Swiss Dent J. 2014;124(10):1042–1046.
289. Haraji A, Rakhshan V, Khamverdi N, Alishahi HK. Effects of intra-alveolar placement of 0.2% chlorhexidine bioadhesive gel on dry socket incidence and postsurgical pain: a double-blind split-mouth randomized controlled clinical trial. J Orofac Pain. 2013 Summer;27(3):256–262.
290. Birn H. Etiology and pathogenesis of fibrinolytic alveolitis (’dry socket’). Int J Oral Surg. 1973;2(5):211–263.

291. Blum IR. Contemporary views on dry socket (alveolar osteitis): a clinical appraisal of standardization, aetiopathogenesis and management: a critical review. Int J Oral Maxillofac Surg. 2002 Jun;31(3):309–317.
292. Hoaglin DR, Lines GK. Prevention of localized osteitis in mandibular third-molar sites using platelet-rich fibrin. Int J Dent. 2013;2013:875380.
293. Eshghpour M, Dastmalchi P, Nekooei AH, Nejat A. Effect of platelet-rich fibrin on frequency of alveolar osteitis following mandibular third molar surgery: a double-blinded randomized clinical trial. J Oral Maxillofac Surg. 2014 Aug;72(8):1463–1467.
294. Al-Hamed FS, Tawfik MA-M, Abdelfadil E. Clinical effects of platelet-rich fibrin (PRF) following surgical extraction of lower third molar. Saudi J Dent Res. 2017;8:19–25.
295. Sammartino G, Dohan Ehrenfest DM, Carile F, Tia M, Bucci P. Prevention of hemorrhagic complications after dental extractions into open heart surgery patients under anticoagulant therapy: the use of leukocyte- and platelet-rich fibrin. J Oral Implantol. 2011 Dec;37(6):681–690.
296. Choukroun J, Diss A, Simonpieri A, Girard MO, Schoeffler C, Dohan SL, Dohan AJ, Mouhyi J, Dohan DM. Platelet-rich fibrin (PRF): a second-generation platelet concentrate. Part IV: clinical effects on tissue healing. Oral Surg Oral Med Oral Pathol Oral Radiol Endod. 2006 Mar;101(3):e56–60.
297. Dohan Ehrenfest DM, Del Corso M, Diss A, Mouhyi J, Charrier JB. Three-dimensional architecture and cell composition of a Choukroun's platelet-rich fibrin clot and membrane. J Periodontol. 2010 Apr;81(4):546–555.
298. Yeaman MR. Platelets: at the nexus of antimicrobial defence. Nat Rev Microbiol. 2014 Jun;12(6):426–437.
299. Ghanaati S, Booms P, Orlowska A, Kubesch A, Lorenz J, Rutkowski J, Landes C, Sader R, Kirkpatrick C, Choukroun J. Advanced platelet-rich fibrin: a new concept for cell-based tissue engineering by means of inflammatory cells. J Oral Implantol. 2014 Dec;40(6):679–689.
300. Turner ML. Cell adhesion molecules: a unifying approach to topographic biology. Biol Rev Camb Philos Soc. 1992 Aug;67(3):359–377.
301. Mócsai A. Diverse novel functions of neutrophils in immunity, inflammation, and beyond. J Exp Med. 2013 Jul 1;210(7):1283–1299.
302. Sinder BP, Pettit AR, McCauley LK. Macrophages: Their Emerging Roles in Bone. J Bone Miner Res. 2015 Dec;30(12):2140–2149.
303. Clark RA. Fibrin and wound healing. Ann N Y Acad Sci. 2001;936:355–367.
304. Kumar YR, Mohanty S, Verma M, Kaur RR, Bhatia P, Kumar VR, Chaudhary Z. Platelet-rich fibrin: the benefits. Br J Oral Maxillofac Surg. 2016 Jan;54(1):57–61.
305. Bilginaylar K, Uyanik LO. Evaluation of the effects of platelet-rich fibrin and piezosurgery on outcomes after removal of ımpacted mandibular third molars. Br J Oral Maxillofac Surg. 2016 Jul;54(6):629–633.

306. Ozgul O, Senses F, Er N, Tekin U, Tuz HH, Alkan A, Kocyigit ID, Atil F. Efficacy of platelet rich fibrin in the reduction of the pain and swelling after impacted third molar surgery: randomized multicenter split-mouth clinical trial. Head Face Med. 2015 Nov 26;11:37.
307. Kumar N, Prasad K, Ramanujam L, Ranganath K, Dexith J, Chauhan A. Evaluation of treatment outcome after impacted mandibular third molar surgery with the use of autologous platelet-rich fibrin: a randomized controlled clinical study. J Oral Maxillofac Surg. 2015 Jun;73(6):1042–1049.
308. Gülşen U, Şentürk MF. Effect of platelet rich fibrin on edema and pain following third molar surgery: a split mouth control study. BMC Oral Health. 2017 Apr 24;17(1):79.
309. Uyanik LO, Bilginaylar K, Etikan I. Effects of platelet-rich fibrin and piezosurgery on impacted mandibular third molar surgery outcomes. Head Face Med. 2015 Jul 26;11:25.
310. Shugars DA, Benson K, White RP Jr, Simpson KN, Bader JD. Developing a measure of patient perceptions of short-term outcomes of third molar surgery. J Oral Maxillofac Surg. 1996 Dec;54(12):1402–8.
311. Atchison KA, Der-Martirosian C, Belin TR, Black EE, Gironda MW. Predictors of risk tolerance among oral surgery patients. J Oral Maxillofac Surg. 2010 Dec;68(12):2947–54.
312. He B, Ou Y, Chen S, Zhao W, Zhou A, Zhao J, Li H, Jiang D, Zhu Y. Designer bFGF-incorporated d-form self-assembly peptide nanofiber scaf-folds to promote bone repair. Mater Sci Eng C Mater Biol Appl. 2017 May 1;74:451–458.
313. Poniatowski ŁA, Wojdasiewicz P, Gasik R, Szukiewicz D. Transforming growth factor Beta family: insight into the role of growth factors in regulation of fracture healing biology and potential clinical applications. Mediators Inflamm. 2015;2015:137823.
314. Boëck-Neto RJ, Artese L, Piattelli A, Shibli JA, Perrotti V, Piccirilli M, Marcantonio E Jr. VEGF and MVD expression in sinus augmentation with autologous bone and several graft materials. Oral Dis. 2009 Mar;15(2):148–54.
315. Fiedler J, Etzel N, Brenner RE. To go or not to go: Migration of human mesenchymal progenitor cells stimulated by isoforms of PDGF. J Cell Biochem. 2004 Nov 15;93(5):990–998.
316. Guihard P, Boutet MA, Brounais-Le Royer B, Gamblin AL, Amiaud J, Renaud A, Berreur M, Rédini F, Heymann D, Layrolle P, Blanchard F. Oncostatin m, an inflammatory cytokine produced by macrophages, supports intramembranous bone healing in a mouse model of tibia injury. Am J Pathol. 2015 Mar; 185(3):765–75.
317. Muller PA, Koscsó B, Rajani GM, Stevanovic K, Berres ML, Hashimoto D, Mortha A, Leboeuf M, Li XM, Mucida D, Stanley ER, Dahan S, Margolis KG, Gershon MD, Merad M, Bogunovic M. Crosstalk between muscularis

macrophages and enteric neurons regulates gastrointestinal motility. Cell. 2014 Jul 17; 158(2):300–313.
318. Kan L, Liu Y, McGuire TL, Berger DM, Awatramani RB, Dymecki SM, Kessler JA. Dysregulation of local stem/progenitor cells as a common cellular mechanism for heterotopic ossification. Stem Cells. 2009 Jan; 27(1):150–6.
319. Shimokado K, Raines EW, Madtes DK, Barrett TB, Benditt EP, Ross R. A significant part of macrophage-derived growth factor consists of at least two forms of PDGF. Cell. 1985 Nov;43(1):277–286.
320. Toulon A, Breton L, Taylor KR, Tenenhaus M, Bhavsar D, Lanigan C, Rudolph R, Jameson J, Havran WL. A role for human skin-resident T cells in wound healing. J Exp Med. 2009 Apr 13;206(4):743–750.
321. Yakar S, Courtland HW, Clemmons D. IGF-1 and bone: New discoveries from mouse models. J Bone Miner Res. 2010 Dec;25(12):2543–2552.
322. Kobayashi Y, Saita Y, Nishio H, Ikeda H, Takazawa Y, Nagao M, Takaku T, Komatsu N, Kaneko K. Leukocyte concentration and composition in platelet-rich plasma (PRP) influences the growth factor and protease concentrations. J Orthop Sci. 2016 Sep;21(5):683–9.
323. Daugela P, Grimuta V, Sakavicius D, Jonaitis J, Juodzbalys G. Influence of leukocyte- and platelet-rich fibrin (L-PRF) on the outcomes of impacted mandibular third molar removal surgery: A split-mouth randomized clinical trial. Quintessence Int. 2018;49(5):377–388.
324. Nandi SK, Roy S, Mukherjee P, Kundu B, De DK, Basu D. Orthopaedic applications of bone graft & graft substitutes: a review. Indian J Med Res. 2010 Jul;132:15–30.

MOKSLINĖS PUBLIKACIJOS DARBO TEMA

Straipsniai leidiniuose, referuojamuose duomenų bazėje „Clarivate Analytics Web of Science“ ir turinčiuose citavimo rodiklį:

1. Daugela P, Pranskunas M, Juodzbalys G, Liesiene J, Baniukaitiene O, Afonso A, Sousa Gomes P. Novel cellulose/hydroxyapatite scaffolds for bone tissue regeneration: In vitro and in vivo study. J Tissue Eng Regen Med. 2018 May;12(5):1195–1208. [Citavimo rodiklis: 3,989 (2017)]
2. Daugela P, Grimuta V, Sakavicius D, Jonaitis J, Juodzbalys G. Influence of leukocyte- and platelet-rich fibrin (L-PRF) on the outcomes of impacted mandibular third molar removal surgery: A split-mouth randomized clinical trial. Quintessence Int. 2018;49(5):377–388. [Citavimo rodiklis: 0,995 (2017)]
3. Ramanauskaite A, Daugela P, Juodzbalys G. Treatment of peri-implantitis: Meta-analysis of findings in a systematic literature review and novel protocol proposal. Quintessence Int. 2016;47(5):379–93. [Citavimo rodiklis: 0,995 (2017)]
4. Palaveniene A, Harkavenko V, Kharchenko V, Daugela P, Pranskunas M, Juodzbalys G, Babenko N, Liesiene J. Cuttlebone as a Marine-Derived Material for Preparing Bone Grafts. Mar Biotechnol (NY). 2018 Apr 3. doi: 10.1007/s10126-018-9816-6. [Epub ahead of print]. [Citavimo rodiklis: 2,748 (2017)]

Straipsniai recenzuojamuose mokslo leidiniuose, referuojamuose kitose duomenų bazėse:

1. Juodzbalys G, Daugela P. Mandibular third molar impaction: review of literature and a proposal of a classification. J Oral Maxillofac Res. 2013 Jul 1;4(2):e1.
2. Daugela P, Cicciù M, Saulacic N. Surgical Regenerative Treatments for Peri-Implantitis: Meta-analysis of Recent Findings in a Systematic Literature Review. J Oral Maxillofac Res. 2016 Sep 9;7(3):e15. eCollection 2016 Jul–Sep.
3. Suárez-López Del Amo F, Faria E Almeida R, Cicciù M, Daugela P, Ramanauskaite A, Saulacic N, Tervonen T, Wang HL, Yu SH. The 1st Baltic Osseointegration Academy and Lithuanian University of Health Sciences Consensus Conference 2016. Summary and Consensus Statements: Group III - Peri-Implantitis Treatment. J Oral Maxillofac Res. 2016 Sep 9;7(3):e16. eCollection 2016 Jul–Sep.

Disertacijos tema pristatytų pranešimų sąrašas:

1. Daugėla, Povilas, Juodžbalys, Gintaras. Natural bone regeneration concept / Penktasis tarptautinis BOA kongresas : programa ir pranešimų santraukos : 2013 m. rugsėjo 13–14 d., Kaunas, Lietuva = The Fifth International BOA Congress : Programme and Abstract Book : Kaunas p. 25–26, no. #20.
2. Juodžbalys, Gintaras, Kubilius, Marius, Daugėla, Povilas. New look at three-dimensional jawbone anatomy evaluation: comprehensive clinical-radiological classifications / Penktasis tarptautinis BOA kongresas : programa ir pranešimų santraukos : 2013 m. rugsėjo 13–14 d., Kaunas, Lietuva = The Fifth International BOA Congress : Programme and Abstract Book : Kaunas p. 13–14, no. #05.
3. Daugėla, Povilas, Juodžbalys, Gintaras. Novel look at growth factors in alveolar ridge regeneration surgeries: literature review in comparison with own clinical experience / SCOI – III Congreso Internacional de Sociedad Científica de Odontología Implantológica : Granada, 27–29 de Marzo 2014 : Libro de Actas / Organiza: Sociedad Científica de Odontología Implant p. 42–43, no. 20.
4. Ramanauskaitė, Aušra, Daugėla, Povilas, Basevičienė, Nomeda. Peri-implantitis bone defect treatment using autologous advanced platelet-rich fibrin in combination with particulated processed human allograft. a case report / 12th ITI World Symposium “Knowledge is Key” : April 24–26 2014, Geneva, Switzerland / ITI International Team for Implantology. ITI Headquarters David L. Cochran, Daniel Buser, Stephen T. Chen p. 1.
5. Baniukaitienė, Odeta, Liesienė, Jolanta, Palavenienė, Alisa, Juodžbalys, Gintaras, Daugėla, Povilas, Pranskūnas, Mindaugas. Cellulose-based grafts for bone regeneration / Biomedical Engineering - 2015 : Proceedings of 19th International conference : [Kaunas, Lithuania, 26–2 November 2015] / Kaunas University of Technology. Biomedical Engineering Institute. Lithuania p. 19–22.
6. Daugėla, Povilas, Cicciù, Marco, Saulacic, Nikola. Current trends in peri-implant bone regeneration / Šeštasis BOA ir LSMU kongresas ir konsensuso konferencija : 2016 m. rugsėjo 9–10 d., Kaunas, Lietuva : programa ir pranešimų santraukos = The Sixth BOA and LUHS congress and consensus confere p. 32–33, no. 23.
7. Fernando Suárez-López del Amo, Ricardo Faria e Almeida, Marco Cicciù, Povilas Daugela, Ausra Ramanauskaite, Nikola Saulacic, Tellervo Tervonen, Hom-Lay Wang, Shan-Huey Yu. The 1st Baltic Osseointegration Academy and Lithuanian University of Health Sciences Consensus Conference 2016, Kaunas, Lithuania. Summary and Consen-

sus Statements: Peri-Implantitis Treatment / Šeštasis BOA ir LSMU kongresas ir konsensuso konferencija : 2016 m. rugsėjo 9–10 d., Kaunas, Lietuva : programa ir pranešimų santraukos = The Sixth BOA and LUHS congress and consensus conference : Kaunas, Lithuania 9–10 September, 2016 : programme and abstract book / Baltijos osteointegracijos akademija/Baltic Osseointegration Academy. Kaunas : Baltijos osteointegracijos akademija, 2016. p. 24–25, no. 15.

8. The Effect of L-PRF after impacted third molar teeth extraction / Vaidas Grimuta, Sakavicius D., Kubilius R., Lukosiunas A., Daugėla P., Sakavičiute E. 9th Congress of Baltic Association for Maxillofacial and Plastic Surgery : May 12–13, 2017 in Tartu, Estonia : programme and abstract book / Baltic AMPS (Baltic Association for Maxillofacial and Plastic Surgery). Tartu : BAMPS, 2017. p. 51.

Received: 8 July 2017 | Revised: 5 November 2017 | Accepted: 17 February 2018
DOI: 10.1002/term.2651

RESEARCH ARTICLE

WILEY

Novel cellulose/hydroxyapatite scaffolds for bone tissue regeneration: *in vitro* and *in vivo* study

Povilas Daugela[1] | Mindaugas Pranskunas[1] | Gintaras Juodzbalys[1] | Jolanta Liesiene[2] | Odeta Baniukaitiene[2] | Américo Afonso[3] | Pedro Sousa Gomes[3,4]

[1] Department of Oral and Maxillofacial Surgery, Lithuanian University of Health Sciences, Kaunas, Lithuania

[2] Department of Polymer Chemistry and Technology, Kaunas University of Technology, Kaunas, Lithuania

[3] Faculty of Dental Medicine, University of Porto, Porto, Portugal

[4] REQUIMTE/LAQV, University of Porto, Porto, Portugal

Correspondence
Povilas Daugela, Department of Oral and Maxillofacial Surgery, Lithuanian University of Health Sciences, Eiveniu str. 2, Kaunas LT-50009, Lithuania.
Email: p.daugela@gmail.com

Funding information
Research Council of Lithuania, Grant/Award Number: MIP019/2014

Abstract

Cellulose scaffolds containing nano- or micro-hydroxyapatite (nHA or μHA) were prepared by the regeneration of cellulose from its acetylated derivative and the mechanical immobilization of inorganic particles, followed by freeze-drying. Microtomographic (micro-computed tomography) evaluation revealed that both scaffolds presented a highly interconnected porous structure, with a mean pore diameter of 490 ± 94 and 540 ± 132 μm for cellulose/nHA and cellulose/μHA, respectively. In vitro and in vivo characterizations of the developed scaffolds were investigated. Commercially available bone allograft was used as a control material. For the in vitro characterization, osteoblastic cell cultures were used and characterized over time to evaluate cell adhesion, metabolic activity, and functional output (alkaline phosphatase activity and osteoblastic gene expression). The results revealed greater spreading cell distribution alongside an increased number of filopodia, higher MTT values, and significantly increased expression of osteoblastic genes (Runx-2, alkaline phosphatase, and BMP-2) for cellulose/nHA, compared with cellulose/μHA and the control. The in vivo biocompatibility was evaluated in a rabbit calvarial defect model. The investigated scaffolds were implanted in circular rabbit calvaria defects. Four- and 12-week bone biopsies were investigated using micro-computed tomography and histological analysis. Although both cellulose/HA scaffolds outperformed the assayed control, a significantly higher amount of newly formed mineralized tissue was found within the defects loaded with cellulose/nHA. Within the limitations of this study, the developed cellulose/HA scaffolds showed promising results for bone regeneration applications. The biological response to the scaffold seems to be greatly dependent on the HA particles' characteristics, with cellulose scaffolds loaded with nHA eliciting an enhanced bone response.

KEYWORDS

bone regeneration, bone tissue engineering, cellulose, hydroxyapatite, osteoblasts, porosity

1 | INTRODUCTION

The aim of bone grafting is to promote new bone formation on sites affected by disease, infection, or resection. A broad range of bone grafts and graft substitutes are currently available. Grafts from the patient's autologous tissues (autografts), together with those donated from human donors (allografts) or from various animal species (xenografts), are mostly used in clinical practice (Bauer & Muschler, 2000; Ebraheim, Elgafy, & Xu, 2001). Autografts contain viable osteogenic cells and osteoinductive growth factors, which stimulate new bone tissue formation. Furthermore, such kinds of grafts possess a microstructure suitable for cellular activity, vascularization, and new bone formation (Oryan, Alidadi, Moshiri, & Maffulli, 2014). Autogenous bone still remains the gold standard due to its mentioned osteogenicity, osteoinductivity, and osteoconductivity apart from the fact that its use causes donor site morbidity, increased postoperative pain, prolonged healing and, eventually, with the use of dense cortical tissue, delayed revascularization (Ebraheim et al., 2001). Allogenic bone allows for osteoconductivity and inconsistent osteoinductivity, despite the risk of immunogenic activation and disease transmission (Oryan et al., 2014). Xenograft bone substitute may originate, for instance, from bovine, porcine, equine, or coral tissues, which can be freeze-dried or demineralized and deproteinized. Xenografts are osteoconductive materials, losing their osteoinductive and osteogenic

properties during graft processing. Major concerns are associated with the potential transmission of zoonotic diseases, prion infections, and immunological activation (Kim, Nowzari, & Rich, 2013). The clinical effectiveness of xenografts is also in dispute in particular clinical situations due to the slow graft turnover and decreased new vital bone formation (Artzi, Tal, & Dayan, 2000; Ramírez-Fernández et al., 2013).

The use of currently available bone grafts is also challenging for the clinicians in some specific clinical situations, where reconstruction of large alveolar bone defects or vertical alveolar bone augmentation is desired (Laino, Iezzi, Piattelli, Lo Muzio, & Cicciù, 2014). Various clinical approaches, including the use of recombinant human bone morphogenetic protein-2 (rhBMP-2) have been suggested for vertical alveolar bone reconstructions (Cicciù, Herford, Cicciù, Tandon, & Maiorana, 2014; Herford, Tandon, Stevens, Stoffella, & Cicciu, 2013). However, the clinical relevance of rhBMP-2 is currently still limited due to safety concerns with "off-label" use and license restrictions in particular countries (Woo, 2012).

The disadvantages of the aforementioned grafts have encouraged the development of alloplastic bone graft substitutes. More recently, significant attention has focused on the fabrication of porous interconnected three-dimensional (3D) scaffolds, which fill the defects and, with a timely degradation process, provide a structure that primes bone regeneration (Hench & Polak, 2002). A wide variety of inorganic materials have been developed and assayed, including β-tricalcium phosphate (β-TCP), hydroxyapatite (HA), bioactive glass (BS), and calcium silicate (CS) (Gao et al., 2014). Polymeric materials were also used, allowing for better handling and more favourable vascularization as well as the capacity to immobilize inorganic material particles into the polymer matrix (Nejati, Mirzadeh, & Zandi, 2008; Saska et al., 2011; Zimmermann, LeBlanc, Sheets, Fox, & Gatenholm, 2011). Aliphatic polyesters, such as poly(caprolactone), poly(glycolic acid), poly(lactic acid), and poly(lactide-co-glycolide), have been preferred (Guo & Ma, 2014). Natural polymers have been found to offer several advantages over synthetic polymers within bone-related applications, namely, an increased biocompatibility profile, adequate hydrophilicity, and biodegradability. A wide variety of natural polymers, including cellulose, starch, chitosan, chitin, collagen, gelatin, and others, have been used for 3D scaffold development (Qiu & Netravali, 2014; Salgado, Coutinho, & Reis, 2004; Wang et al., 2009).

Significant attention has been given to cellulose, due to its unique properties of interest to biological applications: adequate surface chemistry profile, biocompatibility, non-toxicity, and controllable biodegradability (Miyamoto, Takahashi, Ito, Inagaki, & Noishiki, 1989). Cellulose degradation is carried out by cellulases, but they do not exist in mammals (Wilson, 2008). Therefore, the degradation of cellulose in these organisms could possibly be carried out through mechanical erosion and acidic hydrolysis. Cellulose is a linear-chain polymer with an abundance of hydroxyl groups, and its degree of crystallinity and the size of the crystalline regions are largely dependent on the natural source of the cellulose. Different polymorphs of cellulose, including I, II, III, and IV, are known. It should be noted that its biodegradability in vivo depends on its crystallinity. Only amorphous cellulose (cellulose II) implanted in a bone defect could be fully biodegradable in vivo due to its acidic hydrolysis, which does not appear in the crystalline phase.

Although, in the literature, bacterial cellulose is the most investigated in bone tissue engineering (Grande, Torres, Gomez, & Bañó, 2009; Nge & Sugiyama, 2007; Zimmermann et al., 2011), in this work, regenerated cellulose was proposed for the preparation of bone scaffolds. Regenerated cellulose is obtained by the conversion of natural cellulose to its derivatives and subsequent regeneration, forming films, membranes, beads, and hydrogels (Wang, Lu, & Zhang, 2016). Such cellulose has a low degree of crystallinity.

In this work, a regenerated cellulose gel was prepared by saponification of cellulose acetate in an acetone solution. Our previous studies showed that the gel has great potential for the preparation of wound dressings (Kiselioviene, Baniukaitiene, Harkavenko, Babenko, & Liesiene, 2016), sorbents for chromatography (Bryjak, Aniulyte, & Liesiene, 2007), and macroporous 3D scaffolds (Petrauskaite, Juodzbalys, Viskelis, & Liesiene, 2016).

This article is focused on regenerated cellulose-based 3D composites with HA particles for bone tissue regeneration, their fabrication and cytocompatibility, biocompatibility, and functionalities as compared with a commercial product.

2 | MATERIALS AND METHODS

2.1 | Study design

This study involved development of regenerated cellulose scaffolds containing nano- and micro-hydroxyapatite (cellulose/nHA and cellulose/μHA), followed by their in vitro and in vivo characterization.

For the in vitro part, a scanning electron microscopy (SEM) observation, 3-(4,5-dimethylthiazol-2-yl)-2,5-diphenyltetrazolium bromide (MTT) cell proliferation assay, gene expression by reverse transcription-polymerase chain reaction (RT-PCR) and alkaline phosphatase (ALP) activity tests were performed.

The in vivo evaluation involved the biocompatibility assessment of developed cellulose scaffolds following the implantation in surgically created circular calvarial bone defects in a rabbit calvaria model. The biological response of cellulose/nHA and cellulose/μHA was compared with that of a control material—a commercially available biocompatible scaffold allograft cancellous block (Maxgraft, Botiss Biomaterials GmbH, Zossen, and Germany), commonly used for bone tissue regeneration.

2.2 | Preparation of regenerated cellulose-based scaffolds with hydroxyapatite particles

For this study, cellulose acetate with a 2.4° of substitution (Sigma-Aldrich Co., St. Louis, USA), nHA (average particle size 100 nm), and μHA (average particle size 20 μm) spherical particles (Sigma-Aldrich Co., St. Louis, USA) were used for production of the composite cellulose/nHA and cellulose/μHA scaffolds, respectively. Regenerated cellulose gel was prepared as previously described (Petrauskaite et al., 2013). For the preparation of cellulose-based composite scaffolds, nHA or μHA spherical particles were inserted within the polymer during the formation of cellulose gel from cellulose acetate. Composites were formulated with HA particles of 50 wt%. The porous structure was formed using a freeze-drying technique (Christ ALPHA 2-4 LSC

freeze dryer, Martin Christ Gefriertrocknungsanlagen GmbH, Osterode am Harz, Germany).

2.3 | Characterization of the scaffolds

Morphological parameters of the scaffolds were evaluated by micro-computed tomography (μCT; n = 4). The μCT analysis was performed using a μCT40 system (Scanco Medical AG, Bruttisellen, Switzerland). A sample of the scaffold in the form of a cylinder with a diameter of 10 mm and a height of 8 mm was used for the analysis. The following parameters were used for the scans: energy, 45 kVp; integration time, 600 ms; frame averaging, 2×; and nominal resolution, 10 μm. The data were filtered using a constrained 3D Gaussian filter to partially suppress the noise in the images (σ = 0.8, support = 1). 2D and 3D images were generated using image reconstruction software provided by the manufacturer. Scanco 6.0 evaluation software was used for quantitative evaluation of structural parameters of the scaffolds.

Fourier transform infrared spectroscopy was performed using an FTIR spectrometer (Perkin-Elmer, Inc., Waltham, USA). Four milligrams of the sample (n = 4) was mixed with 200 mg of KBr for the preparation of transparent pellets. All spectra were recorded in the range from 4,000 to 400 cm^{-1}.

Chemical composition of the scaffolds was analysed using the Quantax EDS system (Bruker AXS Microanalysis GmbH, Karlsruhe, Germany; n = 4).

X-ray diffraction was used to determine the degree of crystallinity of the cellulose (n = 4). Diffraction patterns were recorded on a DRON-6 using Cu Kα radiation at 30 kV and 20 mA.

2.4 | In vitro cytotoxicity determination

Human osteoblastic-like cells (Mg-63, ATCC number CRL-1427) of passage 27 were used in this study. Cells were grown on α-MEM culture medium, supplemented with 10% fetal bovine serum, 50 $\mu g \cdot ml^{-1}$ ascorbic acid, 50 $\mu g \cdot ml^{-1}$ gentamicin, and 2.5 $\mu g \cdot ml^{-1}$ fungizone, at 37 °C, in a humidified atmosphere of 5% CO_2 in the air. At adequate confluency (around 75%), cultures were detached (0.05% trypsin, 0.25% EDTA; 5 min, 37 °C), and the resultant cell suspension was used in the experiments.

Cells were seeded at 2 × 10^4 cells/cm^{-2} and cultured for 7 days. Cultures were characterized regarding cell morphology (by SEM [n = 4]), metabolic activity (by the MTT assay [n = 6]), gene expression (n = 3), and ALP activity (n = 6).

2.4.1 | SEM observation

Seeded constructs were fixed at 24 hr of culture (1.5% glutaraldehyde in 0.14 M sodium cacodylate buffer, pH = 7.3, 10 min). Samples were further dehydrated in graded alcohols, critical-point dried, sputter-coated with an Au/Pd film (SPI Module Sputter Coater equipment, Structure Probe, Inc., West Chester, USA), and observed in an SEM (Quanta 400 FEG SEM, FEI Co., Hillsboro, USA).

2.4.2 | MTT assay

The cultures' metabolic activity was estimated by the MTT assay, based on the reduction of the 3-(4,5-dimethylthiazol-2-yl)-2,5-diphenyltetrazolium by viable cells to a dark blue formazan product. At adequate time points, MTT (0.5 $mg \cdot ml^{-1}$) was added, and cultures were incubated for 3 hr in the abovementioned culture conditions. Samples were transferred to new wells, and formazan salts were dissolved in dimethylsulphoxide. The absorbance was measured at 550 nm on a plate reader (Synergy HT, BioTek Instruments, Winooski, USA).

2.4.3 | Gene expression by RT-PCR

Cell cultures grown for 7 days were evaluated for the expression of the housekeeping gene GAPDH (glyceraldehydes-3-phosphate dehydrogenase) and the osteoblastic genes runt-related transcription factor 2 (Runx-2), ALP, bone morphogenetic protein 2 (BMP-2) and collagen type I (Col I). RNA was extracted using an RNeasy® Mini Kit (QIAGEN, Hilden, Germany), according to the manufacturer's instructions. RNA yield and purity were assessed by spectrophotometric determination at 260 and 280 nm, and quality was evaluated by 2% (w/v) agarose-gel electrophoresis. RNA, 0.5 μg, was reverse transcribed and amplified with the Titan One Tube RT-PCR System (Roche Diagnostics, Mannheim, Germany) at an annealing temperature of 55 °C. The sequences of the primers used for RT-PCR analysis were as follows: GAPDH, forward primer—CAGGACCAGGTTCACCAACAAGT, reverse primer—GTGGCAGTGATGGCATGGACTGT; Runx-2, forward primer—CAGTTCCCAAGCATTTCATCC, reverse primer—TCAATATGGTCGCCAAACAG; ALP, forward primer—ACGTGGCTAAGAATGTCATC, reverse primer—CTGGTAGGCGATGTCCTTA; BMP-2, forward primer—GCAATGGCCTTATCTGTGAC, reverse primer—GCAATGGCCTTATCTGTGAC; Col I, forward primer—TCCGGCTCCTGCTCCTCTTA, reverse primer—ACCAGCAGGACCAGCATCTC. After electrophoresis on 1% (w/v) agarose gel, the bands were analysed through densitometric analysis with the ImageJ 1.41 (National Institutes of Health, Bethesda, USA) software. Values were normalized to the corresponding GAPDH value of each experimental condition.

2.4.4 | ALP activity

ALP activity was determined in cell lysates (0.1% Triton X-100, 5 min) by the hydrolysis of p-nitrophenyl phosphate (pH – 10.3; 30 min, 37 °C), and p-nitrophenol activity (λ = 400 nm) was determined in a plate reader (Synergy HT, BioTek Instruments, Winooski, USA). ALP activity was normalized to total protein content (quantified by Bradford's method) and expressed as nmol/min/μg protein.

2.5 | In vivo studies

Developed cellulose/nHA and cellulose/μHA round constructs (8.0 mm diameter and 2.0 mm thickness) for implantation in rabbit calvaria defects were used. As a comparative material, a commercially available allograft cancellous block for bone regenerative applications (Maxgraft, Botiss Biomaterials GmbH, Zossen, Germany), prepared in the same manner, was used for control purposes. Scaffolds were pre-operatively rehydrated in a sterile saline solution and randomly distributed. Rabbits were endorsed for the postoperative follow-up in one of the following groups: 4 or 12 weeks (n = 6).

All animal experiments were approved and performed according to Lithuanian State Food and Veterinary Service guidelines and European Community guidelines for animal care (Permission No. G2-18).

Twelve adult male New Zealand white rabbits of 30–35 weeks of age and weighing 3.5–4.0 kg were acquired from a certified vendor. Prior to surgical procedure, the animals were premedicated with an intramuscular injection of acepromazine (0.5 mg/kg), and a subcutaneous injection of buprenorphine (0.03 mg/kg) was used for analgesia. General anaesthesia was induced by intramuscular administration of ketamine hydrochloride (35 mg/kg) and xylazine hydrochloride (5 mg/kg). A trichotomy was conducted on the calvarial area, followed by the disinfection of the skin with an octenidine dihydrochloride solution. After administration of a local injection of 4% articaine hydrochloride with epinephrine 1:100.000, for local anaesthesia and bleeding control, a sagittal incision was made in the midline of the cranium, and the skin and the periosteum were reflected.

In each side of the calvaria, using a trephine drill (speed 2,000 rpm), under copious irrigation with saline solution, two standard 8.0 mm in diameter and approximately 2.0 mm in depth bone defects were made. In total, four circular defects in each animal were created, as shown in Figure 1. Particular care was taken to preserve *dura mater* during defect formation. The defects were randomly press-fitted with either developed cellulose/nHA, cellulose/μHA or commercial allograft scaffolds. Randomization for the selection was performed using specific software, available at http://www.randomization.com. No membranes were used in this study. The wound was closed in layers by suturing with 5–0 polyglycolic acid absorbable suture material (Atramat, Internacional Farmacéutica S.A. de C.V., Mexico City, Mexico).

Postoperative X-rays ensured the correct position of the bone grafts. During the postoperative period, animals were allowed to move freely in their cages, at controlled temperature and light cycle. Water and food were administered ad libitum. An analgesic regimen with buprenorphine was maintained during the first week. No antibiotics were administered.

The animals were sacrificed 4 and 12 weeks after the surgical procedures, initially using a combination of ketamine hydrochloride (50 mg/kg) and xylazine hydrochloride (20 mg/kg) administered intramuscularly, followed by 25 mg/kg of sodium thiopental administered intravenously in the marginal ear vein 20 min thereafter. In order to address systemic toxicology effects, histopathological evaluation of the liver and kidney was conducted. Furthermore, the biological response of the implants within the grafted rabbit calvaria was evaluated by microtomographic and histological analysis, addressing the characterization of the bone grafts' degradation process and the disclosure of the bone formation process in the vicinity of the implanted constructs.

2.5.1 | Microtomographic evaluation

Microtomographic analyses were conducted in a commercially available desktop microtomographic unit (μCT 35, Scanco Medical AG, Bruttisellen, Switzerland) with the following parameters: voxel size of 15 μm, FOV of 30.72 mm, X-ray voltage of 70 kVp, intensity of 114 μA, and an integration time of 800 ms. Structural evaluation of the newly formed tissue was carried out using version 6.0 of the Scanco Medical software. The definition of the volume of interest (VOI) for the analysis was determined with a cylindrical contour, taking into consideration the size of the drill hole (8.0 mm in diameter) and enlarged in the vertical direction to address all the biomaterial and newly formed bone. A fixed VOI was used for all the analyses conducted on different samples. Microstructural measures included the determination of bone volume (BV), total volume (TV), bone volume per total volume ratio (BV/TV), and bone mineral density. The computation of these structural measures has been previously detailed (Silva, Sampaio, Fernandes, & Gomes, 2015). Further, an automated multithreshold segmentation method was employed to highlight and separate the distinct mineralized phases (i.e., scaffold and bone). Briefly, each histogram was partitioned into independent zones, following the manual fixation of thresholds, based on the comparison of microtomographic images with histological images—reference thresholds for "new bone" were set at 3,044 Hounsfield units (HU) and for "new bone & scaffold" at 2,033 HU, allowing for the segmentation and differentiation of the distinct phases within the defect (Calvo-Guirado et al., 2015).

2.5.2 | Histological evaluation

The calvarial bone segments containing the implanted scaffolds were cut and fixed in buffered formaldehyde (10%), dehydrated in graded alcohols, and embedded in a methyl methacrylate resin. Tissue

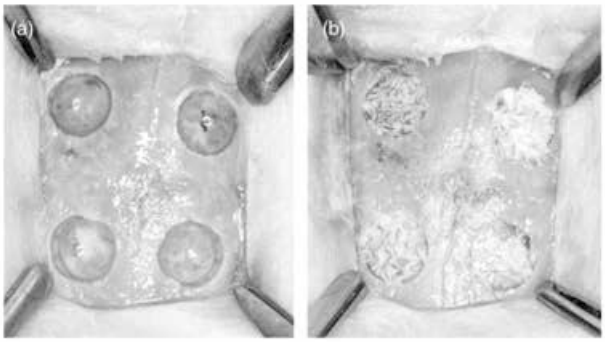

FIGURE 1 (a) Standardized bone defects created in rabbit calvarial bone and (b) Bone defects grafted with cellulose/μHA (top and bottom left defects) and cellulose/nHA (top and bottom right defects) scaffolds [Colour figure can be viewed at wileyonlinelibrary.com]

sections of around 150 μm were cut with a diamond blade microtome and hand-ground to approximately 50–60 μm. Sections were then stained with Solochrome Cyanine R for histological examination with a Nikon light microscope (Eclipse E600, Nikon, Tokyo, Japan), equipped with a calibrated digital camera (Nikon DS-5 M-L1 Digital Sight Camera System, Nikon, Tokyo, Japan).

2.6 | Statistical analysis

For in vitro evaluation, three independent experiments were performed. Sample size was estimated following power analysis computation with G*Power 3 software, following the establishment of a pilot trial for the evaluation of the metabolic activity of the cultures for 3 days. The results are presented as mean ± standard deviation (SD). Data groups were evaluated using a one-way analysis of variance, and no significant differences in the pattern of the cell behaviour were found for the in vitro analysis. Statistical differences between the experimental groups were assessed by Bonferroni's method. Values of $p \leq .05$ were considered statistically significant.

3 | RESULTS

3.1 | Characterization of cellulose-based scaffolds

Cellulose/HA composites were prepared by the regeneration of cellulose from its acetylated derivative and the mechanical immobilization of nHA and μHA particles. Highly porous cellulose/nHA and cellulose/μHA scaffolds were produced by freeze-drying method, as previously described (Petrauskaite et al., 2013).

An infrared analysis of both raw materials and developed composites is presented in Figure 2a. The broad absorption band in the 3,500–3,200 cm^{-1} range was assigned to the stretching vibration of the OH group, regarding the raw cellulose (Figure 2a-E) and prepared composite scaffolds (Figure 2a-C and 2a-D). The peak at 2,893 cm^{-1} corresponded to the symmetric stretching vibration of the CH_2 groups, and the absorption peak, due to the asymmetric C—O—C stretching vibration, which appeared at 1,159 cm^{-1}. Other peaks, at 1,024 and 1,069 cm^{-1}, are related to the stretching of C—O. Regarding the evaluation of HA, IR spectra showed the characteristic absorption peaks of this pure phase material. The sharp peak at 3,571 cm^{-1} was assigned to the stretching vibration of OH ions, whereas the peak at 633 cm^{-1} was assigned to the O—H deformation mode. The absorption peaks at 1,092, 1,044, and 962 cm^{-1} were assigned to the stretching vibration of P—O. The absorption peaks due to the O—P—O stretching vibration appeared at 603, 568, and 474 cm^{-1}. Taking these into account, a similar profile was verified for both μHA (Figure 2a-A) and nHA (Figure 2a-B). Further, the characterized absorption peaks of the raw HA particles were observed in the composite scaffolds (Figure 2 a-C and 2a-D).

Elemental mapping of the scaffolds' surface allowed the identification of Ca and P, fundamental elements of HA composition, permitting the characterization of particles' distribution within the cellulose matrix, the latter identified by C element mapping (Figure 2b,c). In both scaffolds, particles were clearly identified interspersed within the cellulose matrix, and a trend for particle agglomeration was verified.

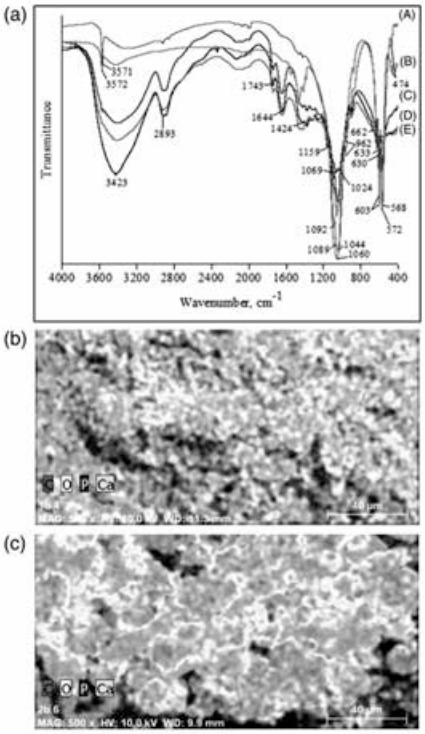

FIGURE 2 (a) The spectra of (A) μHA, (B) nHA, (C) cellulose/μHA, (D) cellulose/nHA, and (E) cellulose. Bottom—SEM-EDS elemental map analysis of the scaffolds: (b) cellulose/nHA and (c) cellulose/μHA [Colour figure can be viewed at wileyonlinelibrary.com]

Comparatively, in cellulose/μHA scaffolds, a higher level of particle aggregation was attained.

Following, the scaffolds were examined by an X-ray diffraction. The typical diffraction peaks of amorphous cellulose (cellulose II) appeared at 12.4°, 20.7°, 21.1°, and 34.9° in 2θ and were also visible in the patterns of the composites (Figure 3a). The diffraction peaks at 25.9°, 31.8°, 32.2°, 34.1°, 46.7°, and 49.6° in 2θ revealed the presence of hydroxyapatite (Figure 3b,c).

Scaffolds were further characterized through microtomographic evaluation. Representative 2D images and 3D reconstructions are presented in Figure 4 as well as data on structural parameters, determined from the 3D analysis. Quantitative data, further supporting what is envisaged from the 2D and 3D reconstructions, revealed that cellulose/nHA scaffolds present slight differences in structural parameters, as compared with cellulose/μHA, namely, a reduced percentage of framework volume, a higher percentage of porosity and an increased specific surface area. Regardless of minor variations, structural parameters were found to be within the same order of magnitude for both assayed compositions. Further, an interconnected porous structure was identified for both scaffolds, with a mean pore diameter of

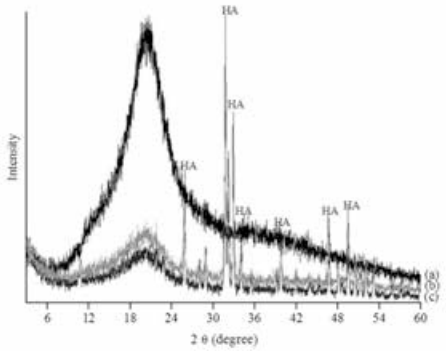

FIGURE 3 X-ray diffraction patterns of (a) regenerated cellulose, (b) cellulose/nHA scaffold, and (c) cellulose/μHA scaffold

490 ± 94 and 540 ± 132 μm, for cellulose/nHA and cellulose/μHA scaffolds, respectively.

3.2 | Cytotoxicity determination

Developed cellulose scaffolds containing μHA and nHA particles were assayed for cytocompatibility through the establishment of direct cultures of human osteoblastic cells. Cultures were characterized for cell adhesion, proliferation, and functional activity at distinct time points up to 7 days of culture.

Cell adhesion and spreading was evaluated by SEM observation at 24 hr of culture (Figure 5, top panel). In cellulose/μHA samples, cell distribution was limited to the scaffolds' regions loaded with μHA particles (Figure 5a,b), with cells establishing thin and short cytoplasmic projections with embedded particles, as evidenced by high-magnification images (Figure 5c). Adhered cells displayed a globular and spherical morphology, with minor cytoplasmic spreading. On cellulose/nHA scaffolds, cells were more distributed over the scaffolds' surface (Figure 5d). In addition, cells at a distinct stage of spreading could be acknowledged, with globular and more elongated cells being visualized concomitantly. Comparatively to cellulose/μHA, whether globular cells could still be identified, generally, a more flattened morphology, associated with increased cytoplasmic spreading and polygonal organization, was acknowledged (Figure 5e). In these, an increased number of filopodia, with greater thickness and length, were further visualized (Figure 5f).

Cells proliferated actively throughout the assayed culture period as MTT reduction values increased from Day 1 to Day 7 in cultures established on both control and cellulose scaffolds. Cellulose/μHA scaffolds presented inferior MTT reduction values, as compared with the control scaffolds, whether cellulose/nHA allowed for increased metabolic activity, with significantly higher values being attained at Days 3 and 7 of culture (Figure 5, bottom).

Cell functional activity was evaluated by the expression of some genes representative of the osteoblastic function—that is, Runx-2, ALP, BMP-2, and Col I—at Day 7 of culture and ALP activity (Figure 6). Comparatively, cultures grown on cellulose/nHA presented a trend for an increased expression of osteoblastic genes, which were found to be significantly higher for Runx-2, ALP, and BMP-2, in comparison with cultures grown on both control and cellulose/μHA substrates. ALP activity was also found to be increased in cultures grown on cellulose/nHA at 7 days of culture. Cultures grown on cellulose/μHA presented a pattern similar to that of the control regarding gene expression and ALP activity.

3.3 | In vivo characterization

During the postoperative period, all animals survived and showed no signs/signals of anxiety or distress. The regions neighbouring the surgical intervention healed adequately without further complications. At the predefined time points, a systematic necropsy was conducted, and no evidence of biomaterial-induced pathological alterations were identified, either locally or systemically.

Microtomographic analysis (Figure 7, top panel) revealed that, at 4 weeks of implantation, control scaffolds showed minimal induction of bone formation, with an evident discontinuity at the native bone/scaffold interface, as clearly identified via both 2D images and 3D

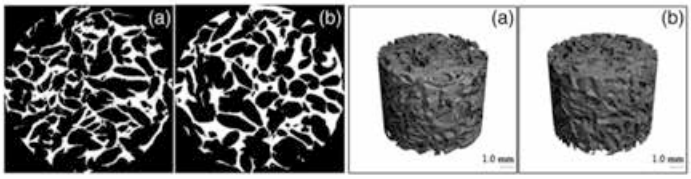

Samples	Structural parameters			
	X_v, %	P, %	SS, mm^{-1}	L, mm
Cellulose/μHA scaffold	34.03 (1.11)	66.12 (2.09)	13.01 (0.50)	0.21 (0.01)
Cellulose/nHA scaffold	28.09 (0.94)*	72.04 (1.72)*	19.06 (0.25)*	0.12 (0.01)*

FIGURE 4 The percent framework volume (Xv), porosity (P), specific surface area (SS), and mean framework thickness (L) of (a) cellulose/μHA and (b) cellulose/nHA scaffolds. *This indicates that the value is significantly different from cellulose/μHA [Colour figure can be viewed at wileyonlinelibrary.com]

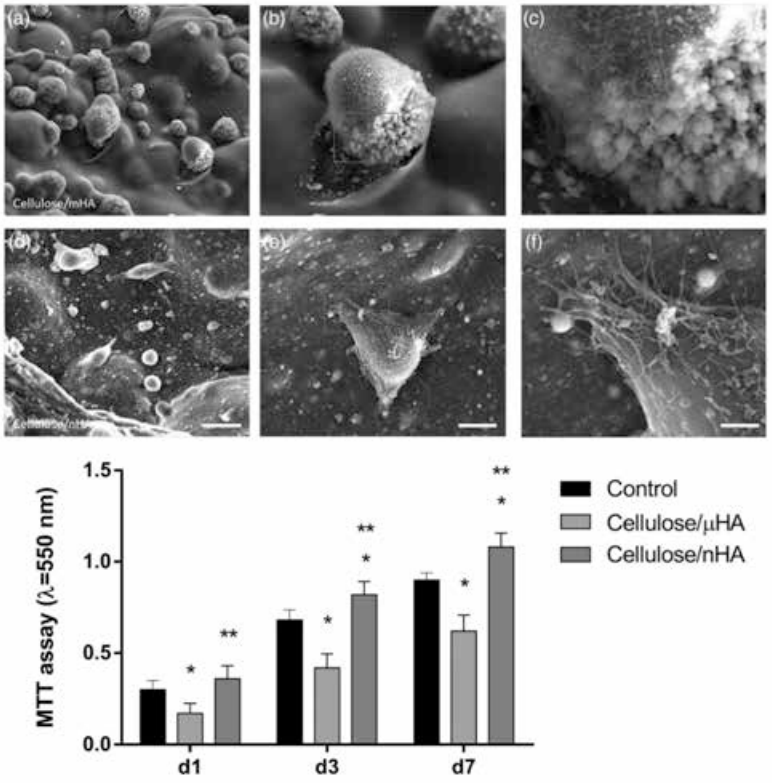

FIGURE 5 Top panel—Representative SEM micrographs of ((a)–(c)) cellulose/μHA and ((d)–(f)) cellulose/nHA scaffolds seeded with human osteoblastic cells, at 24 hr of culture. Scale bar corresponds to 25 μm ((a) and (d)), 10 μm ((b) and (e)), and 4 μm ((c) and (f)). Bottom graph—Cell viability/proliferation (MTT assay) of human osteoblastic cell cultures established on control and cellulose scaffolds, up to 7 days. *This indicates that the value is significantly different from the control; **this indicates that the value is significantly different from cellulose/μHA [Colour figure can be viewed at wileyonlinelibrary.com]

FIGURE 6 Left—Gene expression of human osteoblastic cell cultures established on control and cellulose scaffolds for 7 days. Right—alkaline phosphatase activity of human osteoblastic cell cultures established on control and cellulose scaffolds for 3 and 7 days. *This indicates that the value is significantly different from the control

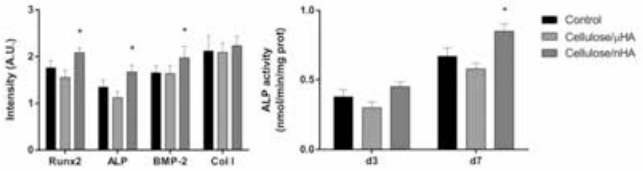

reconstructions. Both cellulose/μHA and cellulose/nHA allowed for an increased bone response, with significant mineralized tissue formation and evidence of scaffold integration into the native bone tissue. In fact, in 2D images, osteoconduction could be seen—particularly noticed within cellulose/nHA scaffolds—with a centripetal bone formation being established from the defect margin into the central region of the defect. At 12 weeks, an increased integration of all assayed scaffolds was verified. Whether the control scaffold seemed to be fully integrated within the native tissue, an increased bone ingrowth was attained for both cellulose scaffolds, with cellulose/nHA being almost encompassed by mineralized tissue. Quantitative assessment of the BV/TV ratio supported the qualitative analysis, revealing increasing levels from Week 4 to Week 12 on all the assayed scaffold structures. Comparatively, cellulose/HA scaffolds presented a significantly higher BV/TV level, as compared with the control, with cellulose/nHA presenting the highest at both time points.

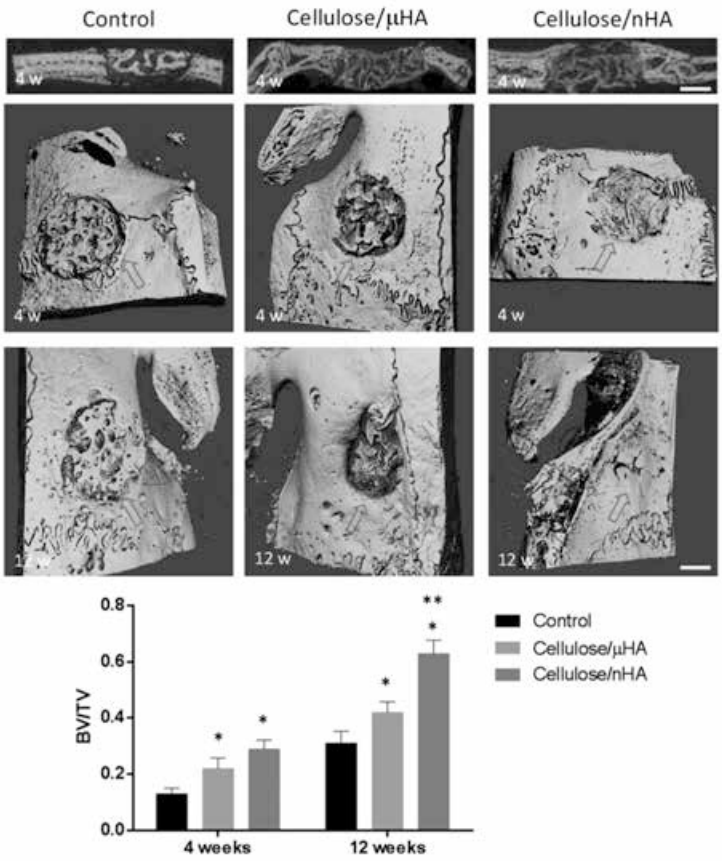

FIGURE 7 Top panel—Representative microtomographic 2D images and 3D reconstructions of the control and cellulose scaffolds, implanted in rabbit's calvarial bone, for 4 and 12 weeks. Scale bar corresponds to 3 mm. Red arrows indicate the margin of the original defect. Bottom graph—BV/TV ratio within the defined volume of interest for the created surgical defect. *This indicates that the value is significantly different from control; **this indicates that the value is significantly different from cellulose/μHA [Colour figure can be viewed at wileyonlinelibrary.com]

Further, microtomographic characterization based on a segmentation analysis with the aim to differentiate the newly formed bone tissue within the VOI was conducted (Figure 7, bottom). Segmental thresholds (Figure 8) were used to differentiate between the mineralized component of the assayed scaffolds (light yellow) and the newly formed bone tissue (dark yellow). Comparatively, minor new bone formation was verified for the control scaffold at Week 4, whereas a higher content of mineralized tissue was verified at Week 12. This trend was verified for both of the assayed cellulose scaffolds, whereas cellulose/nHA induced higher mineralized tissue formation, and, at the 12-week time point, a complete mineralized tissue layer could be identified over the scaffold structure, in accordance with the previous analysis. In addition, no significant differences could be identified regarding the mineral density of the newly formed bone tissue within the analysed VOI (Table 1).

Histological characterization was further conducted, with representative images of the marginal and central regions of the defects implanted with distinct materials (Figure 9). Regarding the defect margin/scaffold interface, within the implanted control material, a fibrous interconnection was verified with vestigial formation of new mineralized tissue within the porous structure of the biomaterial at 4 weeks. At Week 12, an established continuity of mineralized tissue was verified within the defect margin/scaffold interface, with further evidence of active osteoconduction, as new bone formation was verified on the continuity of the scaffold structure. Both cellulose scaffolds allowed for adequate integration with the bone structure at the defect margin, with an established continuity between the remaining bone and the scaffold, verified from Week 4 onward. A dense network of trabecular mineralized tissue was identified

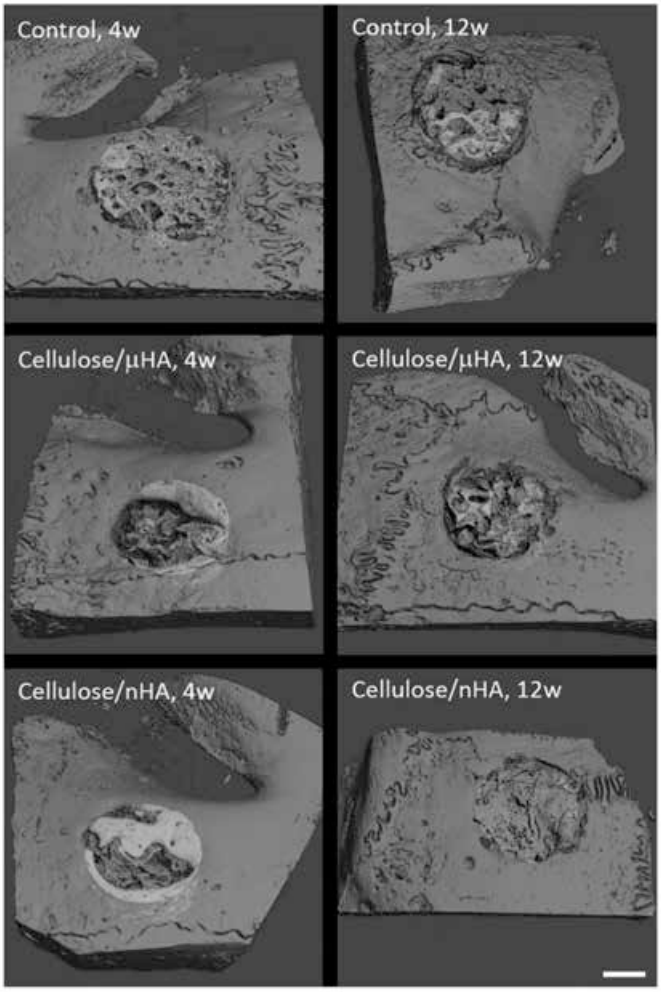

FIGURE 8 Representative microtomographic 3D reconstructions of the control and cellulose scaffolds, implanted in rabbit's calvarial bone, for 4 and 12 weeks. Scale bar corresponds to 3 mm [Colour figure can be viewed at wileyonlinelibrary.com]

TABLE 1 Mineral density of the newly formed bone tissue within the defined VOI, for implanted control and cellulose scaffolds

Bone mineral density (mg-HA/ccm)		
	4 weeks	12 weeks
Control	786.94 ± 120.32	898.27 ± 95.67
Cellulose/µHA	746.80 ± 97.67	801.25 ± 128.45
Cellulose/nHA	766.79 ± 102.34	868.28 ± 138.82

within the porous structure of both scaffolds, early, at the 4-week time point, presenting a more mature appearance at the 12-week time point.

Regarding the evaluation of the central region of the defect, on the implanted control scaffolds, at 4 weeks, the new bone formation process was very limited and restricted to the smaller pores of the structure. At the 12-week time point, increased bone formation was observed, despite the absence of trabecular organization and preservation of sparse areas of mineralized tissue within the scaffold structure. On cellulose-based scaffolds, active bone ingrowth was verified, with the formation of trabecular mineral tissue interspaced within the porous scaffold. Comparatively, cellulose scaffolds allowed for increased bone ingrowth and further maturation of the observed trabecular structure.

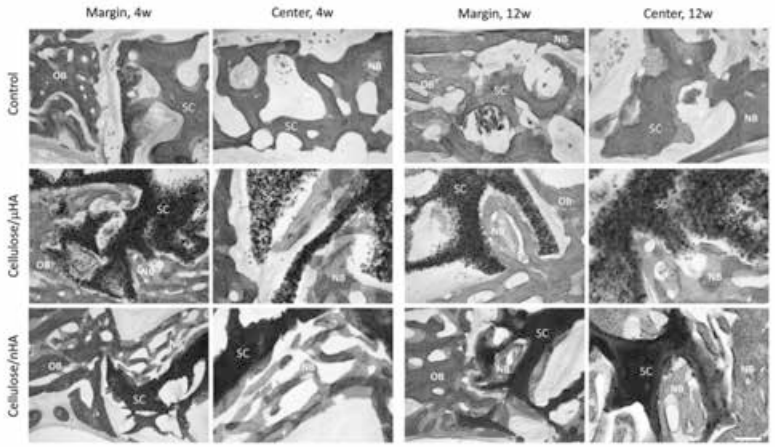

FIGURE 9 Histological micrographs of control and cellulose scaffolds, implanted in rabbit's calvarial bone, for 4 and 12 weeks. Representative sections at the defect margin (margin) and at the centre of the defect (centre) are presented. Scale bar corresponds to 150 μm. OB = old bone; NB = new bone; SC = scaffold [Colour figure can be viewed at wileyonlinelibrary.com]

4 | DISCUSSION

In this study, new porous cellulose scaffolds loaded with HA microparticles or nanoparticles were developed and characterized from a physicochemical and biological point of view. Biological assays were conducted in vitro, with human osteoblastic cells, and in vivo, following the implantation within a rabbit calvaria bone defect model.

For the scaffold preparation, HA particles of either the micrometric or nanometric range were added as matrix ligands, aiming to modulate the scaffolds' surface characteristics for enhanced biological response. Previous studies have shown that unmodified cellulose structures are extremely hydrophilic, which leads to low protein adsorption to the surface and hampers cell–material interaction, precluding the adhesion and proliferation of cells (Bäckdahl et al., 2006; Novotna et al., 2013; Wu, Suen, Chen, & Tzeng, 2003). HA has been shown to favour the specific deposition of proteins and target integrins associated with the cell adhesion process, favouring early cell–substrate interaction (Kilpadi, Chang, & Bellis, 2001; Sawyer, Hennessy, & Bellis, 2007). The initial communication of materials with biological systems relies on the layer of the spontaneously adsorbed proteins, whose composition and bioactivity yield a biological interpretation of the physicochemical characteristics of the underlying material. HA's moderately hydrophilic surface favours the deposition of specific proteins and preserves the bioactivity of adsorbed molecules, enhancing cell adhesion and spreading (Wilson, Clegg, Leavesley, & Pearcy, 2005). In accordance, within the present work, cell-to-substrate contacts were found to be majorly dominated by the scaffold regions loaded with HA microparticles or nanoparticles.

Microtomographic evaluation revealed that both cellulose/μHA and cellulose/nHA scaffolds presented a highly interconnected porous structure, essential for cell metabolism and timely removal of waste products within the regenerative milieu (Polo-Corrales, Latorre-Esteves, & Ramirez-Vick, 2014). Porous interconnection facilitates vascular ingrowth and new tissue formation, set on the interstitial network to assist and guide the anabolic process (Causa, Netti, & Ambrosio, 2007). Interconnection further prevents the development of a low-oxygen-tension micro-environment that can affect cellular behaviour and preclude osteoblastic differentiation (He, Genetos, Yellowley, & Leach, 2010). Further, characterized cellulose/HA scaffolds revealed a high total porosity, clearly above the threshold of 50%, above which induced osteogenesis and vascular ingrowth are expected (Kim, Kim, Vunjak-Novakovic, Min, & Kaplan, 2005; Murphy, Haugh, & O'Brien, 2010). A high porosity also expedites the mechanical interlocking with neighbouring tissues, enhancing the early stabilization of the construct and permitting the effective availability of biofactors for angiogenesis and bone ingrowth (Karageorgiou & Kaplan, 2005). Cellulose/nHA scaffolds presented a slight but significantly higher specific surface area than cellulose/μHA scaffolds. Increasing the scaffolds' surface area allows cells to obtain higher surface reactivity, which can modulate cell behaviour, in terms of both proliferation and differentiation. The combination of a highly porous structure with an open, interconnected geometry allows the achievement of a high surface area, which facilitates the cell adhesion and ingrowth process, further enabling the neovascularization of the construct (Polo-Corrales et al., 2014).

Pore size is another variable of the utmost relevance for successful tissue regeneration, greatly modulating the cellular behaviour within scaffolds' micro-environment. Developed scaffolds presented a similar mean pore size, around the 500-μm range. For hard-tissue regeneration, pores within the 50- to 100-μm range, despite allowing for cell colonization (Schek, Taboas, Segvich, Hollister, & Krebsbach, 2004), lead to a hypoxic environment known to favour the formation of meagerly vascularized tissue with low mechanical properties and to contribute to cell dedifferentiation. A higher mean pore diameter has

been associated with an improved biological outcome, with the added advantage of reducing cell aggregation at the scaffold's edge (Murphy et al., 2010). In fact, a mean pore diameter within the 200- to 600-μm range seems to be more prone to osteogenesis and angiogenesis, greatly contributing to promoting the bone formation process in vivo (Loh & Choong, 2013).

Overall, the physicochemical characteristics of developed cellulose/HA scaffolds, regardless of the loading with particles with distinct morphological characteristics (i.e., microparticles and nanoparticles), were found to be broadly similar and within the same range of magnitude. Notwithstanding, and despite the attained similarities in terms of solid-state characterization, the biological response to either cellulose/μHA or cellulose/nHA scaffolds was found to be quite distinctive.

Cells adhered to cellulose/μHA presented a spherical morphology with short filopodial processes interacting with μHA particles, whereas cells adhered to cellulose/nHA adopted a more polygonal and spread morphology, with the emission of thin and long filopodial processes anchoring in the distributed HA nanoparticle's clusters. Additionally, a significantly higher MTT reduction value was verified for cultures grown on cellulose/nHA for 1 day, suggesting an increased number of active metabolic cells on the scaffold surface. Previous studies have shown that the addition of HA nanoparticles, in comparison with microparticles, enhances the osteoblastic cell adhesion within scaffolds of distinct compositions (Filova et al., 2014). The smaller size of nanoparticles and higher surface area promotes cell adhesion through increased and selective protein adsorption, leading to the formation of a neo-matrix on the scaffold's surface, more suitable for cell interaction (Webster, Ergun, Doremus, Siegel, & Bizios, 2000). Surfaces with nanostructures are found to preferably adsorb vitronectin—a glycoprotein involved in cell adhesion and spreading—due to its structural characteristics and chemical affinity (Lord, Foss, & Besenbacher, 2010). Supporting the enhanced adhesion process, cells adhered to surfaces loaded with nanostructured HA further expressed higher levels of beta-actin and talin—proteins associated with focal adhesions and cytoskeletal activation, whose increased expression leads to a higher degree of cytoplasmic spreading (Filova et al., 2014), as presently verified for seeded cellulose/nHA scaffolds.

Cell proliferation was found to be increased in cellulose/nHA, as compared with cellulose/μHA, as significantly higher MTT reduction values were verified for cultures grown for 3 and 6 days within the seeded materials. Early morphological features may greatly influence the cell proliferative behaviour, as anchorage-dependent cells greatly rely on cytoplasmic expansion over the substrate to switch into the G1 and S phases of the cell cycle (Lee et al., 2017). During the adhesion process, the degree of spreading and the spreading area positively correlate with the proliferative activity and seem to induce cell proliferation through biochemical and mechanical processes, given the activation of integrin-dependent and non-integrin-dependent pathways (Bacakova, Filova, Parizek, Ruml, & Svorcik, 2011). The enhanced cell adhesion and cytoplasmic spreading attained on cellulose/nHA may at least in part sustain the increased cell proliferation verified on this material. Furthermore, HA nanoparticles seem to outperform HA microparticles in the direct enhancement of cell proliferation in osteoblastic populations (Guo, Gough, Xiao, Liu, & Shen, 2007; Shi, Huang, Cai, Tang, & Yang, 2009). Osteoblastic cells can readily uptake nHA particles through endocytosis, clathrin-mediated vesicles or *caveolae*, leading to the formation of endosomes in which nHA particles are partially dissolved, leading to an increased concentration of Ca^{2+} that readily diffuses into the cytoplasm (Chen, Mccrate, Lee, & Li, 2011). The proper Ca^{2+} cytosolic concentration is able to induce osteoblastic functionality, both in terms of proliferation and differentiation (Maeno et al., 2005). Regarding the latter, previous works have shown that, comparatively to μHA, nHA particles greatly enhance osteogenesis through the upregulation of distinct signalling pathways able to induce osteogenic commitment (Huang et al., 2012; Liu et al., 2009). This was further verified within cultures grown on composite structures loaded with either μHA or nHA particles (Filova et al., 2014; Li et al., 2009), with the latter exerting an osteogenic stimulation similar to the one attained with the addition of osteogenic growth factors to the culture environment (Polini, Pisignano, Parodi, Quarto, & Scaglione, 2011).

In accordance with this study, cultures established on cellulose/nHA scaffolds presented a significantly higher expression of osteogenic-related genes (i.e., Runx-2, ALP, and BMP-2) and ALP activity, although no significant differences were found regarding Col I expression. Runx-2 is a key transcription factor greatly associated with osteogenic commitment, regulating osteoblast development through G protein-related signalling pathways and promoting the upregulation of distinct factors such as osteopontin, osteocalcin, and BMP-2 (Lin & Hankenson, 2011). ALP is a membrane-bound glycoprotein involved within the pathway, resulting in the deposition of minerals within the extracellular matrix, being further regarded as an early marker of osteogenic commitment (Czekanska, Stoddart, Richards, & Hayes, 2012). BMP-2 is a secretory signalling molecule belonging to the TGF-β superfamily of growth factors, with the ability to induce different bone cell differentiation processes at different stages, particularly for the generation of mature osteoblasts in vivo. Col I is an essential molecule for the development and maturation of the osteoblastic phenotype, being associated with the formation of the extracellular matrix and highly expressed during the proliferative phase. Overall, a trend for increased osteogenesis was verified for cultures grown on cellulose/nHA, with the upregulation of the assayed osteogenic markers, with the exception of Col I. This may be consistent with the fact that, despite being essential for osteogenesis, Col I is highly expressed by MG-63 cells, in accordance with the immature osteoblast phenotype of this population, being hardly regulated by environmental modifications (Czekanska et al., 2012; Lin & Hankenson, 2011).

The enhanced biological response of cellulose/nHA was further verified in vivo, following the scaffolds' implantation in rabbit calvarial bone defects. Although both cellulose/HA scaffolds outperformed the assayed control—a commercial allograft for bone-healing applications—a significantly higher amount of newly formed mineralized tissue was found within the defects loaded with cellulose/nHA scaffolds.

Previous works have shown that cellulose scaffolds present adequate tissue biocompatibility following implantation, with the absence of chronic inflammation or foreign body reaction, and favourable tissue integration with the establishment of a dense vascular network (Helenius et al., 2006; Luo et al., 2010). The scaffold's loading with HA particles is expected to enhance the biological integration within the bone tissue, improving the scaffold's bioactivity and osteoinductivity, as previously described for distinct composite

structures resulting from the combination of natural or synthetic polymers with HA particles (Gleeson, Plunkett, & O'Brien, 2010; Swetha et al., 2010). Nonetheless, and in accordance with data obtained from the in vitro evaluation, the biological response to the scaffolds seemed to be greatly dependent on the HA particles' characteristics, with scaffolds loaded with nHA eliciting an enhanced bone response. The modulation of distinct stages of the bone-healing process is expected to have contributed to this outcome.

Early tissue response, within the frame of the immune-inflammatory activation, is known to greatly modulate the subsequent bone response. Following bone injury, a set and organized cascade of events is established and able to modulate the early cellular and molecular alterations, enhancing the activation of the repair cascade and influencing the bone-healing process (Thomas & Puleo, 2011). However, the persistency of inflammatory stimuli, embracing cells and mediators, leads to suboptimal bone formation. The implantation of μHA is known to elicit higher immune-inflammatory activation, as compared with nHA implantation (Bota et al., 2010). Concisely, although nHA particles are more readily phagocytosed by immune-competent cells than μHA, the latter seem to attach eagerly to cell membranes and induce more potent inflammatory stimuli, through the activation of the NF-kB pathway (Nicolete, dos Santos, & Faccioli, 2011). The persistent inflammatory stimuli may prorogate the healing activity and delay bone formation.

Apart from the modulatory capability on the immune-inflammatory events associated with bone healing, nHA was further found to directly modulate the bone formation process. nHA, as compared with μHA, was found to accelerate the bone formation process in distinct applications. nHA coatings over distinct metallic implants enhanced fixation and provided better stabilization, bone ingrowth and osteointegration than those of uncoated or μHA-coated implants (Aksakal, Kom, Tosun, & Demirel, 2014). Further, the direct implantation of nHA within experimental bone defects significantly enhanced the bone-formation process, with the deposition of a higher level of mineralized tissue, comparatively to the implantation of μHA (Appleford, Oh, Oh, & Ong, 2009; Zhu et al., 2010). The enhanced bioactivity of nHA was further confirmed with the implantation of composites, based on biodegradable polymers and loaded nHA particles, found to outperform those loaded with μHA, with a higher induction of trabecular bone formation within the scaffold structure and at the tissue–scaffold interface (Chung et al., 2011), as verified in this study.

5 | CONCLUSIONS

Developed cellulose/nHA and cellulose/μHA scaffolds presented similar physicochemical characteristics and a highly interconnected porous structure, favourable to osteogenesis, angiogenesis, and a promoted bone-formation process. Nevertheless, it seems that loading of the cellulose scaffolds with different nHA and μHA particles exhibiting different morphological characteristics has a significant impact on the biological response to either cellulose/μHA or cellulose/nHA composites. In vitro assessment of cellulose/nHA scaffolds revealed superior cell adhesion, increased metabolic activity and osteoblastic gene expression and significantly higher 12-week in vivo formation of newly mineralized tissue, compared with cellulose/μHA scaffolds and a commercially available bone allograft control. Within the limitations of this study, a developed cellulose/nHA scaffold seems to be a promising material for use in a wide range of bone-tissue-engineering applications to achieve desirable osteogenic outcomes.

ACKNOWLEDGEMENT

Financial support from the Research Council of Lithuania (Grant MIP019/2014), European Union (FEDER funds POCI/01/0145/FEDER/007265) and National Funds (FCT/MEC, Fundação para a Ciência e Tecnologia and Ministério da Educação e Ciência) under the Partnership Agreement PT2020 UID/QUI/50006/2013 is acknowledged.

CONFLICT OF INTEREST

The authors have declared that they have no conflict of interest.

ORCID

Povilas Daugela http://orcid.org/0000-0001-7124-6866

REFERENCES

Aksakal, B., Kom, M., Tosun, H., & Demirel, M. (2014). Influence of micro- and nano-hydroxyapatite coatings on the osteointegration of metallic (Ti6Al4 V) and bioabsorbable interference screws: An in vivo study. *European Journal of Orthopaedic Surgery and Traumatology*, *24*, 813–819.

Appleford, M. R., Oh, S., Oh, N., & Ong, J. L. (2009). In vivo study on hydroxyapatite scaffolds with trabecular architecture for bone repair. *Journal of Biomedical Materials Research. Part A*, *89*, 1019–1027.

Artzi, Z., Tal, H., & Dayan, D. (2000). Porous bovine bone mineral in healing of human extraction sockets. Part 1: Histomorphometric evaluations at 9 months. *Journal of Periodontology*, *71*, 1015–1023.

Bacakova, L., Filova, E., Parizek, M., Ruml, T., & Svorcik, V. (2011). Modulation of cell adhesion, proliferation and differentiation on materials designed for body implants. *Biotechnology Advances*, *29*, 739–767.

Bäckdahl, H., Helenius, G., Bodin, A., Nannmark, U., Johansson, B. R., Risberg, B., & Gatenholm, P. (2006). Mechanical properties of bacterial cellulose and interactions with smooth muscle cells. *Biomaterials*, *27*, 2141–2149.

Bauer, T. W., & Muschler, G. F. (2000). Bone graft materials: An overview of the basic science. *Clinical Orthopaedics*, *371*, 10–27.

Bota, P., Collie, A., Puolakkainen, P., Vernon, R. B., Sage, E. H., Ratner, B. D., & Stayton, P. S. (2010). Biomaterial topography alters healing in vivo and monocyte/macrophage activation in vitro. *Journal of Biomedical Materials Research. Part A*, *95*, 649–657.

Bryjak, J., Aniulyte, J., & Liesiene, J. (2007). Evaluation of man-tailored cellulose-based carriers in glucoamylase immobilization. *Carbohydrate Research*, *342*, 1105–1109.

Calvo-Guirado, J. L., Garces, M., Delgado-Ruiz, R. A., Ramirez Fernandez, M. P., Ferres-Amat, E., & Romanos, G. E. (2015). Biphasic β-TCP mixed with silicon increases bone formation in critical site defects in rabbit calvaria. *Clinical Oral Implants Research*, *26*, 891–897.

Causa, F., Netti, P. A., & Ambrosio, L. (2007). A multi-functional scaffold for tissue regeneration: the need to engineer a tissue analogue. *Biomaterials*, *28*, 5093–5099.

Chen, L., Mccrate, J. M., Lee, J. C., & Li, H. (2011). The role of surface charge on the uptake and biocompatibility of hydroxyapatite nanoparticles with osteoblast cells. *Nanotechnology*, *22*, 105708.

Chung, E. J., Qiu, H., Kodali, P., Yang, S., Sprague, S. M., Hwong, J., … Ameer, G. A. (2011). Early tissue response to citric acid-based micro-and nanocomposites. *Journal of Biomedical Materials Research. Part A*, *96*, 29–37.

Cicciù, M., Herford, A. S., Cicciù, D., Tandon, R., & Maiorana, C. (2014). Recombinant human bone morphogenetic protein-2 promote and stabilize hard and soft tissue healing for large mandibular new bone reconstruction defects. *The Journal of Craniofacial Surgery*, *25*, 860–862.

Czekanska, E., Stoddart, M., Richards, R., & Hayes, J. (2012). In search of an osteoblast cell model for in vitro research. *European Cells & Materials*, *24*, 1–17.

Ebraheim, N. A., Elgafy, H., & Xu, R. (2001). Bone-graft harvesting from iliac and fibular donor sites: Techniques and complications. *The Journal of the American Academy of Orthopaedic Surgeons*, *9*, 210–218.

Filova, E., Suchy, T., Sucharda, Z., Supova, M., Zaloudkova, M., Balik, K., … Bacakova, L. (2014). Support for the initial attachment, growth and differentiation of MG-63 cells: A comparison between nano-size hydroxyapatite and micro-size hydroxyapatite in composites. *International Journal of Nanomedicine*, *9*, 3687–3706.

Gao, C., Deng, Y., Feng, P., Mao, Z., Li, P., Yang, B., … Peng, S. (2014). Current progress in bioactive ceramic scaffolds for bone repair and regeneration. *International Journal of Molecular Sciences*, *15*, 4714–4732.

Gleeson, J., Plunkett, N., & O'Brien, F. (2010). Addition of hydroxyapatite improves stiffness, interconnectivity and osteogenic potential of a highly porous collagen-based scaffold for bone tissue regeneration. *European Cells & Materials*, *20*, 218–230.

Grande, C. J., Torres, F. G., Gomez, C. M., & Bañó, M. C. (2009). Nanocomposites of bacterial cellulose/hydroxyapatite for biomedical applications. *Acta Biomaterialia*, *5*, 1605–1615.

Guo, B., & Ma, P. X. (2014). Synthetic biodegradable functional polymers for tissue engineering: A brief review. *Science China: Chemistry*, *57*, 490–500.

Guo, X., Gough, J. E., Xiao, P., Liu, J., & Shen, Z. (2007). Fabrication of nanostructured hydroxyapatite and analysis of human osteoblastic cellular response. *Journal of Biomedical Materials Research. Part A*, *82*, 1022–1032.

He, J., Genetos, D. C., Yellowley, C. E., & Leach, J. K. (2010). Oxygen tension differentially influences osteogenic differentiation of human adipose stem cells in 2D and 3D cultures. *Journal of Cellular Biochemistry*, *110*, 87–96.

Helenius, G., Bäckdahl, H., Bodin, A., Nannmark, U., Gatenholm, P., & Risberg, B. (2006). In vivo biocompatibility of bacterial cellulose. *Journal of Biomedical Materials Research. Part A*, *76*, 431–438.

Hench, L. L., & Polak, J. M. (2002). Third-generation biomedical materials. *Science*, *295*, 1014–1017.

Herford, A. S., Tandon, R., Stevens, T. W., Stoffella, E., & Cicciu, M. (2013). Immediate distraction osteogenesis: The sandwich technique in combination with rhBMP-2 for anterior maxillary and mandibular defects. *The Journal of Craniofacial Surgery*, *24*, 1383–1387.

Huang, Y., Zhou, G., Zheng, L., Liu, H., Niu, X., & Fan, Y. (2012). Micro-/nano-sized hydroxyapatite directs differentiation of rat bone marrow derived mesenchymal stem cells towards an osteoblast lineage. *Nanoscale*, *4*, 2484–2490.

Karageorgiou, V., & Kaplan, D. (2005). Porosity of 3D biomaterial scaffolds and osteogenesis. *Biomaterials*, *26*, 5474–5491.

Kilpadi, K. L., Chang, P., & Bellis, S. L. (2001). Hydroxylapatite binds more serum proteins, purified integrins, and osteoblast precursor cells than titanium or steel. *Journal of Biomedical Materials Research*, *57*, 258–267.

Kim, H. J., Kim, U., Vunjak-Novakovic, G., Min, B., & Kaplan, D. L. (2005). Influence of macroporous protein scaffolds on bone tissue engineering from bone marrow stem cells. *Biomaterials*, *26*, 4442–4452.

Kim, Y., Nowzari, H., & Rich, S. K. (2013). Risk of prion disease transmission through bovine-derived bone substitutes: A systematic review. *Clinical Implant Dentistry and Related Research*, *15*, 645–653.

Kiselioviene, S., Baniukaitiene, O., Harkavenko, V., Babenko, N. A., & Liesiene, J. (2016). Cellulose hydrogel sheets for wound dressings. *Cellulose Chemistry and Technology*, *50*, 915–923.

Laino, L., Iezzi, G., Piattelli, A., Lo Muzio, L., & Cicciù, M. (2014). Vertical ridge augmentation of the atrophic posterior mandible with sandwich technique: bone block from the chin area versus corticocancellous bone block allograft—Clinical and histological prospective randomized controlled study. *BioMed Research International*, *2014*, 982104.

Lee, L. C., Gadegaard, N., de Andrés, M. C., Turner, L., Burgess, K. V., Yarwood, S. J., … Oreffo, R. O. (2017). Nanotopography controls cell cycle changes involved with skeletal stem cell self-renewal and multipotency. *Biomaterials*, *116*, 10–20.

Li, J., Dou, Y., Yang, J., Yin, Y., Zhang, H., Yao, F., … Yao, K. (2009). Surface characterization and biocompatibility of micro-and nano-hydroxyapatite/chitosan-gelatin network films. *Materials Science and Engineering: C*, *29*, 1207–1215.

Lin, G. L., & Hankenson, K. D. (2011). Integration of BMP, Wnt, and notch signaling pathways in osteoblast differentiation. *Journal of Cellular Biochemistry*, *112*, 3491–3501.

Liu, Y., Wang, G., Cai, Y., Ji, H., Zhou, G., Zhao, X., … Zhang, M. (2009). In vitro effects of nanophase hydroxyapatite particles on proliferation and osteogenic differentiation of bone marrow-derived mesenchymal stem cells. *Journal of Biomedical Materials Research. Part A*, *90*, 1083–1091.

Loh, Q. L., & Choong, C. (2013). Three-dimensional scaffolds for tissue engineering applications: Role of porosity and pore size. *Tissue Engineering. Part B, Reviews*, *19*, 485–502.

Lord, M. S., Foss, M., & Besenbacher, F. (2010). Influence of nanoscale surface topography on protein adsorption and cellular response. *Nano Today*, *5*, 66–78.

Luo, L., Zhang, Y., Wang, X., Wan, Y., Chang, P. R., Anderson, D. P., & Chen, Y. (2010). Preparation, characterization, and in vitro and in vivo evaluation of cellulose/soy protein isolate composite sponges. *Journal of Biomaterials Applications*, *24*, 503–526.

Maeno, S., Niki, Y., Matsumoto, H., Morioka, H., Yatabe, T., Funayama, A., … Tanaka, J. (2005). The effect of calcium ion concentration on osteoblast viability, proliferation and differentiation in monolayer and 3D culture. *Biomaterials*, *26*, 4847–4855.

Miyamoto, T., Takahashi, S., Ito, H., Inagaki, H., & Noishiki, Y. (1989). Tissue biocompatibility of cellulose and its derivatives. *Journal of Biomedical Materials Research*, *23*, 125–133.

Murphy, C. M., Haugh, M. G., & O'Brien, F. J. (2010). The effect of mean pore size on cell attachment, proliferation and migration in collagen–glycosaminoglycan scaffolds for bone tissue engineering. *Biomaterials*, *31*, 461–466.

Nejati, E., Mirzadeh, H., & Zandi, M. (2008). Synthesis and characterization of nano-hydroxyapatite rods/poly (l-lactide acid) composite scaffolds for bone tissue engineering. *Composites. Part A, Applied Science and Manufacturing*, *39*, 1589–1596.

Nge, T. T., & Sugiyama, J. (2007). Surface functional group dependent apatite formation on bacterial cellulose microfibrils network in a simulated body fluid. *Journal of Biomedical Materials Research. Part A*, *81*, 124–134.

Nicolete, R., dos Santos, D. F., & Faccioli, L. H. (2011). The uptake of PLGA micro or nanoparticles by macrophages provokes distinct in vitro inflammatory response. *International Immunopharmacology*, *11*, 1557–1563.

Novotna, K., Havelka, P., Sopuch, T., Kolarova, K., Vosmanska, V., Lisa, V., … Bacakova, L. (2013). Cellulose-based materials as scaffolds for tissue engineering. *Cellulose*, *20*, 2263–2278.

Oryan, A., Alidadi, S., Moshiri, A., & Maffulli, N. (2014). Bone regenerative medicine: classic options, novel strategies, and future directions. *Journal of Orthopaedic Surgery and Research*, *9*, 18.

Petrauskaite, O., Gomes Pde, S., Fernandes, M. H., Juodzbalys, G., Stumbras, A., Maminskas, J., … Cicciu, M. (2013). Biomimetic mineralization on a macroporous cellulose-based matrix for bone regeneration. *BioMed Research International*, *2013*, 452750.

Petrauskaite, O., Juodzbalys, G., Viskelis, P., & Liesiene, J. (2016). Control of the porous structure of cellulose-based tissue engineering scaffolds by means of lyophilization. *Cellulose Chemistry and Technology*, *50*, 23–30.

Polini, A., Pisignano, D., Parodi, M., Quarto, R., & Scaglione, S. (2011). Osteoinduction of human mesenchymal stem cells by bioactive composite scaffolds without supplemental osteogenic growth factors. *PLoS One*, *6*, e26211.

Polo-Corrales, L., Latorre-Esteves, M., & Ramirez-Vick, J. E. (2014). Scaffold design for bone regeneration. *Journal of Nanoscience and Nanotechnology*, *14*, 15–56.

Qiu, K., & Netravali, A. N. (2014). A review of fabrication and applications of bacterial cellulose based nanocomposites. *Polymer Reviews*, *54*, 598–626.

Ramirez-Fernández, M. P., Calvo-Guirado, J. L., Maté-Sánchez del Val, J. E., Delgado-Ruiz, R. A., Negri, B., & Barona-Dorado, C. (2013). Ultrastructural study by backscattered electron imaging and elemental microanalysis of bone-to-biomaterial interface and mineral degradation of porcine xenografts used in maxillary sinus floor elevation. *Clinical Oral Implants Research*, *24*, 523–530.

Salgado, A., Coutinho, O., & Reis, R. (2004). Novel starch-based scaffolds for bone tissue engineering: cytotoxicity, cell culture, and protein expression. *Tissue Engineering*, *10*, 465–474.

Saska, S., Barud, H. S., Gaspar, A. M., Marchetto, R., Ribeiro, S. J., & Messaddeq, Y. (2011). Bacterial cellulose-hydroxyapatite nanocomposites for bone regeneration. *Int J Biomater*, *2011*, 175362.

Sawyer, A. A., Hennessy, K. M., & Bellis, S. L. (2007). The effect of adsorbed serum proteins, RGD and proteoglycan-binding peptides on the adhesion of mesenchymal stem cells to hydroxyapatite. *Biomaterials*, *28*, 383–392.

Schek, R. M., Taboas, J. M., Segvich, S. J., Hollister, S. J., & Krebsbach, P. H. (2004). Engineered osteochondral grafts using biphasic composite solid free-form fabricated scaffolds. *Tissue Engineering*, *10*, 1376–1385.

Shi, Z., Huang, X., Cai, Y., Tang, R., & Yang, D. (2009). Size effect of hydroxyapatite nanoparticles on proliferation and apoptosis of osteoblast-like cells. *Acta Biomaterialia*, *5*, 338–345.

Silva, J., Sampaio, P., Fernandes, M., & Gomes, P. (2015). The osteogenic priming of mesenchymal stem cells is impaired in experimental diabetes. *Journal of Cellular Biochemistry*, *116*, 1658–1667.

Swetha, M., Sahithi, K., Moorthi, A., Srinivasan, N., Ramasamy, K., & Selvamurugan, N. (2010). Biocomposites containing natural polymers and hydroxyapatite for bone tissue engineering. *International Journal of Biological Macromolecules*, *47*, 1–4.

Thomas, M. V., & Puleo, D. A. (2011). Infection, inflammation, and bone regeneration: A paradoxical relationship. *Journal of Dental Research*, *90*, 1052–1061.

Wang, S., Lu, A., & Zhang, L. (2016). Recent advances in regenerated cellulose materials. *Progress in Polymer Science*, *53*, 169–206.

Wang, X., Wang, X., Tan, Y., Zhang, B., Gu, Z., & Li, X. (2009). Synthesis and evaluation of collagen–chitosan–hydroxyapatite nanocomposites for bone grafting. *Journal of Biomedical Materials Research. Part A*, *89*, 1079–1087.

Webster, T. J., Ergun, C., Doremus, R. H., Siegel, R. W., & Bizios, R. (2000). Enhanced functions of osteoblasts on nanophase ceramics. *Biomaterials*, *21*, 1803–1810.

Wilson, C. J., Clegg, R. E., Leavesley, D. I., & Pearcy, M. J. (2005). Mediation of biomaterial–cell interactions by adsorbed proteins: A review. *Tissue Engineering*, *11*, 1–18.

Wilson, D. B. (2008). Three microbial strategies for plant cell wall degradation. *Annals of the New York Academy of Sciences*, *1125*, 289–297.

Woo, E. J. (2012). Adverse events reported after the use of recombinant human bone morphogenetic protein 2. *Journal of Oral and Maxillofacial Surgery*, *70*, 765–767.

Wu, C., Suen, S., Chen, S., & Tzeng, J. (2003). Analysis of protein adsorption on regenerated cellulose-based immobilized copper ion affinity membranes. *Journal of Chromatography. A*, *996*, 53–70.

Zhu, W., Zhang, X., Wang, D., Lu, W., Ou, Y., Han, Y., … Peng, L. (2010). Experimental study on the conduction function of nano-hydroxyapatite artificial bone. *IET Micro & Nano Letters*, *5*, 19–27.

Zimmermann, K. A., LeBlanc, J. M., Sheets, K. T., Fox, R. W., & Gatenholm, P. (2011). Biomimetic design of a bacterial cellulose/hydroxyapatite nanocomposite for bone healing applications. *Materials Science and Engineering: C*, *31*, 43–49.

How to cite this article: Daugela P, Pranskunas M, Juodzbalys G, et al. Novel cellulose/hydroxyapatite scaffolds for bone tissue regeneration: *in vitro* and *in vivo* study. *J Tissue Eng Regen Med*. 2018;1–14. https://doi.org/10.1002/term.2651

Povilas Daugela

Influence of leukocyte- and platelet-rich fibrin (L-PRF) on the outcomes of impacted mandibular third molar removal surgery: A split-mouth randomized clinical trial

Povilas Daugela, DDS[1]/Vaidas Grimuta, MD[1]/Dalius Sakavicius DDS, PhD[2]/Juozas Jonaitis DDS, PhD[3]/Gintaras Juodzbalys, DDS, MSD, PhD[4]

Objectives: The purpose of this study was to evaluate the influence of leukocyte- and platelet-rich fibrin (L-PRF) on impacted mandibular third molar (IMTM) extraction wound healing, patient postoperative discomfort, and incidence of alveolar osteitis. **Method and Materials:** Thirty-four patients (20 female, 14 male) who met the inclusion criteria for this split-mouth randomized clinical trial were enrolled and 30 patients completed the study. Patients were randomized and underwent bilateral IMTM surgical extractions. Following extraction, one socket randomly received L-PRF, and the other socket served as a regular blood clot control. Postoperatively, the soft tissue healing index (HI), pain according to visual analog scale (VAS), facial swelling using a horizontal and vertical guide, and incidence of alveolar osteitis were evaluated 1, 3, 7, and 14 days after surgery. **Results:** Sites treated with L-PRF resulted in improved HI ($P = .001$) and lower pain VAS scores ($P = .001$) in the first postoperative week. Significant reduction of facial swelling was recorded on first ($P = .035$) and third ($P = .023$) postoperative days in L-PRF sites versus controls, ceasing to nonsignificant difference at day 7 ($P = .224$). None of the L-PRF sites and four control sites were affected by alveolar osteitis ($P = .001$). **Conclusion:** Within the limitations of this split-mouth study, L-PRF improved soft tissue healing and reduced postoperative pain, swelling, and incidence of alveolar osteitis after IMTM surgical extractions. *(Quintessence Int 2018;49:377–388; doi: 10.3290/j.qi.a40113)*

Key words: impacted tooth, pain, platelet-rich fibrin, third molar, tooth extraction, wound healing

Impacted third molars are developmental pathologic deformities characteristic of modern human civilization. The frequency of mandibular third molar impaction was reported in up to 73% of the young adult population.[1] Consequently, surgical removal of impacted mandibular third molars (IMTMs) became one of the most frequent procedures performed in oral and maxillofacial surgery.[2,3] Notwithstanding some reported concerns regarding necessity of IMTM extraction,[4] there are numerous indications for IMTM surgical removal described in the literature, including orthodontic and prosthodontic reasons, caries, pain, infections, association with cysts or tumors, damage of the neighboring teeth, proximity to mandibular fracture line or orthognathic surgery site,

[1] Lecturer, Department of Oral and Maxillofacial Surgery, Lithuanian University of Health Sciences, Kaunas, Lithuania.

[2] Associate Professor, Department of Oral and Maxillofacial Surgery, Lithuanian University of Health Sciences, Kaunas, Lithuania.

[3] Associate Professor, Department of Dental and Maxillofacial Orthopedics, Lithuanian University of Health Sciences, Kaunas, Lithuania.

[4] Professor, Department of Oral and Maxillofacial Surgery, Lithuanian University of Health Sciences, Kaunas, Lithuania.

Correspondence: Dr Povilas Daugela, Department of Oral and Maxillofacial Surgery, Lithuanian University of Health Sciences, Eiveniu str. 2, LT-50009 Kaunas, Lithuania. Email: p.daugela@gmail.com

infection prophylaxis for cardiac surgery, and endocarditis.[3,5] However, IMTM removal surgery is very often associated with postoperative discomfort, including pain and swelling, significant deterioration in oral health–related quality of life in the immediate postoperative period, and comparatively high incidence of alveolar osteitis (AO).[6,7] The main surgical objective in IMTM surgery is to remove the tooth with minimal sequelae and a complication-free procedure, reducing postoperative morbidity and patient discomfort to the lowest possible level. For this purpose various approaches and techniques were suggested, including corticosteroids and nonsteroidal anti-inflammatory drugs (NSAIDs), cryotherapy, compression, soft laser, piezo surgery, and, eventually, platelet concentrates.[8]

In recent years the use of various autologous platelet concentrates for promotion of wound healing has garnered particular interest. Platelet concentrates are often associated with platelet-rich plasma (PRP), which was the first platelet concentrate offered on the market.[9] In addition, over the last two decades, a large number of publications advocating the use of PRP in oral surgery have been published. However, most of the authors tend to find that there is very limited scientific support regarding PRP capability to enhance extraction wound healing.[10,11] In spite of recently decreasing PRP use in oral and maxillofacial surgery, new interest in platelet concentrates has arisen with the introduction of new-generation platelet-rich fibrin,[12,13] which was later classified as leukocyte- and platelet-rich fibrin (L-PRF), as proposed by Dohan Ehrenfest et al. in 2012.[14]

L-PRF is an autologous fibrin-based biomaterial, enmeshed with platelets, leukocytes, and their cytokines. L-PRF was shown to stimulate biologic functions such as chemotaxis, angiogenesis, and cell proliferation and differentiation,[13,15] all of which may facilitate wound healing. Unlike PRP, L-PRF does not require chemical platelet activation and is an additive-free biomaterial. Also contrary to PRP, L-PRF is a solid biomaterial that does not dissolve quickly after use. Solid-state L-PRF was shown to exhibit a substantial embedding of the growth factors of platelets and leukocytes into fibrin matrix, leading to an increased life span of cytokines.[16] L-PRF was also shown to stimulate proliferation of human osteoblasts and fibroblasts,[15,17] as well as proliferation and osteoblastic differentiation of human bone mesenchymal stem cells.[13] The properties of L-PRF are intended to promote both soft tissue and bone regenerative potential; therefore, L-PRF may be considered as a healing biomaterial. This study was conducted to evaluate the effect of L-PRF on IMTM extraction wound healing, postoperative patient discomfort, and incidence of AO.

METHOD AND MATERIALS

The study was designed as a prospective split-mouth randomized clinical trial on patients who needed bilateral paired IMTM extractions. The study was conducted at the Maxillofacial Surgery Department of the Lithuanian University of Health Sciences. Approval by the local bioethics committee was granted (No. BEC-MF-01). All patients were informed about the operation, healing time, and possible complications, and signed informed consent. The study was registered at ClinicalTrials.gov (www.clinicaltrials.gov) with the ID number NCT03357484.

Patient selection

Based on previously treated pilot cases, a power analysis was conducted for sample size estimation (Statistica 6.0, Dell Software). The calculations revealed a minimum sample size of n = 30, based on a power of 90% and α = 5%.

The inclusion criteria were as follows:

- male and female patients with an age of 18 to 60 years
- healthy patients (American Society of Anesthesiologists Physical Status [ASA PS] index ≤ 2)
- sole bilateral extractions of IMTMs during the same surgery
- complete root formation of mandibular third molars at radiologic examination
- absence of acute inflammation and/or infection in the IMTM areas
- no history of NSAID use in the 4 weeks prior to surgery
- same-difficulty bilateral IMTM extractions, according to both Pederson[18] and Juodzbalys and Daugela[19] classifications
- signed informed consent.

Table 1 Demographic characteristics of the sample

	Males	Females	Total	*P* value
Number of subjects, n (%)	14 (41.18)	20 (58.82)	34 (100.00)	.303*
Age (mean ± SD)	23.35 ± 1.73	22.35 ± 2.13	22.76 ± 2.02	.08†

SD, standard deviation. *P value by chi-square test. †P value by Mann-Whitney test.

The following exclusion criteria were used:

- smoking patients
- IMTM surgery duration difference greater than 10 minutes for each side, seeking to avoid bias
- different surgical manipulations taken at each IMTM surgery site
- presence of any neoplastic lesion (benign or malignant), clinically or radiologically evaluable, at the site or close to the impacted tooth
- presence of any radiolucent lesion > 1 cm at impacted tooth level
- absence of the adjacent tooth
- systemic conditions or pharmacologic treatments altering oral microbiota or immunologic response
- alcohol or drug abuse
- pregnant or breastfeeding women
- lack of compliance by the patient or any other evidence suggesting that the patient was not likely to follow the study protocol.

Preoperatively, two blind expert surgeons assessed patient panoramic radiographs and/or cone beam computed tomography (CBCT) scans, evaluating IMTM extraction difficulty and complexity according to Pederson[18] and Juodzbalys and Daugela[19] indexes for each IMTM bilaterally. The overall kappa index for inter-observer agreement was calculated by using weighted kappa. Only teeth having the same extraction difficulty scores according to both classifications were enrolled in the study. The overall kappa index for inter-observer agreement calculated by using weighted kappa selecting patients was 0.93.

Initially 34 patients (20 females and 14 males), referred to the clinic for bilateral IMTM extraction, were randomly selected for the examination (Table 1); four patients were excluded due to lack of compliance during the investigation period. In total, 30 patients were included for the final investigation (Fig 1).

L-PRF preparation

Prior to surgery, two 9-mL glass-coated tubes (Intra-Spin, Intra-Lock International) of patient venous blood were collected. Tubes were transferred to a centrifuge (EBA 20, Andreas Hettich) and processed for 12 minutes at 2,800 rpm to prepare L-PRF, as described previously.[12]

Surgical procedure

Surgical procedures were performed following a standardized surgical approach[20] by one expert surgeon (PD) (Fig 2). Surgical manipulations required for each tooth extraction were as follows: simple mobilization of the tooth, coronectomy, root separation, incision, and osteotomy. After removal of IMTM and socket curettage (Fig 2b), on the side randomly chosen by the opaque sealed envelope technique to be the study side, the extraction sockets were filled with two L-PRF clots (Fig 2c), whereas on the other side (control), they were allowed to form a natural blood clot and undergo natural healing. Both sides were sutured with absorbable polyglactin (Atramat, Internacional Farmacéutica) interrupted 5-0 sutures (Fig 2d). Patients were blinded to the study or control side selection.

Duration of the surgical procedure was counted from the beginning of surgical manipulations to complete removal of mandibular third molars and wound closure for each side separately. If there was a time difference greater than 10 minutes or if a different surgical

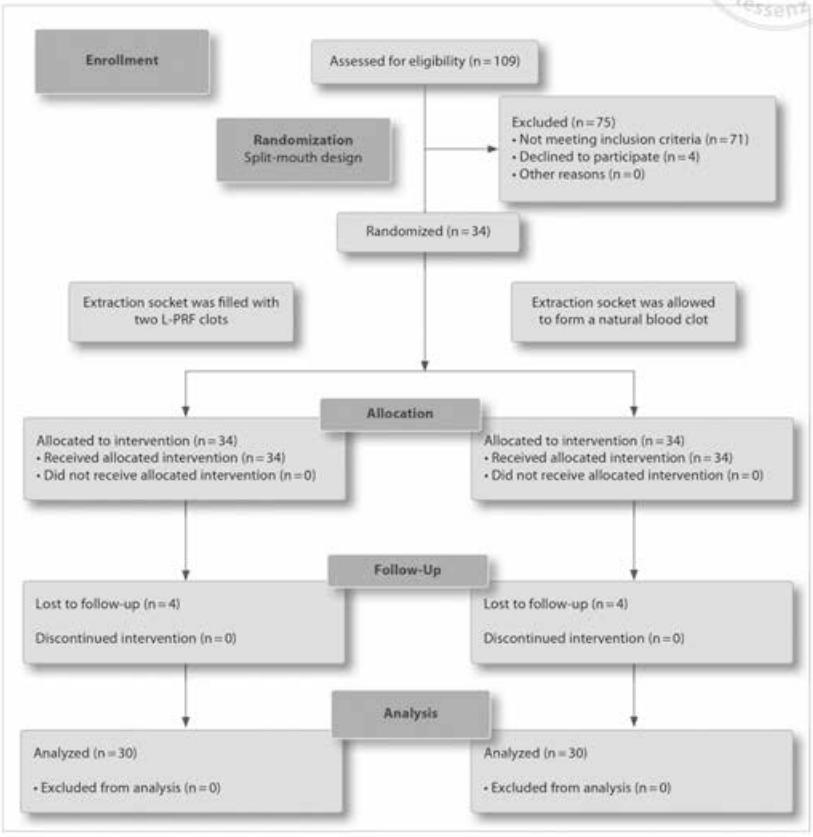

Fig 1 Flow chart of the study, following the CONSORT guidelines.

manipulation was used between each bilateral extraction, the patient was excluded from the study.

Each patient was given systemic antibiotic prophylaxis (clindamycin 600 mg per os) 1 hour before and 6 hours after surgery. Postoperatively oral lornoxicam 8 mg was prescribed to use for pain control when needed. Patients were instructed to rinse with chlorhexidine 0.12% solution three times a day for 2 weeks and provided with both verbal and written postoperative instructions. The sutures were removed 1 week after surgery.

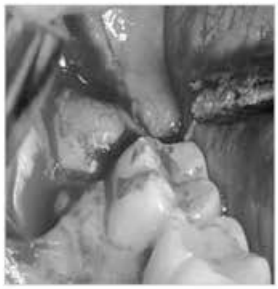

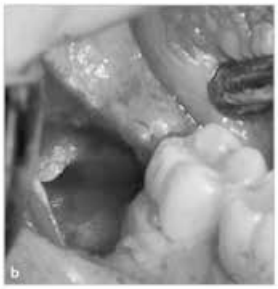

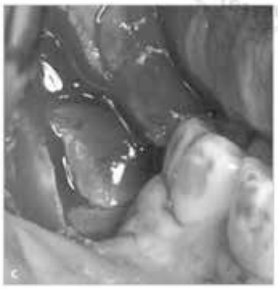

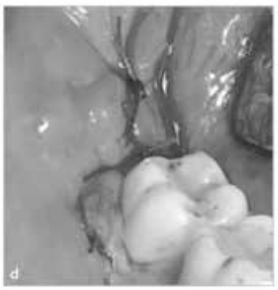

Figs 2a to 2d *(a)* Reflection of mucoperiosteal flap in impacted right mandibular third molar area. *(b)* Surgical site following extraction and socket debridement. *(c)* Mandibular third molar extraction socket filled with two L-PRF clots. *(d)* Closure of the wound site with resorbable 5-0 interrupted sutures.

Postoperative outcome evaluation

Quality of soft tissue healing, incidence of AO, pain, and facial swelling were selected as postoperative outcome measures.

Postextractional wound soft tissue healing

Postextractional wound soft tissue healing was evaluated using a modified postextraction wound healing index (HI),[21] which considered four parameters: bleeding, suppuration, tissue color, and consistency of the healing tissue. Each parameter involved three scoring levels; consequently, the cumulative scoring scale ranged from 4, corresponding to excellent healing, to 12, indicating severely impaired healing. HI was evaluated clinically by the same blinded examiner at days 1, 3, 7, and 14 after surgery.

The examiner for postextractional wound soft tissue HI assessment underwent a calibration course a week before the start of the study, twice repeating measurements on five patients, not included in the study sample. A reliability test was performed to assess the intra-examiner performance.

Alveolar osteitis

AO was characterized as postoperative continuous throbbing pain surrounding the alveolus that was not adequately relieved by analgesics and that increased in severity during a period of 1 to 3 days after tooth extraction. The pain was followed by partial or complete loss of the initial blood clot in the interior of the socket with or without halitosis.[22,23]

Pain

Pain was assessed using a written questionnaire with a visual analog scale (VAS)[24] every day by the patient during the first postoperative week. VAS consisted of

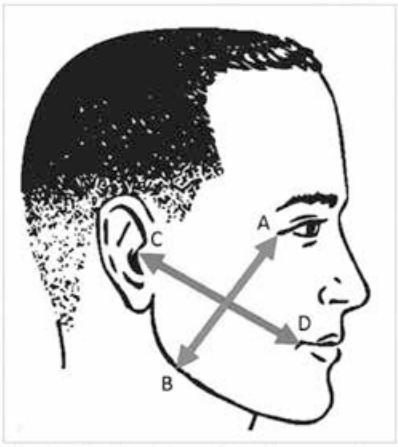

Fig 3 Facial swelling value was taken as the average value of facial measurements in millimeters, according to formula (AB+CD)/2.

10 units in combination with a graphic rating scale, where the leftmost score 0 represented absence of pain and the rightmost score 10 indicated the worst possible, unbearable, excruciating pain. Patients were blind to the knowledge of L-PRF and control sides and were asked to evaluate a VAS pain score for each operated side every day separately for the first week after surgery.

Facial swelling clinical assessment

The examiner for facial swelling assessment underwent a calibration course a week before the start of the study, twice repeating measurements on five patients, not included in the study sample. A reliability test was performed to assess the intra-examiner performance.

Facial swelling clinical assessments for the study patients were performed by the same blinded examiner at baseline (before surgery) and at the day-1, -3, and -7 visits postoperatively at approximately the same time of day.

Patients were seated in a relaxed position with the inferior border of the mandible parallel to the floor. Facial swelling in the operation side was evaluated using two facial measurements with nonexpandable tape, as described previously:[25]

- In the vertical dimension, measurement from the lateral canthus of the eye to the pogonion of the mandible was taken.
- In the horizontal dimension, the distance from the lower border of the tragus to the mouth commissure on both operated sides was measured.

Facial swelling value was taken as the average value of these two measurements (Fig 3). The preoperative measurement was considered as the baseline value.

Statistical analysis

Statistical data analysis was performed using the data mining and statistical analysis software SPSS 22.0 package (IBM). Statistical data were summarized as the mean and standard deviation (SD). Parameters were evaluated using the Kolmogorov-Smirnov test for the normality of distribution. Distribution of quantitative values did not meet normality distribution; therefore *P* values were calculated according to nonparametric tests. The difference between mean values of the variable in two groups was verified using the Mann-Whitney U test. For dependent variables the Wilcoxon test was used. The differences between the results were considered statistically significant when *P* values were less than .05.

RESULTS

According to the split-mouth study design, no significant differences were observed in the demographic variables, including sample size, gender, and age (Table 1). Chi-square and Mann-Whitney statistical analyses did not reveal significant differences according to preoperative and operative variables between the two groups ($P > .05$).

The healing of IMTM extraction sockets proceeded uneventfully with no major complications, except four control sites that experienced AO, which consisted of

13.3% of control cases and was statistically significant compared to no AO development in L-PRF-treated sockets ($P = .001$). AO in control extraction sockets was managed with revision of the wound and new blood clot formation in the socket. There were also two cases of postoperative hematoma in L-PRF and three in control sides, as well as one case of postoperative bleeding in control side, which ceased with repeated compression with the gauze. No potential complications related to harvesting venous blood, anesthesia, adverse reactions to prescribed medications, or other individual related side complications were noted in the study population.

Evaluation of soft tissue healing during the first 2 weeks according to the Wilcoxon rank sum test revealed significantly lower cumulative HI scores and better soft tissue healing in the L-PRF group compared to the control ($P = .001$). Results concerning postextractional wound soft tissue healing at each evaluation point are reported in Table 2. Comparisons between HI values relative to the L-PRF and control sides at days 1, 3, 7, and 14 postoperatively showed better healing and faster extraction wound closure for the group treated with L-PRF, with differences statistically significant at all investigated time points.

Calculation of cumulative pain scores during the first week according to the Wilcoxon rank sum test revealed significantly lower VAS values in the L-PRF group compared to the control ($P = .001$). The distribution of postoperative pain VAS scores in L-PRF and control sides at each evaluation day after the surgery is described in Table 3. L-PRF sides were found to have lower postoperative pain VAS scores compared with the control at each day of the first postoperative week, and this difference was statistically significant ($P < .005$).

There was no significant difference detected in facial swelling measurements prior to surgery ($P = .594$). Results concerning the dynamics of swelling values among the groups during the first postoperative week are reported in Table 4. The extent of facial swelling was significantly lower on L-PRF-treated sides at day 1 and day 3 compared to the controls, ceasing to nonsignificant difference at day 7. However, at day 7 swelling resolved to the baseline in L-PRF group ($P = .593$) only and remained significant at control side ($P = .001$) compared to the baseline.

DISCUSSION

This split-mouth study compared the surgical outcomes (incidence of AO, soft tissue healing, pain, and swelling) after mandibular third molar extraction of filling extraction sockets with L-PRF versus a standard blood clot as the control. As most adverse reactions and peak of patient postoperative discomfort level after IMTM surgeries are expected within first two postoperative weeks,[26] in the present study the estimated follow-up period for incidence of AO and assessment HI was at days 1, 3, 7, and 14 postoperatively. Pain VAS scores were recorded daily for the first postoperative week, and swelling measurements were taken at days 1, 3, and 7 after surgery correspondingly.

L-PRF is a second-generation platelet concentrate that consists predominantly of an equilateral fibrin matrix rich in platelet and leukocyte cytokines.[12] L-PRF preparation is based on a natural coagulation process during centrifugation, without addition of thrombin or calcium chloride, leading to progressive three-dimensional fibrin polymerization and growth factor enmeshment within a fibrin network.[27] The absence of anticoagulant implies the activation of most platelets in the collected blood by contact of Hageman factor (factor XII) with the negatively charged surfaces of glass or silica coating on the tube walls initially, and the release of intrinsic coagulation pathway cascades.[28] During the centrifugation process, fibrinogen is initially concentrated in the high part of the tube, before the circulating thrombin transforms it into fibrin. Gravitational force positions a fibrin clot, enmeshed with platelets and leukocytes, in the middle of the tube, just between the erythrocyte residual base at the bottom and acellular plasma at the top.[29]

Unlike the PRPs, L-PRF does not dissolve quickly after application; instead, the strong fibrin matrix is remodeled slowly in a manner similar to the formation of a natural blood clot. A solid fibrin network of L-PRF

Table 2 Soft tissue healing index score (mean HI ± SD)

Day	1	3	7	14
L-PRF side	5.10 ± 1.30	4.83 ± 0.95	4.33 ± 0.61	4.10 ± 0.40
Control side	6.47 ± 1.36	6.33 ± 1.27	4.97 ± 0.85	4.37 ± 0.62
P value	.001*	.001*	.002*	.023*

HI, healing index; SD, standard deviation. *Statistically significant difference among the groups, by Mann-Whitney test.

Table 3 Postoperative pain evaluation (mean VAS score ± SD)

Day	1	2	3	4	5	6	7
L-PRF side	2.87 ± 0.97	2.67 ± 1.03	1.67 ± 0.88	1.37 ± 0.72	1.13 ± 0.82	0.67 ± 0.76	0.07 ± 0.25
Control side	4.20 ± 1.35	3.53 ± 1.28	3.13 ± 1.28	2.97 ± 1.13	2.57 ± 1.10	1.97 ± 0.85	1.53 ± 0.82
P value	.001*	.004*	.001*	.001*	.001*	.001*	.001*

SD, standard deviation; VAS, visual analog scale. *Statistically significant difference among the groups, by Mann-Whitney test.

Table 4 Postoperative swelling measurements score (mean ± SD)

Day	Preoperatively	1	3	7
L-PRF side	84.20 ± 7.98	87.67 ± 7.21	87.27 ± 7.16	84.23 ± 7.91
Control side	84.70 ± 7.03	91.47 ± 6.88	91.07 ± 7.51	86.53 ± 6.99
P value	.594	.035*	.023*	.224

SD, standard deviation. *Statistically significant differences among the groups, by Mann-Whitney test.

was shown to protect enmeshed cells and growth factors from proteolytic degradation, leading to gradual release of growth factors, including transforming growth factor β1 (TGF-β1), platelet-derived growth factor (PDGF), fibroblast growth factor (FGF), and vascular endothelial growth factor (VEGF) from L-PRF clot for up to 28 days.[16,20,26,30]

Suttapreyasri and Leepong in 2013[31] investigated the impact of L-PRF on postextractional alveolar ridge resorption and soft tissue healing in split-mouth premolar extractions. Although the authors did not find significant impact of L-PRF on alveolar ridge preservation, L-PRF was found to accelerate soft tissue healing in the first four postoperative weeks, which is in accordance with recent studies by Marenzi et al,[32] Singh et al,[33] and Varghese et al,[34] who also found improvement in the soft tissue HI alongside a reduction of postoperative pain in L-PRF-treated premolar sockets at the early stages of healing. Additionally, Yelamali and Saikrishna[35] compared PRP- and L-PRF-treated IMTM extraction sites and found L-PRF significantly better in promoting soft tissue healing after third molar extraction, in comparison with PRP. These findings are in accordance with HI improvement in the present study, where the better HI values, associated with soft tissue healing enhancement, were found in the L-PRF-treated sockets ($P = .001$).

L-PRF is considered a weak osteoconductive material, losing 84% to 98% of its weight after extraction of the exudate from the L-PRF clot.[36] Thus L-PRF is not expected to serve as an osteoconductive scaffold for ridge preservation, in contrast to slow resorption biomaterials, like xenografts, allografts, or alloplasts, used for socket grafting surgeries. Unless inert slow resorption biomaterials may partially counteract postextractional ridge contraction, they were also shown to

delay the healing process.[37,38] On the other hand, L-PRF can improve the capacity of tissues to regenerate by enhancing cellular chemoattraction, angiogenesis, and epithelial proliferation,[39] leading to enhanced wound healing in clinical IMTM extraction situations, where fast and complication-free healing is desired.

AO is the most common complication after IMTM extraction, with the varying incidence of 4.1% to 32.6% reported in the literature.[40,41] AO is a multifactorial condition, associated with a local increase in fibrinolytic activity and consequent failure of maturation of the initially formed blood clot.[22,42] Comparatively high incidence of AO in IMTM surgeries can be attributed to increased bone density, decreased vascularity, and a reduced capacity to produce granulation tissue.[43] Jain et al[39] suggested that L-PRF supports the three primary aspects of wound healing: angiogenesis, immunity, and epithelial proliferation. A retrospective study evaluating the prevention of AO at 200 mandibular third molar extractions in 100 patients found incidence of AO of 1% in L-PRF treated sockets versus 9.5% in non-treated sites.[44] These findings correspond with the findings of two other studies[45,46] and the results of the present study ($P = .001$), demonstrating that preventative treatment of AO can be accomplished using L-PRF. The lower frequency of AO following L-PRF application could be related to its strong fibrin architecture,[30] increased hemostasis and blood clot stabilization,[47] ability to guide epithelial cell migration, and cicatricial properties.[26,48] Erythrocyte elimination from the socket by placing in L-PRF and the increased concentration of platelets and leukocytes within the extraction wound also may account for the enhanced socket healing capability.[44] In addition to the enhancement of wound healing by growth factors released by platelets and leukocytes, the latter cells also play an important role in the local immunomodulatory process of the healing extraction site. Tang et al[49] found that activated platelets release antimicrobial peptides, including platelet factor 4, RANTES, connective tissue activating peptide-III, platelet basic protein, thymosin β-4, fibrinopeptide B, and fibrinopeptide A. These bioactive substances were shown to be potent against *Escherichia coli* and *Staphylococcus aureus*.[49] Moreover, platelet antimicrobial peptides together with fibrinogen degradation products play an immunomodulatory role recruiting and amplifying leukocyte antimicrobial responses in the healing site.[49-51] The leukocytes trapped within the L-PRF clot mainly consist of lymphocytes, followed by neutrophils, monocytes, eosinophil, and basophil granulocytes.[50,52] Although there are some controversies in the literature regarding the influence of leukocytes on wound healing,[53,54] overpopulation of lymphocytes within the L-PRF clot compared to regular blood samples has an important role in immunomodulatory healing processes as lymphocytes are responsible for antigen-specific immune response.[55,56] Neutrophils, enmeshed within the fibrin clot, are known to participate in antimicrobial host defense both as the first line of innate immune defense and as effectors of adaptive immunity.[57] This contributes toward the prevention of bacterial contamination within the surgical site. Monocytes, recruited to the tissue, differentiate into tissue macrophages. Macrophages are key mediators of osseous wound healing and fracture repair, playing a pivotal role in the transition between wound inflammatory and repair phase during osteogenesis.[58,59] Functions of macrophages also involve phagocytosis and the release of enzymes, such as collagenase, elastase, and plasminogen activator, facilitating tissue debridement and wound repair.[59]

Relief of postoperative pain and swelling is crucial for the reduction of patient discomfort and improvement of overall success of IMTM surgery. Recently, studies have evaluated the effect of L-PRF on IMTM extraction socket healing, addressing postoperative pain[33,46,60-65] and swelling.[61-65] The impact of L-PRF on postoperative patient discomfort after IMTM extraction, as reported in the literature, is inconsistent. Some studies report no significant influence of L-PRF on postoperative pain[33,62,64] and swelling[61,64,65] values after IMTM surgeries, while others found reduced postoperative pain[46,60,61,63,65] and swelling[62,63] in L-PRF-treated sites during the first postoperative week. In accordance with the latter, the present study demonstrated significant reduction of pain in L-PRF group during the first post-

operative week ($P = .001$), and significant reduction of swelling at day 1 ($P = .035$) and day 3 ($P = .023$) postoperatively compared to the controls. It is important to note that at day 7 postoperatively in the present study pain scores were significantly different to the baseline in both L-PRF-treated ($P = .001$) and control ($P = .001$) groups. At the same time point the resolution of swelling was observed in L-PRF group ($P = .593$) only and remained significantly different to the baseline at the control side ($P = .001$). These findings are in correspondence with other studies,[26,44,46,60,63] where occurrence of postoperative complications were registered above 1-week postoperatively; therefore, it can be recommended to follow up patients for at least 2 weeks after IMTM surgeries to monitor incidence of AO, and assess soft tissue HI. Additionally, a prolonged time frame for pain and swelling reduction observation might be recommended, as these values tend not to resolve completely to the baseline within the first postoperative week, with the exception of swelling in L-PRF-treated sites. Clinically, the reduction of postoperative pain and swelling results in decrease of postoperative discomfort, lower demand of postoperative emergency appointments, and increase of patient satisfaction during the period of healing.[7,66] The beneficial effect of L-PRF in diminishing postoperative discomfort might be attributed to the release of growth factors and cytokines immersed in platelets, leukocytes, and the fibrin mesh.

Platelets have been shown to contain alpha granules, which degranulate upon platelet activation following the release of growth factors, stimulate cell migration, and enhance cellular-level events to expedite wound healing. Many experimental and clinical studies have found that platelet growth factors, such as FGF and TGF-β1, stimulate bone formation during osseous healing.[67,68] PDGF regulates the migration and proliferation of mesenchymal stem cells in the extraction site and stimulates osseous, endothelial, and fibroblastic proliferation to facilitate wound healing.[27,48,69] Additionally, VEGF, released from platelets, stimulates the proliferation and differentiation of numerous cell types essential for vascular formation during angiogenesis and vasculogenesis, helping to transport nutrients and oxygen mandatory for the extraction wound healing process.[70]

Leukocytes are not only inflammatory cells, as they also release growth factors at the extraction wound site. Macrophages release TGF to stimulate keratinocytes, interleukin 1 (IL-1), FGF, and tumor necrosis factor α (TNF-α) that stimulate collagen production by the fibroblasts and improve angiogenesis. PDGF, which was formerly considered to be specific to platelets, was also found to be produced by macrophages.[71] Lymphocytes were shown to release insulin-like growth factor 1 (IGF-1),[72] which plays a central role in cellular growth, differentiation, survival, and cell cycle progression.[73] Leukocytes present anti-nociceptive effects through different chemokines, anti-inflammatory interleukins (IL-4, IL-10, and IL-13), and opioid peptides (β-endorphin, metenkefalin, and dynorphin A), and can, therefore, promote a clinically relevant inhibition of postoperative pain. During the inflammatory phase of wound healing, these cytokines counteract the effects of the pro-inflammatory mediators generated naturally in the early stages of inflammation.[74]

It is important to note that L-PRF should be described not only as a source of growth factors; it is a fibrin-based living biomaterial containing living cells, as well as matrix proteins (thrombospondin-1, fibronectin, and vitronectin), glycosaminoglycans (heparin, hyaluronic acid), and a complex of regulatory cytokines including interleukins (IL-1β, IL-4, IL-6) and TNF-α. Therefore, the introduction of L-PRF to an extraction wound modulates the immune-inflammatory response; promotes primary hemostasis, chemotaxis, angiogenesis, and mitogenesis of endothelial cells; and acts as a bioactive cicatricial matrix for a complex cascade of wound healing.[27,30,48]

CONCLUSIONS

Within the limitations of this study, L-PRF showed potential in improving soft tissue healing and reducing postoperative pain, swelling, and incidence of AO following mandibular third molar extraction surgery.

However, further investigation with higher numbers of patients, a longer follow-up period, and attention to L-PRF impact on bone healing are needed to justify L-PRF use in oral surgery applications.

REFERENCES

1. Hugoson A, Kugelberg CF. The prevalence of third molars in a Swedish population. An epidemiological study. Community Dent Health 1988;5:121–138.
2. Eklund SA, Pittman JL. Third-molar removal patterns in an insured population. J Am Dent Assoc 200;132:469–475.
3. Costa MG, Pazzini CA, Pantuzo MC, Jorge ML, Marques LS. Is there justification for prophylactic extraction of third molars? A systematic review. Braz Oral Res 2013;27:183–188.
4. Friedman JW. The prophylactic extraction of third molars: a public health hazard. Am J Public Health 2007;97:1554–1559.
5. Guerrouani A, Zeinoun T, Vervaet C, Legrand W. A four-year monocentric study of the complications of third molars extractions under general anesthesia: about 2112 patients. Int J Dent 2013;2013:763837.
6. Mantovani E, Arduino PG, Schierano G, et al. A split-mouth randomized clinical trial to evaluate the performance of piezosurgery compared with traditional technique in lower wisdom tooth removal. J Oral Maxillofac Surg 2014;72:1890–1897.
7. Lee CT, Zhang S, Leung YY, Li SK, Tsang CC, Chu CH. Patients' satisfaction and prevalence of complications on surgical extraction of third molar. Patient Prefer Adherence 2015;9:257–263.
8. Barone A, Marconcini S, Giacomelli L, Rispoli L, Calvo JL, Covani U. A randomized clinical evaluation of ultrasound bone surgery versus traditional rotary instruments in lower third molar extraction. J Oral Maxillofac Surg 2010; 68: 330–336.
9. Marx RE, Carlson ER, Eichstaedt RM, Schimmele SR, Strauss JE, Georgeff KR. Platelet-rich plasma: growth factor enhancement for bone grafts. Oral Surg Oral Med Oral Pathol Oral Radiol Endod 1998;85:638–646.
10. Del Fabbro M, Bortolin M, Taschieri S. Is autologous platelet concentrate beneficial for post-extraction socket healing? A systematic review. Int J Oral Maxillofac Surg 2011;40:891–900.
11. Barona-Dorado C, González-Regueiro I, Martín-Ares M, Arias-Irimia O, Martínez-González JM. Efficacy of platelet-rich plasma applied to post-extraction retained lower third molar alveoli. A systematic review. Med Oral Patol Oral Cir Bucal 2014;19:e142–e148.
12. Choukroun J, Adda F, Schoeffler C, Vervelle A. Une opportunite en paro-implantologie: le PRF. Implantodontie 2001;42:55–62.
13. Dohan Ehrenfest DM, Doglioli P, de Peppo GM, Del Corso M, Charrier JB. Choukroun's platelet-rich fibrin (PRF) stimulates in vitro proliferation and differentiation of human oral bone mesenchymal stem cell in a dose-dependent way. Arch Oral Biol 2010;55:185–194.
14. Dohan Ehrenfest DM, Bielecki T, Mishra A, et al. In search of a consensus terminology in the field of platelet concentrates for surgical use:platelet-rich plasma (PRP), platelet-rich fibrin (PRF), fibrin gel polymerization and leukocytes. Curr Pharm Biotechnol 2012;13:1131–1137.
15. Dohan Ehrenfest DM, Diss A, Odin G, Doglioli P, Hippolyte MP, Charrier JB. In vitro effects of Choukroun's PRF (platelet-rich fibrin) on human gingival fibroblasts, dermal prekeratinocytes, preadipocytes, and maxillofacial osteoblasts in primary cultures. Oral Surg Oral Med Oral Pathol Oral Radiol Endod 2009;108:341–352.
16. He L, Lin Y, Hu X, Zhang Y, Wu H. A comparative study of platelet-rich fibrin (PRF) and platelet-rich plasma (PRP) on the effect of proliferation and differentiation of rat osteoblasts in vitro. Oral Surg Oral Med Oral Pathol Oral Radiol Endod 2009;108:707–713.
17. Chang IC, Tsai CH, Chang YC. Platelet-rich fibrin modulates the expression of extracellular signal-regulated protein kinase and osteoprotegerin in human osteoblasts. J Biomed Mater Res A 2010;95:327–332.
18. Pederson GW. Surgical removal of tooth. In: Pederson GW (ed). Oral surgery. Philadelphia: WB Saunders, 1988.
19. Juodzbalys G, Daugela P. Mandibular third molar impaction: review of literature and a proposal of a classification. J Oral Maxillofac Res 2013;4:e1.
20. Farish SE, Bouloux GF. General technique of third molar removal. Oral Maxillofac Surg Clin North Am 2007;19:23–43.
21. Mozzati M, Gallesio G, di Romana S, Bergamasco L, Pol R. Efficacy of plasma-rich growth factor in the healing of postextraction sockets in patients affected by insulin-dependent diabetes mellitus. J Oral Maxillofac Surg 2014;72: 456–462.
22. Cardoso CL, Rodrigues MT, Ferreira Júnior O, Garlet GP, de Carvalho PS. Clinical concepts of dry socket. J Oral Maxillofac Surg 2010;68:1922–1932.
23. Cheung LK, Chow LK, Tsang MH, Tung LK. An evaluation of complications following dental extractions using either sterile or clean gloves. Int J Oral Maxillofac Surg 2001;30:550–554.
24. Campbell WI, Lewis S. Visual analogue measurement of pain. Ulster Med J 1990;59:149–154.
25. Rakprasitkul S, Pairuchvej V. Mandibular third molar surgery with primary closure and tube drain. Int J Oral Maxillofac Surg 1997;26:187–190.
26. Shugars DA, Benson K, White RP Jr, Simpson KN, Bader JD. Developing a measure of patient perceptions of short-term outcomes of third molar surgery. J Oral Maxillofac Surg 1996;54:1402–1048.
27. Dohan DM, Choukroun J, Diss A, et al. Platelet-rich fibrin (PRF): a second-generation platelet concentrate. Part II: Platelet-related biologic features. Oral Surg Oral Med Oral Pathol Oral Radiol Endod 2006;101:e45–e50.
28. Nishimoto S, Fujita K, Sotsuka Y, et al. Growth factor measurement and histological analysis in platelet rich fibrin: a pilot study. J Maxillofac Oral Surg 2015;14:907–913.
29. Dohan DM, Choukroun J, Diss A, et al. Platelet-rich fibrin (PRF): a second-generation platelet concentrate. Part I: technological concepts and evolution. Oral Surg Oral Med Oral Pathol Oral Radiol Endod 2006;101:e37–e44.
30. Dohan Ehrenfest DM, Bielecki T, Jimbo R, et al. Do the fibrin architecture and leukocyte content influence the growth factor release of platelet concentrates? An evidence-based answer comparing a pure platelet-rich plasma (P-PRP) gel and a leukocyte- and platelet-rich fibrin (L-PRF). Curr Pharm Biotechnol 2012;13:1145–1152.
31. Suttapreyasri S, Leepong NJ. Influence of platelet-rich fibrin on alveolar ridge preservation. Craniofac Surg 2013;24:1088–1094.
32. Marenzi G, Riccitiello F, Tia M, di Lauro A, Sammartino G. Influence of leukocyte- and platelet-rich fibrin (L-PRF) in the healing of simple postextraction sockets: a split-mouth study. Biomed Res Int 2015;2015:369273.
33. Singh A, Kohli M, Gupta N. Platelet rich fibrin: a novel approach for osseous regeneration. J Maxillofac Oral Surg 2012;11:430–434.
34. Varghese MP, Manuel S, Kumar LKS. Potential for osseous regeneration of platelet-rich fibrin: a comparative study in mandibular third molar impaction sockets. J Oral Maxillofac Surg 2017;75:1322–1329.
35. Yelamali T, Saikrishna D. Role of platelet rich fibrin and platelet rich plasma in wound healing of extracted third molar sockets: a comparative study. J Maxillofac Oral Surg 2015;14:410–416.
36. Kobayashi M, Kawase T, Horimizu M, Okuda K, Wolff LF, Yoshie H. A proposed protocol for the standardized preparation of PRF membranes for clinical use. Biologicals 2012;40:323–329.
37. Iasella JM, Greenwell H, Miller RL, et al. Ridge preservation with freeze-dried bone allograft and a collagen membrane compared to extraction alone for implant site development: a clinical and histologic study in humans. J Periodontol 2003;74:990–999.
38. Araújo MG, Lindhe J. Ridge preservation with the use of Bio-Oss collagen: a 6-month study in the dog. Clin Oral Implants Res 2009;20:433–440.
39. Jain V, Triveni MG, Kumar AB, Mehta DS. Role of platelet-rich-fibrin in enhancing palatal wound healing after free graft. Contemp Clin Dent 2012;3 (Suppl 2):S240–S243.

40. Sigron GR, Pourmand PP, Mache B, Stadlinger B, Locher MC. The most common complications after wisdom-tooth removal: part 1: a retrospective study of 1,199 cases in the mandible. Swiss Dent J 2014;124:1042–1046.
41. Haraji A, Rakhshan V, Khamverdi N, Alishahi HK. Effects of intra-alveolar placement of 0.2% chlorhexidine bioadhesive gel on dry socket incidence and postsurgical pain: a double-blind split-mouth randomized controlled clinical trial. J Orofac Pain 2013;27:256–262.
42. Birn H. Etiology and pathogenesis of fibrinolytic alveolitis ("dry socket"). Int J Oral Surg 1973;2:211–263.
43. Blum IR. Contemporary views on dry socket (alveolar osteitis): a clinical appraisal of standardization, aetiopathogenesis and management: a critical review. Int J Oral Maxillofac Surg 2002;31:309–317.
44. Hoaglin DR, Lines GK. Prevention of localized osteitis in mandibular third-molar sites using platelet-rich fibrin. Int J Dent 2013;2013:875380.
45. Eshghpour M, Dastmalchi P, Nekooei AH, Nejat A. Effect of platelet-rich fibrin on frequency of alveolar osteitis following mandibular third molar surgery: a double-blinded randomized clinical trial. J Oral Maxillofac Surg 2014;72:1463–1467.
46. Al-Hamed FS, Tawfik MA-M, Abdelfadil E. Clinical effects of platelet-rich fibrin (PRF) following surgical extraction of lower third molar. Saudi J Dent Res 2017;8:19–25.
47. Sammartino G, Dohan Ehrenfest DM, Carile F, Tia M, Bucci P. Prevention of hemorrhagic complications after dental extractions into open heart surgery patients under anticoagulant therapy: the use of leukocyte- and platelet-rich fibrin. J Oral Implantol 2011;37:681–690.
48. Choukroun J, Diss A, Simonpieri A, et al. Platelet-rich fibrin (PRF): a second-generation platelet concentrate. Part IV: clinical effects on tissue healing. Oral Surg Oral Med Oral Pathol Oral Radiol Endod 2006;101:e56–e60.
49. Tang YQ, Yeaman MR, Selsted ME. Antimicrobial peptides from human platelets. Infect Immun 2002;70:6524–6533.
50. Dohan Ehrenfest DM, Del Corso M, Diss A, Mouhyi J, Charrier JB. Three-dimensional architecture and cell composition of a Choukroun's platelet-rich fibrin clot and membrane. J Periodontol 2010;81:546–555.
51. Yeaman MR. Platelets: at the nexus of antimicrobial defence. Nat Rev Microbiol 2014;12:426–437.
52. Ghanaati S, Booms P, Orlowska A, et al. Advanced platelet-rich fibrin: a new concept for cell-based tissue engineering by means of inflammatory cells. J Oral Implantol 2014;40:679–689.
53. Anitua E, Zalduendo MM, Prado R, Alkhraisat MH, Orive G. Morphogen and proinflammatory cytokine release kinetics from PRGF-endoret fibrin scaffolds: evaluation of the effect of leukocyte inclusion. J Biomed Mater Res A 2015;103:1011–1020.
54. Dohan Ehrenfest DM, Zhang CQ, Pinto NR, Bielecki T. Merchants shall be expelled from the temple: the PRGF(®) (Plasma-Preparation Rich in Growth Factors)-Endoret(®) case. Muscles Ligaments Tendons J 2015;4:473–477.
55. Turner ML. Cell adhesion molecules: a unifying approach to topographic biology. Biol Rev Camb Philos Soc 1992;67:359–377.
56. Cieslik-Bielecka A, Dohan Ehrenfest DM, Lubkowska A, Bielecki T. Microbicidal properties of leukocyte- and platelet-rich plasma/fibrin (L-PRP/L-PRF): new perspectives. J Biol Regul Homeost Agents 2012;26(2 Suppl 1):435–525.
57. Mócsai A. Diverse novel functions of neutrophils in immunity, inflammation, and beyond. J Exp Med 2013;210:1283–1299.
58. Sinder BP, Pettit AR, McCauley LK. Macrophages: their emerging roles in bone. J Bone Miner Res 2015;30:2140–2149.
59. Clark RA. Fibrin and wound healing. Ann N Y Acad Sci 2001;936:355–367.
60. Kumar YR, Mohanty S, Verma M, et al. Platelet-rich fibrin: the benefits. Br J Oral Maxillofac Surg 2016;54:57–61.
61. Bilginaylar K, Uyanik LO. Evaluation of the effects of platelet-rich fibrin and piezosurgery on outcomes after removal of impacted mandibular third molars. Br J Oral Maxillofac Surg 2016;54:629–633.
62. Ozgul O, Senses F, Er N, et al. Efficacy of platelet rich fibrin in the reduction of the pain and swelling after impacted third molar surgery: randomized multicenter split-mouth clinical trial. Head Face Med 2015;11:37.
63. Kumar N, Prasad K, Ramanujam L, Ranganath K, Dexith J, Chauhan A. Evaluation of treatment outcome after impacted mandibular third molar surgery with the use of autologous platelet-rich fibrin: a randomized controlled clinical study. J Oral Maxillofac Surg 2015;73:1042–1049.
64. Gülşen U, Şentürk MF. Effect of platelet rich fibrin on edema and pain following third molar surgery: a split mouth control study. BMC Oral Health 2017;17:79.
65. Uyanik LO, Bilginaylar K, Etikan I. Effects of platelet-rich fibrin and piezosurgery on impacted mandibular third molar surgery outcomes. Head Face Med 2015;11:25.
66. Atchison KA, Der-Martirosian C, Belin TR, Black EE, Gironda MW. Predictors of risk tolerance among oral surgery patients. J Oral Maxillofac Surg 2010;68:2947–2954.
67. He B, Ou Y, Chen S, et al. Designer bFGF-incorporated d-form self-assembly peptide nanofiber scaffolds to promote bone repair. Mater Sci Eng C Mater Biol Appl 2017;74:451–458.
68. Poniatowski ŁA, Wojdasiewicz P, Gasik R, Szukiewicz D. Transforming growth factor beta family: insight into the role of growth factors in regulation of fracture healing biology and potential clinical applications. Mediators Inflamm 2015;2015:137823.
69. Fiedler J, Etzel N, Brenner RE. To go or not to go: migration of human mesenchymal progenitor cells stimulated by isoforms of PDGF. J Cell Biochem 2004;93:990–998.
70. Boëck-Neto RJ, Artese L, Piattelli A, Shibli JA, Perrotti V, Piccirilli M, Marcantonio E Jr. VEGF and MVD expression in sinus augmentation with autologous bone and several graft materials. Oral Dis 2009;15:148–154.
71. Shimokado K, Raines EW, Madtes DK, Barrett TB, Benditt EP, Ross R. A significant part of macrophage-derived growth factor consists of at least two forms of PDGF. Cell 1985;43:277–286.
72. Toulon A, Breton L, Taylor KR, et al. A role for human skin-resident T cells in wound healing. J Exp Med 2009;206:743–750.
73. Yakar S, Courtland HW, Clemmons D. IGF-1 and bone: new discoveries from mouse models. J Bone Miner Res 2010;25:2543–2552.
74. Dohan Ehrenfest DM, Andia I, Zumstein MA, Zhang CQ, Pinto NR, Bielecki T. Classification of platelet concentrates (platelet-rich plasma-PRP, platelet-rich fibrin-PRF) for topical and infiltrative use in orthopedic and sports medicine: current consensus, clinical implications and perspectives. Muscles Ligaments Tendons J 2014;4:3–9.

Ausra
Ramanauskaite

Treatment of peri-implantitis: Meta-analysis of findings in a systematic literature review and novel protocol proposal

Ausra Ramanauskaite, DDS[1]/Povilas Daugela, DDS[2]/Gintaras Juodzbalys, DDS, MSD, PhD[3]

Objective: To test the effectiveness of nonsurgical and surgical treatment methods for clinical and radiographic peri-implantitis symptoms resolution with respect to pocket probing depth (PD), bleeding on probing (BOP), and marginal bone-loss reduction (RBL); to propose guidelines for managing peri-implantitis. **Method and Materials:** An electronic literature search was conducted of the MEDLINE and EMBASE databases for articles published between 2002 and 2015. Sequential screening at the title/abstract and full-text levels was performed. Clinical human studies in the English language that had reported changes in PD and/or BOP and/or radiologic marginal bone level (RBL) changes after peri-implantitis treatment at 6-month follow-up or longer were included. A meta-analysis was performed using the random-effects model on the selected qualifying articles. **Results:** The search resulted in 29 articles meeting the inclusion criteria. The meta-analysis demonstrated improved BOP values ($P = .001$; OR = 1.567; 95% CI, 1.405 to 1.748) after the nonsurgical treatment but did not reveal a statistically significant difference in the PD changes ($P = .8093$; standardized mean difference [SMD] = 0.346 mm; 95% CI, 0.181 to 0.512). There was a significant improvement in PD ($P < .001$; SMD = 1.647 mm; 95% CI, 1.414 to 1.880) and BOP values ($P < .001$; OR = 4.044; 95% CI, 3.571 to 4.381) after surgical treatment and an intrabony defect fill was found to be 1.66 mm (1.0) using a regenerative treatment modality. Our meta-analysis confirms there is a significant reduction in RBL after nonsurgical ($P = 0.037$; SMD = 0.157 mm; 95% CI, −0.183 to 0.496), resective ($P = .0212$; SMD = −0.116 mm; 95% CI, −0.433 to 0.201), and regenerative ($P = .0305$; SMD = 1.703 mm; 95% CI, 1.266 to 2.139) surgical treatment. A novel complex management and maintenance (CMM) six-step protocol is thus suggested for treatment of peri-implantitis. **Conclusion:** Regenerative surgical treatment of peri-implantitis was found to be most effective. A novel six-step protocol aimed at managing patients with peri-implantitis can be a useful tool in peri-implantitis treatment. *(doi: 10.3290/j.qi.a35131)*

Key words: peri-implantitis, review, treatment, therapy

Replacing missing teeth with titanium dental implants has become a routine procedure. Several longitudinal studies have reported high survival rates of the implants, ranging from 95% to 98% over a period up to 10 years, and have encouraged clinicians to consider this type of oral rehabilitation.[1,2] However, complications do occur. Plaque-induced peri-implantitis, which generally occurs more than 1 year after placement, is considered to be the most common late biologic complication.[3]

Peri-implantitis has been characterized by an inflammatory process around a rough-surface, solid

[1]PhD Student, Clinic of Dental and Oral Pathology, Lithuanian University of Health Sciences, Kaunas, Lithuania.

[2]PhD Student, Department of Maxillofacial Surgery, Lithuanian University of Health Sciences, Kaunas, Lithuania.

[3]Professor, Department of Maxillofacial Surgery, Lithuanian University of Health Sciences, Kaunas, Lithuania.

Correspondence: Dr Ausra Ramanauskaite, Clinic of Dental and Oral Diseases, Faculty of Dentistry, Lithuanian University of Health Sciences, Eiveniu 2, 5009, Kaunas, Lithuania. Email: ausra.ramanauskaite@gmail.com

screw-type implant, which includes both soft-tissue inflammation and progressive loss of supporting bone beyond biologic bone remodeling.[4] It is often associated with bleeding at the peri-implant margin after the insertion of a periodontal probe into the peri-implant space, increased peri-implant pocket probing depth (PD), mucosal recession, and/or suppuration.[5] Peri-implantitis was reported to occur in 18.8% of subjects and 9.6% of implants.[6] If not properly managed, it is a debilitating condition that results in loss of function and esthetics.[7]

The evidence that microorganisms are essential for the development of infections around dental implants has been well documented.[8] The microbiota associated with peri-implant diseases have been reported to be similar to the bacteria that cause periodontal diseases.[7] Marginal bone loss around dental implants may also be caused by occlusal overload.[9] However, this review will focus on the treatment of peri-implantitis induced by plaque infection.

Various clinical protocols for the treatment of peri-implantitis have been proposed, including mechanical debridement, the use of antiseptics, and local or systemic antibiotics,[10-18] surgical access,[19,20] and regenerative[21-33] or resective procedures.[34-36] The aim of peri-implantitis treatment is the management of the surrounding soft-tissue inflammation and progressive loss of supporting bone as well as the reestablishment and maintenance of healthy soft and hard tissues.[37] Furthermore, clinical and radiographic peri-implant tissue parameters (eg, bleeding on probing (BOP), PD, and radiologic bone level changes/bone defect fill) have been established as indicators for evaluating the effectiveness of various treatment procedures.[38] However, even though plenty of methods for peri-implantitis treatment have been described in the literature, it is still hard to clarify which method is most effective at eliminating soft-tissue inflammation and arresting continuous bone loss.

The purposes of the present article were to test the effectiveness of nonsurgical and surgical treatment methods for clinical and radiographic peri-implantitis symptoms resolution with respect to PD, BOP, and marginal bone-loss reduction (RBL), as well as to propose guidelines for managing peri-implantitis.

METHOD AND MATERIALS

Protocol and registration

The methods of the analysis and inclusion criteria were specified in advance and documented in a protocol. The review was registered in PROSPERO, an international prospective register of systematic reviews. The protocol can be accessed at: http://www.crd.york.ac.uk/PROSPERO/display_record.asp?ID=CRD42015023781; registration number: CRD42015023781. The reporting of this systematic analysis adhered to the Preferred Reporting Items for Systematic Review and Meta-Analyses (PRISMA) statement.[39]

Focus question

The following focus question was developed according to the population, intervention, comparison, and outcome (PICO) study design: What is the effectiveness of nonsurgical and surgical treatment methods for clinical and radiographic peri-implantitis symptoms resolution with respect to PD, BOP, and marginal bone loss?

Types of publications

The review included studies on humans published in the English language. Letters, editorials, literature reviews, PhD theses, and abstracts were excluded.

Types of studies

The review included all human prospective and retrospective follow-up studies, clinical trials, cohort studies, case-control studies, and case series studies published between 1 January 2002, and 1 February 2015, that reported on nonsurgical and surgical treatment modalities for peri-implantitis. Case report studies were excluded.

Information sources

The search strategy incorporated the examination of electronic databases, supplemented by hand searches. A search was conducted on the National Library of

doi: 10.3290/j.qi.a35131

Medicine database (MEDLINE) through its online site (PubMed) and EMBASE databases. Additionally, a hand search was conducted in the following journals: Clinical Oral Implants Research, Clinical Implant Dentistry and Related Research, European Journal of Oral Implantology, Implant Dentistry, International Journal of Oral and Maxillofacial Implants, International Journal of Periodontics and Restorative Dentistry, Journal of Clinical Periodontology, Journal of Oral Implantology, International Journal of Oral and Maxillofacial Surgery, Journal of Periodontology, and Journal of Prosthetic Dentistry.

The references of each relevant study were screened to discover additional relevant publications and to improve the sensitivity of the search.

Search

The PubMed and EMBASE resource databases were explored through advanced searches. The keywords and search inquiries used during the primary stage were as follows: ("peri-implantitis" OR "peri-implant complication" OR "peri-implant infection" OR ("implant" AND "failure") AND ("treatment" OR "therapy" OR "management" OR "nonsurgical therapy" OR "surgical therapy" OR "regeneration" OR "open flap" OR "access surgery" OR "resection" OR "laser"). The choice of keywords was intended to be broad to collect as much relevant data as possible without relying on electronic means alone to refine the search results.

Selection of studies

Titles derived from this broad search were independently screened by two reviewers based on the inclusion criteria. The reviewers compared decisions and resolved differences through discussion, consulting a third party when consensus could not be reached. The third party was an experienced senior reviewer. Full reports were obtained for all the studies deemed eligible for inclusion in this paper. At the title and abstract stage, one reviewer accepted the citations that appeared to meet the inclusion criteria and sent them on for full-text review, with a second reviewer assessing only those citations the first reviewer deemed ineligible.

Population

Subjects in the included studies must have had at least one osseointegrated rough-surface, solid screw-type implant that presented with signs of peri-implantitis. The definition of peri-implantitis included continuous marginal bone loss beyond biologic bone remodeling (eg, more than 2 mm) with signs of inflammation (eg, purulent, BOP, and more than 6 mm PD).[3]

Inclusion and exclusion criteria

The applied inclusion criteria for the studies were as follows:

- investigated nonsurgical and surgical treatment outcomes for peri-implantitis in patients with at least one osseointegrated rough-surface, solid screw-type implant that presented the signs of peri-implantitis
- followed up after at least 6 months on clinical and radiographic peri-implant tissue parameter changes and reported clear data
- all human prospective or retrospective follow-up studies and clinical trials, cohort studies, case-control studies and case series studies were included with at least 10 patients
- studies from which smokers were not excluded
- treatment outcomes had to include changes in PD and/or BOP as primary outcome variables and/or radiologic bone level changes/bone defect fill as a secondary outcome variable.

The following types of articles were excluded as follows:

- in vitro and animal studies; studies based on charts or questionnaires
- studies of patients with immunologic diseases, uncontrolled diabetes mellitus, osteoporosis, or other contraindicating systemic conditions
- studies of patients with machined and hydroxyapatite surface implants or ceramic implants
- studies including fewer than 10 patients
- studies involving less than 6 months of follow-up after peri-implantitis treatment

- studies not focused specifically on the selected topic or that included unclear data or had authors who could not be contacted for any reason.

Sequential search strategy

Following the initial literature search, all article titles were screened to eliminate irrelevant publications, review articles, case reports, and in vitro and animal studies. Next, studies were excluded based on data obtained from screening the abstracts. The final stage of screening involved reading the full texts to confirm each study's eligibility based on the inclusion and exclusion criteria.

Data extraction

The data were independently extracted from studies in the form of variables, according to the aims and themes of the present review, as listed as follows.

Data items

Data were collected from the included articles and arranged in the following fields:

- "Year" revealed the year of publication
- "Type of study" indicated the type of study
- "Treatment method" described the treatment protocol performed
- "Sample size" described the number of patients examined
- "Follow-up" described the duration of the observed outcomes
- "Probing depth changes" described the probing depth changes (in mm) before and after the treatment
- "Bleeding on probing changes" described the BOP (%) before and after the treatment
- "Radiologic bone level changes" described the marginal bone level changes (in mm; measured from implant shoulder to the bone) before and after the treatment; and/or intrabony defect depth changes (in mm; measured from the bottom of the defect to the interproximal bone).

Assessment of methodologic quality

The quality of all included studies was assessed during the data extraction process. The quality appraisal involved evaluating the methodologic elements that might influence the outcomes of each study.

The Cochrane Collaboration's two-part tool for assessing risk of bias (Higgins and Green[40]) was used to assess bias across the studies and identify papers with intrinsic methodologic and design flaws (Table 1).[40]

Synthesis of results

Relevant data of interest regarding the previously stated variables were collected and organized into two tables based on the assessed treatment method.

Statistical analysis

A meta-analysis integrates the quantitative findings from separate but similar studies and provides a numerical estimate of the overall effect of interest. All meta-analyses were performed on studies that reported the clinical and/or radiologic outcomes of different peri-implantitis treatment methods. Thus, each study provided estimates of outcome measures (eg, odds ratio, relative risk). The goal was to obtain global estimates of these measures and to test whether they differed significantly. Global estimates of a proportion can be obtained by simply pooling together the data from each study. However, a test for significance cannot be applied to such pooled data, as these studies are heterogeneous with respect to study population and treatment protocol. Therefore, individual trials were pooled, and the overall rates of PD reduction, BOP reduction, bone-level changes, and bone defect fill among the treatment groups, together with their 95% confidence intervals (CIs), were calculated. Under the fixed-effects model, it is assumed that all studies come from a general population and that the size (eg, relative risk, odds ratio) is not significantly different among the different trials. This assumption was tested by the heterogeneity test using the Cochran Q statistics. We considered that in our case the random-effects model (the Der Simonian and Liard method)[41] was more appropriate to use since it took into account both the random

doi: 10.3290/j.qi.a35131

Table 1 Assessment of the risk of bias

Study	Random sequence generation	Allocation concealment	Blinding	Incomplete outcome data	Selective reporting	Other bias
Karring et al[10]	?	?	+	+	?	+
Schwarz et al[11]	+	?	-	-	-	-
Renvert et al[12]	+	+	+	-	?	+
Renvert et al[13]	+	?	+	+	?	+
Renvert et al[14]	+	?	+	+	?	+
Sahm et al[15]	+	?	?	+	?	+
Renvert et al[16]	+	?	+	+	?	+
Schär et al[17]	+	?	+	+	?	+
Deppe et al[18]	?	?	?	+	-	-
Bassetti et al[44]	+	?	+	+	?	+
John et al[45]	?	?	-	+	?	+
Heitz-Mayfield et al[19]	?	?	?	-	-	-
Papadopoulos et al[20]	+	?	+	+	?	+
de Waal et al[24]	+	+	+	+	-	+
Romeo et al[35]	-	-	-	+	-	+
Romeo et al[36]	-	-	-	+	-	+
Schwarz et al[21]	+	?	+	-	?	+
Roos-Jansåker et al[22]	?	?	?	-	?	+
Schwarz et al[23]	+	?	+	-	?	+
Romanos et al[24]	?	?	?	-	-	-
Schwarz et al[25]	+	?	+	-	?	+
Roos-Jansåker et al[26]	?	?	+	-	?	+
Roccuzzo et al[27]	?	?	+	+	?	+
Aghazadeh et al[28]	?	?	+	+	?	+
Wiltfang et al[29]	?	?	?	-	-	+
Schwarz et al[30]	+	?	+	?	-	+
Roos-Jansåker et al[31]	?	?	+	-	?	+
Schwarz et al[32]	?	?	?	-	?	+
Matarasso et al[33]	?	?	?	-	?	+

+ low risk; ? unclear risk; - high risk.

variation within the studies and the variation among different studies, especially because in some cases the heterogeneity test yielded a log *P* value. Later findings indicated the fixed-effects model might be invalid. Indeed, the random-effects model tended to give a more conservative estimate (ie, with a wider CI), but the results from the two models usually agreed well. Kappa index was used to evaluate the level of agreement between two independent researchers.

RESULTS

Study selection

Article review and data extraction were performed according to the PRISMA flow diagram (Fig 1). The initial search displayed 753 results from the MEDLINE (NCBI PubMed and PMC) and EMBASE databases and three results from other sources. A total of 758 search results were initially screened. The inclusion and exclusion criteria were applied to 62 full-text articles. Finally, 29 articles were included in the review. A total of 718 patients diagnosed with peri-implantitis were treated in the included studies, 319 of them using various non-surgical methods and 399 with surgical treatment methods.

The κ value for inter-reviewer agreement for potentially relevant articles was 1 (titles and abstracts) and > 0.9 (full-text articles), indicating a "very good" agreement between the two reviewers, according to the criteria of Landis and Koch.[42]

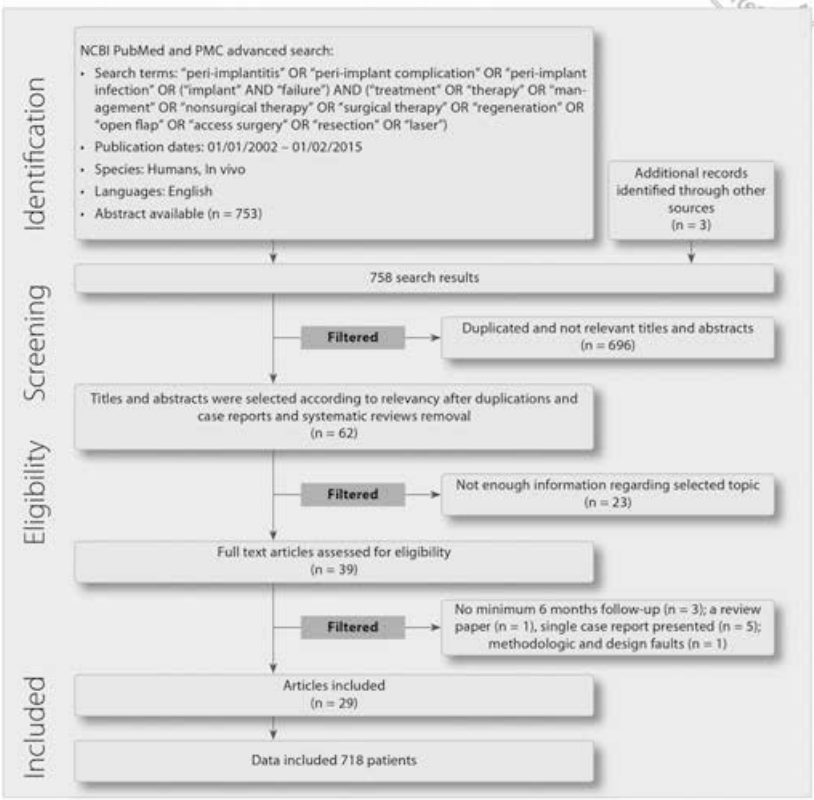

Fig 1 PRISMA flow diagram.

Study exclusion

The reasons for excluding studies after full-text assessment were as follows: insufficient amount of information about the results obtained on the selected topic (n = 24), follow-up time < 6 months (n = 3), being a review paper (n = 1), and single case reports presented (n = 5). One study (n = 1) was excluded due to methodologic and design faults.[43]

Quality assessment

Summarizing the risk of bias for each study, 26 studies were classified as unclear risk (of bias for one or more key domains),[10-33,44,45] and three studies were judged to have a high risk (of bias for more than one domain) (Table 1).[34-36]

doi: 10.3290/j.qi.a35131

Study characteristics

The included studies were further divided into two groups, characterized by the method of peri-implantitis treatment: nonsurgical (Appendix 1, available in the online version of this article, at http://quintessenz.de) and surgical (Appendix 2). The division provided a better understanding of peri-implantitis treatment outcomes and contributed to the sensitivity of the review. The studies were compared regarding the type of study, the number of patients treated, the follow-up period, the treatment methods used, the clinical parameters (ie, PD and BOP) evaluated, and the preoperative and postoperative radiographic intrabony defect evaluation (Appendixes 1 and 2).

Nonsurgical treatment

Eleven studies reporting the effectiveness of various nonsurgical peri-implantitis treatment methods included 319 patients (Appendix 1). Eight studies were randomized controlled trials,[12-17,44,45] and the rest were pilot studies.[10,11,18] Seven studies[10,11,14-18] out of the 11 included up to 6 months of follow-up, and the rest[12,13,44,45] included up to 1 year of follow-up.

Reduced BOP scores from baseline were found following all the treatments.[10-18,44,45] However, a significant improvement in BOP scores was indicated in four studies.[11,16,17,44]

No significant difference in PD changes was found between the submucosal scaling with piezoelectric ultrasonic scaler,[10,14] or subgingival air polishing[15,45] compared with the hand instrumentation using either carbon fiber or titanium curettes.

Adjunctive local delivery of minocycline microspheres resulted in significantly lower BOP scores when compared with submucosal debridement alone.[12,13]

Nonsurgical laser therapy using Er:YAG laser resulted in significantly greater reduction of BOP in the Er:YAG treatment group compared with mechanical submucosal debridement.[11]

Photodynamic therapy as an adjunct to mechanical debridement demonstrated significantly greater reduction in PD between the two groups in one study.[44]

Three studies reported on marginal bone loss following treatment.[10,13,16] Deppe et al[18] reported on progressive bone loss in peri-implantitis cases diagnosed as severe (PD 5 to 8 mm) at baseline.

Surgical treatment

Eighteen studies on surgical treatment of peri-implantitis included 399 patients (Appendix 2). Four of the studies were randomized controlled studies,[20,28,35,36] three were case series,[24,32,33] and the rest were prospective clinical studies.[19,21-23,25-27,29-31,34] Only three studies[20,21,32] involved up to 6 months of follow-up; the rest called for 1 to 5 years of follow-up.[19,22-31,33-36]

All surgical treatment methods were divided into three groups: access surgery,[19,20] resective,[34-36] and regenerative.[21-33]

Access surgery

Surgical treatment of peri-implantitis by access flaps resulted in improvement of all clinical parameters.[19,20] Bone-level changes were evaluated in the study by Heitz-Mayfield et al,[19] where three implants out of 36 demonstrated bone gain, and three implants had bone loss not exceeding 1 mm.

Resective approach

Three studies reported on a resective surgical approach[34-36] and improved clinical parameters (ie, PD and BOP)[34,35] and marginal bone loss compared with the baseline were observed in both treatment groups, with no significant difference between them.[35]

Randomized clinical studies by Romeo et al[36] performed resective surgery together with the modification of the implant surface (implantoplasty) for the test group and without implantoplasty for the control group. Significantly extended marginal bone loss was reported in the group without implantoplasty, demonstrating implant surface modification could be considered an effective procedure for peri-implantitis treatment.[36]

Regenerative approach

Different regenerative procedures involving bone grafts (xenogenous, autogenous, or allogenous), with or without barrier membranes, were proposed for the management of peri-implantitis in 13 of the studies

included. Twelve of them reported improved clinical parameters (ie, PD and BOP) compared with baseline,[21-25,27-33] and in four of the studies these improvements were statistically significant.[24,28,32,33]

Roccuzzo et al[27] used xenograft bone for intrabony defect regeneration around two implant types: titanium plasma-sprayed surface (TPS) and sand-blasted and acid-etched surface (SLA) implants. As clinical parameters around moderately rough implants were better than around rough implants, the authors concluded that "surface characteristics may have an impact on the clinical outcomes".[27]

A membrane over the grafting materials failed to show any additional benefit to the use of barrier materials, as no significant difference in terms of clinical or radiologic outcomes were reported between the groups in two studies.[26,31] An improved outcome of healing was observed when a collagen membrane was used in the two studies by Schwarz et al.[23,25]

Two studies[24,28] reported the efficacy of autogenous bone and bovine-derived xenograft covered with a collagen membrane for peri-implantitis treatment. The bovine xenograft provided more radiographic bone fill than autogenous bone,[24,28] and the mean bone-level gain was statistically significantly higher for the group treated with the xenograft compared with the group treated with autogenous bone.[28]

Four studies reported marginal bone loss following treatment.[27,28,31,33] Radiologic bone defect fill was reported in seven studies.[22,24,26,28,29,31,33] Bone defect fill expected after regenerative treatment was found to be 1.66 mm (±1.0) (min. 0.2 mm; max. 3.5 mm) on average, according to these data. This indicated it is possible to obtain defect fill of peri-implantitis bone defects following regenerative surgical modalities.

SYNTHESIS OF RESULTS

Nonsurgical treatment

Meta-analyses were performed only if there were studies with similar comparisons reporting the same outcome measures.

In total, there were 277 patients from 10 studies[10-15,17,18,44,45] included in the meta-analysis of PD changes using nonsurgical treatment methods. Overall, PD reduction was not found to be statistically significantly different after the treatments compared with the baseline ($P = .8093$). There was no significant heterogeneity among studies (Q = 13.5496, degrees of freedom [df] = 19, $P = .8093$; standardized mean difference [SMD] = 0.346 mm; 95% CI, 0.181 to 0.512). In conclusion, nonsurgical methods were not found to be efficient at reducing PD in peri-implantitis treatment.

Six studies were included in the meta-analysis to evaluate BOP changes using nonsurgical treatment methods.[10-13,15,45] These data included 150 patients. All of these studies' data revealed BOP statistically significantly decreased after the treatments ($P = .001$), and there was a significant heterogeneity among studies (Q = 37.0847, df = 11, $P = .001$; odds ratio = 1.567; 95% CI: 1.405 to 1.748). Thus, it could be posited that nonsurgical treatments are effective at reducing soft-tissue inflammation in peri-implantitis.

According to the data of three studies, which included a total of 59 patients,[10,13,18] a significant decrease in marginal bone level ($P = .037$) was found after nonsurgical peri-implantitis treatment. A statistically significant difference was found between the studies (Q = 11.8444, df = 5, $P = .011$; SMD = 0.157 mm; 95% CI, −0.183 to 0.496).

Forest plots of odds ratios (95% CI) for PD, BOP reduction, and bone-level changes using nonsurgical treatment methods are demonstrated in Appendixes 3 to 5.

Surgical treatment

Resective surgery

Two studies reporting on a resective surgical treatment modality presented results of marginal bone level before and after treatment and were included in the meta-analysis.[34,35] According to the data of these studies, bone level statistically significantly decreased after resective surgical treatment ($P = .021$), and there was a significant heterogeneity between the studies (Q = 13.245, df = 5, $P = .021$; SMD = −0.116 mm; 95% CI,

doi: 10.3290/j.qi.a35131

−0.433 to 0.201). A forest plot of the odds ratio (95% CI) comparing bone level using nonsurgical treatment methods is presented in Appendix 6.

Regenerative treatment

The rest of the meta-analysis calculations were made using the data from the studies that presented results of regenerative surgical treatments.

Eleven studies[21-25,27,28,30-33] with a total of 256 patients with reported PD changes before and after regenerative surgical peri-implantitis treatment were included in the meta-analysis. The results demonstrated PD statistically significantly reduced ($P < .001$), and a significant heterogeneity was found between the studies ($Q = 100.046$, $df = 17$, $P < .001$; SMD = 1.647 mm; 95% CI, 1.414 to 1.880).

Nine studies[21,23,25,27-30,32,33] (with 187 patients) were included in the meta-analysis of BOP changes after regenerative surgical treatment. BOP statistically significantly decreased ($P < .001$). There was heterogeneity among the studies ($Q = 64.5872$; $df = 14$; $P < 0.001$; SMD = 4.044 mm; 95% CI, 3.571 to 4.581).

These findings suggest surgical peri-implantitis treatment methods are effective at reducing peri-implant PD and BOP scores.

Marginal bone-level changes were evaluated and included in the meta-analysis in three studies with a total of 49 patients.[27,31,33] Marginal bone level statistically significantly decreased ($P = .0305$), with a significant heterogeneity among the studies ($Q = 10.6697$, $df = 4$, $P = .0305$).

Forest plots of the odds ratios (95% CI) for PD, BOP reduction, and bone-level changes using regenerative surgical treatments are demonstrated in Appendixes 7 to 9.

DISCUSSION

The present investigation included studies reporting the clinical and/or radiologic outcomes of different nonsurgical and surgical peri-implantitis treatment methods. An electronic search of MEDLINE (PubMed) and EMBASE databases was performed including studies published in the English language between 1 January 2002 and 1 February 2015. Additionally, a hand search was carried out in the dental implants–related journals.

Our findings suggest peri-implantitis treatment using different nonsurgical treatment modalities are of limited effectiveness. Reduction in signs of inflammation (decreased BOP index) could be expected, but the reduction of the PD and the arrestment of continuous bone loss are limited. The present meta-analyses demonstrated improved BOP values ($P = .001$) after nonsurgical treatments but did not reveal a statistically significant difference in the PD changes ($P = .8093$), and a significant reduction in marginal bone level ($P = .037$) after nonsurgical treatment was noted.

These findings correspond to the Third European Association for Osseointegration (EAO) Consensus Conference (2012) statement, which claims peri-implantitis does not respond to nonsurgical therapy and, thus, surgical treatment should be considered.[46] Even access flap surgery[19,20] and resective techniques[34-36] were effective in reducing PD and BOP values;[19,20,34] however, marginal bone loss occurred. Our meta-analyses used the data reported in two studies and confirmed there was a significant reduction in bone level after resective surgical treatment ($P = .0212$).[34,36]

As the majority of the studies reporting on regenerative surgical treatment demonstrated significant improvement in PD and BOP values as well as an intrabony defect fill,[22,25,28-31,33] we suggest a regenerative approach should be the treatment of choice. The present meta-analyses confirmed a significant reduction in PD ($P < .001$) and decreased BOP ($P < .001$). Nevertheless, according to the data of three studies included in the meta-analysis of marginal bone-level changes after regenerative surgical treatment, a significant reduction in marginal bone could be expected as well after the treatment ($P = .0305$).[27,31,33]

The results of the present review are in agreement with the systematic review by Chan et al[47] that aimed to investigate the efficacy of different surgical approaches, including access flap debridement, surgical resection, application of bone-grafting materials and guided bone regeneration (GBR), to treat peri-implanti-

tis. The authors found the application of grafting materials and barrier membranes resulted in a greater PD reduction and radiologic bone fill, but there was a lack of high-quality comparative studies to support this statement.[47] Similar conclusions were made in a review by Mombelli et al,[48] who reviewed the literature on the surgical treatment of peri-implantitis and came to the conclusion that currently available evidence does not provide any firm, specific recommendations for the surgical therapy of peri-implantitis; however, the stabilization of the defect with a bone substitute may be advantageous.[48]

More controversial results were found in the review by Khoshkam et al,[49] which stated currently there is a lack of evidence to support the additional benefit of reconstructive procedures compared to other treatment modalities for managing peri-implantitis.

It is evident that successful peri-implant lesion treatment is a comprehensive procedure. Thus, summarizing literature data and their own experience, the authors recommend a complex peri-implantitis management and maintenance approach consisting of several steps.

Surgical treatment should be performed only when the soft tissues are free of inflammation. This is essential during the surgical phase to ensure proper management of the wound. As concluded in the review above, nonsurgical subgingival mechanical debridement in conjunction with local antibacterials, like chlorhexidine digluconate or locally delivered antibiotics, are effective in reducing soft-tissue inflammation[12,13,15] and should be the first step in successful treatment (Figs 2 and 3).

The results of the study by Serino and Ström[50] indicated proper oral hygiene at the implant sites seems to be related to the presence or absence of peri-implantitis.[50] Oral hygiene instructions and the importance of plaque control must be stressed to patients before and after the treatment.

After soft tissue health has been achieved and patient's oral hygiene improved, the treatment could be continued with the surgical step. Surgical therapy should at least include removal of the granulation tissues and a thorough cleaning of the contaminated surface.[46] Therefore, access flap surgery that ensures thorough debridement of the defect should be performed (Fig 4a). Carbon fiber and/or titanium curettes are recommended because they have been shown to cause minimal damage to implant surfaces.[51]

Decontamination of the implant surface is considered mandatory for the successful treatment of peri-implantitis. The goal of such decontamination is to eliminate bacteria and render the surface conducive to bone regeneration and re-osseointegration.[52] Different decontamination methods, including chemical, mechanical, and laser decontaminations were suggested.[53] Combined mechanical and chemical removal of biofilm from the implant surface is recommended.[53] According to the in-vitro study, airflow devices using glycine powders were shown to constitute an efficient therapeutic option for the debridement of implants in peri-implantitis defects.[54] Chlorhexidine digluconate (0.2%) and ethylenediaminetetraacetic acid (EDTA; 24%) demonstrated a great decontamination capacity with respect to both the killing and the removal of biofilm cells.[55] Therefore, we suggest to use three-step implant surface decontamination: air-powder polishing with glycine powders, application of EDTA (24%), and irrigation with chlorhexidine gluconate (0.12%) (Fig 4b).

According to the results of the present review, the regenerative approach should be a treatment option in peri-implantitis cases. We would recommend use of bioactive materials to obtain optimal treatment results. Leucocyte- and platelet-rich fibrin (L-PRF), first described by Choukroun et al,[56] is a second-generation platelet concentrate that consists predominantly of a fibrin matrix rich in platelet and leukocyte cytokines such as interleukin 1β (IL-1β), IL-4, and IL-6, and growth factors such as vascular endothelial growth factor (VEGF), platelet-derived growth factor (PDGF), and transforming growth factor β (TGF-β).[56-58] Studies have demonstrated that fibrin matrix is able to enmesh leukocytes, platelets, and their growth factors and has a slow sustained release of key growth factors for 7 to 28 days,[59-61] which means that the L-PRF stimulates its environment for a significant time during wound heal-

doi: 10.3290/j.qi.a35131

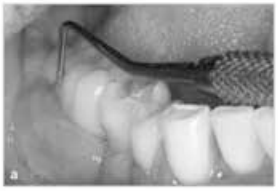

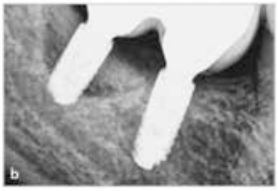

Figs 2a and 2b Pretreatment intraoral *(a)* and radiographic *(b)* view.

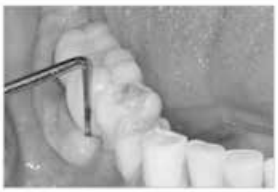

Fig 3 Four weeks after conservative treatment (Step I); signs of inflammation were reduced significantly.

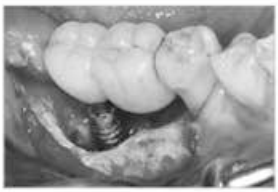

Fig 4a Reflection of a full-thickness flap and removal of granulation tissues (Step III).

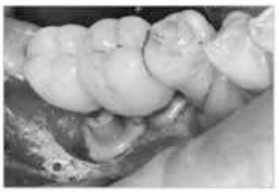

Fig 4b The first step of decontamination: application of EDTA acid for 2 minutes (Step IV).

ing. Various matrix components found in L-PRF (fibronectin, vibronectin, glycosaminoglycans, and fibrin itself) and enmeshed growth factors accelerate angiogenesis, and stimulate quicker proliferation and differentiation of the osteoblasts and mesenchymal stem cells; therefore L-PRF functions as a complex active regenerative bioscaffold for vascularization, promoting both alveolar bone and surrounding soft tissue regeneration.[57,62]

L-PRF clots may be also compressed into membranes in the PRF and growth-factor-rich fibrin (GRF) box.[63] In contrast to traditional guided-tissue regeneration (GTR) membranes, L-PRF membranes allow vascularization from highly vascularized periosteum and do not block migration of osteogenic cells from the periosteum to the defect; thus the periosteum is not excluded from bone defect healing. Besides, growth factors found within L-PRF may stimulate periosteum and contribute to periosteal bone healing.[57,58]

Although L-PRF is a bioactive material and has been shown to accelerate bone healing and promote bone graft maturation,[59,64] it has weak osteoconductive properties. Demineralized freeze-dried bone allograft (DFDBA) is suggested to be used as the osteoconductive component of the composite graft. DFDBA was not only shown to be osteoconductive, but also to exhibit potential in stimulating an osteoinductive response and allowing for improved bone growth and fusion.[65] DFDBA was also shown to provide faster particle incorporation and greater vital bone formation compared to common mineralized freeze-dried bone allografts (FDBAs) and xenografts, which is important for promoting rapid bone regeneration around titanium dental implants.[66,67]

The third component of the composite graft, gentamicin, is suggested to be used for DFDBA particle rehydration, to boost the antibacterial effects of the graft and prevent grafted site contamination. Van Winkelhoff[68] stated that local antibiotic delivery in addition to mechanical debridement and irrigation with an antimicrobial agent may be an effective option for treating peri-implantitis lesions. Gentamicin is a broad-spectrum aminoglycoside bactericidal antibiotic that acts against a wide variety of both Gram-positive and Gram-negative bacteria. Gentamicin-impregnated allogeneic demineralized bone matrix was shown to release clinically relevant levels of the drug for at least 13 days in vitro, allowing for the inhibition of bacterial

doi: 10.3290/j.qi.a35131

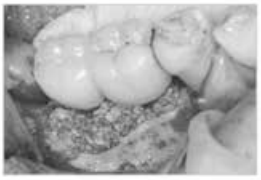

Fig 5a Intrabony defect filled with processed human allograft mixed with autologous platelet-rich fibrin (L-PRF) (Step V).

Fig 5b The graft was covered using a double layer of autologous L-PRF membranes on the buccal, interproximal, and lingual aspects (Step V).

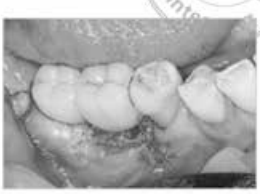

Fig 5c The flap sutured with resorbable sutures (Step V).

growth in the graft. Gentamicin was also shown to have an antibacterial effect on *Staphylococcus aureus* and *Staphylococcus epidermidis*, which are frequently associated with implant-related bone infections.[69] Stavropoulos et al[70] found that impregnation of grafting biomaterial with gentamicin before implantation tended to improve healing outcomes after GBR. Additionally, in a previous study by Holck et al,[71] gentamicin-enhanced bone grafts were shown to present significantly more vascular ingrowth compared with untreated controls after 2 weeks.

Therefore, we would recommend to fill the intrabony defect with composite L-PRF, DFDBA, and gentamicin (gentamicin sulfate 2 mg/mL) graft and cover it using a double layer of autologous L-PRF membranes (Fig 5).

The last step of peri-implantitis treatment should be the maintenance. The necessity for regular maintenance after peri-implantitis treatment was well illustrated in a study by Serino et al.[72] Their results demonstrated that in patients with a high standard of oral hygiene and enrolled in a recall system every 6 months, the peri-implant conditions obtained following peri-implant surgery were maintained stable for the majority of subjects and implants during a 5-year period (Figs 6 to 8).

Taking into account the present review results and our own clinical experience, we suggest the following novel complex management and maintenance (CMM) six-step protocol for the treatment of peri-implantitis. The CMM protocol includes all consecutive steps of required nonsurgical and regenerative surgical treatments: conservative treatment including proper oral hygiene institution, debridement, triple decontamination protocol, and regeneration of the bone defect utilizing a bioactive composite graft (Table 2).

LIMITATIONS

This systematic review was not limited to only randomized, controlled clinical studies. The included studies were of relatively short follow-up period and included relatively small numbers of patients. There were various degrees of heterogeneity in the study design and treatment provided among the pooled studies. The absence of a control group (no treatment or placebo) was also a limitation. The current review used two databases and only included studies written in English, which could introduce a publication bias.

All of the studies included in this review revealed an unclear or high risk of bias. According to the Cochrane Collaboration's tool for assessing risk of bias,[40] the proportion of information from studies with unclear or high risk of bias is sufficient to affect the interpretation of results. Therefore, the strength of evidence of this review is low because of the risk of bias and the significant variations observed in the included studies.

CONCLUSION

The present systematic review and meta-analyses revealed peri-implantitis treatments using different

doi: 10.3290/j.qi.a35131

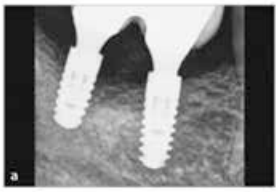

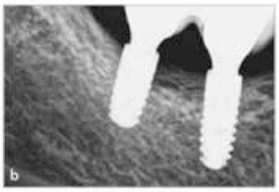

Figs 6a and 6b Periapical radiograph taken 6 *(a)* and 24 *(b)* months after surgery. Nearly complete intrabony defect fill.

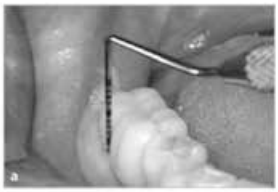

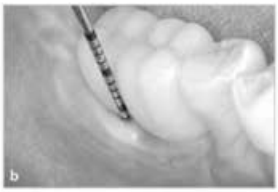

Figs 7a and 7b Probing 6 *(a)* and 24 months *(b)* after surgery reveals PD of 3.5 mm on the mesial buccal aspect (Step VI).

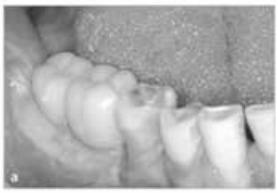

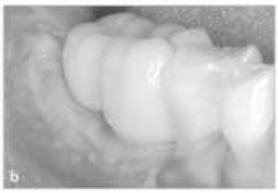

Figs 8a and 8b Healthy mucosa around the implant can be noted during 6 *(a)* and 24 *(b)* months after the surgery (Step VI).

Table 2 A complex management and maintenance (CMM) protocol for the treatment of peri-implantitis

Treatment step (I, II conservative; III–VI surgical)	Peri-implantitis management procedures
Step I: Subgingival debridement and local antimicrobial treatment	Subgingival mechanical debridement and local antimicrobial treatment
Step II: Proper oral hygiene institution	Oral hygiene training and control after 4 weeks
Step III: Open flap debridement	Open flap debridement using titanium or carbon fiber curettes to protect implant surface
Step IV: Triple decontamination	Implant surface decontamination: *(a)* Air polishing with glycine powder for 60 s; *(b)* Application of 24% EDTA for 2 mins; *(c)* 60 s continuous irrigation with chlorhexidine gluconate solution (0.12%)
Step V: Bone defect regeneration	Leukocyte- and platelet-rich fibrin (L-PRF) clot and membranes preparation: 2,800 rpm, 12 mins centrifugation. Bone defect regeneration with composite L-PRF, demineralized freeze-dried bone allograft (DFDBA), and gentamicin (gentamicin sulfate 2 mg/mL) graft
Step VI: Maintenance treatment	Follow-up and oral hygiene control every 3 months in the first year and every 6 months thereafter

nonsurgical modalities are of limited effectiveness. As the majority of the studies reporting on regenerative surgical treatments demonstrated significant improvement in clinical parameters and intrabony defect fill, we suggest a regenerative approach should be the treatment of choice. However, our meta-analyses confirmed there was a significant reduction in radiologic peri-implant marginal bone level using either treatment approach. Therefore, the novel peri-implantitis CMM six-step protocol was proposed based on all consecutive

and most effective steps of nonsurgical and regenerative surgical treatments: conservative treatment including proper oral hygiene institution, debridement, triple decontamination protocol, and regeneration of the bone defect utilizing a bioactive composite graft. A six-step protocol aimed at managing patients with peri-implantitis could be a useful tool in peri-implantitis treatment. However, more randomized controlled trials with follow-ups of several years and large sample sizes are needed to determine the best treatment to control peri-implantitis. Further clinical studies should be conducted for new peri-implantitis complex management and maintenance protocol efficacy evaluation.

REFERENCES

1. Lang NP, Berglundh T, Heitz-Mayfield LJ, et al. Consensus statements and recommended clinical procedures regarding implant survival and complications. Int J Oral Maxillofac Implants 2004;19:150–154.
2. Pjetursson BE, Tan K, Lang NP, et al. A systematic review of the survival and complication rates of fixed partial dentures (FPDs) after an observation period of at least 5 years. Clin Oral Implants Res 2004;15:667–676.
3. American Academy of Periodontology. Academy report: Peri-Implant Mucositis and Peri-Implantitis: a current understanding of their diagnoses and clinical implications. J Periodontol 2013;84:436–443.
4. Berglundh T, Persson L, Klinge B. A systematic review of the incidence of biological and technical complications in implant dentistry reported in prospective longitudinal studies of at least 5 years. J ClinPeriodontol 2002;29(Suppl 3): 197–212.
5. Fransson C, Wennström L, Berghlundh T. Clinical characteristics at implants with a history of progressive bone loss. Clin Oral Implants Res 2008;19: 142–147.
6. Atieh MA, Alsabeeha NH, Faggion CM Jr, Duncan WJ. The frequency of peri-implant diseases: a systematic review and meta-analysis. J Periodontol 2013;84:1586–1598.
7. Fransson C, Thomasi C, Pikner SS, et al. Severity and pattern of peri-implantitis-associated bone loss. J Clin Periodontol 2010;37:442–448.
8. Lang NP, Berghlundh T; Working Group 4 of Seventh European Workshop on Periodontology. Peri-implant diseases: where are we now? Consensus of the Seventh European Workshop on Periodontology. J Clin Periodontol 2011;38: 178–181.
9. Isidor F. Loss of osseointegration caused by occlusal load of oral implants. A clinical and radiographic study in monkeys. Clin Oral Implants Res 1996;7: 143–152.
10. Karring ES, Stavropoulos A, Ellegaard B, et al. Tretament of peri-implantitis by the Vector system. Clin Oral Implants Res 2005;16:288–293.
11. Schwarz F, Sculean A, Rothamel D, et al. Clinical evaluation of an Er:YAG laser for nonsurgical treatment of peri-implantitis: a pilot study. Clin Oral Implants Res 2005;16:44–52.
12. Renvert S, Lessem J, Dahlen G, et al. Topical minocycline microspheres versus topical chlorhexidine gel as an adjunct to mechanical debridement of incipient peri-implant infections: a randomized clinical trial. J Clin Periodontol 2006;33:362–369.
13. Renvert S, Lessem J, Dahlen G, et al. Mechanical and repeated antimicrobial therapy using local drug delivery system in the treatment of peri-implantitis: a randomized clinical trial. J Periodontol 2008;79:836–844.
14. Renvert S, Samuelsson E, Lindahl C, et al. Mechanical non-surgical treatment of peri-implantitis: a double blind randomized longitudinal clinical study. I: clinical results. J Clin Periodontol 2009;36:604–609.
15. Sahm N, Becker J, Santel T, et al. Non-surgical treatment of peri-implantitis using an air-abrasive or mechanical debridement and local application of chlorhexidine: a prospective, randomized, controlled clinical trial. J Clin Periodontol 2011;38:872–878.
16. Renvert S, Lindahl C, Roos-Jansaker AM. Treatment of peri-implantitis using an Er:YAG laser or an abrasive device: a randomized clinical trial. J Clin Periodontol 2011;38:65–73.
17. Schär D, Ramseier CA, Eick S, et al. Anti-infective therapy of peri-implantitis with adjunctive local drug delivery or photodynamic therapy: six-month outcomes of a randomized controlled clinical trial. Clin Oral Implants Res 2013;24:104–110.
18. Deppe H, Mücke T, Wagenpfeil S, et al. Nonsurgical antimicrobial photodynamic therapy in moderate vs severe peri-implant defects: a clinical pilot study. Quintessence Int 2013;44:609–618.
19. Heitz-Mayfield LJA, Salvi GE, Mombelli A, et al. Anti-infective surgical therapy of peri-implantitis. A 12-month prospective clinical study. Clin Oral Implants Res 2012;23:205–210.
20. Papadopoulos CA, Vouros I, Menexes G, Konstantinidis A. The utilization of a diode laser in the surgical treatment of peri-implantitis. A randomized clinical trial. Clin Oral Investig 2015;19:1851–1860.
21. Schwarz F, Bieling K, Latz T, et al. Healing of intrabony peri-implantitis defects following application of a nanocrystalline hydroxyapatite (Ostim) or a bovine-derived xenograft (Bio-Oss) in combination with a collagen membrane (Bio-Guide). A case series. J Clin Periodontol 2006;33:491–499.
22. Roos-Jansåker AM, Renvert H, Lindahl C, et al. Submerged healing following surgical treatment of peri-implantitis: a case series. J Clin Periodontol 2007;34: 723–727.
23. Schwarz F, Sculean A, Bieling K, et al. Two year clinical results following treatment of peri-implantitis lesions using a nanocrystalline hydroxyapatite or a natural bone mineral in combination with collagen membrane. J Clin Periodontol 2008;35:80–87.
24. Romanos GE, Nentwig GH. Regenerative therapy of deep peri-implant infrabony defects after CO_2 laser implant surface decontamination. Int J Periodontics Restorative Dent 2008;28:245–255.
25. Schwarz F, Sahm N, Bieling K, et al. Surgical regenerative treatment of peri-implantitis lesions using a nanocrystalline hydroxyapatite or a natural bone mineral in combination with a collagen membrane: a four year clinical follow-up report. J Clin Periodontol 2009;36:807–814.
26. Roos-Jansåker AM, Lindahl C, Persson GR, et al. Long term stability of surgical bone regenerative procedures of peri-implantitis lesions in a prospective case-control study over 3 years. J Clin Periodontol 2011;38:590–597.
27. Roccuzzo M, Bonino F, Bonino L, Dalmasso P. Surgical therapy of peri-implantitis lesions by means of a bovine-derived xenograft: comparative results of a prospective study on two different implant surfaces. J Clin Periodontol 2011;38:738–745.
28. Aghazadeh A, Rutger Persson G, Renvert S. A single-centre randomized controlled clinical trial on the adjunct treatment of intra-bony defects with autogenous bone or a xenograft: results after 12 months. J Clin Periodontol 2012;39:666–673.
29. Wiltfang J, Zernial O, Behrens E, et al. Regenerative treatment of peri-implantitis bone defects with a combination of autologous bone and a demineralized xenogenic bone graft. A series of 36 defects. Clin Implant Dent Relat Res 2012;14:421–427.
30. Schwarz F, Hegewald A, John G, Sahm N, Becker J. Four-year follow-up of combined surgical therapy of advanced peri-implantitis evaluating two methods of surface decontamination. J Clin Periodontol 2013;40:962–967.
31. Roos-Jansåker AM, Persson GR, Lindahl C, Renvert S. Surgical treatment of peri-implantitis using a bone substitute with or without a resorbable membrane: a 5-year follow-up. J Clin Periodontol 2014;41:1108–1114.
32. Schwarz F, Sahm N, Becker J. Combined surgical therapy of advanced peri-implantitis lesions with concomitant soft tissue volume augmentation. A case series. Clin Oral Implants Res 2014;25:132–136.

doi: 10.3290/j.qi.a35131

33. Matarasso S, Iorio Siciliano V, Aglietta M, Andreuccetti G, Salvi GE. Clinical and radiographic outcomes of a combined resective and regenerative approach in the treatment of peri-implantitis: a prospective case series. Clin Oral Implants Res 2014;25:761–767.
34. de Waal YC, Raghoebar GM, Huddleston Slater JJ, Meijer HJ, Winkel EG, van Winkelhoff AJ. Implant decontamination during surgical peri-implantitis treatment: a randomized, double-blind, placebo-controlled trial. J Clin Periodontol 2013;40:186–195.
35. Romeo E, Ghisolfi M, Murgolo N, et al. Therapy of peri-implantitis with resective surgery. A 3-year clinical trial on rough screw-shaped oral implants. Part I: clinical outcome. Clin Oral Implants Res 2005;16:9–18.
36. Romeo E, Lops D, Chiapasco M, et al. Therapy of peri-implantitis with resective surgery. A 3-year clinical trial on rough screw-shape oral implants. Part II: radiographic outcome. Clin Oral Implants Res 2007;18:179–187.
37. Mombelli A. Criteria for success. Monitoring. In: Lang NP, Karring T (eds). Proceedings of the 1st European Workshop on Periodontology. London: Quintessence Publishing, 1994:317–325.
38. Faggion CM,Jr, Listl S, Tu YK. Assessment of endpoints in studies on peri-implantitis treatment: A systematic review. J Dent 2010;38:443–450.
39. Moher D, Liberati A, Tetzlaff J, Altman DG; PRISMA Group. Preferred reporting items for systematic reviews and meta-analyses: the PRISMA statement. J Clin Epidemiol 2009;62:1006–1012.
40. Higgins JPT, Green S. Cochrane Handbook for Systematic Reviews of Interventions. Available at: http://www.cochrane.org/cochrane-interventions-handbook. Accessed 24 September 2015.
41. DerSimonian R, Kacker R. Random-effects model for meta-analysis of clinical trials: an update. Contemp Clin Trials 2007;28:105–114.
42. Landis JR, Koch GG. The measurement of observer agreement for categorical data. Biometrics 1977;33:159–174.
43. Serino G, Turri A. Outcome of surgical treatment of peri-implantitis: results from a 2-year prospective clinical study in humans. Clin Oral Implants Res 2011;22:1214–1220.
44. Bassetti M, Schär D, Wicki B, et al. Anti-infective therapy of peri-implantitis with adjunctive local drug delivery or photodynamic therapy: 12-month outcomes of a randomized controlled clinical trial. Clin Oral Implants Res 2014;25:279–297.
45. John G, Sahm N, Becker J, Schwarz F. Nonsurgical treatment of peri-implantitis using an air-abrasive device or mechanical debridement and local application of chlorhexidine. Twelve-month follow-up of a prospective, randomized, controlled clinical study. Clin Oral Investig 2015;19:1807–1814.
46. Klinge B, Meyle J, Working Group 2. Peri-implant tissue destruction. The Third EAO Concensus Conference 2012. Clin Oral Implants Res 2012;23:108–110.
47. Chan HL, Lin GH, Suarez F, MacEachern M, Wang HL. Surgical management of peri-implantitis: a systematic review and meta-analysis of treatment outcomes. J Periodontol 2014;85:1027–1041.
48. Mombelli A, Moëne R, Décaillet F. Surgical treatments of peri-implantitis. Eur J Oral Implantol 2012;5(Suppl):S61–S70.
49. Khoshkam V, Chan HL, Lin GH, et al. Reconstructive procedures for treating peri-implantitis: a systematic review. J Dent Res 2013;92(Suppl 12):1315–1385.
50. Serino G, Ström C. Peri-implantitis in partially edentulous patients: association with inadequate plaque control. Clin Oral Implants Res 2009;20:169–174.
51. Louropoulou A, Slot DE, Van der Weijden FA. Titanium surface alterations following the use of different mechanical instruments: a systematic review. Clin Oral Implants Res 2012;23:643–658.
52. Mombelli A. Microbiology and antimicrobial therapy of peri-implantitis. Periodontology 2000;28:177–189.
53. Mellado-Valero A, Buitrago-Vera P, Solá-Ruiz MF, Ferrer-García JC. Decontamination of dental implant surface in peri-implantitis treatment: a literature review. Med Oral Patol Oral Cir Bucal 2013;18:e869–e876.
54. Sahrmann P, Ronay V, Sener B, Jung RE, Attin T, Schmidlin PR. Cleaning potential of glycine air-flow application in an in vitro peri-implantitis model. Clin Oral Implants Res 2013;24:666–670.
55. Ntrouka V, Hoogenkamp M, Zaura E, van der Weijden F. The effect of chemotherapeutic agents on titanium-adherent biofilms. Clin Oral Implants Res 2011;22:1227–1234.
56. Choukroun J, Adda F, Schoeffler C, et al. Une opportunite en paro-implantologie: le PRF. Implantodontie 2001;42:55–62.
57. Del Corso M, Vervelle A, Simonpieri A, et al. Current knowledge and perspectives for the use of platelet-rich plasma (PRP) and platelet-rich fibrin (PRF) in oral and maxillofacial surgery part 1: periodontal and dentoalveolar surgery. Curr Pharm Biotechnol 2012;13:1207–1230.
58. Simonpieri A, Del Corso M, Vervelle A, et al. Current knowledge and perspectives for the use of platelet-rich plasma (PRP) and platelet-rich fibrin (PRF) in oral and maxillofacial surgery part 2: Bone graft, implant and reconstructive surgery. Curr Pharm Biotechnol 2012;13:1231–1256.
59. Choukroun J, Diss A, Simonpieri A, et al. Platelet-rich fibrin (PRF): a second generation platelet concentrate. Part V: histologic evaluations of PRF effects on bone allograft maturation in sinus sift. Oral Surg Oral Med Oral Pathol Oral Radiol Endod 2006;101:299–303.
60. He L, Lin Y, Hu X, et al. A comparative study of platelet-rich fibrin (PRF) and platelet-rich plasma (PRP) on the effect of proliferation and differentiation of rat osteoblasts in vitro. Oral Surg Oral Med Oral Pathol Oral Radiol Endod 2009;108:707–713.
61. Schär MO, Diaz-Romero J, Kohl S, et al. Platelet-rich concentrates differentially release growth factors and induce cell migration in vitro. Clin Orthop Relat Res 2015;473:1635–1643.
62. Kang YH, Jeon SH, Park JY, et al. Platelet-rich fibrin is a bioscaffold and reservoir of growth factors for tissue regeneration. Tissue Eng Part A 2011;17:349–359.
63. Dohan Ehrenfest DM. How to optimize the preparation of leukocyte- and platelet-rich fibrin (L-PRF, Choukroun's technique) clots and membranes: introducing the PRF box. Oral Surg Oral Med Oral Pathol Oral Radiol Endod 2010;110:275–278.
64. Xuan F, Lee CU, Son JS, Jeong SM, Choi BH. A comparative study of the regenerative effect of sinus bone grafting with platelet-rich fibrin-mixed Bio-Oss® and commercial fibrin-mixed Bio-Oss®: An experimental study. J Craniomaxillofac Surg 2014;42:e47–e50.
65. Chemsel KD, Branger J, Wertheim H, Scarborough N. Healing response to various forms of human demineralised bone matrix in athymic rat cranial defects. J Oral Maxillofac Surg 1998;56:857–863.
66. Wood RA, Mealey BL. Histologic comparison of healing after tooth extraction with ridge preservation using mineralized versus demineralized freeze-dried bone allograft. J Periodontol 2012;83:329–336.
67. Yang S, Lan L, Miron RJ, et al. Variability in particle degradation of four commonly employed dental bone grafts. Clin Implant Dent Relat Res 2015;17:996–1003.
68. van Winkelhoff AJ. Antibiotics in the treatment of peri-implantitis. Eur J Oral Implantol 2012;5(Suppl):S43–S50.
69. Lewis CS, Supronowicz PR, Zhukauskas RM, et al. Local antibiotic delivery with demineralised bone matrix. Cell Tissue Bank 2012;13:119–127.
70. Stavropoulos A, Karrings ES, Kostopoulos L, Karring T. Deproteinized bovine bone and gentamicin as an adjunct to GTR in the treatment of intrabony defects: a randomized controlled clinical study. J Clin Periodontol 2003;30:486–495.
71. Holck DE, Dutton JJ, Proia A, et al. Rate of vascularization of coralline hydroxyapatite spherical implants pretreated with saline/gentamicin, rTGF-beta 2, and autogenous plasma. Ophthal Plast Reconstr Surg 1998;14:73–80.
72. Serino G, Turri A, Lang NP. Maintenance therapy in patients following the surgical treatment of peri-implantitis: a 5-year follow-up study. Clin Oral Implants Res 2015;26:950–956.

Appendix 1 Nonsurgical treatments for peri-implantitis

Study (year)	Type of study	Treatment method used	Sample size	Follow-up (months)	PD* changes (mm; mean ± SD)
Karring et al[10] (2005)[10,11]	Pilot study	Group 1: ultrasonic device (Vector system); Group 2: mechanical debridement with carbon fiber curettes	11 (each exhibiting 2 implants with peri-implantitis)	6	Group 1: baseline 5.8 ± 1.1; after 6 months 5.8 ± 1.2; Group 2: baseline 6.2 ± 1.6; after 6 months 6.3 ± 2.2; In both treatment groups, PD did not change between baseline and 6 months.
Schwarz et al[11] (2005)[14]	Pilot study	Group 1: Er:YAG laser (ERL); Group 2: mechanical debridement using plastic curettes and antiseptic therapy with chlorhexidine digluconate (0.2%)	20 (Group 1: 10; Group 2: 10)	6	Group 1: baseline 5.4 ± 1.2; after 6 months 4.6 ± 1.1 ($P < .01$); Group 2: baseline 5.5 ± 1.5; after 6 months 4.9 ± 1.4 ($P < .01$); No statistically significant differences between the two groups ($P > .01$)
Renvert et al[12] (2006)[19]	Randomized clinical study	Subgingival antimicrobial treatment using: Group 1: minocycline microspheres; Group 2: chlorhexidine gel	30 (Group 1: 14; Group 2: 16)	12	Group 1: baseline 1: 3.9 ± 0.7; at 12 months 3.6 ± 0.6; Group 2: baseline 3.9 ± 0.3; at 12 months 3.9 ± 0.4; No significant differences between the groups ($P > .01$)
Renvert et al[13] (2008)[19]	Randomized clinical study	Group 1: mechanical debridement with local minocycline microspheres; Group 2: chlorhexidine gel treatments were performed on three occasions: baseline and days 30 and 90	32 (Group 1: 17; Group 2: 15)	12	Group 1: 3.85 ± 1.04; at 12 months 3.55 ± 0.98; Group 2: baseline 3.87 ± 1.16; at 12 months 3.72 ± 1.02; No difference between the groups ($P > .01$)
Renvert et al[14] (2009)[5]	Randomized longitudinal clinical study	Group 1: mechanical debridement with titanium hand-instruments; Group 2: mechanical debridement with an ultrasonic device	31 (Group 1: 17; Group 2: 14)	6	Group 1: 4.0 ± 0.8; at 6 months 4.0 ± 0.8; Group 2: baseline 4.3 ± 0.6; at 6 months 3.9 ± 0.8
Sahm et al[15] (2011)[16]	Randomized controlled clinical study	Group 1: amino acid glycine powder (AAD); Group 2: mechanical debridement using carbon curettes and antiseptic therapy with chlorhexidine digluconate	32 (Group 1: 16; Group 2: 16)	6	Group 1: baseline 3.8 ± 0.8; at 6 months 3.2 ± 0.9; difference 0.6 ± 0.6; Group 2: baseline 4.0 ± 0.8; at 6 months 3.9 ± 0.8; difference 0.5 ± 0.6; No significant difference in PD reductions between the groups ($P > .05$)
Renvert et al[16] (2011)	Randomized clinical study	Group 1: Er:YAG laser; Group 2: air-borne-particle abrasion device	42 (Group 1: 21; Group 2: 21)	6	PD reduction in group 1: 0.8 ± 0.5; group 2: 0.9 ± 0.8; ($P = .55$)
Schär et al[17] (2013)[3]	Randomized clinical study	All implants underwent mechanical debridement with titanium curettes followed by a glycine-based powder air polishing. Group 1 (test): Implants received adjunctive PDT. Group 2: Minocycline microspheres were locally delivered into the peri-implant pockets.	40 (Group 1: 20; Group 2: 20)	6	Group 1: baseline 4.19 ± 0.55; after 6 months 3.83 ± 0.58 mm; Group 2: baseline 4.39 ± 0.77; after 6 months 3.90 ± 0.78; Statistically significant reduction from the baseline ($P < .05$) in both groups. No statistically significant difference between the groups ($P > .05$)
Deppe et al[18] (2013)[19]	Pilot study	PDT without surgical intervention; Group 1: moderate bone loss (< 5 mm); Group 2: implants with severe defects (5–8 mm)	16 patients, 18 implants; Group 1: 10 implants; Group 2: 8 implants	6	Group 1: baseline 3.3 ± 0.8; after 6 months 2.9 ± 0.5 (t value = −2.4); Group 2: baseline 5.8 ± 0.8; after 6 months 6.5 ± 0.9 (t value = 2.05)

continued on next page

doi: 10.3290/j.qi.a35131

BOP+ changes (%; mean ± SD)	Radiologic marginal bone-level changes/bone defect fill	Comments
Group 1: baseline 63.6; after 6 months 36.4; Group 2: baseline 72.7; after 6 months 81.8; BOP was reduced in group 1, when compared with baseline, while it was increased in group 2 ($P > .1$).	Bone-level changes: Group 1 at baseline 6.8 ± 1.7 mm; after 6 months 7.1 ± 1.9 mm; difference −0.3 ± 1 mm; Group 2: at baseline 7.4 ± 2.1 mm; at 6 months 7.7 ± 2.6 mm; difference −0.3 ± 0.8 mm; Intrabony component changes: Group 1: baseline 4.1 ± 2.2 mm; after 6 months 4.5 ± 2.2 mm; difference −0.4 ± 0.8 mm; Group 2: at baseline 4 ± 1.5 mm; after 6 months 4.1 ± 1.5 mm; difference −0.1 ± 0.4 mm. No statistically significant differences between baseline and the 6-month control either within each treatment group or between treatments	No significant difference between ultrasonic device and mechanical subgingival debridement in terms of clinical and radiologic changes.
BOP reduction: group 1 at baseline 83; after 6 months 31 ($P < .01$); Group 2: baseline 80; after 6 months 58 ($P < .01$). Statistically significantly greater reduction in group 1($P < .01$)		Significantly greater reduction in BOP in the Er:YAG treatment group compared with mechanical submucosal debridement.
Group 1: baseline 88 ± 12, after 12 months 71 ± 22; Group 2: baseline 86 ± 14; after 12 months 78 ± 13. Significantly greater BOP reduction in group 1 ($P < .01$)		Adjunctive local delivery of minocycline microspheres resulted in significantly lower BOP scores when compared with submucosal debridement alone.
Group 1: baseline 86.5 ± 20.1; after 12 months 48.1 ± 20.7; Group 2: baseline 89.2 ± 17.2; after 12 months 63.5 ± 19.2; Significantly greater reduction in group 1 ($P < .01$)	Bone level changes: Group 1: baseline 0.77 ± 0.85 mm; after 12 months 0.7 ± 0.84 mm; Group 2: baseline: 0.41 ± 0.7 mm; after 12 months 0.46 ± 0.76 mm; No statistical differences in radiographic bone levels were found	The use of a repeated local antibiotic as an adjunct to the mechanical treatment of peri-implantitis lesions demonstrated improvements in PD that were significantly different from controls.
Mean bleeding at implant: Group 1: baseline 1.7 ± 0.9; after 6 months 1.4 ± 1.0; Group 2: baseline 1.7 ± 0.6; after 6 months 1.2 ± 0.7		No group differences were found in the treatment outcomes.
Group 1: baseline 94.6 ± 15.8; after 6 months 51.1 ± 24.7; difference 43.5 ± 27.7; Group 2: baseline 95.3 ± 9.6 after 6 months 84.3 ± 15.5; difference 11.0 ± 15.7; Significantly higher ($P < .05$) reduction in group 1		Subgingival air polishing resulted in significantly lower BOP scores compared to mechanical debridement with chlorhexidine digluconate.
BOP decreased in both the groups ($P < .01$) compared to baseline, but there was no difference between the groups ($P = .22$)	Bone-level decrease was diagnosed in 39% of implants in group 1 and 41.5% of implants in group 2. No bone changes occurred in 2.1% of the implants in group 1 and 2.4% of the implants in group 2. Increases in bone level ranging from 2.1 up to 3 mm occurred in 6.3% of the implants in group 1, none in group 2; 0.1–1 mm increase in 52% of implants in group 1, 56% in group 2. No difference between the groups ($P = .42$)	Clinical parameters (eg, BOP and PD) improved in both treatment groups without significant differences between the groups.
Decrease in BOP positive sites: Group 1: baseline 4.03 ± 1.66, after 6 months 1.51 ± 1.41 ($P < 0.05$); Group 2: baseline 4.41 ± 1.47; after 6 months 2.10 ± 1.55 ($P < .05$). No statistically significant difference ($P > .05$) between groups		Nonsurgical mechanical debridement with adjunctive use of PDT is equally effective in the reduction of BOP and PD as with the adjunctive use of minocycline microspheres.
Comparable sulcus bleeding index in the two groups; no difference between the baseline and 6 months	Distance from implant shoulder to bone: Group 1: baseline 3.9 ± 0.8 mm; after 6 months 3.6 ± 0.8 mm (t value = −1.125); Group 2: baseline 8.7 ± 0.7 mm; after 6 months 6.8 ± 0.8 mm (t value = −6.27)	Nonsurgical treatment with PDT could stop bone resorption in moderate peri-implant defects but not in severe defects.

continued on next page

continuation from previous page

Bassetti et al[44] (2014)[†]	Randomized controlled clinical study	All implants were mechanically debrided with titanium curettes and with a glycine-based powder air-polishing system. Group 1 (test): Implants received adjunctive PDT. Group 2 (control): Minocycline microspheres were locally delivered into the peri-implant pockets of control implants	40 (Group 1: 20; Group 2: 20)	12	Group 1: baseline 4.39 ± 0.77; after 12 months 3.83 ± 0.85; Group 2: baseline 4.19 ± 0.55; after 9 months 3.89 ± 0.68. A statistically significant decrease in PD from baseline was observed in group 1 after 12 months and group 2 after 9 months ($P < .05$)
John et al[45] (2015)[†‡]	Randomized controlled clinical study	Group 1: amino acid glycine powder (AAD); Group 2: mechanical debridement using carbon curettes and antiseptic therapy with chlorhexidine digluconate	25 (Group 1: 12; Group 2: 13)	12	Group 1: baseline 3.7 ± 1; after 12 months 3.2 ± 1; difference 0.5 ± 0.9; Group 2: baseline 3.9 ± 1.1; after 12 months 3.5 ± 1.2; difference 0.4 ± 0.8, $P > .05$

+BOP, bleeding on probing; *PD, probing-pocket depth; PDT, photodynamic therapy.
†Included to the meta-analysis of PD.
‡Included to the meta-analysis of BOP.
§Included to the meta-analysis of bone level.

doi: 10.3290/j.qi.a35131

Decrease in BOP positive sites: Group 1: baseline 4.03 ± 1.66; after 12 months 1.74 ± 1.37 ($P < .05$); Group 2: baseline 4.41 ± 1.47; after 12 months 1.55 ± 1.26 ($P < .05$)	Nonsurgical mechanical debridement with adjunctive use of PDT is equally effective in the reduction of BOP and PD as with the adjunctive use of minocycline microspheres.
Group 1: baseline 99.0 ± 4.1; after 12 months 57.8 ± 30.7; difference 41.2 ± 29.5; Group 2: baseline 94.7 ± 13.7; after 12 months 78.1 ± 30; difference 16.6 ± 33.4; Group 1 revealed a significantly higher BOP reduction ($P < .05$) when compared with group 2	Nonsurgical therapy of peri-implantitis in both groups resulted in comparable PD and BOP reduction. Adjunctive use of air polishing resulted in significantly higher BOP reduction in comparison to the chlorhexidine digluconate.

Appendix 2 Surgical treatments of peri-implantitis

Surgical treatment	Study (year)	Type of study	Treatment method used	Sample size	Follow-up (months)	PD* changes (mean ± SD)
Access surgery	Heitz-Mayfield et al[19] (2012)	Prospective cohort study	Open flap debridement and implant surface decontamination with adjunctive systemic amoxicillin and metronidazole	24 patients; 36 implants	12	Baseline: mean PD ≥ 6 mm—20%; 5 ≤ PD < 6 mm—25%; 4 ≤ PD < 5 mm—28%; < 4 mm—7%; After 12 months: ≥ 6 mm—0%; 5 ≤ PD < 6 mm—0%; 4 ≤ PD < 5 mm—11%; < 4 mm—89%; Statistically significant ($P < .01$) reduction in mean PD
	Papadopoulos et al[20] (2015)	Randomized controlled clinical study	Group 1: open flap debridement alone; Group 2: open flap debridement with the additional use of a diode laser for the treatment of peri-implantitis	16 (Group 1: 8; Group 2: 8)	6	Group 1: baseline mean PD 5.92 mm; after 6 months 4.44 mm; reduction of 1.38 mm; Group 2: baseline mean PD 5.52 mm; after 6 months 4.31 mm; reduction of 1.19 mm. No statistically significant difference between the two groups
Resective surgery	de Waal[14] (2014)[§]	Prospective clinical study	Resective surgery with bone recontouring and surface decontamination; Group 1: 0.2% chlorhexidine solution; Group 2: 0.12% chlorhexidine + 0.05% cetylpiridinum chloride	44 (Group 1: 22; Group 2: 22)	12	Mean PD ≥ 5 mm: Group 1: baseline 57.5 ± 26.6%; after 12 months 7.3 ± 12.6%; Group 2: baseline 60.2 ± 28.3%; after 12 months 5.3 ± 12.5%; Mean PD ≥ 6 mm: Group 1: baseline 29.1 ± 31.6%; after 12 months 2.1 ± 7.0%; Group 2: baseline 34.4 ± 31.8%; after 12 months 1.4 ± 5.8%. No significant difference between the groups ($P = .6$)
	Romeo et al[23] (2005)	Randomized clinical study	Group 1 (test): resective surgery and modification of surface topography (implantoplasty); Group 2: resective surgery only (control group)	17 (Group 1: 10; Group 2: 7)	36	Group 1: baseline 5.79 ± 1.69 mm; after 36 months 3.21 ± 0.56 mm (Student's *t*-value of +11.63); Group 2: baseline 6.52 ± 1.62 mm; after 24 months 5.5 ± 1.47 mm (Student's *t*-value of +3.18)
	Romeo et al[24] (2007)[§]	Randomized clinical study	Group 1 (test): resective surgery and implantoplasty; Group 2 (control): resective surgery alone	19 (Group 1: 10; Group 2: 9)	36	
Regenerative surgery	Schwarz et al[21] (2006)[†‡]	Prospective clinical study	Group 1: access flap surgery and the application of nanocrystalline hydroxyapatite; Group 2: access flap surgery and the application of a bovine-derived xenograft in combination with a collagen membrane	22 (Group 1: 11; Group 2: 11)	6	Group 1: baseline 7.0 ± 0.6 mm; after 6 months 4.9 ± 0.6 mm; difference 2.1 ± 0.5 mm; Group 2: baseline 7.1 ± 0.8 mm; after 6 months 4.5 ± 0.7 mm; difference 2.6 ± 0.4 mm
	Roos-Jansåker et al[22] (2007)[†]	Prospective clinical study	The bone defects were filled with a bone substitute, a resorbable membrane was placed over the grafted defect, and a cover screw was connected to the fixture.	12	12	Mean PD at baseline (5.1 ± 1.0 mm) was reduced by 4.2 ± 1.5 mm at 12 months.
	Schwarz et al[21] (2008)[†‡]	Prospective clinical study	Group 1: access flap surgery and the application of nanocrystalline hydroxyapatite; Group 2: access flap surgery and the application of natural bone mineral in combination with a collagen membrane	22 (Group 1: 11; Group 2: 11)	24	Group 1: baseline 6.9 ± 0.6 mm; after 2 years 5.4 ± 0.7 mm; difference 1.5 ± 0.6 mm; Group 2: baseline 7.1 ± 0.8 mm; after 2 years 4.7 ± 0.7 mm; difference 2.4 ± 0.8 mm. Better improvement in group 2
	Romanos et al[24] (2008)[†]	Case series	CO_2 laser was used to decontaminate the implant surface. Ten defects were filled with autogenous bone and nine with xenografts. All grafted sites were covered with a collagen membrane.	15	27 (± 17.83)	Baseline 6.00 ± 2.03 mm; after treatment 2.48 ± 0.63 mm; significant reduction ($P < .01$)
	Schwarz et al[25] (2009)[†‡]	Prospective clinical study	Group 1 (test): natural bone mineral in combination with a collagen membrane; Group 2 (control): access flap surgery and the application of nanocrystalline hydroxyapatite	20 (Group 1: 11; Group 2: 9)	48	Group 1: baseline 7.1 ± 0.7 mm; after 48 months 4.5 ± 0.9 mm; difference 2.5 ± 0.9 mm; Group 2: baseline 6.9 ± 0.6 mm; after 48 months 5.8 ± 0.7 mm; difference 1.1 ± 0.3 mm

continued on next page

doi: 10.3290/j.qi.a35131

BOP+ changes (mean ± SD)	Radiographic marginal bone level changes/bone defect fill	Comments
Number of sites with BOP: baseline: 2.5 ± 1; after 12 months: 1 ± 1.2. Statistically significant ($P < .01$) reduction in BOP	Three implants in three patients had 0.6–1 mm bone loss at 12 months. Three implants in three patients showed bone gain, while the remaining implants had stable marginal bone levels.	Access flap surgery in combination with systemic antibiotics was an effective treatment resulting in significantly reduced BOP and PD scores.
Group 1: baseline 93.5%; after 6 months 31.3%; mean reduction 72.9%; Group 2: baseline 81.2%; after 6 months 23.8%; mean reduction 66.7% ($P < .05$). No statistically significant difference between groups		Surgical treatment of peri-implantitis by access flap surgery resulted in improvement of clinical parameters. The additional use of a diode laser did not have any extra beneficial effect.
Group 1: baseline 82.1 ± 23.9%; after 12 months 42.7 ± 34.2%. Group 2: baseline 74.2 ± 27.8%; after 12 months 37.0 ± 35.3%. No significant difference between the groups ($P = .6$)	Mean marginal bone loss: Group 1: baseline 4.0 ± 1.5 mm; after 12 months 4.3 ± 1.7 mm; Group 2: baseline 4.1 ± 1.6 mm; after 12 months 4.1 ± 1.7 mm. Radiologic bone loss was not significantly different between the groups ($P = .8$).	Improved clinical parameters (eg, BOP and PD) and marginal bone loss compared with the baseline were observed in both groups, with no significant difference between them.
Mean bleeding index: Group 1: 2.83 ± 0.47; after 36 months 0.61 ± 0.67 (Student's *t*-value of +16.02); Group 2: baseline 2.86 ± 0.35; after 24 months 2.33 ± 0.75 (Student's *t*-value of +3.33)		Clinical parameters improved in both treatment groups, without a significant difference between them.
	Group 1: baseline mesially 3.82 ± 1.52 mm, distally 3.94 ± 1.64 mm; after 3 years mesially 3.81 ± 3.94 mm, distally 1.72 ± 1.79 mm; Group 2: baseline mesially 3.45 ± 1.93 mm, distally 3.49 ± 1.8 mm; after 3 years mesially 5.35 ± 1.99 mm, distally 5.42 ± 1.91 mm. Significantly higher ($P < .05$) mean marginal bone loss was recorded in group 2 than in group 1.	A significantly extended marginal bone loss was reported in the group without implantoplasty.
Group 1: baseline 82%; after 6 months 30%; Group 2: baseline 78%; after 6 months 28%	Radiologic observation revealed a decreased translucency within the intrabony component of the respective peri-implant bone defects.	Both therapies resulted in clinically important PD and BOP reduction.
BOP reduced	The distance not supported by bone or bone substitute at the mesial and distal site of the implant was evaluated. Mean defect fill was of 2.3 ± 1.2 mm	Treatment of peri-implant defect using a bone graft substitute combined with a resorbable membrane and submerged healing resulted in defect fill and clinical healthier situations.
Group 1: baseline 80%; after 2 years 44%; Group 2: baseline 78%; after 2 years 34%	In both treatment groups, radiologic observation at 24 months revealed a decreased translucency within the intrabony component of the respective peri-implant bone defects.	Both treatment procedures have shown efficacy; however, the application of natural bone mineral in combination with a collagen membrane may result in an improved outcome of healing.
Sulcus bleeding index: Baseline 2.76 ± 0.35; after treatment 1.03 ± 0.85; significant reduction ($P < .01$)	Complete bone fill was observed in all cases after the use of xenogenic bone-grafting material. In all sites treated with autogenous bone alone, at least two-thirds of the bony defect was filled with bone.	Bovine xenograft provided more radiographic bone fill than autogenous.
Group 1: baseline 79%; after 48 months 28%; Group 2: baseline 80%; after 48 months 48%	Decreased translucency in the former peri-implant defect area noticed at 8 sites in group 1 and 5 sites in group 2	While the application of natural bone mineral with a collagen membrane resulted in clinical improvements, a long-term outcome obtained with nanocrystalline hydroxyapatite without a barrier membrane must be considered as poor.

continued on next page

continuation from previous page

	Roos-Jansåker et al[26] (2011)	Prospective clinical study	Group 1 (test): bone substitute and a resorbable membrane; Group 2 (control): bone substitute alone	32 (Group 1:17 [29 implants]; Group 2: 15 [27 implants])	36	
	Roccuzzo et al[27] (2011)[†‡§]	Prospective clinical study	The implant surface was mechanically debrided and treated using a 24% EDTA gel and a 1% chlorhexidine gel. The bone defect was filled with a bovine-derived xenograft (BDX), and the flap was sutured around the non-submerged implant. Group 1 (control): TPS (titanium plasma-sprayed surface) dental implants; Group 2 (test): SLA (sand-blasted large-grit and acid-etched surface) dental implants	26	12	Group 1: baseline 7.2 ± 1.5 mm; after 12 months 5.1 ± 2.0 mm (P = .001); Group 2: baseline 6.8 ± 1.2 mm; after 12 months 3.4 ± 1.0 (P = .003)
	Aghazadeh et al[28] (2012)[†‡]	Randomized controlled clinical study	Group 1: surgical debridement and placement of autogenous bone with a collagen membrane; Group 2: surgical debridement and placement of bovine-derived xenograft with a collagen membrane	45 (Group 1: 22; Group 2: 23)	12	Group 1: baseline 6.0 ± 1.3 mm; after 12 months 3.8 ± 0.2 mm; Group 2: baseline 6.2 ± 1.4 mm; after 12 months 3.3 ± 0.2 mm (P = .06); Greater PD reduction in group 2 (P < .01)
Regenerative surgery	Wiltfang et al[29] (2012)[‡]	Prospective case series	The implants were decontaminated with etching gel, and the defects were filled with autologous bone mixed 1:1 with a xenogenic bone graft. The prosthetic reconstructions did not have to be removed.	22 patients; 36 implants	12	Average reduction of PD was 4 mm (95% CI: 3.3–4.6 mm).
	Schwarz et al[30] (2013)[†‡]	Prospective clinical study	Group 1: access flap surgery and the application of nanocrystalline hydroxyapatite + collagen membrane and implant surface decontamination with Er:YAG laser; Group 2: access flap surgery and the application of natural bone mineral + collagen membrane and implant surface decontamination with plastic curettes + sterile saline	17 (Group 1: 7; Group 2: 10)	48	Group 1: baseline 5.1 ± 1.5 mm; after 48 months 3.8 ± 1.1 mm; difference 1.3 ± 1.8 mm; Group 2: baseline 5.1 ± 1.7 mm; after 48 months 4.3 ± 1.2 mm; difference 1.2 ± 1.9 mm
	Roos-Jansåker et al[31] (2014)[†§]	Prospective clinical study	Group 1: bone substitute and a resorbable membrane; Group 2: bone substitute alone	25 (Group 1:13 [23 implants]; Group 2: 12 [22 implants])	60	Group 1: baseline 5.6 ± 1.9 mm; after 5 years 3.0 ± 2.4 mm; Group 2: baseline 6.0 ± 2.2 mm; after 5 years 3.3 ± 2.0 mmm (P = .56)
	Schwarz et al[32] (2014)[†‡]	Case series	Access flap surgery, implantoplasty, and augmentation using a natural bone mineral + a collagen membrane; a subepithelial connective tissue graft was harvested and adapted to the wound area to support transmucosal healing.	10 patients, 13 implants	6	PD baseline 6.15 ± 0.8 mm; after 6 months 3.61 ± 1.24 mm; difference: 2.53 ± 1.80 mm (P < .01)
	Matarasso et al[33] (2014)[†§]	Case series	Application of a deproteinized bovine bone mineral + a collagen membrane and implantoplasty in the suprabony component of the peri-implant lesion	11	12	Baseline mean PD 8.1 ± 1.8 mm; after 12 months: 4.0 ± 1.3 mm (P = .01)

+BOP: bleeding on probing; *PD, pocket-probing depth.
†Included in the meta-analysis of PD.
‡Included in the meta-analysis of BOP.
§Included in the meta-analysis of bone level.

doi: 10.3290/j.qi.a35131

	The mean defect fill was 1.6 ± 1.2 mm in group 1 and 1.3 ± 1.3 mm in group 2 ($P = .40$). In both groups, radiographic evidence of bone gain was significant ($P < .01$). In group 1, 51.7% of the implants had a defect fill ≥ 1.8 mm. In group 2, 44.4% of the implants gained >1.8 mm in defect fill. No difference in bone changes as a result of treatment modality ($P = .89$)	No significant difference in terms of radiologic outcomes between the groups.
Group 1: baseline 91.1 ± 12.4%; after 12 months 57.1 ± 38.5% ($P = .04$); Group 2: baseline 75.0 ± 30.2%; after 12 months 14.6 ± 16.7% ($P = .03$)	Group 1: baseline 3.9 ± 1.6 mm; after 12 months 2.2 ± 1.3 mm; Group 2: baseline 3.0 ± 0.9 mm; after 12 months 1.1 ± 0.8 mm. In both groups bone reduction was statistically significant ($P < .05$), but the difference between the two groups was not statistically significant.	Clinical parameters around moderately rough implants were better than around rough implants.
Group 1: baseline 87 ± 20.1%; after 12 months 48.4 ± 5.4%; Group 2: baseline 79.4 ± 28.4%; after 12 months 26.7 ± 4.7% ($P = .004$). No differences in BOP changes between the groups	Radiologic bone defect depth (the mesial and distal distances from the implant platform to the bottom of the defect): Group 1: baseline mesially 5.9 ± 1.8 mm, distally 5.8 ± 1.6 mm; after 12 months mesially 5.8 ± 0.3 mm, distally 5.7 ± 0.3 mm; Group 2: baseline mesially 5.2 ± 1.8 mm, distally 5.3 ± 1.8 mm; after 12 months mesially 4.0 ± 0.3 mm, distally 4.3 ± 9.3 mm. Mean bone-level gain: Group 1: 0.2 ± 0.3 mm; Group 2: 1.1 ± 0.3 ($P = .05$). Radiographic defect fill was greater in group 2 (mesially $P < .01$ and distally $P < .05$, respectively).	Mean bone-level gain was statistically significantly higher for the group treated with the xenograft compared with the group treated with autogenous bone.
BOP was observed in 61% of the implants at baseline and in 25% after 12 months.	The radiologic evaluation of the bone defects resulted in a regeneration from 5.1 mm (95% CI, 4.4–5.9 mm) prior to surgery to 1.6 mm (95% CI, 1.1–2.2 mm) after 12 months, a mean reduction of 3.5 mm (95% CI, 2.7–4.3 mm).	For the bone defects larger than 4 mm in case of peri-implantitis, the single surgical intervention provided a reliable method to reduce bone defects.
Group 1: baseline 95.2 ± 12.6%; after 48 months 23.5 ± 23.4%; difference 71.6 ± 24.9%; Group 2: baseline 100 ± 0.0%; after 48 months 14.8 ± 16.4%; difference 85.2 ± 16.4%		A combined surgical respective/regenerative therapy of peri-implantitis were not influenced by the method of surface decontamination.
BOP decreased in both groups.	Bone loss: Group 1: baseline 4.6 ± 1.3 mm; after 5 years 1.5 ± 1.2 mm; Group 2: baseline 4.0 ± 0.8 mm; after 5 years 1.1 ± 1.2 mm. Average defect fill was 1.3 ± 1.4 mm in group 1 and 1.1 ± 2.0 mm in group 2 ($P = .24$).	No significant difference in terms of clinical and radiologic outcomes between the groups.
BOP baseline 92.30 ± 16.12%; after 6 months 17.91 ± 19.7%; difference 74.39 ± 28.52% ($P < .01$)		The combined surgical procedure was effective in controlling peri-implantitis lesion without compromising the overall esthetic outcome.
BOP at baseline 19.7 ± 40.1% after 12 months 6.1 ± 24.0% ($P = .032$)	Marginal bone level (distance between the implant shoulder and the bottom of the defect) decreased: baseline 8.0 ± 3.7 mm; after 12 months 5.2 ± 2.2 mm ($P = .01$). Intrabony defect depth (distance between the bottom of the defect and the line connecting the distal and mesial interproximal bone crest) decreased: baseline 2.5 ± 3.5 mm; after12 months 0.5 ± 1.1 mm ($P < .01$). The radiographic fill of the intrabony defect was 93.3 ± 13.0%.	A combined regenerative and respective approach for the treatment of peri-implant defects yielded positive outcomes in terms of PD and BOP reduction and radiographic defect fill.

Q = 13.5496, df = 19, P = .8093						Standardized Mean Difference
Study	N1	N2	Total	SMD	95% CI	-2 -1 0 1 2
Karring et al[10] (2005) group 1	11	11	22	0.000	−0.889 to 0.889	
Karring et al[10] (2005) group 2	11	11	22	−0.0500	−0.940 to 0.840	
Renvert et al[13] (2008) group 1	17	17	34	0.290	−0.413 to 0.993	
Renvert et al[13] (2008) group 2	15	15	30	0.134	−0.615 to 0.883	
Deppe et al[18] (2013) group 1	10	10	20	0.574	−0.389 to 1.538	
Deppe et al[18] (2013) group 2	8	8	16	−0.777	−1.902 to 0.348	
Renvert et al[14] (2009) group 1	17	17	34	0.000	−0.699 to 0.699	
Renvert et al[14] (2009) group 2	14	14	28	0.549	−0.245 to 1.343	
John et al[45] (2015) group 1	12	12	24	0.483	−0.379 to 1.344	
John et al[45] (2015) group 2	13	13	26	0.337	−0.480 to 1.153	
Sahm et al[15] (2011) group 1	16	16	32	0.687	−0.059 to 1.433	
Sahm et al[15] (2011) group 2	16	16	32	0.122	−0.601 to 0.845	
Renvert et al[12] (2006) group 1	14	14	28	0.447	−0.341 to 1.235	
Renvert et al[12] (2006) group 2	16	16	32	0.000	−0.722 to 0.722	
Schwarz et al[11] (2005) group 1	10	10	20	0.666	−0.306 to 1.637	
Schwarz et al[11] (2005) group 2	10	10	20	0.396	−0.555 to 1.347	
Bassetti et al[44] (2014) group 1	20	20	40	0.677	0.017 to 1.337	
Bassetti et al[44] (2014) group 2	20	20	40	0.475	−0.175 to 1.126	
Schär et al[17] (2013) group 1	20	20	40	0.624	−0.033 to 1.282	
Schär et al[17] (2013) group 2	20	20	40	0.620	−0.037 to 1.277	
Total (fixed effects)	290	290	580	0.346	0.181 to 0.512	
Total (random effects)	290	290	580	0.346	0.181 to 0.512	

Appendix 3 Forest plot of odds ratio (95% CI) for probing depth using nonsurgical treatment methods.

Q = 37.0847, df = 11, P = .0001					Odds ratio
Study	Intervention	Controls	Odds ratio	95% CI	0,1 1 10
Karring et al[10] (2005) group 1	63/290	36/290	1.957	1.254 to 3.054	
Karring et al[10] (2005) group 2	72/290	81/290	0.852	0.589 to 1.231	
Renvert et al[13] (2008) group 1	86/290	48/290	2.138	1.435 to 3.185	
Renvert et al[13] (2008) group 2	89/290	63/290	1.585	1.090 to 2.302	
John et al[45] (2015) group 1	99/290	57/290	2.082	1.429 to 3.035	
John et al[45] (2015) group 2	94/290	78/290	1.316	0.920 to 1.880	
Sahm et al[15] (2011) group 1	94/290	51/290	2.263	1.534 to 3.341	
Sahm et al[15] (2011) group 2	95/290	84/290	1.194	0.840 to 1.699	
Renvert et al[12] (2006) group 1	88/290	71/290	1.344	0.931 to 1.939	
Renvert et al[12] (2006) group 2	86/290	78/290	1.146	0.798 to 1.645	
Schwarz et al[11] (2005) group 1	83/290	31/290	3.350	2.133 to 5.260	
Schwarz et al[11] (2005) group 2	80/290	58/290	1.524	1.036 to 2.242	
Total (fixed effects)	1,029/3,480	736/3,480	1.567	1.405 to 1.748	
Total (random effects)	1,029/3,480	736/3,480	1.600	1.306 to 1.961	

Appendix 4 Forest plot of odds ratio (95% CI) for bleeding on probing using nonsurgical treatment methods.

doi: 10.3290/j.qi.a35131

Q = 11.8444, df = 5, P = .0370

Study	N1	N2	Total	SMD	95% CI
Karring et al[10] (2005) group 1	11	11	22	−0.160	−1.051 to 0.731
Karring et al[10] (2005) group 2	11	11	22	−0.122	−1.013 to 0.768
Renvert et al[13] (2008) group 1	17	17	34	0.081	−0.618 to 0.780
Renvert et al[13] (2008) group 2	15	15	30	−0.067	−0.815 to 0.682
Deppe et al[18] (2013) group 1	10	10	20	0.359	−0.590 to 1.308
Deppe et al[18] (2013) group 2	8	8	16	2.390	0.893 to 3.886
Total (fixed effects)	72	72	144	0.157	−0.183 to 0.496
Total (random effects)	72	72	144	0.253	−0.284 to 0.790

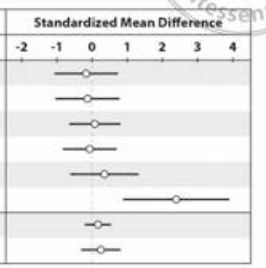

Appendix 5 Forest plot of odds ratio (95% CI) for bone level using nonsurgical treatment methods.

Q = 13.2455, df = 5, P = .0212

Study	N1	N2	Total	SMD	95% CI
de Waal et al[34] (2014)	22	22	44	−0.184	−0.794 to 0.426
de Waal et al[34] (2014)	22	22	44	0.000	−0.608 to 0.608
Romeo et al[36] (2007, mesial)	10	10	20	0.003	−0.936 to 0.943
Romeo et al[36] (2007, mesial)	9	9	18	−0.923	−1.988 to 0.142
Romeo et al[36] (2007, distal)	10	10	20	1.239	0.193 to 2.284
Romeo et al[36] (2007, distal)	9	9	18	−0.993	−2.069 to 0.082
Total (fixed effects)	82	82	164	−0.116	−0.433 to 0.201
Total (random effects)	82	82	164	−0.131	−0.669 to 0.407

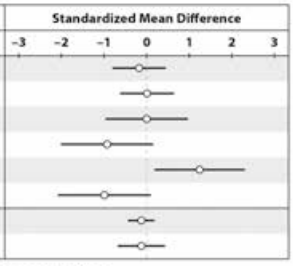

Appendix 6 Forest plot of odds ratio (95% CI) for bone level using surgical resective treatment methods.

Q = 100.0462, df = 17, P < .0001						Standardized Mean Difference
Study	N1	N2	Total	SMD	95% CI	−2 −1 0 1 2 3 4 5
Roccuzzo et al[27] (2011)	13	13	26	1.150	0.265 to 2.035	
Roccuzzo et al[27] (2011)	13	13	26	2.981	1.751 to 4.211	
Roos-Jansåker et al[31] (2014)	13	13	26	−0.188	−1.000 to 0.623	
Roos-Jansåker et al[31] (2014)	12	12	24	−0.131	−0.979 to 0.717	
Roos-Jansåker et al[32] (2007)	12	12	24	0.682	−0.194 to 1.557	
Schwarz et al[25] (2009)	11	11	22	3.102	1.706 to 4.499	
Schwarz et al[25] (2009)	9	9	18	1.607	0.419 to 2.795	
Schwarz et al[21] (2006)	11	11	22	3.367	1.898 to 4.836	
Schwarz et al[21] (2006)	11	11	22	3.328	1.870 to 4.785	
Schwarz et al[23] (2008)	11	11	22	2.214	1.038 to 3.389	
Schwarz et al[23] (2008)	11	11	22	3.072	1.683 to 4.460	
Schwarz et al[30] (2013)	7	7	14	0.925	−0.323 to 2.174	
Schwarz et al[30] (2013)	10	10	20	0.521	−0.438 to 1.480	
Schwarz et al[32] (2014)	10	10	20	2.331	1.055 to 3.608	
Aghazadeh et al[28] (2012)	22	22	44	2.323	1.520 to 3.126	
Aghazadeh et al[28] (2012)	23	23	46	2.850	1.987 to 3.714	
Romanos et al[24] (2008)	15	23	38	2.537	1.620 to 3.454	
Matarasso et al[33] (2014)	11	11	22	2.512	1.267 to 3.758	
Total (fixed effects)	225	233	458	1.647	1.414 to 1.880	
Total (random effects)	225	233	458	1.894	1.321 to 2.468	

Appendix 7 Forest plot of odds ratio (95% CI) for probing depth using surgical regenerative treatment methods.

Q = 64.5872, df = 14, P < .0001					Odds ratio
Study	Intervention	Controls	Odds ratio	95% CI	1 10 100
Roccuzzo et al[27] (2011)	91/188	57/188	2.155	1.413 to 3.288	
Roccuzzo et al[27] (2011)	75/188	14/188	7.883	4.289 to 14.489	
Wiltfang et al[29] (2012)	61/188	25/188	3.132	1.862 to 5.268	
Schwarz et al[25] (2009)	79/188	28/188	4.142	2.524 to 6.795	
Schwarz et al[25] (2009)	80/188	48/188	2.160	1.395 to 3.345	
Schwarz et al[21] (2006)	82/188	30/188	4.074	2.508 to 6.619	
Schwarz et al[21] (2006)	78/188	28/188	4.052	2.469 to 6.650	
Schwarz et al[23] (2008)	80/188	44/188	2.424	1.554 to 3.781	
Schwarz et al[23] (2008)	78/188	34/188	3.212	2.005 to 5.145	
Schwarz et al[30] (2013)	95/188	23/188	7.181	4.277 to 12.057	
Schwarz et al[30] (2013)	100/188	14/188	13.299	7.275 to 24.309	
Schwarz et al[32] (2014)	93/188	17/188	9.457	5.377 to 16.632	
Aghazadeh et al[28] (2012)	87/188	48/188	2.484	1.608 to 3.838	
Aghazadeh et al[28] (2012)	79/188	26/188	4.417	2.675 to 7.293	
Matarasso et al[33] (2014)	91/188	24/188	6.507	3.888 to 10.891	
Total (fixed effects)	1,249/2,820	460/2,820	4.044	3.571 to 4.581	
Total (random effects)	1,249/2,820	460/2,820	4.257	3.235 to 5.602	

Appendix 8 Forest plot of odds ratio (95% CI) for bleeding on probing using surgical regenerative treatment methods.

doi: 10.3290/j.qi.a35131

Q = 10.6697, df = 4, P = .0305						Standardized Mean Difference
Study	**N1**	**N2**	**Total**	**SMD**	**95% CI**	-1 0 1 2 3 4
Roccuzzo et al[27] (2011)	13	13	26	1.129	0.247 to 2.012	
Roccuzzo et al[27] (2011)	13	13	26	2.161	1.109 to 3.213	
Roos-Jansåker et al[31] (2014)	13	13	26	2.400	1.299 to 3.500	
Roos-Jansåker et al[31] (2014)	12	12	24	2.746	1.511 to 3.981	
Matarasso et al[33] (2014)	11	11	22	0.885	−0.056 to 1.826	
Total (fixed effects)	62	62	124	1.703	1.266 to 2.139	
Total (random effects)	62	62	124	1.802	1.082 to 2.523	

Appendix 9 Forest plot of odds ratio (95% CI) for bone level using surgical regenerative treatment methods.

Marine Biotechnology
https://doi.org/10.1007/s10126-018-9816-6

ORIGINAL ARTICLE

Cuttlebone as a Marine-Derived Material for Preparing Bone Grafts

Alisa Palaveniene[1] · Volodymyr Harkavenko[2] · Vitalina Kharchenko[2] · Povilas Daugela[3] · Mindaugas Pranskunas[3] · Gintaras Juodzbalys[3] · Nataliya Babenko[2] · Jolanta Liesiene[1]

Received: 1 February 2017 / Accepted: 4 December 2017

Abstract
The use of synthetic materials for biomedical applications still presents issues owing to the potential for unfavourable safety characteristics. Currently, there is increasing interest in using natural, marine-derived raw materials for bone tissue engineering. In our study, the endoskeleton of the mollusc *Sepia*, i.e. cuttlebone (CB), was used with regenerated cellulose (RC) to prepare three-dimensional composite bone grafts. CB microparticles were mechanically immobilised within a cellulose gel, resulting in a macroporous structure upon lyophilisation. The interconnected porous structure of the regenerated cellulose/cuttlebone (RC/CB) composite was evaluated by micro-computed tomography. The porosity of the composite was 80%, and the pore size predominantly ranged from 200 to 500 μm. The addition of CB microparticles increased the specific scaffold surface by almost threefold and was found to be approximately 40 mm^{-1}. The modulus of elasticity and compressive strength of the RC/CB composite were 4.0 ± 0.6 and 22.0 ± 0.9 MPa, respectively. The biocompatibility of the prepared RC/CB composite with rat hepatocytes and *extensor digitorum longus* muscle tissue was evaluated. The obtained data demonstrated that both the composite and cellulose matrix samples were non-cytotoxic and had no damaging effects. These results indicate that this RC/CB composite is a novel material suitable for bone tissue-engineering applications.

Keywords Cuttlebone · Regenerated cellulose · Bone tissue engineering · Cytotoxicity

Introduction

Great concern has been shown for the unfavourable safety aspects of synthetic materials in clinical practice (Anderson et al. 2008; Givissis et al. 2010; Franz et al. 2011). Alongside the development of different synthetic bone substitute materials, there has been a growing interest in biological material resources over the last decade. A significant amount of attention has been focused on material resources of marine origin, e.g. the bones of aquatic animals and fishes, mollusc shells, sponges, algae, and corals (Meyers et al. 2008; Cunningham et al. 2010; Clarke et al. 2011; Lin et al. 2011; Silva et al. 2012; Mayer et al. 2013; Zhang and Vecchio 2013; Brennan et al. 2015).

Cuttlebone (CB), also known as cuttlefish backbone, the endoskeleton of cuttlefish or *Os Sepiae*, represents a potential biological material for bone tissue engineering. CB is an internal shell of marine animals known as cuttlefish (*Sepia*), belonging to the phylum *Mollusca*, class *Cephalopoda*, order *Sepiida*. CB is listed in the Chinese Pharmacopoeia; in traditional Chinese medicine, it is known as *Hai Piao Xiao* (Zhao et al. 2011). Curative applications of CB exist in traditional Ayurvedic Indian medicine, in which it is known as *Jhaag-e-Darya/Samudra Phena* (Siddiquee et al. 2013).

The use of CB in particular biomedicine and material science branches is possible by preserving the CB structure or modifying the original material. The main constituents of CB are aragonite (carbonate mineral, a crystal form of calcium carbonate) and β-chitin linked with proteins (Denton et al. 1961; Cadman et al. 2012). The properties of chitin have been thoroughly studied in the biomedical science field. Chitin is a non-toxic and biodegradable natural polymer (Kurita 2006). Chitin has potential as a polymer matrix in tissue engineering for facilitating progenitor cell activity, inducing in vivo calcification, and enhancing surrounding tissue ingrowth

✉ Jolanta Liesiene
jolanta.liesiene@ktu.lt

[1] Department of Polymer Chemistry and Technology, Kaunas University of Technology, Radvilenu str. 19, 50254 Kaunas, Lithuania

[2] Department of Ontogenetic Physiology, V. N. Karazin Kharkiv National University, 4 Svobody Sq., Kharkiv 61022, Ukraine

[3] Department of Oral and Maxillofacial Surgery, Lithuanian University of Health Sciences, Eiveniu str. 2, LT-50009 Kaunas, Lithuania

Published online: 03 April 2018

(Jayakumar et al. 2011). Osteoinductive activity followed by neovascularisation was achieved on a chemically modified hyaluronan-chitin composite material (Muzzarelli 2009). Chitin nanofibrils have shown antimicrobial activity and improved physical and mechanical properties in a composition of a carrageenan film (Shankar et al. 2015). Chitin membranes exhibited a high degradation rate, low swelling degree, and good mechanical properties and allowed fibroblast growth in vitro in a study by Nagahama et al. (2008). In another study, chitin was characterised as a biocompatible natural material and a regulator of collagen synthesis in soft tissues (Morganti and Morganti 2008). Other studies have shown high levels of CB-based material osteoconductivity, bioactivity, and chemical and structural conformity towards human bone tissue (Dogan and Okumus 2014; Won et al. 2015).

CB is of great interest for bone tissue engineering as a bioactive mineral filler owing to the presence of biogenic calcium and bioinorganic trace elements, such as phosphorus, sodium, magnesium, potassium, sulphur, silicon, chlorine, iron, and strontium, among others. Generally, bone homeostasis is related to the quantitative expression, particular ratios, and specific properties of the inorganic fraction of bone. Trace elements, such as magnesium, iron, zinc, silicon, and copper, influence the enzymatic activity of bone, as well as cartilage formation and collagen synthesis (Dermience et al. 2015). Few researchers have previously produced and examined scaffolds retaining the primary structure of the organic CB matrix or containing milled CB.

The potential of using small pieces of crushed CB for xenogeneic grafts promoting the healing of bone defects in vivo was examined by Dogan and Okumus (2014). Desirable decreased formation of free radicals in surrounding soft tissue was observed around CB xenografts, and grafts containing immobilised demineralised bone matrix, bovine cancellous graft, or tricalcium phosphate showed no advantages over the CB xenografts. In this study, CB grafts also resulted in accelerated osteogenesis and osteointegration, and no signs of secondary infection were observed. An in vivo study performed using a rabbit model showed that applying pieces of crushed CB could withstand the required mechanical workload. These results have strongly contributed to the recognition of CB as a bioactive marine-derived material.

A few researchers have developed a thin monolayer material from a demineralised CB lamellar microstructure. The approach appears to be effective for further specific biotechnological applications (Ogasawara et al. 2000; Culverwell et al. 2008; Jia et al. 2009; Xu et al. 2009). Original and successful results were achieved in converting CB aragonite to hydroxyapatite (HAp) by Rocha et al. (2005) and Kannan et al. (2007). Powdered CB materials have been also used as fillers in synthetic polymeric matrices.

A study of the in vivo osteointegration of prepared acrylic bone cements toughened by CB microparticles revealed that the CB-based material has potential as a bioactive filler for medical applications (Garcia-Enriquez et al. 2010). The composite showed a higher modulus of elasticity compared with that of an unfilled scaffold. However, no improvements in the compressive strength, bending modulus, bending strength, or fracture toughness of the composite were achieved by incorporating CB microparticles. According to another study, similar trends in mechanical properties were observed for β-tricalcium phosphate in an acrylic polymer framework. An acrylic matrix that did not incorporate β-tricalcium phosphate showed superior mechanical strength compared with that of acrylic bone cements incorporating β-tricalcium phosphate, but the modulus of elasticity was not superior (Vázquez et al. 2005).

A polycaprolactone (PCL) scaffold with embedded CB particles was prepared by Park et al. (2012) using a salt-leaching method for the formation of pores. Scaffolds with pore sizes of approximately 200–300 μm and an interconnected porous network were obtained. However, scaffolds produced using this technique could exhibit limited mechanical properties and undesirable residual cytotoxic solvents and porogens (Subia et al. 2010). In a study by Kim et al. (2013a), a CB-derived HAp scaffold was coated with PCL. The results demonstrated decreased osteoblast adhesion and proliferation in scaffolds coated with 10% PLC. The authors explained the negative cell behaviour by reductions in scaffold porosity of up to 77%. However, it has been shown that insufficient scaffold porosity for bone tissue ingrowth is only 50% (Whang et al. 1999; Yang et al. 2001); thus, this factor cannot be considered the only parameter affecting cell-scaffold behaviour in the study.

Three-dimensional (3D) composite scaffolds developed from polymers and inorganics have already been recognised as promising grafts for bone tissue engineering (Amini et al. 2012). Results have been obtained using polymers of natural origin, such as collagen and gelatine, silk fibroin, gellan gum and its derivatives, hyaluronic acid, chitin and chitosan, alginate, and bacterial cellulose for bone tissue-engineering applications (Pina et al. 2015; Zaborowska et al. 2010). Cellulose is a widespread, naturally occurring polysaccharide. It is a biocompatible and non-immunogenic material applicable for various biomedical applications (Baptista et al. 2013). Biocomposite scaffolds from bacterial cellulose and inorganic materials showed promising results for a bone scaffold design (Nge and Sugiyama 2007; Chen et al. 2009). Osteoconductive properties of the regenerated cellulose/inorganic composite were recently described by our scientific group, showing promising results for bone tissue-engineering applications (Petrauskaite et al. 2013).

The aim of our study was to prepare porous 3D scaffolds with embedded CB microparticles on an RC base. The cytotoxicity and morphological and physicochemical characteristics of the prepared RC/CB composites were examined.

Materials and Methods

Materials

Dried CBs were purchased from Vital Pet Products, Ltd., UK. The raw material was crushed, ground in an agate mortar, and sieved. A fraction of CB particles between 325 and 400 mesh was collected (the particle size in 32–45-μm range). Acetylcellulose and chitin (degree of acetylation [DA] ≥ 95%) were purchased from Sigma-Aldrich. All other reagents were of a chemically pure grade.

Preparation of a Scaffold with CB Microparticles Based on a Cellulose Matrix

A cellulose gel was prepared as previously described (Petrauskaite et al. 2013). To prepare the RC/CB composites, CB microparticles were mechanically immobilised within the viscous cellulose gel (7:150 ratio, *w*/*v*). The porous structure was formed using a Christ Alpha 2-4 LSC (Martin Christ Gefriertrocknungsanlagen GmbH, Osterode am Harz, Germany) freeze dryer (Petrauskaite et al. 2016).

Evaluation of the Physicochemical Characteristics of the CB Material and RC/CB Composite

The elemental composition of the dorsal and lamellar CB layers was evaluated by X-ray fluorescence spectrometry using a Bruker X-ray S8 Tiger WD (Bruker AXS GmbH, Karlsruhe, Germany) and the Spectra^{plus} quant-express method. The experimental parameters were as follows: a rhodium tubule, a voltage up to 60 kV, and an electric current up to 130 mA.

The morphology of the CB sections was examined by scanning electron microscopy using an FEI Quanta 200 FEG. Organic Element Analyser Flash 2000 was used to evaluate the total nitrogen content in the dorsal and lamellar CB layers. The chitin content in the CB material was calculated according to the theoretical content of nitrogen (6.9%) in a fully acetylated chitin monomer (Florek et al. 2009).

Fourier transform infrared (FTIR) spectroscopy was performed using a FTIR spectrometer (Perkin-Elmer, Inc., Waltham, USA). The samples for this analysis were prepared by mixing the finely powdered material with potassium bromide in an agate mortar at a 1:50 ratio and pressing the mixture into homogeneous pellets. Mid-infrared spectral range data, corresponding to 4000–400 cm^{-1}, was used; the resolution was 4 cm^{-1}.

To evaluate changes in the DA, powdered chitin was immersed in an alkaline medium (pH = 11) for 10 days; then, the material was washed with distilled water until reaching neutrality and dried. The elemental analysis (for C, H, and N) was performed using an Exeter Analytical CE-440 elemental analyser (Exeter Analytical, Inc., Chelmsford, USA). The DA was calculated from the elemental analysis data according to Formula 1 (Xu et al. 1996):

$$\mathrm{DA}(\%) = \frac{(C/N)5.14}{1.72} \times 100. \quad (1)$$

Morphological parameters of the RC matrix and RC/CB composite were evaluated by micro-computed tomography (μCT). Samples were scanned with a μCT 40 system (Scanco Medical AG, Brüttisellen, Switzerland). The following parameters were used for the scans: energy, 70 kVp; integration time, 600 ms; frame averaging, 2×; and nominal resolution, 10 μm. Morphometric parameters, such as the scaffold volume fraction (SV/TV), the specific scaffold surface (SS/SV), and the mean partition thickness (Pr.Th), were computed from 3D images. The porosity and pore sizes of the scaffold were determined directly from two-dimensional (2D) images. Partition spacing (Pr.Sp) and partition number (Pr.N) indices were also calculated from the primary indices (Hildebrand et al. 1999).

Determination of the Mechanical Properties of the RC/CB Composite

Dry samples in a cylindrical form with dimensions of approximately 1.0 × 1.5 cm were prepared. Mechanical tests were performed using a benchtop Tinius Olsen H10KT testing machine (Tinius Olsen Ltd., Surrey, England) at cross-head speed of 1 mm/min with a 5000-N load cell.

Cytotoxicity Evaluation of the RC/CB Composite and RC Matrix

The effect of the RC/CB composite or RC matrix samples on hepatocyte viability was analysed. The preparation of ex vivo hepatocyte primary cell cultures was achieved through a non-enzymatic method (Petrenko and Sukach 1991). The livers of healthy 3-month-old Wistar rats were used to obtain isolated cells. The viability of the isolated cells was initially estimated by trypan blue staining and was determined to be greater than 95%. The term "cell viability" used in the article is mainly related to the detection of dead-or-alive cell number, but not the specific apoptotic process. The dead-or-alive cell number is significant in comparison with the intact control cells for the biocompatibility testing, because it is related to an adaptability of the experimental composite. For the test, ≥ 600 freshly isolated hepatocytes were used for every sample. Cells were incubated in Petri dishes at 37 °C temperature for 90 min with milled RC/CB composites or RC matrix samples at 50 mg/mL of cell suspension. After incubation, aliquots were collected for cell viability testing. Cells were stained with trypan blue dye and counted using a haemocytometer. Control cell

viability was greater than 92% in all experiments; ≥ 600 cells were tested for each group.

To evaluate the cell plasma membrane integrity of the isolated rat hepatocytes and *extensor digitorum longus* (EDL) muscle tissue, lactate dehydrogenase (LDH) and aldolase activities were measured. Hepatocytes were centrifuged after incubation with the samples, and supernatants were collected for LDH testing. LDH release into the supernatant was analysed using a commercial kit from Felicit Diagnostic (Dnepropetrovsk, Ukraine). To investigate potential membrane damage in the myocytes, EDL muscle tissue was isolated from 3-month-old rats and incubated with the scaffolds at 37 °C temperature for 90 min in oxygen-enriched Krebs saline buffer. Aldolase activity was measured using the method described by Sibley and Lehninger (1949).

Metabolic effects of the RC/CB composites and RC matrix were studied by evaluating the sensitivity of EDL tissue to insulin and the glucose uptake rate after incubation with the samples. For the insulin sensitivity investigation, the twofold [^{3}H] glucose uptake rate was determined in isolated EDL cells during incubation in oxygen-enriched Krebs saline buffer, as determined using the method described by Brutman-Barazani et al. (2012). Glucose uptake over 90 min was investigated both in the presence of 0.9% NaCl (basal level) and under the action of 10 nM insulin in the media with milled scaffold samples; 0.1 μCi/mL twofold [^{3}H]-glucose was used. The reaction was stopped by ice-cold 0.9% NaCl, and the radiolabelled glucose content in EDL cells was evaluated by a scintillation analysis.

Statistical Analysis

Data are expressed as the mean value ± standard deviation of 5 and 3 tests for the mechanical property and cytotoxicity tests, respectively. ANOVA was performed, and $P \leq 0.05$ was considered statistically significant.

Results

Characterisation of the CB Material

The structure and composition of CB are closely related to the physiological functions of the endoskeleton in cuttlefish. The hierarchical structures of the dorsal and lamellar layers contribute to the mechanical properties of CB, while buoyancy control is achieved by the diffusion of gases between thin calcareous pillars (Birchall and Thomas 1983). Images of the CB fragments showed significant structural differences between the dorsal and lamellar layers (Fig. 1). Two layers of the dorsal shield were observed (Fig. 1a). The outer layer had a burgeoned shape with an open core structure approximately 200 μm in diameter, while the underlying layer had a smooth, non-porous structure. The presence of holes in the outer layer of the dorsal shield could be explained by the need for a nutrients supply and for metabolic activity product elimination from the CB to the surrounding mantle. In association with aragonite, β-chitin fibres of the dorsal shield were arranged in a compact manner and served as a shield for the underlying porous lamellar structure. A transverse section of the lamellar CB layer is presented in Fig. 1b. As shown in Fig. 1c, demineralised dorsal CB is a transparent film of β-chitin.

The presence of macro- and microelements, such as Ca, P, Mg, Sr, Fe, Na, Cl, S, K, Cu, and Br, was evaluated in both sample groups. The lamellar and dorsal CB layers had similar elemental compositions. However, the iron concentration was higher in the dorsal shield (0.02%); chromium and zinc were also detected in this layer. The lamellar CB layer was richer in calcium (51%), while the concentration of phosphorus was almost the same in both samples (0.07 and 0.08% for the dorsal and lamellar layers, respectively). The total nitrogen content was determined to be 0.6 and 1.5% in the lamellar and dorsal CB layers, respectively. The maximum amount of chitin in the lamellar and dorsal CB layers was calculated as 8 and 22%, respectively, according to the detected nitrogen content. Since the protein content is negligible as a source of nitrogen in CB (Xiao et al. 2005), it was ignored.

The contributions of biogenic counterparts towards cellulose-based scaffold structural and mechanical properties are presented in the following sections.

Characterisation of the RC/CB Composite and RC Matrix

CB microparticles were used for preparing the cellulose-based composite; the porous composite structure was achieved by lyophilisation.

FTIR spectra for the CB, RC matrix, and RC/CB composite samples are presented in Fig. 2. The characteristic absorption peaks assigned to aragonite at 1077 cm^{-1} for ν_1, a doublet at 713 and 700 cm^{-1} for ν_4, and 856 cm^{-1} for ν_2 are visible (Fig. 2(a)). Regarding carbonate ions, peaks at 1790 cm^{-1} for ν_2 and 2519 and 1481 cm^{-1} for ν_3 are also visible. A broad absorption band in the 3650–3200-cm^{-1} range was assigned to the stretching vibration of O–H groups. A weak absorption peak at 1630 cm^{-1} was attributed to amide groups, confirming the presence of chitin (Rocha et al. 2005; Kasaai 2008). The stretching vibrations of O–H and C–H groups at 3429 and 2890 cm^{-1}, respectively, were assigned to RC (Fig. 2(b)). Absorption peaks in the 1800–1600-cm^{-1} region were attributed to C=O groups (1746 cm^{-1}) and absorbed water (1642 cm^{-1}). The stretching of C–H groups appears at 1377 cm^{-1}. The vibrational frequencies of C–O–C at the β-glucoside linkage were observed at 1164 and 895 cm^{-1}. The absorption peak at 660 cm^{-1} was assigned to out-of-plane C–O–H stretching (Oh et al. 2005).

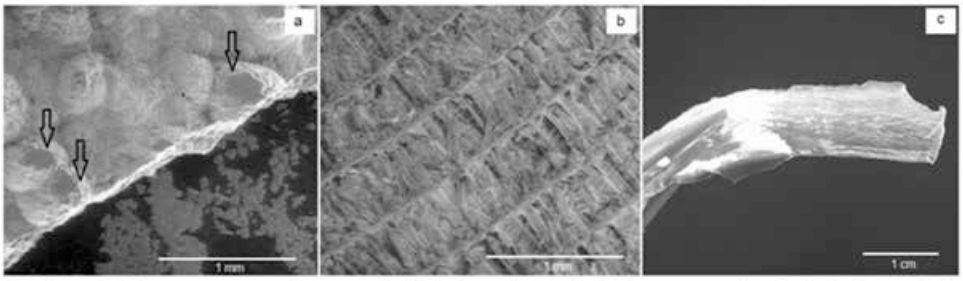

Fig. 1 Images of CB fragments: (a) top view of the outer and underlying layers of the dorsal shield, (b) transverse section of the lamellar layer, and (c) the demineralised dorsal layer

Absorption peaks arising from the presence of CB and RC were also observed in the RC/CB composite sample spectrum (Fig. 2(c)). Most characteristic CB peaks, such as those at 2519, 1790, 1481, 856, 713, and 700 cm^{-1}, were observed in the RC/CB composite sample spectrum. However, slight shifts of these frequencies to lower or higher absorption regions were clearly visible. The absorption peaks at 2890 and 1164 cm^{-1} in the RC spectrum remained in the RC/CB spectrum, while the absorption peaks at 1746, 1377, and 895 cm^{-1} decreased or almost disappeared.

Morphometric indices of the RC/CB composite and RC matrix were evaluated using μCT scanning (Table 1). The information provided by the 2D images suggested a macroporous structure of the RC/CB composite and RC matrix (Fig. 3a, b). Similar SV/TV values were calculated for both sample groups, as follows: 19.8 and 24.9% for the RC/CB composite and RC matrix, respectively. The SS/SV of the RC/CB composite was broader than that of the RC matrix, at 39.7 and 15.0 mm^{-1}, respectively. The Pr.Th of the RC/CB composite was 0.07 mm and had an influence on the larger SS/SV (39.7 mm^{-1}). The Pr.Sp values of the RC matrix and RC/CB composite samples were 0.4 and 0.2 mm, respectively, indicating that the latter had a more compact structure. These results were confirmed by 2D images, which also provided information regarding Pr.N values. As indicated by the Pr.N values, the density of internal partitions was greater in the RC/CB sample than in the RC sample, at 3.93 and 1.81 mm^{-1}, respectively. 3D reconstructions of the RC matrix and RC/CB composite are presented in Fig. 3c, d, respectively.

As shown in Fig. 4, RC/CB composites with pore sizes over a multi-scale range were obtained using the lyophilisation technique. Pore sizes ranging from 200 to 500 μm were predominant and accounted for nearly 84% of all pores. RC/CB composite pores ranging from 10 to 100 μm constituted only 3.5% of all pores, and only 1.2% of all pores were ranged from 800 to 900 μm in size. No pores larger than

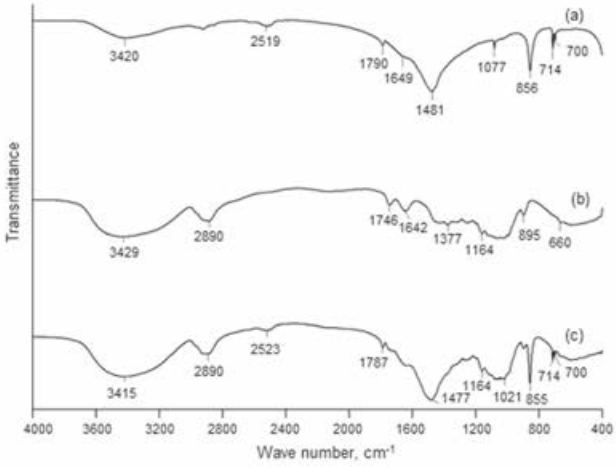

Fig. 2 FTIR spectra of (a) CB, (b) RC, and (c) the RC/CB composite

Table 1 Morphometric indices of the RC/CB composite and RC matrix

Sample name	Morphometric indices						
	SV/TV (%)	SS/SV (mm^{-1})	Pr.Th (mm)	Pr.Sp (mm)	Pr.N (mm^{-1})	Mean pore size (mm)	Porosity (%)
RC/CB composite	19.8	39.7	0.07	0.20	3.93	0.32	80.2
RC matrix	24.9	14.5	0.21	0.42	1.81	0.75	75.1

1000 μm were observed in the RC/CB composite structure. The mean pore sizes of the mineralised scaffold and the RC differed, as they were 324 and 750 μm, respectively.

Mechanical Properties of the RC/CB Composite and RC Matrix

The modulus of elasticity of the mineralised scaffold was 2.3-fold greater than that of the RC scaffold, at 3.5 ± 0.6 and 1.0 ± 0.2 MPa, respectively. A similar trend was observed for the compressive strength, which increased from 13.8 ± 0.3 MPa for the RC matrix to 21.5 ± 0.9 MPa for the RC/CB composite, respectively.

Cytotoxicity Evaluation of the RC/CB Composite and RC Matrix

In this section, the effects of the RC/CB composite vs those of the RC matrix on membrane integrity and cell metabolism were evaluated. No significant cell viability changes were observed after incubating the hepatocytes with RC/CB composite or RC matrix samples (Fig. 5). The RC/CB composites reduced cell viability only slightly in comparison with the control and RC matrix. Thus, the CB microparticles within the scaffold had no influence on cell viability.

Furthermore, to study the influence of the RC/CB composite on cell membrane integrity, the release of specific enzymes through cell membrane pores into the culture medium was investigated. Both the RC/CB and RC matrix samples demonstrated no effect on LDH release into the medium (Fig. 6a). Compared with the control, the RC/CB composite and RC matrix samples resulted in a slight but insignificant increase in the aldolase activity of the EDL muscle samples (Fig. 6b). The LDH release and aldolase activity tests clearly demonstrated that the presence of CB microparticles in the polymer framework had a positive influence on the plasma membrane integrity of liver and muscle cells relative to that of the RC matrix alone.

Discussion

This study presented the significance of CB for bone grafting through examining features of the raw material and its natural polymer-based composite that are essential for this purpose. The elements of the CB material might replace those in the mineral phase of bone when used as a bone substitute material. The CB elemental composition data obtained in our study and by other authors appeared to be incomparable (Table 2). Several authors have presented elemental data obtained via inductively coupled plasma atomic emission spectroscopy

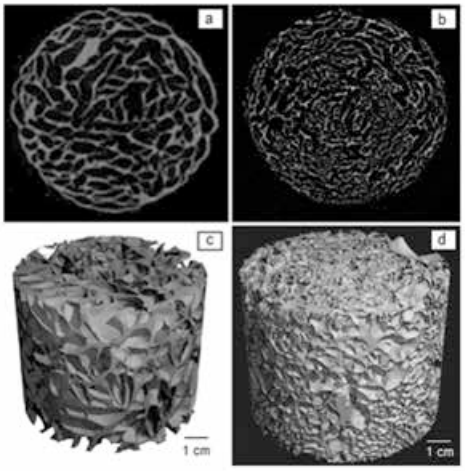

Fig. 3 Architecture of the RC matrix and RC/CB composite as evaluated by μCT: (a, b) 2D images and (c, d) 3D reconstructions, respectively

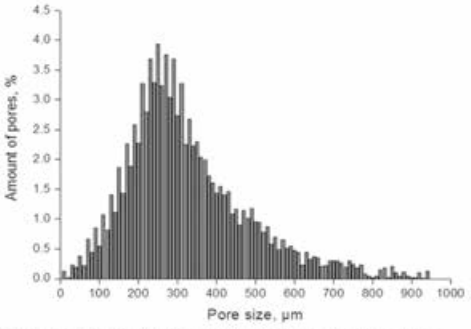

Fig. 4 Pore size distribution percentage within the RC/CB composite

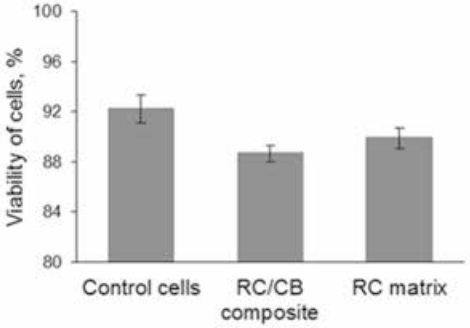

Fig. 5 Effect of the RC/CB composite and RC matrix on hepatocyte using trypan blue assay: (a) untreated cells, (b) cells treated with powdered RC/CB composite particles, and (c) cells treated with powdered RC matrix particles. $P < 0.05$ compared with the control group

measurements of CB (Florek et al. 2009; García-Enriquez et al. 2010; Turan and Yaglioglu 2010; Park et al. 2012). However, this technique has some obvious limitations; thus, only incomplete data regarding the lamellar CB elemental composition are available. Additionally, 1.4% of nitrogen was found in CB by Florek et al. (2009); however, the region of investigation was not clearly mentioned. To the best of our knowledge, the dorsal layer of CB has not been studied, and only the elemental composition of CB fossils is available (Doguzhaeva et al. 2012). There are multiple explanations for these deviations. Obtained data depends on the sensitivity of the selected analytical tool and the potential variability in the elemental constituents of different species. Marine environmental factors, such as climate, seasonal changes, and medium salinity, as well as cephalopod age and health, also have a significant influence on the formation of a living organism and the composition of its organs, e.g. the endoskeleton of cuttlefish (Gauvrit et al. 1998; Sherrard 2000; Kassahn et al. 2003; Özyurt et al. 2006; Zumholz et al. 2007; Gutowska et al. 2010; Dorey et al. 2013; Zhang et al. 2014).

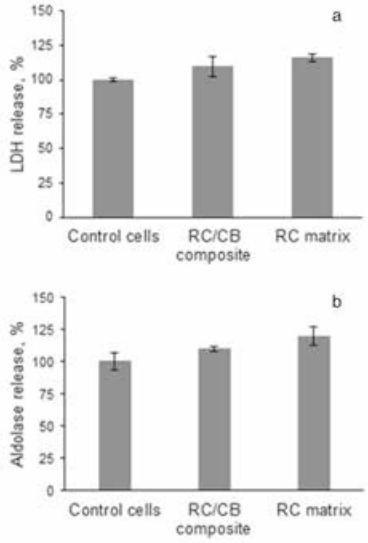

Fig. 6 Impact of the RC/CB composite and RC matrix specimens on (**a**) LDH release into the incubation medium of the hepatocytes and (**b**) aldolase release into the incubation medium of the EDL cells. $P < 0.05$ compared with the control group

Dermience et al. (2015) presented a complete review of the importance of various bioinorganic elements for enzymatic and metabolic activities during the bone growth process. In CB, the bioinorganic element structure is closely connected to that of the chitin fibres. The *Sepia* endoskeleton structure is based on the β-chitin arrangement, which therefore plays a significant role in mineralisation. An organised pillar structure repeats layer by layer, constructing a porous interconnected framework (Birchall and Thomas 1983). While mineral formation centres enter the chitin fibres, the initiation of mineral phase ingrowth occurs (Falini and Fermani 2004). Organic fibres in association with aragonite are arranged in a compact manner and serve as a shield for an underlying lamellar frame (Checa et al. 2015). The distribution of the chitin fibres and further mineralisation organises and strengthens the endoskeleton of a mollusc. CB chitin makes a framework by organising thin pillar walls for mineral phase ingrowth (Kayano et al. 2011). Thus, the concept of CB compositional-architectural performance could be beneficial for new bone tissue ingrowth.

The high DA of chitin indicates improved mechanical properties of the material (Aranaz et al. 2009). To verify the mechanical properties of chitin in the RC/CB composites, the DA of chitin was measured before and after composite formation. The DA of chitin decreased from 90.0% in CB to 88.5% in the RC/CB composites. This slight decrease in chitin DA resulting from RC/CB composite preparation suggests that the mechanical properties of chitin were preserved (Pillai et al. 2009). The presence of chitin in the cellulose-based scaffold leads to a synergetic behaviour of both biopolymers regarding their mechanical properties (Marsano et al. 2002). Considering the results of other authors (Zheng et al. 2002; Zhang et al. 2009), some interaction between cellulose and chitin could be expected.

The interconnected porous structure with a randomly ordered pore distribution in the RC/CB composites and RC matrix was achieved by lyophilisation. As shown in the 2D images (Fig. 3a, b), the RC/CB composite exhibited a more compact structure than that of the RC matrix because of the formation of smaller pores. Immobilising CB microparticles in the RC gel increased the porosity of the resultant framework; however, the mean pore size was approximately halved,

Table 2 Comparative elemental composition (%) data of the dorsal and lamellar CB layers

Element	CB dorsal layer		CB lamellar layer			
	Our study	Doguzhaeva et al. (2012)	Our study	Doguzhaeva et al. (2012)	García-Enriquez et al. (2010)	Florek et al. (2009)
Calcium	43.90	10.1	50.80	12.87–60.35	48.00	n. d.
Phosphorus	0.07	n. d.	0.08	2.10–12.87	2.09	n. d.
Magnesium	0.14	1.5	0.18	0.03–0.93	n. d.	0.13
Strontium	0.36	3.2	0.48	0.15–3.45	n. d.	0.28
Zinc	0.14	n. d.	n. d.	0.07	n. d.	n. d.
Iron	0.02	n. d.	0.004	0.16–8.89	n. d.	0.03
Sodium	0.37	2.6	0.65	0.06–0.65	0.57	1.00
Chlorine	1.83	11.3	1.41	0.76–26.93	n. d.	n. d.
Sulphur	0.44	n. d.	0.22	n. d.	n. d.	n. d.
Potassium	0.05	n. d.	0.05	0.37–0.92	0.05	0.26
Cuprum	56.00	n. d.	46.00	n. d.	n. d.	n. d.
Bromine	97.00	n. d.	45.00	n. d.	n. d.	n. d.
Chromium	0.004	n. d.	n. d.	n. d.	n. d.	n. d.
Silicon	0.01	n. d.	n. d.	0.1–10.21	n. d.	n. d.
Fluorine	n. d.	n. d.	n. d.	0.19–4.53	n. d.	n. d.
Aluminium	n. d.	n. d.	n. d.	0.05–4.35	n. d.	n. d.

Cu and Br concentrations are presented in ppm

n. d. not detected

with values of 0.75 and 0.32 mm for the RC matrix and RC/CB composite, respectively. Smaller pores result in a smaller volume fraction and a more compact and stable framework (Fig. 3). These results contribute to the improvements in the mechanical properties of the mineralised scaffold. Thus, the modulus of elasticity and compressive stress values of the RC/CB composite were higher than those of the RC matrix. The obtained mechanical properties are comparable with those of other composites and human cancellous bone (Table 3). For instance, the modulus of elasticity of human bone has an optimal value ranging from 20 to 500 MPa, while compressive strength ranged from 4 to 12 MPa (Yang et al. 2001). It could be concluded that RC/CB scaffold composition and morphology were able to resolve essential question regarding the mechanical properties of cuttlebone material.

The architecture of a scaffold is an extremely important characteristic in the design of bone substitutes. Determinant requirements are usually related to the morphological parameters of trabecular bone. Optimal porosity, pore sizes, and pore geometry are the main structural characteristics that could guarantee the satisfaction of basic demands by a scaffold in vivo, e.g. vascularisation, osteoconductive properties, and mechanical performance (Olszta et al. 2007; Stevens 2008; Liu et al. 2013).

Numerous in vivo studies have confirmed the necessity of optimal scaffold porosity for successful osteogenesis (Colombo et al. 2010; Murphy et al. 2010; Han et al. 2014). The pore sizes of healthy adult trabecular bone are distributed over multiple scales, ranging from 30 to 90% (Johnson and Herschler 2011). A similar pore arrangement was observed in the 2D images of the RC/CB composite (Fig. 3a, b). The minimum required pore size of a bone scaffold is ≥ 100 μm, while diameters greater than 800 μm could negatively affect the mechanical properties of a graft. Moreover, when the pore sizes of a scaffold are less than 50 μm, fibrous tissue is expected to form, disturbing normal bone restoration (Karageorgiou and Kaplan 2005). Pore sizes ranging from 200 to 500 μm are desirable for successful vascularisation.

Table 3 Comparative mechanical properties data of the RC/CB composite, RC matrix, other composites, and cancellous human bone

Mechanical property	RC/CB composite	RC matrix	PLGA/collagen Lee et al. 2006	PCL/HAp Razak et al. 2012	Cancellous bone Yang et al. 2001
Modulus of elasticity (MPa)	3.5 ± 0.6	1.0 ± 0.2	5.56	–	20–500
Compressive strength (MPa)	21.5 ± 0.9	13.8 ± 0.3	0.83	0.6–15.9	4–12

The proper arrangement of pores mimics the structural performance of natural bone and maintains the crucial stages of new osseous tissue formation (Mastrogiacomo et al. 2006). The pore size distribution within the RC/CB composite was multidimensional, ranging from 100 to 900 μm. Taking into consideration the correlation of SV/TV to the structural model index (Hildebrand and Rüegsegger 1997), the porous architecture of both scaffolds should be useful for bone growth. Owing to its larger SS/SV, the RC/CB composite could be expected to be more beneficial for cell adhesion, proliferation, and differentiation (Wang et al. 2014; Florencio-Silva et al. 2015).

Porosity is closely related to scaffold pore size and has a large influence on vascularisation. For instance, no bone tissue ingrowth or fibrous tissue formation appeared when the scaffold porosity was insufficient, i.e. ranging from 34 to 47% (Whang et al. 1999; Yang et al. 2001). The RC/CB composite and RC matrix had similar porosity values, at 80 and 75%, respectively. These data appeared to correlate well with the porosities of both polymer/mineral composites prepared by other authors and those of natural bone samples. For instance, HAp/PCL, collagen/HAp, and poly(lactide-*co*-glycolide)/collagen/apatite composites have shown porosity values of 87, 79, and 87%, respectively (Karageorgiou and Kaplan 2005). The trabecular regions of the maxilla and mandible have porosities ranging from 51 to 93% (Kim et al. 2013b).

To support the clinical application of RC/CB composites, the biocompatibility of the grafts must first be investigated. In our study, the effects of the RC/CB composite vs the RC matrix on cytotoxicity, membrane integrity, and cell metabolism were evaluated. Hepatocytes were selected for the cell viability tests as they are highly sensitive to toxic influences and physical damage and are thus good indicators of metabolic disruption and adverse effects. Compared with the control, no significant changes in hepatocyte viability were observed after incubation in the presence of the RC/CB composite (Fig. 5). LDH or aldolase outflow from cells into the culture medium indicates disrupted membrane integrity, i.e. the formation of pores large enough to allow the passage of large protein molecules. LDH is found in many body tissues, including the liver. Elevated levels of LDH may indicate liver damage. LDH test is a common clinical procedure to estimate body tissue damage. Moreover, LDH assay is a very common procedure to detect the cytotoxicity effects and even could be applied to detect cell growth inhibition (Smith et al. 2011). Aldolase is an enzyme that catalyses a reversible reaction that splits fructose 1,6-bisphosphate into dihydroxyacetone phosphate (DHAP) and glyceraldehyde 3-phosphate (GAP). It is found in high amount in muscle tissue. In case of cell damage, aldolase can come out of the cell and be detected by biochemical methods (Achalandabaso et al. 2014). Muscle cells were used in these experiments because of their direct interaction with bone tissue during the recovery process, and their significant role under normal circumstances in bone graft regeneration. EDL muscle samples were selected to allow the simultaneous representation of all three muscle fibre types: I, IIa, and IIb. The obtained results clearly demonstrate that the RC/CB composites and RC matrix had no damaging effects on the plasma membrane of the liver and muscle cells (Fig. 6a, b).

The insulin sensitivity of target cells is highly influenced by various stressors, and insensitivity to insulin indicates that a cell is under abnormal physiological conditions. Muscle tissue is one of the main targets of insulin. Estimating the basal- and insulin-stimulated radiolabelled glucose, uptake rates in the EDL muscle samples showed only insignificant differences, indicating that the composite scaffolds did not have a disruptive impact on the metabolic integrity of the muscle cells (Fig. 7). Both the RC/CB composites and RC matrix had no influence on the basal- or insulin-stimulated glucose uptake. The cytotoxicity data demonstrate that the prepared RC/CB composite could be safely applied in vivo without inducing any toxic effects or acute metabolic disorders.

Conclusions

Macroporous regenerated cellulose/cuttlebone composite scaffolds were prepared via lyophilisation. The obtained scaffolds were characterised as possessing optimal morphometric features with respect to those of trabecular bone. The contents of trace elements in the cuttlebone lamellar and dorsal layers were similar to those in human bone tissue. The cuttlebone components improved the structural and, therefore, mechanical properties of the cellulose framework. The present research demonstrated the non-cytotoxicity of the regenerated cellulose/cuttlebone composite in terms of its compatibility with living tissues. It could be concluded that cuttlebone is a promising material of marine origin for bone tissue engineering.

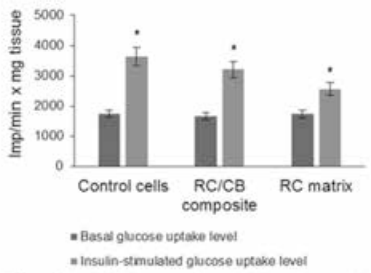

Fig. 7 Effect of the RC/CB composite and RC matrix on the insulin-stimulated glucose uptake by isolated EDL cells. $^{*}P < 0.05$ compared with the basal glucose uptake level

Acknowledgements The authors want to thank Springer Nature Author Services for English grammar proof on the paper.

Funding Information The study was financially supported by the Lithuanian Research Council in the form of grant MIP019/2014.

Compliance with Ethical Standards

Ethical Approval All animal procedures were performed in accordance with approved animal handling guidelines (Directive 2010/63/EU of the European Parliament and of the Council of 22 September 2010 on the protection of animals used for scientific purposes).

Conflict of Interest The authors declare that they have no conflicts of interest.

References

Achalandabaso A, Plaza-Manzano G, Lomas-Vega R, Martínez-Amat A, Camacho MV, Gassó M, Hita-Contreras F, Molina F (2014) Tissue damage markers after a spinal manipulation in healthy subjects: a preliminary report of a randomized controlled trial. Dis Markers 2014:1–7

Amini AR, Laurencin CT, Nukavarapu SP (2012) Bone tissue engineering: recent advances and challenges. Crit Rev Biomed Eng 40:363–408

Anderson JM, Rodriguez A, Chang DT (2008) Foreign body reaction to biomaterials. Semin Immunol 20:86–100

Aranaz I, Mengíbar M, Harris R, Paños I, Miralles B, Acosta N, Galed G, Heras Á (2009) Functional characterization of chitin and chitosan. Curr Chem Biol 3:203–230

Baptista A, Ferreira I, Borges JP (2013) In: Thakur VK, Singha AS (eds) Biomass-based biocomposites. Smithers Rapra Technology, Shrewsbury

Birchall J, Thomas N (1983) On the architecture and function of cuttlefish bone. J Mater Sci 18:2081–2086

Brennan O, Stenson B, Widaa A (2015) Incorporation of the natural marine multi-mineral dietary supplement Aquamin enhances osteogenesis and improves the mechanical properties of a collagen-based bone graft substitute. J Mech Behav Biomed 47:114–123

Brutman-Barazani T, Horovitz-Fried M, Aga-Mizrachi S, Brand C, Brodie C, Rosa J, Sampson SR (2012) Protein kinase Cδ but not PKCα is involved in insulin-induced glucose metabolism in hepatocytes. J Cell Biochem 113:2064–2076

Cadman J, Zhou S, Chen Y, Li Q (2012) Cuttlebone: characterisation, application and development of biomimetic materials. J Bionic Eng 9:367–376

Checa AG, Cartwright JH, Sánchez-Almazo I, Andrade JP, Ruiz-Raya F (2015) The cuttlefish Sepia officinalis (Sepiidae, Cephalopoda) constructs cuttlebone from a liquid-crystal precursor. Sci Rep 5:11513

Chen YM, Xi T, Zheng Y, Guo T, Hou J, Wan Y, Gao C (2009) In vitro cytotoxicity of bacterial cellulose scaffolds used for tissue-engineered bone. J Bioact Compat Polym 24:137–145

Clarke S, Walsh P, Maggs C, Buchanan F (2011) Designs from the deep: marine organisms for bone tissue engineering. Biotechnol Adv 29:610–617

Colombo P, Vakifahmetoglu C, Costacurta S (2010) Fabrication of ceramic components with hierarchical porosity. J Mater Sci 45:5425–5455

Culverwell E, Wimbush SC, Hall SR (2008) Biotemplated synthesis of an ordered macroporous superconductor with high critical current density using a cuttlebone template. Chem Commun 0:1055–1057

Cunningham E, Dunne N, Walker G, Maggs C, Wilcox R, Buchanan F (2010) Hydroxyapatite bone substitutes developed via replication of natural marine sponges. J Mater Sci Mater Med 21:2255–2261

Denton E, Gilpin-Brown J, Howarth J (1961) The osmotic mechanism of the cuttlebone. J Mar Biol Assoc UK 41:351–363

Dermience M, Lognay G, Mathieu F, Goyens P (2015) Effects of thirty elements on bone metabolism. J Trace Elem Med Biol 32:86–106

Dogan E, Okumus Z (2014) Cuttlebone used as a bone xenograft in bone healing. Vet Med Czech 59:254–260

Doguzhaeva LA, Weaver PG, Ciampaglio CN (2012) A unique late Eocene coleoid cephalopod Mississaepia from Mississippi, USA: new data on cuttlebone structure, and their phylogenetic implications. Acta Palaeontol Pol 59:147–162

Dorey N, Melzner F, Martin S, Oberhänsli F, Teyssié J, Bustamante P, Gattuso J, Lacoue-Labarthe T (2013) Ocean acidification and temperature rise: effects on calcification during early development of the cuttlefish Sepia officinalis. Mar Biol 160:2007–2022

Falini G, Fermani S (2004) Chitin mineralization. Tissue Eng 10:1–6

Florek M, Fornal E, Gómez-Romero P, Zieba E, Paszkowicz W, Lekki J, Nowak J, Kuczumow A (2009) Complementary microstructural and chemical analyses of Sepia officinalis endoskeleton. Mater Sci Eng C 29:1220–1226

Florencio-Silva R, Sasso G, Sasso-Cerri E, Simões MJ, Cerri PS (2015) Biology of bone tissue: structure, function, and factors that influence bone cells. Biomed Res Int 2015:1–17

Franz S, Rammelt S, Scharnweber D, Simon JC (2011) Immune responses to implants—a review of the implications for the design of immunomodulatory biomaterials. Biomaterials 32:6692–6709

García-Enriquez S, Guadarrama H, Reyes-González I, Mendizábal E, Jasso-Gastinel C, García-Enríquez B, Rembao-Bojórquez D, Pane-Pianese C (2010) Mechanical performance and in vivo tests of an acrylic bone cement filled with bioactive sepia officinalis cuttlebone. J Biomat Sci Polym Ed 21:113–125

Gauvrit E, Du Sel GP, Daguzan J (1998) Age group determination by analysis of the cuttlebone of the cuttlefish Sepia officinalis L. in reproduction in the Bay of Biscay. J Molluscan Stud 64:183–193

Givissis PK, Stavridis SI, Papagelopoulos PJ, Antonarakos PD, Christodoulou AG (2010) Delayed foreign-body reaction to absorbable implants in metacarpal fracture treatment. Clin Orthop Relat Res 468:3377–3383

Gutowska MA, Melzner F, Pörtner HO, Meier S (2010) Cuttlebone calcification increases during exposure to elevated seawater pCO_2 in the cephalopod Sepia officinalis. Mar Biol 157:1653–1663

Han X, Li X, Lin H, Ma J, Chen X, Bian C, Wu X, Qu F (2014) Hierarchical meso–macroporous bioglass for bone tissue engineering. J Sol Gel Sci Technol 70:33–39

Hildebrand T, Rüegsegger P (1997) Quantification of bone microarchitecture with the structure model index. Comput Methods Biomech 1:15–23

Hildebrand T, Laib A, Müller R, Dequeker J, Rüegsegger P (1999) Direct three-dimensional morphometric analysis of human cancellous bone: microstructural data from spine, femur, iliac crest, and calcaneus. J Bone Miner Res 14:1167–1174

Jayakumar R, Chennazhi KP, Srinivasan S, Nair SV, Furuike T, Tamura H (2011) Chitin scaffolds in tissue engineering. Int J Mol Sci 12:1876–1887

Jia X, Qian W, Wu D, Wei D, Xu G, Liu X (2009) Cuttlebone-derived organic matrix as a scaffold for assembly of silver nanoparticles and application of the composite films in surface-enhanced Raman scattering. Colloid Surface B 68:231–237

Johnson AJW, Herschler BA (2011) A review of the mechanical behavior of CaP and CaP/polymer composites for applications in bone replacement and repair. Acta Biomater 7:16–30

Kannan S, Rocha J, Agathopoulos S, Ferreira J (2007) Fluorine-substituted hydroxyapatite scaffolds hydrothermally grown from aragonitic cuttlefish bones. Acta Biomater 3:243–249

Karageorgiou V, Kaplan D (2005) Porosity of 3D biomaterial scaffolds and osteogenesis. Biomaterials 26:5474–5491
Kasaai MR (2008) A review of several reported procedures to determine the degree of N-acetylation for chitin and chitosan using infrared spectroscopy. Carbohydr Polym 71:497–508
Kassahn K, Donnellan S, Fowler A, Hall K, Adams M, Shaw P (2003) Molecular and morphological analyses of the cuttlefish Sepia apama indicate a complex population structure. Mar Biol 143:947–962
Kayano K, Saruwatari K, Kogure T, Shiraiwa Y (2011) Effect of coccolith polysaccharides isolated from the coccolithophorid, Emiliania huxleyi, on calcite crystal formation in in vitro $CaCO_3$ crystallization. Mar Biotechnol 13:83–92
Kim B, Kang HJ, Lee J (2013a) Improvement of the compressive strength of a cuttlefish bone-derived porous hydroxyapatite scaffold via polycaprolactone coating. J Biomed Mater Res B 101:1302–1309
Kim J, Shin J, Oh S, Yi W, Heo M, Lee S, Choi S, Huh KH (2013b) The three-dimensional microstructure of trabecular bone: analysis of site-specific variation in the human jaw bone. Imaging Sci Dent 43:227–233
Kurita K (2006) Chitin and chitosan: functional biopolymers from marine crustaceans. Mar Biotechnol 8:203–226
Lee SJ, Lim GJ, Lee J, Atala A, Yoo JJ (2006) In vitro evaluation of a poly(lactide-co-glycolide)–collagen composite scaffold for bone regeneration. Biomaterials 27:3466–3472
Lin Z, Solomon KL, Zhang X, Pavlos NJ, Abel T, Willers C, Dai K, Xu J, Zheng Q, Zheng M (2011) In vitro evaluation of natural marine sponge collagen as a scaffold for bone tissue engineering. Int J Biol Sci 7:968–977
Liu Y, Lim J, Teoh S (2013) Review: development of clinically relevant scaffolds for vascularised bone tissue engineering. Biotechnol Adv 31:688–705
Marsano E, Conio G, Martino R, Turturro A, Bianchi E (2002) Fibers based on cellulose-chitin blends. J Appl Polym Sci 83:1825–1831
Mastrogiacomo M, Scaglione S, Martinetti R, Dolcini L, Beltrame F, Cancedda R, Quarto R (2006) Role of scaffold internal structure on in vivo bone formation in macroporous calcium phosphate bioceramics. Biomaterials 27:3230–3237
Mayer A, Rodríguez AD, Taglialatela-Scafati O, Fusetani N (2013) Marine pharmacology in 2009–2011: marine compounds with antibacterial, antidiabetic, antifungal, anti-inflammatory, antiprotozoal, antituberculosis, and antiviral activities; affecting the immune and nervous systems, and other miscellaneous mechanisms of action. Mar Drugs 11:2510–2573
Meyers MA, Chen P, Lin AY, Seki Y (2008) Biological materials: structure and mechanical properties. Prog Mater Sci 53:1–206
Morganti P, Morganti G (2008) Chitin nanofibrils for advanced cosmeceuticals. Clin Dermatol 26:334–340
Murphy CM, Haugh MG, O'Brien FJ (2010) The effect of mean pore size on cell attachment, proliferation and migration in collagen–glycosaminoglycan scaffolds for bone tissue engineering. Biomaterials 31:461–466
Muzzarelli RA (2009) Chitins and chitosans for the repair of wounded skin, nerve, cartilage and bone. Carbohydr Polym 76:167–182
Nagahama H, Nwe N, Jayakumar R, Koiwa S, Furuike T, Tamura H (2008) Novel biodegradable chitin membranes for tissue engineering applications. Carbohydr Polym 73:295–302
Nge TT, Sugiyama J (2007) Surface functional group dependent apatite formation on bacterial cellulose microfibrils network in a simulated body fluid. J Biomed Mater Res A 81:124–134
Ogasawara W, Shenton W, Davis SA, Mann S (2000) Template mineralization of ordered macroporous chitin-silica composites using a cuttlebone-derived organic matrix. Chem Mater 12:2835–2837
Oh SY, Yoo DI, Shin Y, Kim HC, Kim HY, Chung YS, Park WH, Youk JH (2005) Crystalline structure analysis of cellulose treated with sodium hydroxide and carbon dioxide by means of X-ray diffraction and FTIR spectroscopy. Carbohydr Res 340:2376–2391
Olszta MJ, Cheng X, Jee SS, Kumar R, Kim Y, Kaufman MJ, Douglas EP, Gower LB (2007) Bone structure and formation: a new perspective. Mater Sci Eng R 58:77–116
Özyurt G, Duysak Ö, Akamca E, Tureli C (2006) Seasonal changes of fatty acids of cuttlefish Sepia officinalis L. (Mollusca: Cephalopoda) in the north eastern Mediterranean Sea. Food Chem 95:382–385
Park J, Lim Y, Youn M, Gwon H, Nho Y (2012) Biodegradable polycaprolactone/cuttlebone scaffold composite using salt leaching process. Korean J Chem Eng 29:931–934
Petrauskaite O, Gomes PS, Fernandes MH, Juodzbalys G, Stumbras A, Maminskas J, Liesiene J, Cicciù M (2013) Biomimetic mineralization on a macroporous cellulose-based matrix for bone regeneration. Biomed Res Int 2013:1–9
Petrauskaite O, Juodzbalys G, Viskelis P, Liesiene J (2016) Control of the porous structure of cellulose-based tissue engineering scaffolds by means of lyophilization. Cellul Chem Technol 50:23–30
Petrenko AY, Sukach A (1991) Isolation of intact mitochondria and hepatocytes using vibration. Anal Biochem 194:326–329
Pillai C, Paul W, Sharma CP (2009) Chitin and chitosan polymers: chemistry, solubility and fiber formation. Prog Polym Sci 34:641–678
Pina S, Oliveira JM, Reis RL (2015) Natural-based nanocomposites for bone tissue engineering and regenerative medicine: a review. Adv Mater 27:1143–1169
Razak SIA, Sharif N, Rahman W (2012) Biodegradable polymers and their bone applications: a review. J Basic Appl Sci 12:31–49
Rocha J, Lemos A, Agathopoulos S, Valério P, Kannan S, Oktar F, Ferreira J (2005) Scaffolds for bone restoration from cuttlefish. Bone 37:850–857
Shankar S, Reddy JP, Rhim J, Kim H (2015) Preparation, characterization, and antimicrobial activity of chitin nanofibrils reinforced carrageenan nanocomposite films. Carbohydr Polym 117:468–475
Sherrard KM (2000) Cuttlebone morphology limits habitat depth in eleven species of Sepia (Cephalopoda: Sepiidae). Biol Bull 198:404–414
Sibley JA, Lehninger AL (1949) Determination of aldolase in animal tissues. J Biol Chem 177:859–872
Siddiquee MRA, Sultana A, Siddiquee A (2013) Scientific review of Os Sepia (Jhaag-e-Darya/Samudra Phena) with respect to Indian medicine and its characterization on physicochemical parameters. Int J Pharm India 2:669–678
Silva TH, Alves A, Ferreira B, Oliveira JM, Reys L, Ferreira R, Sousa R, Silva SS, Mano JF, Reis RL (2012) Materials of marine origin: a review on polymers and ceramics of biomedical interest. Int Mater Rev 57:276–306
Smith SM, Wunder MB, Norris DA, Shellman YG (2011) A simple protocol for using a LDH-based cytotoxicity assay to assess the effects of death and growth inhibition at the same time. PLoS One 6:1–6
Stevens MM (2008) Biomaterials for bone tissue engineering. Mater Today 11:18–25
Subia B, Kundu J, Kundu S (2010) In: Eberli D (ed) Tissue engineering. InTech, Rijeka
Turan C, Yaglioglu D (2010) Population identification of common cuttlefish (Sepia officinalis) inferred from genetic, morphometric and cuttlebone chemistry data in the NE Mediterranean Sea. Sci Mar 74:77–86
Vázquez B, Ginebra MP, Gil X, Planell JA, San Román J (2005) Acrylic bone cements modified with β-TCP particles encapsulated with poly (ethylene glycol). Biomaterials 26:4309–4316
Wang C, Wang X, Xu X, Yuan X, Gou W, Wang A, Guo Q, Peng J, Lu S (2014) Bone microstructure and regional distribution of osteoblast and osteoclast activity in the osteonecrotic femoral head. PLoS One 9:1–10
Whang K, Healy KE, Elenz DR, Nam EK, Tsai DC, Thomas CH, Nuber GW, Glorieux FH, Travers R, Sprague SM (1999) Engineering bone

regeneration with bioabsorbable scaffolds with novel microarchitecture. Tissue Eng 5:35–51
Won S, Lee JM, Cheong J, Park H, Seo J (2015) Evaluation of the biocompatibility of cuttlebone in mouse. J Vet Clin 32:417–421
Xiao S, Zheng X, Wang Z, Wang R (2005) A study of the organic matrix of cuttlebone: molecular weights, characterized infrared spectrum and amino acid composition. Res Bull Phuket Mar Biol Cent 66: 235–241
Xu J, McCarthy SP, Gross RA, Kaplan DL (1996) Chitosan film acylation and effects on biodegradability. Macromolecules 29:3436–3440
Xu G, Li H, Ma X, Jia X, Dong J, Qian W (2009) A cuttlebone-derived matrix substrate for hydrogen peroxide/glucose detection. Biosens Bioelectron 25:362–367
Yang S, Leong K, Du Z, Chua C (2001) The design of scaffolds for use in tissue engineering. Part I. Traditional factors. Tissue Eng 7:679–689
Zaborowska M, Bodin A, Bäckdahl H, Popp J, Goldstein A, Gatenholm P (2010) Microporous bacterial cellulose as a potential scaffold for bone regeneration. Acta Biomater 6:2540–2547
Zhang X, Vecchio KS (2013) Conversion of natural marine skeletons as scaffolds for bone tissue engineering. Front Mater Sci 7:103–117
Zhang S, Li F, Yu J (2009) Preparation of cellulose/chitin blend bio-fibers via direct dissolution. Cellul Chem Technol 43:393–398
Zhang Y, Cheng Q, Yao Y, Guo X, Wang R, Peng Z (2014) A preliminary study: saltiness and sodium content of aqueous extracts from plants and marine animal shells. Eur Food Res Technol 238:565–571
Zhao Z, Liang Z, Ping G (2011) Macroscopic identification of Chinese medicinal materials: traditional experiences and modern understanding. J Ethnopharmacol 134:556–564
Zheng H, Zhou J, Du Y, Zhang L (2002) Cellulose/chitin films blended in NaOH/urea aqueous solution. J Appl Polym Sci 86:1679–1683
Zumholz K, Hansteen TH, Piatkowski U, Croot PL (2007) Influence of temperature and salinity on the trace element incorporation into statoliths of the common cuttlefish (Sepia officinalis). Mar Biol 151:1321–1330

Mandibular Third Molar Impaction: Review of Literature and a Proposal of a Classification

Gintaras Juodzbalys[1], Povilas Daugela[1]

[1]Department of Maxillofacial Surgery, Lithuanian University of Health Sciences, Kaunas, Lithuania.

Corresponding Author:
Gintaras Juodzbalys
Vainiku 12
LT- 46383, Kaunas
Lithuania
Phone: +370 37 29 70 55
Fax: +370 37 32 31 53
E-mail: gintaras@stilusoptimus.lt

ABSTRACT

Objectives: The purpose of present article was to review impacted mandibular third molar aetiology, clinical anatomy, radiologic examination, surgical treatment and possible complications, as well as to create new mandibular third molar impaction and extraction difficulty degree classification based on anatomical and radiologic findings and literature review results.
Material and Methods: Literature was selected through a search of PubMed, Embase and Cochrane electronic databases. The keywords used for search were mandibular third molar, impacted mandibular third molar, inferior alveolar nerve injury third molar, lingual nerve injury third molar. The search was restricted to English language articles, published from 1976 to April 2013. Additionally, a manual search in the major anatomy and oral surgery journals and books was performed. The publications there selected by including clinical and human anatomy studies.
Results: In total 75 literature sources were obtained and reviewed. Impacted mandibular third molar aetiology, clinical anatomy, radiographic examination, surgical extraction of and possible complications, classifications and risk factors were discussed. New mandibular third molar impaction and extraction difficulty degree classification based on anatomical and radiologic findings and literature review results was proposed.
Conclusions: The classification proposed here based on anatomical and radiological impacted mandibular third molar features is promising to be a helpful tool for impacted tooth assessment as well as for planning for surgical operation. Further clinical studies should be conducted for new classification validation and reliability evaluation.

Keywords: tooth impacted; molar, third; alveolar nerve, inferior; lingual nerve injuries; mandibular canal; classification.

Accepted for publication: 11 June 2013
To cite this article:
Juodzbalys G, Daugela P. Mandibular Third Molar Impaction: Review of Literature and a Proposal of a Classification.
URL: http://www.ejomr.org/JOMR/archives/2013/2/e1/v4n2e1ht.pdf
doi: 10.5037/jomr.2013.4201

INTRODUCTION

In early 1954 Mead [1] has defined an impacted tooth as a tooth that is prevented from erupting into position because of malposition, lack of space, or other impediments. Later Peterson [2], characterized impacted teeth as those teeth that fails to erupt into the dental arch within the expected time. In 2004 Farman [3] wrote that impacted teeth are those teeth that prevented from eruption due to a physical barrier within the path of eruption.

According to Elsey and Rock [4] impaction of the third molar is occurring in up to 73% of young adults in Europe. Generally, third molars have been found to erupt between the ages of 17 and 21 years [5,6]. Furthermore, third molar eruption time have been reported to vary with races [5-8]. For example, mandibular third molars may erupt as early as 14 years of age in Nigerians [7], and up to the age of 26 years in Europeans [8]. The average age for the eruption of mandibular third molars in male is approximately 3 to 6 months ahead of females [9]. Most authors claim that the incidence of mandibular third molar impaction is higher in females [8,10].

Third molar eruption and continuous positional changes after eruption can be related not only with race but also with nature of the diet, the intensity of the use of the masticatory apparatus and possibly due to genetic background [11].

Impaction of mandibular third molars is a common condition related with different difficulty degree of extraction operation and risk of complications, including iatrogenic trigeminal nerve injury. The purpose of present article was to review impacted mandibular third molar aetiology, clinical anatomy, radiologic examination, surgical treatment and possible complications, as well as to create new mandibular third molar impaction and extraction difficulty degree classification based on anatomical and radiologic findings and literature review results.

MATERIAL AND METHODS

Literature was selected through a search of PubMed, Embase and Cochrane electronic databases. The keywords used for search were mandibular third molar, impacted mandibular third molar, inferior alveolar nerve injury third molar, lingual nerve injury third molar. The search was restricted to English language articles, published from 1976 to April 2013. Additionally, a manual search in the major anatomy and oral surgery journals and books was performed. The publications there selected by including clinical and human anatomy studies.

RESULTS

Aetiology

Many theories have been proposed owing to high incidence of mandibular third molar impaction. One of the most popular theory is insufficient development of the retromolar space [12,13]. Mandibular ramus growth is related to resorption at its anterior surface and deposition at its posterior surface, but in case of disbalance of this process, the mandibular third molars don't get enough space to erupt [14]. Proper mandibular third molars eruption also depends on their favourable path of eruption. For example, if the tooth bud is medially angulated during the initial stages of calcification and root development the path of eruption will be unfavourable [15]. However, impaction of mandibular third molars can develop due to a decrease in the angulation of the mandible and an increase in the angulation of the mandibular plane [16]. Yamaoka et al. [18] found the relation between the root angulation and impaction: angulated roots were more common in impacted mandibular third molars as compared to erupted mandibular third molars. Some authors indicates other important third molar impaction causes: malposition of the tooth germ, hereditary factors [19], lack of sufficient eruption force for third molars, and the theory of phylogenetic regression of the jaw size - insufficient mesial movement of the dentition of modern human due to lack of interproximal attrition [20,21].

Clinical anatomy

Mandibular third molar is situated at the distal end of the body of the mandible where is connection with relatively thin ramus. There is the region of weakness and the fracture can occur if excessive force will be applied during impacted wisdom tooth elevation without preliminary and adequate removing of surrounding bone [22]. The buccal alveolar bone in this region is thicker than the lingual. The external oblique ridge forms the buttress that reinforced the buccal plate. The lingual nerve often lies close to the cortical plate. There is high risk of lingual nerve damage using lingual split technique or elevating third molar flap medially to the distoangular recess [23]. Rood and Shehab [24] showed on panoramic radiographs that in most cases the roots of third molars are in close proximity to the mandibular canal. Furthermore, in some cases third molar roots can contact or penetrate into mandibular canal or they can be deflected. Close relationship of

the canal with the roots can evoke inferior alveolar nerve damage during the surgery [22].

Radiologic examination

The location and configuration of impacted third molar, surrounding bone, mandibular canal and adjacent tooth are important in imaging diagnosis for the proper surgical operation planning. Periapical radiographs have been used for many years to assess the jaws during impacted teeth surgery. Long cone paralleling technique for taking periapical X-ray is the technique of choice for the following reasons: reduction of radiation dose; less magnification; a true relationship between the bone height and adjacent teeth is demonstrated [25]. One of the shortcomings of the present method is the use of film. Since the film is highly flexible, literally and figuratively, its processing can be suboptimal and it often leads poor image [26]. During the last decade, many dental practices replaced the film with digital imaging systems [28].

Nevertheless, the biggest concern of periapical radiographs is that mandibular canal could not be clearly identified in the third molar region. Furthermore, the angulation of the periapical film can affect the perceived location of the canal with respect to the bone crest [28]. When a specific region that is too large to be seen on a periapical view, panoramic radiograph can be the method of choice. The major advantages of panoramic images are the broad coverage of oral structures, low radiation exposure (about 10% of a full-mouth radiographs), and relatively inexpensive of the equipment. The major drawbacks of panoramic imaging are: lower image resolution, high distortion, and presence of phantom images. These can artificially produce apparent changes thus may hide some of important vital structures [12]. For example, cervical spine images often overlap on the anterior mandible. Furthermore, it depicts a two-dimensional view of an intricate three-dimensional anatomic relationship and also fails to accurately project the buccolingual relation between the tooth and the inferior alveolar canal [30,31].

Cone Beam Computed Tomography (CBCT) have been advocated as method of choice than there is need to have a three dimensional view of the mandibular third molar and adjacent anatomical structures [32,33]. Ghaeminia et al. [32] in prospective study evaluated the role of CBCT in the treatment of patients with impacted mandibular third molars (n = 53) at increased risk of inferior alveolar nerve injury. After reviewing the CBCT images, significantly more subjects were reclassified to a lower risk for IAN injury compared with the panoramic radiograph assessments. This change in risk assessment also resulted in a significantly different surgical approach ($P < 0.03$). Authors concluded that CBCT contributes to optimal risk assessment and, as a consequence, to more adequate surgical planning, compared with panoramic radiography. It was reconfirmed by study of Matzen et al. [33], where CBCT influenced the treatment plan for 12% of cases. Direct contact in combination with narrowing of the canal lumen and canal positioned in a bending or a groove in the root complex observed in CBCT images were significant factors for deciding to change treatment plan.

Indications for mandibular third molar extraction

According to the recommendations of National Institute of Health (NIH) [34] both impacted and erupted mandibular third molars with evidence of follicular enlargement should be removed electively and that the associated soft tissue should be submitted for microscopic examination. Impacted teeth with pericoronitis should also be extracted electively because of their known potential for repetitive infection and morbidity. Furthermore, third molars with non-restorable carious lesions and third molars contributing to resorption of adjacent teeth should be also extracted. Following indications for mandibular third molar extraction were highlighted by Koerner [35]: existing pathology or pain due to pericoronitis, periodontitis, periapical abscess, cysts or neoplasms, resorption of adjacent roots, and inflammation of the opposing soft tissue; aberrant positions in which the tooth is oriented buccally or lingually; preceding dental work with fixed or removable appliances; arch length discrepancy in cases when the impacted third molars are affecting the stability of orthodontic treatment. Lytle [20] added infection around the impaction; loss of bone around the impacted teeth; dental caries and damage of adjacent teeth; crowding of the dental arch; cysts and tumours associated with impacted teeth; pre-irradiation removal of impacted teeth; for prosthodontic reasons; and for chronic facial pain. The National Institute of Clinical Excellence (NICE) of England introduced guidelines relating to third molars surgery. These recommended against the prophylactic removal of third molars and listed specific clinical indications for surgery.

Surgical extraction of impacted mandibular third molar and possible complications

There are two main intraoral approaches for surgical removal of impacted mandibular third molars: one through the sublingual space and the other buccally through the entire mandibular thickness. There is also extraoral method from the submandibular space [36-38]. Sublingual access requires incision

and elevation of a wide mucoperiosteal intrasulcular flap on the lingual side of the mandible, in the molar and premolar regions. Dissection of the mylohyoid muscle attachment is necessary to reach the impacted molar. The buccal approach requires the elevation of a wide mucoperiosteal flap localized around the molar–premolar region. An extensive osteotomy is made underneath the apical area of the mandibular teeth. However there are many modifications of flap techniques, including envelope flap, two sided flap, and coma shaped flap [39]. In every case the third molar flap should provide adequate visualisation of the surgical field.

After mucoperiosteal flap elevation excessive bone must be excised using bur before third molar extraction. In most cases there will be necessary to remove buccal and distal bone borders. In difficult cases the tooth should be sectioned with a fissure bur in a high-speed handpiece. The wound should be irrigated with cool sterile physiologic saline solution. After tooth extraction using elevator or forceps it is necessary to clean operation area and to suture the wound without tension [40].

The frequency and severity of untoward events associated with surgical procedures are influenced by multiple factors that may be related to the procedure, patient, and/or surgeon [41]. Complications related to mandibular third molar extraction can be classified to intraoperative and postoperative [2]. Intraoperative complications are as follows: mandibular fracture, damage of adjacent teeth, tooth or tooth fragments displacement into soft tissues and bleeding. In cases if the excessive intraoral force was applied or/and part of bone was removed, risk of mandibular fracture or damage of adjacent teeth is increased [2,40]. Tooth or tooth fragments displacement into soft tissues can occur in case of wrong operation technique [41].

The most serious and unpleasant iatrogenic complication that arise from third molar surgery is inferior alveolar and/or lingual nerve injury and neurosensory function disturbance. The incidence of inferior alveolar nerve injury according to different authors varies from 0.81% to 22% of cases [42-47]. 1% to 4% of patients are at risk of permanent injury [48]. Lingual nerve injury incidence was reported between 0.4% and 25% [49-53]. Inferior alveolar nerve injury can cause paresthesia to complete numbness and/or pain [54] in the region of the skin of the mental area, the lower lip, mucous membranes, and the gingiva as far posteriorly as the second premolar [55]. Furthermore this commonly interferes with speech, eating, kissing, make-up application, shaving and drinking [56]. The injury of the lingual nerve leads to numbness of the ipsilateral anterior two thirds of the tongue and taste disturbance [50].

Typical postoperative complications are pain, swelling, bruising, trismus [57], osteitis and surgical site infection [58].

Classifications and risk factors identification

In order to minimise number of complications during mandibular third molar extraction several classifications have been developed that are assessing the difficulty of surgical procedure and helping to create an optimal treatment plan. The most popular are Winter's [59] and Pell and Gregory's [60] systems who are classifying the inclinations and positions of the third molars based on the relation among the dental longitudinal axis, occlusal plane and ascending mandibular ramus. These systems have been extensively adopted and applied in clinical practice. However some authors claim that these scales have little value for predicting the degree of extraction difficulty, [61] mainly because these systems of classification introduce error of interpretation by the observer [62]. Later Peterson [2] proposed a modification of the Pell and Gregory scale that included a third factor, the angulation of the molar (mesio-angular, horizontal, vertical or disto-angular). Clinical studies showed that there is no doubt about the importance of individual parameters of mentioned above classifications. Chuang et al. [58] demonstrated in their study that the level of impaction is associated with an increased risk of inflammatory complications following third molar surgery. Carvalho and Vasconcelos [63] extracted 473 mandibular third molars for 285 patients and concluded that root number ($P < 0.004$ and morphology ($P < 0.031$), tooth position ($P = 0.001$), periodontal space ($P < 0.004$) and second molar relation ($P = 0.001$) were significant predictors of surgical difficulty. Authors mentioned that not all significant predictors of surgical difficulty should be considered indicators of complications. Akadiri and Obiechina [64] demonstrated in their study wisdom tooth depth angulation and root morphology as the most consistent determinants of extraction difficulty.

Eruption status of the lower third molar is important risk factor for inferior alveolar nerve injury. Incidences of inferior alveolar nerve injury in fully erupted, partially erupted and unerupted lower wisdom teeth were 0.3%, 0.7% and 3.0%, respectively [65,66]. The risk of nerve injury is increasing with the depth of the impacted mandibular wisdom teeth [23,66]. It was demonstrated the relationship between pattern of impaction and inferior alveolar nerve injury. The incidence of nerve injury was highest in horizontally impacted lower wisdom teeth (1.7%), followed by distal impaction (1.4%), mesial impaction (1.3%) and vertical impaction (1.1%) [23,65,66].

In general the proximity of the mandibular third molar to the mandibular canal is considered a risk

factor for damage to the inferior alveolar nerve. This fact inspirited further studies for the predictive radiographic parameters identification. Rood and Shehab [24] distinguished four radiographic indicators observed in the tooth root (darkening, deflection and narrowing of the root, and a bifid root apex), and the other three in the canal (diversion, narrowing, and interruption in the white line of the canal). Studies demonstrated that the most important parameters for inferior alveolar nerve injury prediction are third molar root apices inside or in contact with the mandibular canal [46,67-69]. Furthermore, the prevalence of post-extraction complications correlated with the absence of cortication around the mandibular canal. It was reconfirmed by Park et al. [70] in their retrospective cohort study (179 patients and 259 teeth) where the overall prevalence of paresthesia was 4.2%. In contrast, the prevalence of paresthesia in group involving an interrupted mandibular canal cortex was 11.8%. Ueda et al. [71] performed similar study (99 patients and 145 teeth) and showed that inferior alveolar nerve injury was observed in 7 of 145 cases (4.8%). All 7 cases exhibited absence of cortication. Leung and Cheung [72] in literature review demonstrated that 16.2% of the surgery with the inferior alveolar nerve exposed developed postoperative inferior alveolar nerve deficit, whilst only 1.1% of the surgeries without nerve exposure developed inferior alveolar nerve deficit ($P < 0.0001$). The risk ratio of inferior alveolar nerve injury from intraoperative nerve exposure is 14.9 times more likely than if the nerve is not exposed.

Iatrogenic injury to the lingual nerve may happen during third molar surgery due to the anatomical proximity of the cortex region of the molar to the nerve, being separated from it by the periosteum alone [52]. Surgery on unerupted mandibular third molars was at higher risk (5.8%) of lingual nerve injury compared with erupted (0.3%) or partially erupted (2.0%) teeth ($P < 0.0001$) [66,73]. The incidence of lingual nerve injury was highest in distally impacted lower wisdom teeth (4.0%, $P < 0.01$), followed by horizontal impaction (2.8%), mesial impaction (2.4%) and vertical impaction (1.9%) [23,46,66]. The risk ratio of lingual nerve injury was 1.94 times more likely to occur if the lingual flap was raised than if it was not and 4.1 times more likely to occur if the lingual split technique was used in comparison with the buccal approach [72].

Mandibular third molar impaction classification based on anatomical and radiologic features

New mandibular third molar impaction and extraction difficulty degree classification based on anatomical and radiologic findings and literature review results is suggested (Table 1).

Table 1. Mandibular third molar impaction classification

Position of the mandibular third molar	Risk degree of presumptive intervention (score)			
	Conventional (0)	Simple (1)	Moderate (2)	Complicated (3)
Mesiodistal position in relation to the second molar – M and the mandibular ramus – R				
Relation to the second molar - M	Crown directed at or above the equator of the second molar	Crown directed below the equator to the coronal third of the second molar root	Crown/roots directed to the middle third of the second molar root	Crown/roots directed to the apical third of the second molar root
Relation to the mandibular ramus – R	Sufficient space in the dental arch	Partially impacted in the ramus	Completely impacted in the ramus	Completely impacted in the ramus in distoangular or horizontal position
Apicocoronal position in relation to the alveolar crest – A and the mandibular canal – C (IAN injury risk)				
Relation to the adjacent alveolar crest (from the uppermost point of the tooth) - A	Tooth is completely erupted	Partially impacted, but widest part of the crown (equator) is above the bone	Partially impacted, but widest part of the crown (equator) is below the bone	Completely encased in the bone
Relation to the mandibular canal (from the lowermost point of the tooth) - C	≥ 3 mm to the mandibular canal	Contacting or penetrating the mandibular canal, wall of the mandibular canal may be identified	Contacting or penetrating the mandibular canal, wall of the mandibular canal is unidentified	Roots surrounding the mandibular canal
Buccolingual position in relation to mandibular lingual and buccal walls – B (LN injury risk)				
Relation to mandibular lingual and buccal walls – B	Closer to buccal wall	In the middle between lingual and buccal walls	Closer to lingual wall	Closer to lingual wall, when the tooth is partially impacted or completely encased in the bone (A2 or A3)
Spatial position - S				
Spatial position - S	Vertical (90°)	Mesioangular ≤ 60°	Distoangular ≥ 120°	Horizontal (0°) or inverted (270°)

IAN = inferior alveolar nerve; LN = lingual nerve.

Classification of mandibular third molar impaction and extraction difficulty degree enables the clinician to determine the difficulty in removal of the impacted tooth, to choose optimal treatment and to avoid the majority of possible complications. This classification describes wisdom tooth relation to the adjacent anatomical structures: mandibular ramus, second molar, alveolar crest, mandibular canal, and the spatial position of the tooth. Wisdom tooth position assessment should be performed clinically and using CBCT and panoramic radiographic images. The tooth position according to the all aforementioned landmarks has been not completely classified yet. Proposed classification is determining mandibular third molar mesiodistal position (in relation to the second molar - M and the mandibular ramus - R), apicocoronal position (in relation to the alveolar crest - A, and the mandibular canal - C), buccolingual position (in relation to mandibular lingual and buccal walls - B) and spatial tooth position - S.

Risk degree of presumptive intervention is scored as follows:

- conventional extraction is determined, when all parameters are equal to score 0;
- simple, when at least one parameter is equal to score 1 and surgical extraction with coronectomy and/or sectioning of roots is determined;
- moderate, when at least one parameter is equal to score 2 and surgical extraction with coronectomy and/or sectioning of roots is determined;
- complicated, when at least one parameter is equal to score 3 and surgical extraction with coronectomy and/or sectioning of roots is determined. Extraoral approach can be indicated.

To make the classification more informative, each component of the indices (M,R,A,C,B and S) is described independently. For example, position, extraction difficulty degree of tooth 48 and risk of trigeminal nerve damage during surgery is described as following: M1,R1,A2,C2,B1,S3 (Figure 1A, B). This description determines complicated extraction, because one of the parameters – S is equal to 3. Detailed explanation: crown is in contact below the equator to the coronal third of the second molar (M1), partially impacted in the ramus (R1), widest part of the crown (equator) is below the bone (A2), roots are contacting or penetrating the mandibular canal, wall of the mandibular canal is unidentified (C2), tooth is located in the middle between lingual and buccal walls (B1); horizontal spatial position (S3). Complicated extraction is anticipated and C2 value presumes moderate risk of inferior alveolar nerve damage.

There are some new approaches in assessing different anatomical and radiological parameters in the present classification. For example, the depth of tooth impaction in Pell and Gregory's [60] classification was assessed according to the occlusal plane, but in some cases the crown of wisdom tooth is small in size and located below occlusal plane. However the tooth can be completely erupted and easily extracted. The assessment of tooth impaction (coronal position) should be evaluated from the alveolar crest, because the extraction difficulty is determined predominantly by the depth of impaction in the bone. Furthermore, it is necessary to highlight the lower landmark of the possible apicocoronal wisdom tooth position which is determined by mandibular canal. It was mentioned above that the proximity of the mandibular third molar to the mandibular canal is considered a risk factor for damage to the inferior alveolar nerve. In contrast, some previous classifications recommended assessing too many radiological parameters determining wisdom tooth roots relationship with mandibular canal. For example, Rood and Shehab [24] distinguished four radiographic indicators observed in the tooth

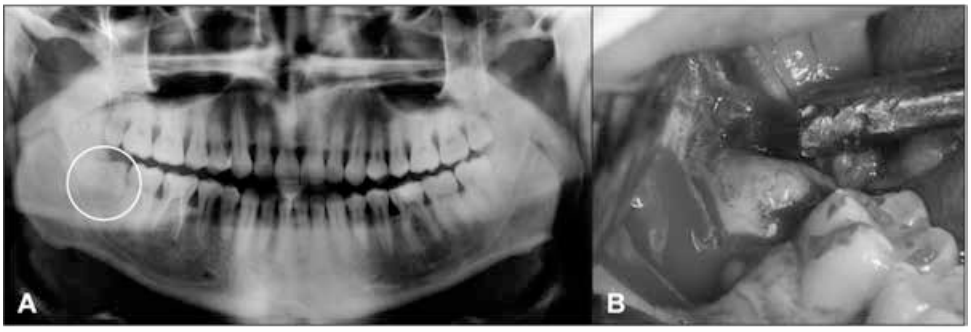

Figure 1. A = Tooth No. 48 is classified as M1,R1,A2,C2,B1,S3 on the ortopantomograph.
B = Impaction in horizontal spatial position index (S3) predicts complicated surgical extraction.

root (darkening, deflection and narrowing of the root, and a bifid root apex), and the other three in the canal (diversion, narrowing, and interruption in the white line of the canal). Latest clinical studies demonstrated that the most important parameters for inferior alveolar nerve injury prediction are third molar root apices inside or in contact with the inferior alveolar canal [46,67-69] and absence of cortication around the inferior alveolar canal [70-72], this is why mentioned above parameters were included into inferior alveolar nerve injury risk evaluation assessment. In such cases clinicians should avoid apical pressure during root elevation or even to perform multiple sectioning of the tooth to reduce any stress to a root on elevation. CBCT scan should be also accomplished for detailed surgery planning in cases when C2 or C3 relation to the mandibular canal is expected on two-dimensional radiographs (Figure 2A, B). Some authors are recommending to perform coronectomy of impacted wisdom tooth if roots are surrounding the mandibular canal because there is high risk or inferior alveolar nerve injury [33,74,75]. In contrast, it was considered that in cases when wisdom tooth position is ≥ 3 mm away from the mandibular canal, there is no risk to damage mandibular canal during surgical extraction (Figure 3).

Mesiodistal position is defined in relation to the second molar and the mandibular ramus. It is important to assess impacted tooth relationship to the second molar in order to avoid iatrogenic tooth traumatisation. The impaction degree of mandibular third molar in the ramus of mandible is associated with extraction operation difficulty score and postoperative complications manifestation. For example, high risk degree is registered when tooth is completely impacted in the mandibular ramus in distoangular or horizontal position (Figure 4).

Buccolingual third molar position in relation to mandibular lingual and buccal walls is reflecting risk of lingual nerve injury. It was discussed previously that iatrogenic injury to the lingual nerve may happen during

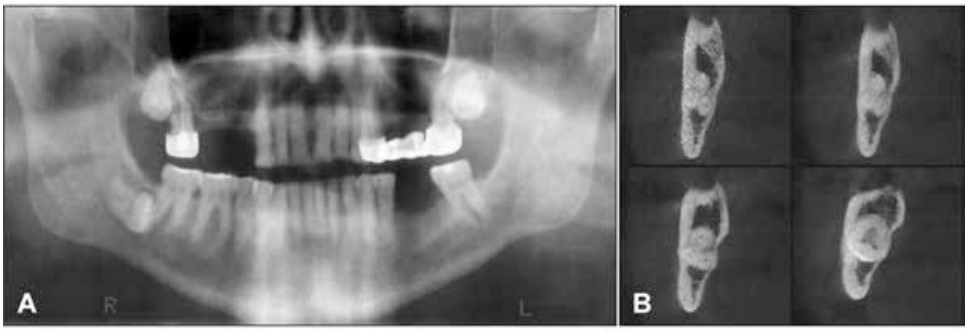

Figure 2. A = On orthopantomograph close contact between impacted right mandibular third molar and mandibular canal is suspected. B = More detailed view on the CBCT images reveals tooth penetration through the mandibular canal wall (C2) and moderate risk of inferior alveolar nerve damage.

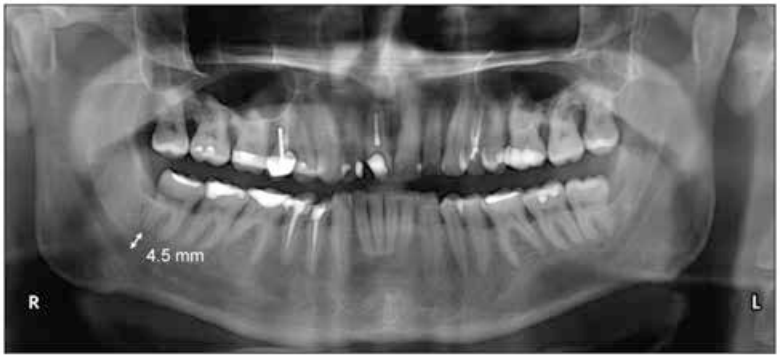

Figure 3. Roots of tooth No. 48 are ≥ 3 mm away from the mandibular canal (C0) on the orthopantomograph. There is no risk to damage inferior alveolar nerve during surgical extraction.

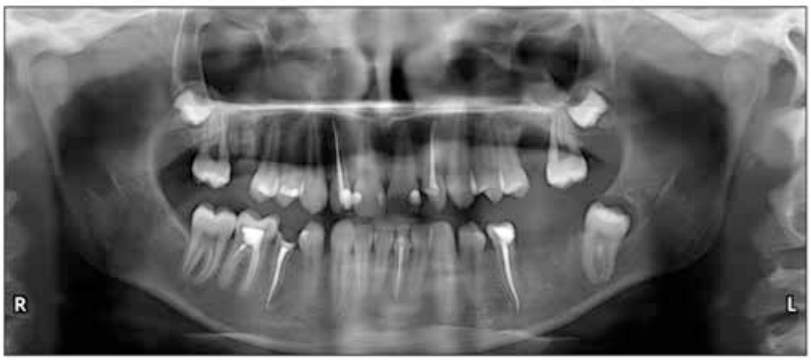

Figure 4. Tooth No. 38, completely impacted in the mandibular ramus in distoangular position and classified as A3 and R3 according to the relation to alveolar crest and mandibular ramus, is noticed on the orthopantomograph. Complicated surgical extraction is anticipated..

third molar surgery due to the anatomical proximity of the cortex region of the molar to the nerve [52]. Surgery on unerupted mandibular third molars was at higher risk (5.8%) of lingual nerve injury compared with erupted (0.3%) or partially erupted (2.0%) teeth ($P < 0.0001$) [66,73]. Thus the highest risk of lingual nerve injury was scored in case when the tooth is partially impacted or completely encased in the bone (A2 or A3) and is located closer to the lingual wall.

Spatial mandibular third molar position is reflecting extraction difficulty degree especially in combination with other indices. For example distoangular or horizontal impacted tooth position in combination with deep impaction in the mandibular ramus, can be complicated case even for experienced clinician.

CONCLUSIONS

There are selected only the most informative parameters in presented herein classification, because it is impossible to reflect all important parameters, such as periodontal ligament width, soft tissue condition, patient characteristic, clinician's experience, and et cetera in one classification which should be useful in daily practice. The classification proposed here based on anatomical and radiological impacted mandibular third molar features is promising to be a helpful tool for impacted tooth assessment as well as for planning for surgical operation. Further clinical studies should be conducted for new classification validation and reliability evaluation.

AKNOWLEDGEMENT AND DISCLOSURE STATEMENTS

The authors report no conflict of interest related to the present study.

REFERENCES

1. Archer WH. Oral Surgery: A Step-By-Step Atlas of Operative Techniques, 4th ed. Philadelphia: W.B. Saunders Company; 1966. p. 507-10.
2. Peterson LJ. Principles of Management of Impacted Teeth. In: Peterson LJ, Ellis E III, Hupp JR, Tuker MR, editors. Contemporary Oral and Maxillofacial Surgery, 3rd ed. St. Louis: Mosby; 1998. p. 215-48.
3. Agarwal KN, Gupta R, Faridi MM, Kalra N. Permanent dentition in Delhi boys of age 5-14 years. Indian Pediatr. 2004 Oct;41(10):1031-5. [Medline: 15523129]
4. Khan NB, Chohan AN, AlMograbi B, AlDeyab S, Zahid T, AlMoutairi M. Eruption Time of Permanent First Molars and Incisors Among a Sample of Saudi Male Schoolchildren. Saudi Dent J. 2006 Jan-Apr;18(1):18-24.
5. Elsey MJ, Rock WP. Influence of orthodontic treatment on development of third molars. Br J Oral Maxillofac Surg. 2000 Aug;38(4):350-3. [Medline: 10922167] [doi: 10.1054/bjom.2000.0307]
6. Pahkala R, Pahkala A, Laine T. Eruption pattern of permanent teeth in a rural community in northeastern Finland. Acta Odontol Scand. 1991 Dec;49(6):341-9. [Medline: 1776401] [doi: 10.3109/00016359109005930]
7. Odusanya SA, Abayomi IO. Third molar eruption among rural Nigerians. Oral Surg Oral Med Oral Pathol. 1991 Feb;71(2):151-4. [Medline: 2003009] [doi: 10.1016/0030-4220(91)90457-N]

8. Kruger E, Thomson WM, Konthasinghe P. Third molar outcomes from age 18 to 26: findings from a population-based New Zealand longitudinal study. Oral Surg Oral Med Oral Pathol Oral Radiol Endod. 2001 Aug;92(2):150-5. [Medline: 11505260] [doi: 10.1067/moe.2001.115461]
9. Hattab FN, Alhaija ES. Radiographic evaluation of mandibular third molar eruption space. Oral Surg Oral Med Oral Pathol Oral Radiol Endod. 1999 Sep;88(3):285-91. [Medline: 10503855] [doi: 10.1016/S1079-2104(99)70029-6]
10. Yuasa H, Sugiura M. Clinical postoperative findings after removal of impacted mandibular third molars: prediction of postoperative facial swelling and painbased on preoperative variables. Br J Oral Maxillofac Surg. 2004 Jun;42(3):209-14. [Medline: 15121265] [doi: 10.1016/j.bjoms.2004.02.005]
11. Alling CC, Alling RD. Indications for management of impacted teeth. In: Alling CC, Helfrick JF, Alling RD, editors. Impacted Teeth. Philadelphia: W.B. Saunders; 1993. p. 49-54.
12. Bishara SE, Andreasen G. Third molars: a review. Am J Orthod. 1983 Feb;83(2):131-7. [Medline: 6572040] [doi: 10.1016/S0002-9416(83)90298-1]
13. Grover PS, Lorton L. The incidence of unerupted permanent teeth and related clinical cases. Oral Surg Oral Med Oral Pathol. 1985 Apr;59(4):420-5. [Medline: 3858781] [doi: 10.1016/0030-4220(85)90070-2]
14. Björk A. Prediction of mandibular growth rotation. Am J Orthod 1969;55:585–99. [doi: 10.1016/0002-9416(69)90036-0]
15. Richardson M. Changes in lower third molar position in the young adult. Am J Orthod Dentofacial Orthop. 1992 Oct;102(4):320-7. [Medline: 1456216] [doi: 10.1016/0889-5406(92)70047-E]
16. Richardson M. The development of third molar impaction. Br J Orthod. 1975 Oct;2(4):231-4. [Medline: 1065361]
17. Odusanya SA. Third molar impaction among Nigerian youths. Odontostomatol Trop. 1984 Jun;7(2):79-83. [Medline: 6593696]
18. Yamaoka M, Tambo A, Furusawa K. Incidence of inflammation in completely impacted lower third molars. Aust Dent J. 1997 Jun;42(3):153-5. [Medline: 9241923] [doi: 10.1111/j.1834-7819.1997.tb00112.x]
19. Peck S, Peck L, Kataja M. Concomitant occurrence of canine malposition and tooth agenesis: evidence of orofacial genetic fields. Am J Orthod Dentofacial Orthop. 2002 Dec;122(6):657-60. [Medline: 12490878] [doi: 10.1067/mod.2002.129915]
20. Bermúdez de Castro JM. Third molar agenesis in human prehistoric populations of the Canary Islands. Am J Phys Anthropol. 1989 Jun;79(2):207-15. [Medline 2662782]
21. Lytle JJ. Etiology and indications for the management of impacted teeth. Northwest Dent. 1995 Nov-Dec;74(6):23-32. [Medline: 9462087]
22. Kay LW, Killey HC. The extraction of teeth. The impacted third molar. Dent Update. 1976 Mar-Apr;3(2):49-52. [Medline: 1074729]
23. Blondeau F, Daniel NG. Extraction of impacted mandibular third molars: postoperative complications and their risk factors. J Can Dent Assoc. 2007 May;73(4):325. [Medline: 17484797] [FREE Full Text]
24. Rood JP, Shehab BA. The radiological prediction of inferior alveolar nerve injury during third molar surgery. Br J Oral Maxillofac Surg. 1990 Feb;28(1):20-5. [Medline: 2322523] [doi: 10.1016/0266-4356(90)90005-6]
25. Denio D, Torabinejad M, Bakland LK. Anatomical relationship of the mandibular canal to its surrounding structures in mature mandibles. J Endod. 1992 Apr;18(4):161-5. [Medline: 1402570] [doi: 10.1016/S0099-2399(06)81411-1]
26. van der Stelt PF. Filmless imaging: the uses of digital radiography in dental practice. J Am Dent Assoc. 2005 Oct;136(10):1379-87. [Medline: 16255462]
27. Kim IS, Kim SG, Kim YK, Kim JD. Position of the mental foramen in a Korean population: a clinical and radiographic study. Implant Dent. 2006 Dec;15(4):404-11. [Medline: 17172959] [doi: 10.1097/01.id.0000243319.66845.15]
28. Misch CE. Diagnostic imaging techniques. In: Misch CE, editors. Contemporary Implant Dentistry, 3rd ed. St Louis: CV Mosby Company; 2008. p. 38-67.
29. White SC, Heslop EW, Hollender LG, Mosier KM, Ruprecht A, Shrout MK; American Academy of Oral and Maxillofacial Radiology, ad hoc Committee on Parameters of Care. Parameters of radiologic care: An official report of the American Academy of Oral and Maxillofacial Radiology. Oral Surg Oral Med Oral Pathol Oral Radiol Endod. 2001 May;91(5):498-511. [Medline: 11346726] [doi: 10.1067/moe.2001.114380]
30. Khan I, Halli R, Gadre P, Gadre KS. Correlation of panoramic radiographs and spiral CT scan in the preoperative assessment of intimacy of the inferior alveolar canal to impacted mandibular third molars. J Craniofac Surg. 2011 Mar;22(2):566-70. [Medline: 21403569] [doi: 10.1097/SCS.0b013e3182077ac4]
31. Juodzbalys G, Wang HL. Guidelines for the Identification of the Mandibular Vital Structures: Practical Clinical Applications of Anatomy and Radiological Examination Methods. J Oral Maxillofac Res 2010;1(2):e1. URL: http://www.ejomr.org/JOMR/archives/2010/2/e1/e1ht.htm [doi: 10.5037/jomr.2010.1201]
32. Ghaeminia H, Meijer GJ, Soehardi A, Borstlap WA, Mulder J, Vlijmen OJ, Bergé SJ, Maal TJ. The use of cone beam CT for the removal of wisdom teeth changes the surgical approach compared with panoramic radiography: a pilot study. Int J Oral Maxillofac Surg. 2011 Aug;40(8):834-9.Epub 2011 Apr 19. [Medline: 21507612] [doi: 10.1016/j.ijom.2011.02.032]
33. Matzen LH, Christensen J, Hintze H, Schou S, Wenzel A. Influence of cone beam CT on treatment plan before surgical intervention of mandibular third molars and impact of radiographic factors on deciding on coronectomy vs surgical removal. Dentomaxillofac Radiol. 2013;42(1):98870341.Epub 2012 Aug 29. [Medline: 22933533] [doi: 10.1259/dmfr/98870341]

34. Removal of third molars. Sponsored by the National Institute of Dental Research, November 28-30, 1979. Natl Inst Health Consens Dev Conf Summ. 1979;2:65-8. Review. [Medline: 398969]
35. Koerner KR. The removal of impacted third molars. Principles and procedures. Dent Clin North Am. 1994 Apr;38(2):255-78. Review. [Medline: 8206177]
36. Bux P, Lisco V. Ectopic third molar associated with a dentigerous cyst in the subcondylar region: report of case. J Oral Maxillofac Surg. 1994 Jun;52(6):630-2. [Medline: 8189304] [doi: 10.1016/0278-2391(94)90105-8]
37. Medici A, Raho MT, Anghinoni M. Ectopic third molar in the condylar process: case report. Acta Biomed Ateneo Parmense. 2001;72(5-6):115-8. [Medline: 12233269]
38. Wassouf A, Eyrich G, Lebeda R, Grätz KW. Surgical removal of a dislocated lower third molar from the condyle region: case report. Schweiz Monatsschr Zahnmed. 2003;113(4):416-20. [Medline: 12768887]
39. Nageshwar. Comma incision for impacted mandibular third molars. J Oral Maxillofac Surg. 2002 Dec;60(12):1506-9. [Medline: 12465020] [doi: 10.1053/joms.2002.36152]
40. Susarla SM, Blaeser BF, Magalnick D. Third molar surgery and associated complications. Oral Maxillofac Surg Clin North Am. 2003 May;15(2):177-86. [Medline: 18088673] [doi: 10.1016/S1042-3699(02)00102-4]
41. Pippi R, Perfetti G. Lingual displacement of an entire lower third molar. Report of a case with suggestions for prevention and management. Minerva Stomatol. 2002 Jun;51(6):263-8. English, Italian. [Medline: 12147979]
42. Marciani RD. Complications of third molar surgery and their management. Atlas Oral Maxillofac Surg Clin North Am. 2012 Sep;20(2):233-51. [Medline: 23021398] [doi: 10.1016/j.cxom.2012.06.003]
43. Kim JW, Cha IH, Kim SJ, Kim MR. Which risk factors are associated with neurosensory deficits of inferior alveolar nerve after mandibular third molar extraction? J Oral Maxillofac Surg. 2012 Nov;70(11):2508-14. Epub 2012 Aug 15. [Medline: 22901857] [doi: 10.1016/j.joms.2012.06.004]
44. Renton T, Yilmaz Z, Gaballah K. Evaluation of trigeminal nerve injuries in relation to third molar surgery in a prospective patient cohort. Recommendations for prevention. Int J Oral Maxillofac Surg. 2012 Dec;41(12):1509-18. Epub 2012 Sep 25. [Medline: 23017786] [doi: 10.1016/j.ijom.2012.06.025]
45. Leung YY, Cheung LK. Correlation of radiographic signs, inferior dental nerve exposure, and deficit in third molar surgery. J Oral Maxillofac Surg. 2011 Jul;69(7):1873-9. Epub 2011 Mar 3. [Medline: 21371801] [doi: 10.1016/j.joms.2010.11.017].
46. Smith WP. The relative risk of neurosensory deficit following removal of mandibular third molar teeth: the influence of radiography and surgical technique. Oral Surg Oral Med Oral Pathol Oral Radiol. 2013 Jan;115(1):18-24. Epub 2012 Aug 22. [Medline: 22921833] [doi: 10.1016/j.oooo.2012.03.017]
47. Umar G, Obisesan O, Bryant C, Rood JP. Elimination of permanent injuries to the inferior alveolar nerve following surgical intervention of the "high risk" third molar. Br J Oral Maxillofac Surg. 2013 Jun;51(4):353-7.Epub 2012 Sep 23. [Medline: 23010201] [doi: 10.1016/j.bjoms.2012.08.006]
48. Renton T, Hankins M, Sproate C, McGurk M. A randomised controlled clinical trial to compare the incidence of injury to the inferior alveolar nerve as a result of coronectomy and removal of mandibular third molars. Br J Oral Maxillofac Surg. 2005 Feb;43(1):7-12. [Medline: 15620767] [doi: 10.1016/j.bjoms.2004.09.002]
49. Blackburn CW, Bramley PA. Lingual nerve damage associated with the removal of lower third molars. Br Dent J. 1989 Aug 5;167(3):103-7. [Medline: 2765316] [doi: 10.1038/sj.bdj.4806922]
50. Hillerup S, Stoltze K. Lingual nerve injury in third molar surgery I. Observations on recovery of sensation with spontaneous healing. Int J Oral Maxillofac Surg. 2007 Oct;36(10):884-9. Epub 2007 Sep 4. [Medline: 17766086] [doi: 10.1016/j.ijom.2007.06.004]
51. Zuniga JR. Management of third molar-related nerve injuries: observe or treat? Alpha Omegan. 2009 Jun;102(2):79-84. [Medline: 19591333] [doi: 10.1016/j.aodf.2009.04.014]
52. Janakiraman EN, Alexander M, Sanjay P. Prospective analysis of frequency and contributing factors of nerve injuries following third-molar surgery. J Craniofac Surg. 2010 May;21(3):784-6. [Medline: 20485048] [doi: 10.1097/SCS.0b013e3181d7f29a]
53. Lata J, Tiwari AK. Incidence of lingual nerve paraesthesia following mandibular third molar surgery. Natl J Maxillofac Surg. 2011 Jul;2(2):137-40. [Medline: 22639500] [doi: 10.4103/0975-5950.94467]
54. Alhassani AA, AlGhamdi AS. Inferior alveolar nerve injury in implant dentistry: diagnosis, causes, prevention, and management. J Oral Implantol. 2010;36(5):401-7. Epub 2010 Jun 14. Review. [Medline: 20545547] [doi: 10.1563/AAID-JOI-D-09-00059]
55. Roy TS, Sarkar AK, Panicker HK. Variation in the origin of the inferior alveolar nerve. Clin Anat. 2002 Mar;15(2):143-7. [Medline: 11877794] [doi: 10.1002/ca.1110]
56. Ziccardi VB, Assael LA. Mechanisms of trigeminal nerve injuries. Atlas Oral Maxillofac Surg Clin North Am. 2001 Sep;9(2):1-11. [Medline: 11665372]
57. Bouloux GF, Steed MB, Perciaccante VJ. Complications of third molar surgery. Oral Maxillofac Surg Clin North Am. 2007 Feb;19(1):117-28, vii. Review. [Medline: 18088870]
58. Chuang SK, Perrott DH, Susarla SM, Dodson TB. Risk factors for inflammatory complications following third molar surgery in adults. J Oral Maxillofac Surg. 2008 Nov;66(11):2213-8. [Medline: 18940482] [doi: 10.1016/j.joms.2008.06.067]

59. Winter G.B. Impacted mandibular third molars. St Louis: American Medical Book Co.; 1926. p. 241–79.
60. Pell GJ, Gregory BT. Impacted mandibular third molars: classification and modified techniques for removal. Dent Digest 1933;39:330–338.
61. García AG, Sampedro FG, Rey JG, Vila PG, Martin MS. Pell-Gregory classification is unreliable as a predictor of difficulty in extracting impacted lower third molars. Br J Oral Maxillofac Surg. 2000 Dec;38(6):585-587. [Medline: 11092770] [doi: 10.1054/bjom.2000.0535]
62. Almendros-Marqués N, Berini-Aytés L, Gay-Escoda C. Evaluation of intraexaminer and interexaminer agreement on classifying lower third molars according to the systems of Pell and Gregory and of Winter. J Oral Maxillofac Surg. 2008 May;66(5):893-9. [Medline: 18423277] [doi: 10.1016/j.joms.2007.09.011]
63. Carvalho RW, do Egito Vasconcelos BC. Assessment of factors associated with surgical difficulty during removal of impacted lower third molars. J Oral Maxillofac Surg. 2011 Nov;69(11):2714-21. Epub 2011 Jul 12. [Medline: 21752507] [doi: 10.1016/j.joms.2011.02.097]
64. Akadiri OA, Obiechina AE. Assessment of difficulty in third molar surgery--a systematic review. J Oral Maxillofac Surg. 2009 Apr;67(4):771-4. Review. [Medline: 19304033] [doi: 10.1016/j.joms.2008.08.010]
65. Carmichael FA, McGowan DA. Incidence of nerve damage following third molar removal: a West of Scotland Oral Surgery Research Group study. Br J Oral Maxillofac Surg. 1992 Apr;30(2):78-82. Review. [Medline: 1567807] [doi: 10.1016/0266-4356(92)90074-S]
66. Cheung LK, Leung YY, Chow LK, Wong MC, Chan EK, Fok YH. Incidence of neurosensory deficits and recovery after lower third molar surgery: a prospective clinical study of 4338 cases. Int J Oral Maxillofac Surg. 2010 Apr;39(4):320-6. Epub 2010 Jan 12. [Medline: 20061121] [doi: 10.1016/j.ijom.2009.11.010]
67. Hasegawa T, Ri S, Umeda M, Komori T. Multivariate relationships among risk factors and hypoesthesia of the lower lip after extraction of the mandibular third molar. Oral Surg Oral Med Oral Pathol Oral Radiol Endod. 2011 Jun;111(6):e1-7. [Medline: 21569985] [doi: 10.1016/j.tripleo.2011.02.013]
68. Jun SH, Kim CH, Ahn JS, Padwa BL, Kwon JJ. Anatomical differences in lower third molars visualized by 2D and 3D X-ray imaging: clinical outcomes after extraction. Int J Oral Maxillofac Surg. 2013 Apr;42(4):489-96. Epub 2013 Jan 24. [Medline: 23352698] [doi: 10.1016/j.ijom.2012.12.005]
69. Xu GZ, Yang C, Fan XD, Yu CQ, Cai XY, Wang Y, He D. Anatomic relationship between impacted third mandibular molar and the mandibular canal as the risk factor of inferior alveolar nerve injury. Br J Oral Maxillofac Surg. 2013 Feb 11. [Epub ahead of print] [Medline: 23411471] [doi: 10.1016/j.bjoms.2013.01.011]
70. Park W, Choi JW, Kim JY, Kim BC, Kim HJ, Lee SH. Cortical integrity of the inferior alveolar canal as a predictor of paresthesia after third-molar extraction. J Am Dent Assoc. 2010 Mar;141(3):271-8. [Medline: 20194382]
71. Ueda M, Nakamori K, Shiratori K, Igarashi T, Sasaki T, Anbo N, Kaneko T, Suzuki N, Dehari H, Sonoda T, Hiratsuka H. Clinical significance of computed tomographic assessment and anatomic features of the inferior alveolar canal as risk factors for injury of the inferior alveolar nerve at third molar surgery. J Oral Maxillofac Surg. 2012 Mar;70(3):514-20. Epub 2011 Nov 12. [Medline: 22079065] [doi: 10.1016/j.joms.2011.08.021]
72. Leung YY, Cheung LK. Risk factors of neurosensory deficits in lower third molar surgery: an literature review of prospective studies. Int J Oral Maxillofac Surg. 2011 Jan;40(1):1-10. Epub 2010 Oct 28. Review. [Medline: 21035310] [doi: 10.1016/j.ijom.2010.09.005]
73. Chossegros C, Guyot L, Cheynet F, Belloni D, Blanc JL. Is lingual nerve protection necessary for lower third molar germectomy? A prospective study of 300 procedures. Int J Oral Maxillofac Surg. 2002 Dec;31(6):620-4. [Medline: 12521318] [doi: 10.1054/ijom.2002.0236]
74. Pogrel MA, Lee JS, Muff DF. Coronectomy: a technique to protect the inferior alveolar nerve. J Oral Maxillofac Surg. 2004 Dec;62(12):1447-52. [Medline: 15573343] [doi: 10.1016/j.joms.2004.08.003]
75. O'Riordan BC. Coronectomy (intentional partial odontectomy of lower third molars). Oral Surg Oral Med Oral Pathol Oral Radiol Endod. 2004 Sep;98(3):274-80. [Medline: 15356463] [doi: 10.1016/j.tripleo.2003.12.040]

To cite this article:
Juodzbalys G, Daugela P. Mandibular Third Molar Impaction: Review of Literature and a Proposal of a Classification.
J Oral Maxillofac Res 2013;4(2):e1
URL: http://www.ejomr.org/JOMR/archives/2013/2/e1/v4n2e1ht.pdf
doi: 10.5037/jomr.2013.4201

Surgical Regenerative Treatments for Peri-Implantitis: Meta-analysis of Recent Findings in a Systematic Literature Review

Povilas Daugela[1], Marco Cicciù[2], Nikola Saulacic[3]

[1]Department of Maxillofacial Surgery, Lithuanian University of Health Sciences, Kaunas, Lithuania.
[2]Human Pathology Department, Messina University, Messina, Italy.
[3]Department of Cranio-Maxillofacial Surgery, Faculty of Medicine, University of Bern, Bern, Switzerland.

Corresponding Author:
Povilas Daugela
Department of Oral and Maxillofacial Surgery
Lithuanian University of Health Sciences
Eiveniu str. 2, LT-50009, Kaunas
Lithuania
Phone: +370 600 61999
E-mail: p.daugela@gmail.com

ABSTRACT

Objectives: The purpose of the present study was to systematically review the literature on the surgical regenerative treatment of the peri-implantitis and to determine an effective therapeutic predictable option for their clinical management.
Material and Methods: The study searched MEDLINE and EMBASE databases from 2006 to 2016. Clinical human studies that had reported changes in probing depth (PD) and/or bleeding on probing (BOP) and/or radiologic marginal bone level (RBL) changes after peri-implantitis surgical treatment at 12-month follow-up or longer were included accordingly to PRISMA guidelines.
Results: The initial search obtained 883 citations. After screening and determination of eligibility, 18 articles were included in the review. The meta-analysis of selected studies revealed that the weighted mean RBL fill was 1.97 mm (95% confidence interval [CI] = 1.58 to 2.35 mm), PD reduction was 2.78 mm (95% CI = 2.31 to 3.25 mm), and BOP reduced by 52.5% (95% CI = 41.6 to 63.1%). Defect fill in studies using and not using barrier membranes for graft coverage was 1.86 mm (95% CI = 1.36 to 2.36 mm) and 2.12 mm (95% CI = 1.46 to 2.78 mm) correspondingly. High heterogeneity among the studies regarding defects morphology, surgical protocols, and selection of biomaterials were found.
Conclusions: All included studies underlined an improvement of clinical conditions after the surgical regenerative treatment of peri-implantitis, however, there is a lack of scientific evidence in the literature regarding the superiority of the regenerative versus non-regenerative surgical treatment. The presence of a barrier membrane or submergence in the regenerative procedure does not seem to be fundamental in order to obtain clinical success of the surgery.

Keywords: alveolar bone grafting; biocompatible materials; alveolar bone loss; bone regeneration; oral surgery; peri-implantitis.

Accepted for publication: 19 August 2016
To cite this article:
Daugela P, Cicciù M, Saulacic N.
Surgical Regenerative Treatments for Peri-Implantitis: Meta-analysis of Recent Findings in a Systematic Literature Review
J Oral Maxillofac Res 2016;7(3):e15
URL: http://www.ejomr.org/JOMR/archives/2016/3/e15/v7n3e15.pdf
doi: 10.5037/jomr.2016.7315

INTRODUCTION

In the recent years, dental implant rehabilitation has confronted requests for optimal functional and aesthetic outcomes which require an inflammation of the predictable surgical techniques and long-term clinical results. Besides of the successful functioning on a long-term, several types of complications have been recently encountered. The clinical condition involving dental implants, characterized by the inflammation, bleeding, suppuration of peri-implant tissues and rapid bone loss is widely known as peri-implantitis [1-6].

Peri-implantitis is associated with the presence of a sub-marginal plaque, which contains a large variety of Gram-negative anaerobic rods, fusiform bacteria, motile and curved rods and spirochetes [7]. It contains large amounts of densely packed inflammatory cells (neutrophilis, macrophages, lymphocytes and plasma cells), frequently accompanied by a crater like bone defects that surround the contaminated implant [8,9]. Several lines of evidence indicated that an accumulation of bacteria on the implant surface plays an important role in the aetiology of peri-implantitis – an inflammatory condition affecting the tissues around osseointegrated implants, leading to loss of supporting bone [10]. Nevertheless, peri-implant tissues can be kept in a healthy clinical state and some endosseous implants successfully used as prosthetic abutments for the oral rehabilitation of fully and partially edentulous patients for a prolonged period of time [11]. Besides of a numerous patient-related factors (insufficient bone quality, smoking, systemic diseases or chemotherapy), surgical trauma or bacterial contamination during implant insertion, non-fit dental implant prosthesis and abnormal masticatory load are reported to be the most important causes of early implant failure [12-14].

Peri-implantitis can be defined as a site-specific infectious disease associated to an inflammatory process involving periodontal soft tissues, and causing bone loss around an osseointegrated implant. Numerous aetiological factors may play a decisive role for the progress of peri-implant infection. The implant design, the degree of roughness, the external morphology, the abutment connection, the passivation of the prosthesis and excessive mechanical load are all related with the disease [6,15]. Diagnosis can be referred on altered clinical condition like the colour in the gingiva, bleeding on probing (BOP), increased probing depth (PD), suppuration, and gradual loss of peri-implant bone as diagnosed by decrease of radiologic bone level (RBL) in standardized radiography.

The diagnosis and therapies for the soft tissue inflammation and peri-implant bone loss is quite challenging for the clinician. Diagnostic measures, such as probing pocket depth, radiographic tools, and microbial sampling have been shifted from the periodontal area and utilized during the maintenance phase of the dental implant treatment [16]. The main aim in the treatment of peri-implantis is to arrest the progression of the disease and at the same time to keep the dental implant in function solving the inflammatory signs of bleeding and pain [17]. Peri-implant bony defects around dental implants can be treated with either non-surgical or surgical (resective or regenerative) techniques. Bone tissue regeneration is the objective therapeutic option in selected peri-implant bony defects of functioning implants if appropriate surgical techniques are utilized and the aetiologic cause is fully eradicated [18].

The purpose of this systematic review is to screen recent literature on various approaches of surgical regenerative treatment of peri-implantitis in order to give the clinicians valuable suggestions for the most appropriate treatment modality.

MATERIAL AND METHODS

Protocol and registration

The methods of the analysis and inclusion criteria were specified in advance and documented in a protocol. The review was registered in PROSPERO, an international prospective register of systematic reviews. The protocol can be accessed through the following link:
http://www.crd.york.ac.uk/PROSPERO/display_record.asp?ID=CRD42016033664
Registration number: CRD42016033664.
The reporting of this systematic analysis adhered to the Preferred Reporting Items for Systematic Review and Meta-Analyses (PRISMA) statement [19].

Focus question

The following focus questions were developed according to the population, intervention, comparison, and outcome (PICO) study design:

1. What are the overall treatment outcomes of reconstructive procedures in treating peri-implantitis?
2. Does the use of barrier membranes or submergence of the healing site provide beneficial clinical outcomes in the treatment of peri-implantitis?

Information sources

The search strategy incorporated examinations of electronic databases, supplemented by hand searches. A search of four electronic databases, including Ovid MEDLINE, PubMed, EMBASE, and Dentistry and Oral Sciences Source was carried out for relevant studies published in the English language from January 2006 to March 2016.

Additionally, a hand search performed in dental and implant-related journals limited to English language for the same period included: 1) "Journal of Periodontology"; 2) "Clinical Implant Dentistry and Related Research"; 3) "International Journal of Oral and Maxillofacial Implants"; 4) "Clinical Oral Implants Research"; 5) "Implant Dentistry"; 6) "International Journal of Oral and Maxillofacial Surgery"; 7) "Journal of Oral and Maxillofacial Surgery"; 8) "Journal of Dental Research"; 9) "Journal of Prosthetic Dentistry"; 10) "International Journal of Prosthodontics"; 11) "Journal of Oral Implantology"; 12) "Journal of Clinical Periodontology"; 13) "International Journal of Periodontics & Restorative Dentistry"; 14) "European Journal of Oral Implantology". A hand search of the reference lists in the articles retrieved was carried out to source additional relevant publications and to improve the sensitivity of the search.

Search

The keywords used in the search of the selected electronic databases included the following: "peri-implantitis" OR "periimplantitis" OR "peri-implant" OR "periimplant" or ("implant" AND "failure") AND "surgery" OR "surgical" OR "regeneration" OR "regenerative" OR "treatment" OR "therapy" OR "bone graft" OR "bone substitute" OR "laser" OR "lasers".

The choice of keywords was intended to be extensive, to collect as much relevant data as possible without relying on electronic means alone to refine the search results.

Selection of studies

The resulting articles were independently subjected to clear inclusion and exclusion criteria by 2 independent reviewers as follows. Reviewers compared decisions and resolved differences through discussion, consulting a third party when consensus could not be reached. The third party was an experienced senior reviewer. The level of agreement between the reviewers regarding study inclusion was calculated using κ statistics. At the title and abstract stage, one reviewer accepted the citations that appeared to meet inclusion criteria and send them to full-text review, with a second reviewer assessing only those citations and abstracts that the first reviewer deemed ineligible. At the stage of reviewing of full-text articles, a complete independent dual review was undertaken.

Types of publications

The review included studies on humans published in the English language. Letters, editorials, case reports, literature reviews, and PhD theses were excluded.

Types of studies

The review included all human prospective and retrospective follow-up studies and clinical trials, cohort studies, case-control studies, and case series studies on surgical regenerative treatment of peri-implantitis, published between January 2006 and March 2016.

Types of participants/population

Subjects in the included studies must have had at least one osseointegrated titanium screw-shaped dental implant that presented signs of peri-implantitis.

Disease definition

The authors of this review classified the case definition of peri-implantitis of each study, if there was a clear radiographic threshold > 2 mm of continuous marginal bone loss beyond biologic peri-implant bone remodelling, presence of BOP and/or suppuration on probing with probing depth more than 6 mm [20].

Inclusion and exclusion criteria

The full text of all studies of possible relevance was obtained for assessment against the following inclusion criteria:

- Investigated surgical regenerative treatment in patients with at least one osseointegrated titanium screw-shaped dental implant, that presented signs of peri-implantitis;
- Studies involving at least one surgical regenerative treatment method of peri-implantitis applied;
- All human prospective or retrospective follow-up studies and clinical trials, cohort studies, case-control studies, and case series studies

with a minimal sample size of 10 implants and not less than 12 months follow-up after surgical regenerative treatment of peri-implantitis;
- Clear report on clinical and radiographic peri-implant tissues changes, including RBL and/or PD change as primary outcome measure and/or BOP as secondary outcome measure.

The applied exclusion criteria for studies were as follows:
- Animal or *in vitro* studies;
- Studies involving patients with specific diseases, immunologic disorders, uncontrolled diabetes mellitus, osteoporosis, or other implant risk related systemic conditions;
- Studies investigating ceramic or coated surface implants;
- Not enough information regarding the selected topic;
- No access to the title and abstract in English language.

Sequential search strategy

Following the initial literature search, all article titles were screened to eliminate irrelevant publications, considering the exclusion criteria. Next, studies were excluded based on data obtained from screening the abstracts. The final stage of screening involved reading the full texts to confirm each study's eligibility, based on the inclusion criteria.

Data extraction

The data were independently extracted from studies in the form of variables, according to the aims and themes of the present review, as listed onwards.

Data items

Data were collected from the included articles and arranged in the following fields:
- "Author (Year)" – revealed the author and year of publication.
- "Type of study" – indicated the type of the study.
- "Sample size" – described the number of patients examined.
- "Detoxification method" – described additional implant surface detoxification measures applied in addition to the instrumental debridement, full thickness flap, and degranulation.
- "Bone substitute/membrane" – described types of bone grafts and membranes used for regeneration.
- "Antimicrobial" – described antimicrobial agents (e.g. systemic antibiotics, chlorhexidine mouth rinse) used adjunctive to the surgery.
- "Follow-up" – described the duration of the observed outcomes after applied surgical regenerative treatment of peri-implantitis.
- "Probing depth change (ΔPD)" – described probing depth difference (in mm) before and after surgical treatment.
- "Bleeding on probing change (ΔBOP)" – described BOP difference (in %) before and after surgical treatment.
- "Radiologic bone level change (ΔRBL)" – described the marginal bone level difference (in mm; measured from implant shoulder to the bone surface) before and after the treatment; and/or intrabony defect depth difference (in mm; measured from the bottom of the defect to the interproximal bone) before and after treatment.

Risk of bias assessment

Assessment of risk of bias was undertaken independently, and in duplicate by the two authors during the data extraction process. For the included studies, this was conducted using the Cochrane Collaboration's two-part tool for assessing risk of bias [21].

The following possible sources of bias were addressed: random sequence generation (selection bias); allocation concealment (selection bias); blinding of participants and personnel (performance bias and detection bias); incomplete outcome data (attrition bias);

selective reporting (reporting bias); and other bias (examiner blinding, examiner calibration, standardized probing force, standardized radiographic assessment). The authors' judgment for each source of bias item was assigned for each study in the data extraction table (Table 1). An overall risk of bias was then assigned to each trial according to Higgins et al. [21]. The degrees of bias were categorized as follows: low risk, if all the criteria were met; moderate risk, when only one criterion was missing; high risk, if two or more criteria were missing; and unclear risk, if too few details were available to make a judgement of certain risk assessment.

Statistical analysis

A meta-analysis was performed to integrate the quantitative findings from separate but similar studies and to provide a numerical estimate to the overall effect of interest. All meta-analyses were performed on studies that reported the clinical and/or radiologic outcomes of regenerative peri-implantitis treatment

Table 1. Risk of bias within the studies

Study	Year of publication	Random sequence generation	Allocation concealment	Blinding	Incomplete outcome data	Selective reporting	Other bias
Deppe et al. [22]	2007	?	?	?	-	+	+
Roos-Jansåker et al. [23]	2007	?	?	+	-	?	+
Roos-Jansåker et al. [24]	2007	?	?	?	-	?	+
Schwarz et al. [25]	2008	+	?	+	-	?	+
Romanos et al. [26]	2008	?	?	?	-	-	-
Schwarz et al. [27]	2009	+	?	+	-	?	+
Schwarz et al. [28]	2010	?	?	+	-	?	+
Roccuzzo et al. [29]	2011	?	?	+	+	?	+
Froum et al. [30]	2012	?	?	+	-	-	-
Aghazadeh et al. [31]	2012	+	-	+	+	+	+
Wohlfahrt et al. [32]	2012	+	+	+	+	+	+
Wiltfang et al. [33]	2012	?	?	?	-	-	+
Schwarz et al. [34]	2013	+	?	+	?	-	+
Matarasso et al. [35]	2014	?	?	?	-	?	+
Roos-Jansåker et al. [36]	2014	?	?	+	-	?	+
Jepsen et al. [37]	2015	+	+	+	+	+	+
Froum et al. [38]	2015	?	?	+	+	+	-
Roccuzzo et al. [39]	2016	?	?	-	+	+	+

+ = low risk; ? = unclear risk; - = high risk.

approach. The primary outcome measures were ΔRBL and/or ΔPD, evaluating ΔBOP as secondary outcome measure. The pooled weighted mean (WM) and the 95% confidence interval (CI) of each measure were estimated with Comprehensive Meta-analysis (Version 2, Biostat, Englewood, NJ, USA) statistical software. Parametric data were expressed as mean and standard deviation (M [SD]). The random effect model was applied when performing meta-analysis to account for methodologic differences among studies. Forest plots were produced to graphically represent WM and 95% CI for the primary and secondary outcomes, with the implant as the analysis unit. Heterogeneity was assessed with the I^2 test. To evaluate the potential influences of different treatment modalities, WM and 95% CI were calculated separately for membrane use, and type of the flap manipulation (submerged/nonsubmerged healing). The reporting of this meta-analysis adhered to the PRISMA statement [19].

RESULTS

Study selection

Article review and data extraction were performed according to PRISMA flow diagram (Figure 1). The initial electronic and hand search retrieved 883 citations, 802 of which were eliminated as duplicates or not relevant articles. After titles and abstracts were reviewed, additional 34 articles were filtered as having not enough information regarding selecting topic. 47 articles were identified as full-text articles, 18 of which were included in this review [22-39]. Reasons for studies exclusion after full-text assessment were as follows: no minimum 12 months follow-up (n = 7) [40-46]; a review paper (n = 3) [47-49], single case report presented (n = 15) [50-64]; methodological and design faults (n = 4) [66-69]. The κ value for the interreviewer agreement of the included publications was 0.92.

Study characteristics

Eight prospective clinical studies [22,23,28,29,34,36,38,39], seven case series [24-27,30,33,35], and three randomized clinical trials (RCTs) [31,32,37] were included for the final review. A total of 528 patients (713 implants) were treated. The mean age of the patients was 61 years (ranged from 20 to 83 years) with the mean observation period of 37 months (ranging from 12 to 236 months). Eleven studies [23-25,27,29,31,32,35-37,39] reported smoking status of the patients, ranging from 14% [39] to 72% [36]. The summarized individual study characteristics are described in Table 2.

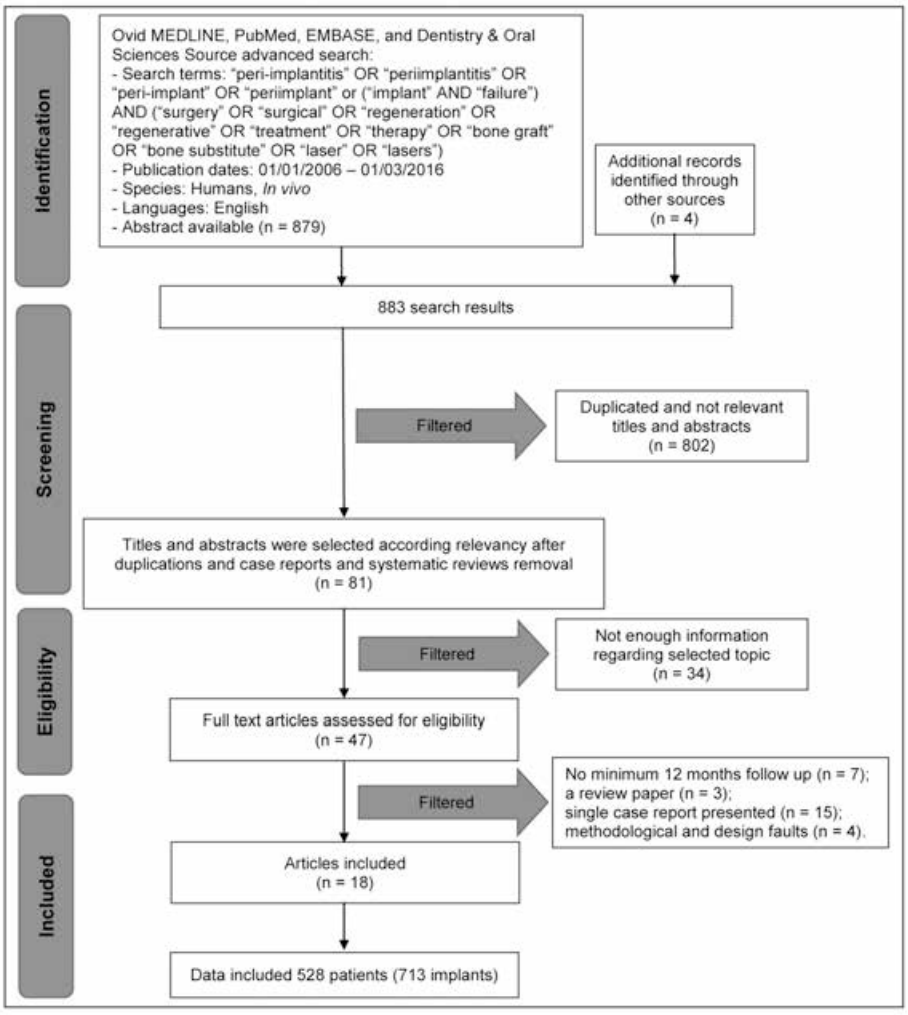

Figure 1. PRISMA flow diagram.

Eight studies included rough surface dental implants [26,29,30,31,32,35,37,39], three studies investigated machined surface implants [23,24,36] and five studies - both rough and machined surface dental implants [22,25,27,28]. The remaining two studies did not reveal implant surface specifications [33,38].

Initial radiologic bone defect depth was measured in twelve studies [22-24,29-33,35-38]. In nine studies [22,29-33,35,37,38] the distance was measured from the implant shoulder to the first bone contact on dental radiographs with the mean from 3 to 8 mm [29,35]. In three studies [23,24,36] the measurement reference point of the radiologic defect depth was the first thread of the implant. The mean initial PD was measured clinically in all included studies, ranging from 4.8 to 8.8 mm [22,30]. After applied surgical regenerative treatment, the PD reduction was ranging from 1.1 to 5.4 mm [27,30]. All studies except three [22,26,32] provided BOP data: the mean initial BOP was ranging from 19.7 to 100% [35,30,34,38]. The mean BOP reduction from 25.9 to 91.1% was obtained after surgical regenerative treatment of peri-implantitis [28,38].

Table 2. Selected studies

Author	Type of study	Sample size (implants)	Detoxification method	Bone substitute/membrane	Antimicrobial	Follow-up (months)	PD Mean (SD) mm		BOP* Mean, %		Radiologic bone level Mean (SD) mm		Complications	Comments	Submerge
							IN	APD	IN	ABOP	IN	ABRL			
Deppe et al. [22]	Prospective clinical study	19 (6 patients)#		No augmentation		20 - 236	5.1 (1.3)	0.8 (1.2)	No data	No data	7.6 (1.4)	0.3 (1.3)	8 implants were lost in augmented bone groups due to infection and 5 implants lost in non-augmented sites	With the respect to the long term results of augmentation procedures, the method used for decontamination seems to play a subordinate role. Augmentation with 1:1 mix of AB and βTCP can lead to reduction of the defect depth.	Y
		15 (7 patients)		AB mixed with βTCP 1:1/PTFE			4.8 (1.4)	2.3 (1.2)			6.8 (1.2)	2.1 (1.1)			
		22 (10 patients)#	CO_2 laser	No augmentation			6.1 (1.6)	2.7 (1.5)			7.2 (1.3)	0.4 (1.1)			
		17 (9 patients)		AB mixed with βTCP 1:1/PTFE			5 (1.3)	2.5 (1.3)			6.7 (1.5)	2.2 (1.3)			
Roos-Jansåker et al. [23]	Prospective clinical study	29 (17 patients)	3% H_2O_2, Saline	FHA/SRM	0.1% CHX rinse for 5 weeks. Amx (375 mg x 3) + Metro (400 mg x 2) for 10 days.	12	5.4 (1.8)	2.9 (1)	79.3%	57.7%	3.4 (1.2)	1.5 (1.2)	Membrane exposure after 2 weeks was noted in 43.8% of the treated implants.	It is possible to treat peri-implant defects with a bone substitute, with or without a resorbable membrane.	N
		36 (19 patients)		FHA			5.6 (1.8)	3.4 (1.7)	92.9%	67.9%	2.8 (0.8)	1.4 (1.3)	Uneventful		
Roos-Jansåker et al. [24]	Case series	16 (12 patients)	3% H_2O_2, Saline	FHA/SRM	0.1% CHX rinse for 5 weeks. Amx (375 mg x 3) + Metro (400 mg x 2) for 10 days.	12	5.1 (1)	4.2 (1.5)	75%	62.5%	3.8 (1)	2.3 (1.2)	62.5% implant sites demonstrated inadequate primary healing with the presence of soft tissue craters. Membrane exposure 75.1%	Treatment of peri-implantitis defect using a bone graft substitute combined with a resorbable membrane and submerged healing resulted in defect fill and clinical healthier situations.	Y
Schwarz et al. [25]	Case series	11 (11 patients)	Saline	nanoHA	0.2% CHX rinse for 2 weeks.	24	6.9 (0.6)	1.5 (0.6)	80%	36%	No data		Suppuration around 2 implants	Both treatment procedures have shown efficacy, however, the application of natural bone mineral in combination with a collagen membrane may result in an improved outcome of healing.	N
		11 (11 patients)		BDX/CM			7.1 (0.8)	2.4 (0.8)	78%	44%					N
Romanos et al. [26]	Case series	19 (15 patients)	CO_2 laser	AB or BDX/CM		27	6 (2)	3.5 (1.3)	No data		No data		No data	Bovine xenograft provided more radiographic bone fill than autogenous graft, because of autogenous graft resorption over time.	YN
Schwarz et al. [27]	Case series	9 (9 patients)	Saline	nanoHA	0.2% CHX rinse for 2 weeks.	48	6.9 (0.6)	1.1 (0.3)	80%	32%	Decreased translucency in the former peri-implant defect area noticed at 8 sites in nanoHA and 5 sites in BDX/ resorbable membrane group.		Uneventful	While the application of natural bone mineral with a collagen membrane resulted in clinical improvements, a long-term outcome obtained with nanocrystaline hydroxyapatite without a barrier membrane must be considered as poor.	N
		10 (10 patients)		BDX/CM			7.1 (0.7)	2.5 (0.9)	79%	51%					N
Schwarz et al. [28]	Prospective clinical study	9 (9 patients)	Saline	DBX/CM	0.2% CHX rinse for 2 weeks.	12	6.7 (0.7)	1.6 (0.9	81.5%	38.9%	No data		Uneventful	Defect configuration may have an impact on the clinical outcome following surgical regenerative therapy of peri-implantitis lesions.	N
		9 (9 patients)					7.1 (0.6)	1.6 (0.7)	83.3%	25.9%					
		9 (9 patients)					7 (0.5)	2.7 (0.7)	85.2%	61.1%					
Roccuzzo et al. [29]	Prospective clinical study	14 TPS implants (14 patients)	24% EDTA gel, 1% CHX gel, Saline	BDX	Axm and Clavulanic acid (1000 mg x 2) for 6 days. 0.2% CHX rinse for 3 weeks.	12	7.2 (1.5)	2.1 (1.2)	91.1%	33.9%	3.9 (1.6)	1.6 (0.7)	No complications	Clinical parameters around moderately rough implants were better than around rough implants. Surgical regenerative technique described resulted in a clinical healthier situation around many of the treated implants so that their function could be fully maintained. Complete fill of the bony defect seems not to be a predictable result.	N
		12 SLA implants (12 patients)					6.8 (1.2)	3.4 (1.7)	75%	60.4%	3 (0.9)	1.9 (1.3)			
Froum et al. [30]	Case series	19 (15 patients)	AA, Saline, Tetracycline (50 mg/mL), 0.12% CHX	DBX or MBA/Enamel matrix derivative/ /PDGF/CM or SCTG	Amx 500 mg x 3 for 10 days. 0.12% CHX rinse for 2 weeks.	36 - 90	8.8 (1.9)	5.4 (1.5)	100%	78.9%	6.4 (1.9)	3.8 (1.5)		Regenerative approach for the treatment of peri-implantitis appear to be encouraging.	N
Aghazadeh et al. [31]	Randomized controlled clinical study	34 (22 patients)	3% H_2O_2, Saline	AB/resorbable bovine collagen	Azithromycin (250 mg x1) for 4 days. 0.1% CHX rinse for 6 weeks.	12	6 (1.3)	7 (1.2)	87.5%	44.8%	5.8 (1.7)	0.2 (1.8)		BDX provided more radiographic bone fill than AB. The success for both surgical regenerative procedures was limited.	N
		37 (23 patients)		BDX/resorbable bovine collagen			6.2 (1.4)	3.1 (1.2)	79.4%	50.4%	5.2 (1.8)	1.1 (1.9)			
Wohlfahrt et al. [32]	Randomized clinical trial	16 (16 patients)	24% EDTA gel, Saline	Porous titanium granules	0.2% CHX rinse for 4 weeks. Amx (500 mg x 3) + Metro (400 mg x 2) for 10 days.	12	6.5 (1.9)	1.7 (1.7)	No data	No data	6.8 (2.7)	2 (1.7)	Uneventful	Reconstruction with porous titanium granules resulted in significantly better radiographic peri-implant defect fill compared with controls.	Y
		16 (16 patients)#		No augmentation			6.5 (2.3)	2 (2.3)	No data	No data	6.8 (3.9)	0.1 (1.9)			
Wilfang et al. [33]	Case series	36 (22 patients)	Implantoplsty, 20% Phosphoric Acid	AB mixed with BDX 1:1	Ampicillin/sulbactam 1500 mg preoperatively.	12	7.5 (1.8)	4 (1.8)	61%	36%	5.1 (2.4)	3.5 (2.4)	One local infection 1 week after surgery causing loss of the augmentation material without loss of the implant.	Surgical regenerative treatment provided a reliable method to reduce peri-implantitis induced bone defects.	N
Schwarz et al. [34]	Prospective clinical study	7 (7 patients)	Implantoplasty, Saline	BDX/CM	Non specified antibiotic medication for 5 days.	48	5.5 (1.7)	1.2 (1.9)	100%	85.2%	No data		Reinfection in 4 patients occurred between 24 - 36 months postoperatively.	A combined surgical respective/regenerative therapy of peri-implantitis were not influenced by the method of surface decontamination.	N
		10 (10 patients)	Implantoplasty, Er:YAG laser				5.1 (1.5)	1.3 (1.8)	95.2%	71.6%					
Matarasso et al. [35]	Case series	11 (11 patients)	Implantoplasty, AA, Saline	DBX/CM	Amx 875 mg and clavulanic acid 125 mg x 2 for 5 days. 0.12% CHX rinse for 4 weeks.	12	8.1 (1.8)	4.1 (1.5)	19.7%	13.6%	8 (3.7)	2.7 (3.3)	Membrane exposure in 18% of cases.	Combined regenerative/resective surgical approach for the treatment of peri-implantitis defects yielded positive clinical and radiographic results after 12 months.	N
Roos-Jansåker et al. [36]	Prospective clinical study	23 (13 patients)	3% H_2O_2, Saline	FHA/SRM	0.1% CHX rinse for 5 weeks. Amx (375 mg x 3) + Metro (400 mg x 2) for 10 days.	60	5.6 (1.9)	3 (2.4)	75%	42.4%	4.6 (1.3)	1.5 (1.2)	Membrane exposure	The use of a resorbable membrane in combination with a bone substitute did not add to the predictability or extent of bone fill.	N
		22 (12 patients)		FHA			6 (2.2)	3.3 (2)	94.3%	82.9%	4 (0.8)	1.1 (1.2)			
Jepsen et al. [37]	Randomized clinical trial	33 (33 patients)	Titanium brush, 3% H_2O_2, Saline	Porous titanium granules	0.2% CHX rinse for 4 weeks. Amx (500 mg x 3) + Metro (400 mg x 2) for 8 days.	12	6.3 (1.3)	2.8 (1.3)	89.4%	56.1%	4.6 (2)	3.6 (2)	Uneventful	Reconstructive surgery using porous titanium granules resulted in significantly enhanced radiographic defect fill compared with open flap debridement. The radiographic findings must be interpreted with caution, because it is difficult to discern biomaterial and newly formed osseous tissue.	N
		30 (30 patients)#		No augmentation			6.3 (1.6)	2.6 (1.4)	85.8%	44.9%	4 (2.5)	1.1 (1.4)			
Froum et al. [38]	Prospective clinical study	168 (100 patients)	AA, Saline, Tetracycline (50 mg/mL), 0.12% CHX	DBX or MBA/Enamel matrix derivative/ /PDGF/CM or SCTG		24 - 120	8.1 (2.5)	5.1 (2.2)	100%	91.1%	3.8 (2.3)	1.8 (2)	2 implants were lost at 6 months follow up 16.7% of cases needed additional surgeries to obtain desired result.	Regenerative protocol used in treating peri-implantitis produced positive clinical outcomes in terms of reduction in BOP and PD, bone gain, and implant survival.	N
Roccuzzo et al. [39]	Prospective clinical study	71 (71 patients)	Titanium brush, 24% EDTA gel, 1% CHX gel, Saline	DBX	Axm and Clavulanic acid (1000 mg x 2) for 6 days. 0.2% CHX rinse for 3 weeks.	12	7.2 (1.6)	2.9 (1.7)	71.5%	53.2%	No data	No data	6 implants were explanted due to persistent pus formation after 12 months.	Partial defect fill was obtained. Complete resolution does not seem a predictable outcome.	N

#Non augmented control groups were excluded for evaluation.
NanoHA = nanocrystalline hydroxyapatite; BDX = bovine-derived xenograft; CHX = chlorhexidine solution; Saline = Sterile physiologic saline solution; FHA = fluorohydroxyapatite, Amx = Amoxicillin; Metro = Metronidazole; AB = autogenous bone; SCTG = Subepithelial connective tissue graft; PDGF = Platelet-derived growth factor; MBA = mineralized bone allograft; βTCP = beta tricalcium phosphate; CM = collagen membrane; PTFE = polytetrafluoroethylene membrane; SRM = synthetic resorbable membrane; AA = air abrasive.

All included studies used grafting materials for peri-implant bone defect augmentation. Most commonly xenografts [25-31,34,35,38,39] were utilized as well as other grafting materials, including flourhydroxyapatites [23,24,36], autografts [26,31], allografts [30,39], porous titanium granules [32,37], and comixtures of several different grafts [22,33]. There were more study groups using barrier membranes [22-28,30,31,34-36,38], than study groups, without barrier membranes utilized to cover the grafted area [23,25,27,29,32,33,36,37,39]. Due to high heterogeneity of the studies, statistical comparisons among different grafting materials and membrane types were not intended.

Risk of bias within studies

Summarizing the risk of bias for each study, most of the studies were classified as unclear risk [22-25,27-29,34-36,38,39]. Two studies were considered as having low risk of bias [32,37], where as another one was classified as moderate risk [31], and three studies were attributed to high risk of bias [26,30,33]. The risk of bias assessment for the included studies is summarized in Table 1.

Results of meta-analysis

The results and forest plots of the meta-analyses for ΔRBL, ΔPD and ΔBOP are demonstrated in Figures 2 - 4.

Following surgical regenerative treatment of peri-implantitis, the reported WM of ΔRBL was 1.97 mm (95% CI = 1.58 to 2.35 mm; Figure 2A). WM of ΔRBL was 1.86 mm (95% CI = 1.36 to 2.36 mm; Figure 2B) in ten study groups with membranes used, whereas WM of ΔRBL was calculated 2.12 mm (95% CI = 1.46 to 2.78 mm; Figure 2C) in seven study groups without membranes used to cover the grafted area. ΔRBL in submerged healing cases was evaluated in four study groups, with WM 2.17 mm (95% CI = 1.87 to 2.47 mm; Figure 2D), whereas thirteen groups of non-submerged healing presented WM 1.91 mm (95% CI = 1.44 to 2.39 mm; Figure 2E).

All included studies investigated probing depth change prior and post treatment. The pooled WM of ΔPD was 2.78 mm (95% CI = 2.31 to 3.25 mm; Figure 3A). WM of ΔPD 2.88 mm (95% CI = 2.31 to 3.45 mm; Figure 3B) was calculated in eighteen study groups using the barrier membrane. Similarly, WM of ΔPD 2.6 mm (95% CI = 1.9 to 3.3 mm; Figure 3C) was obtained in ten study groups, without membranes used to cover the graft. In four study groups, that evaluated submerged healing, WM of ΔPD 2.68 mm (95% CI = 1.71 to 3.64 mm; Figure 3D) was obtained, meanwhile WM of ΔPD 2.77 mm (95% CI = 2.23 to 3.3 mm; Figure 3E) was granted in twenty three study groups of non-submerged healing.

The percentage of BOP reduction was reported in fifteen studies, with the WM being 55% (95% CI = 45.2 to 64.4%; Figure 4A).

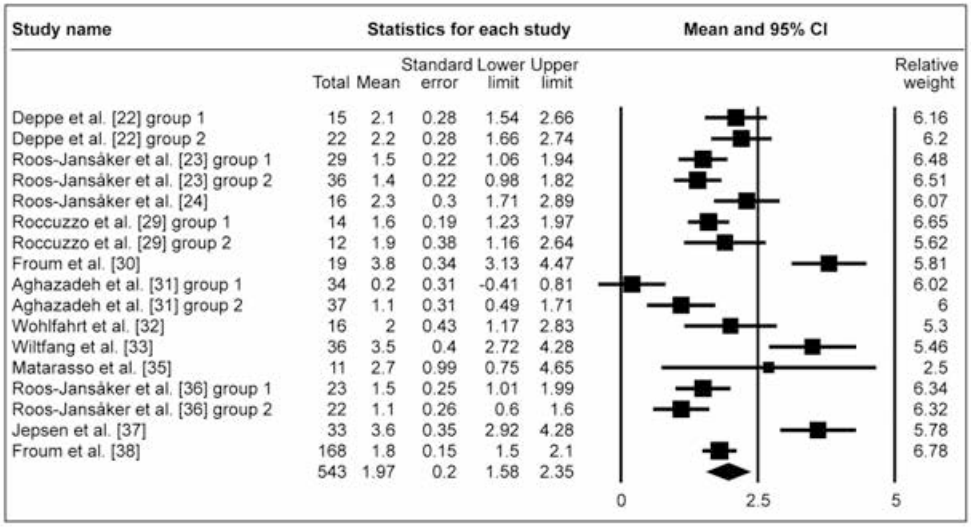

Figure 2A. Meta-analysis for radiologic bone level change (ΔRBL). The calculated WM was 1.97 mm (95% CI = 1.58 to 2.35 mm).

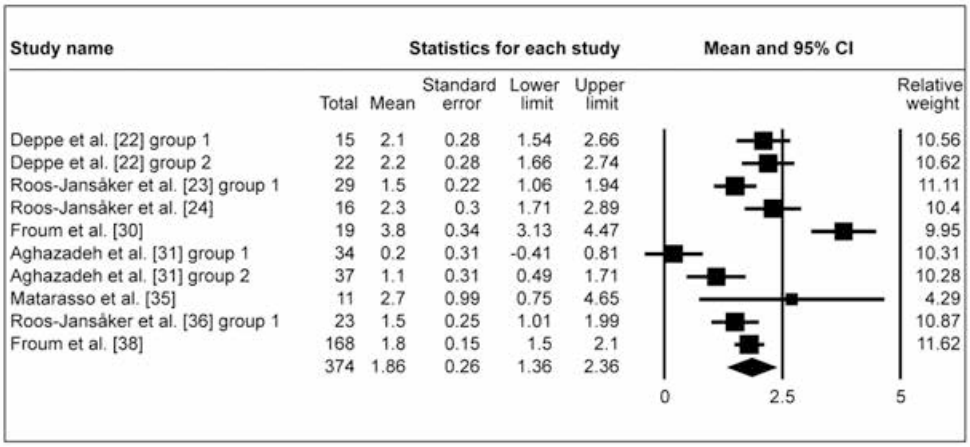

Figure 2B. Meta-analysis for radiologic bone level change (ΔRBL) with membrane coverage of the grafted area. The calculated WM was 1.86 mm (95% CI = 1.36 to 2.36 mm).

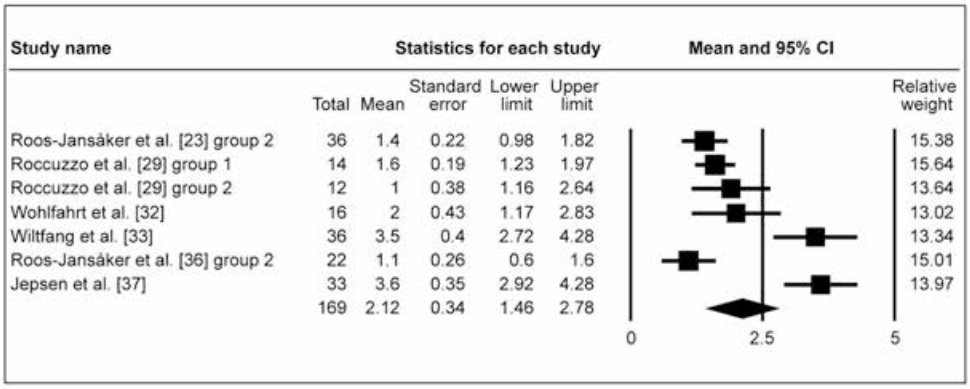

Figure 2C. Meta-analysis for radiologic bone level change (ΔRBL) without membrane coverage of the grafted area. The calculated WM was 2.12 mm (95% CI = 1.46 to 2.78 mm).

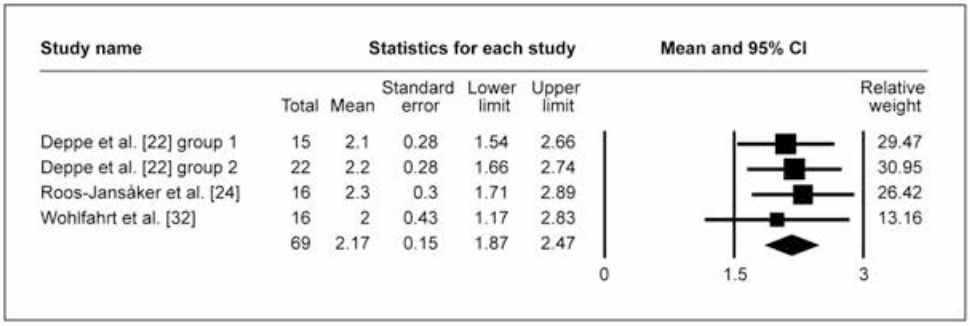

Figure 2D. Meta-analysis for radiologic bone level change (ΔRBL) in submerged peri-implant defect healing. The calculated WM was 2.17 mm (95% CI = 1.87 to 2.47 mm).

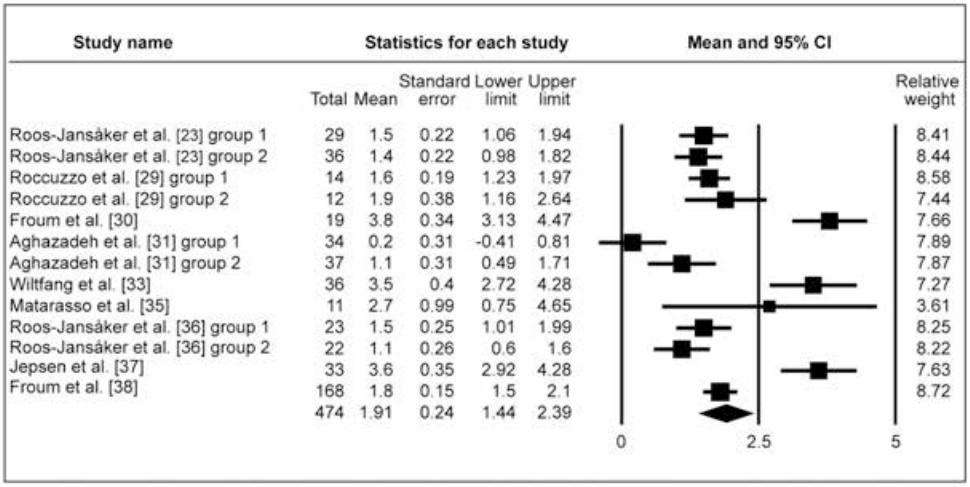

Figure 2E. Meta-analysis for radiologic bone level change (ΔRBL) in non-submerged peri-implant defect healing. The calculated WM was 1.91 mm (95% CI = 1.44 to 2.39 mm).

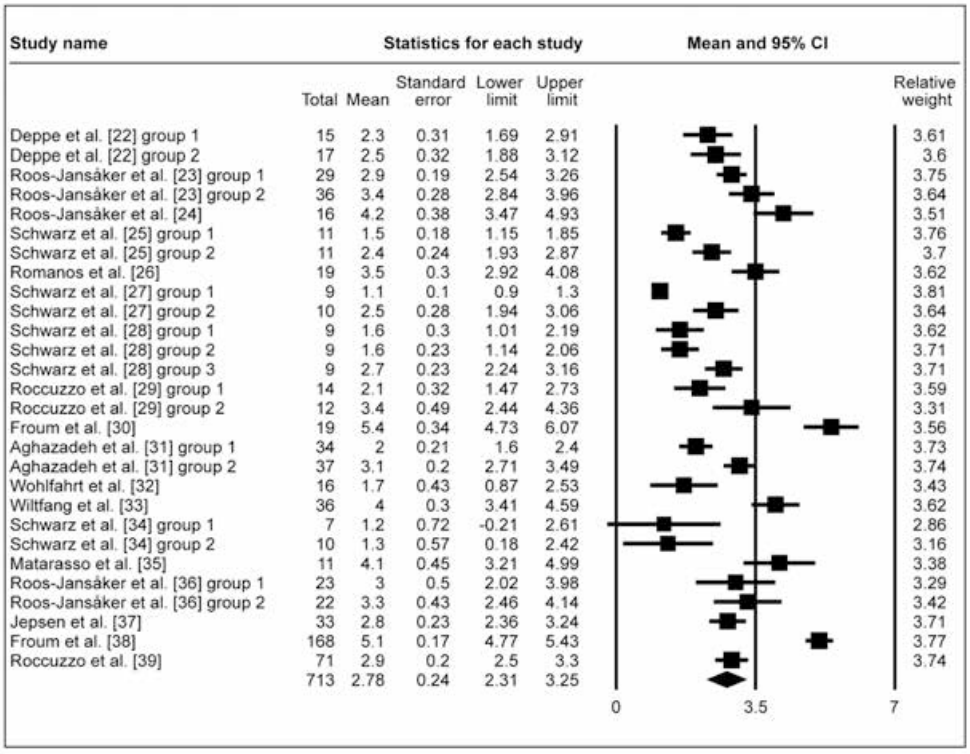

Figure 3A. Meta-analysis for probing depth change (ΔPD). The calculated WM was 2.78 mm (95% CI = 2.31 to 3.25 mm).

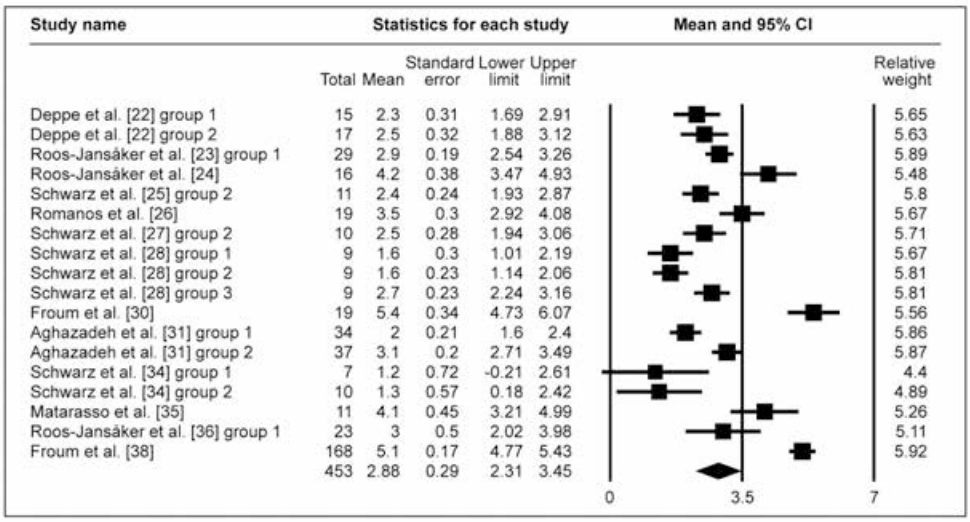

Figure 3B. Meta-analysis for probing depth change (ΔPD) with membrane coverage of the grafted area. The calculated WM was 2.88 mm (95% CI = 2.31 to 3.45 mm).

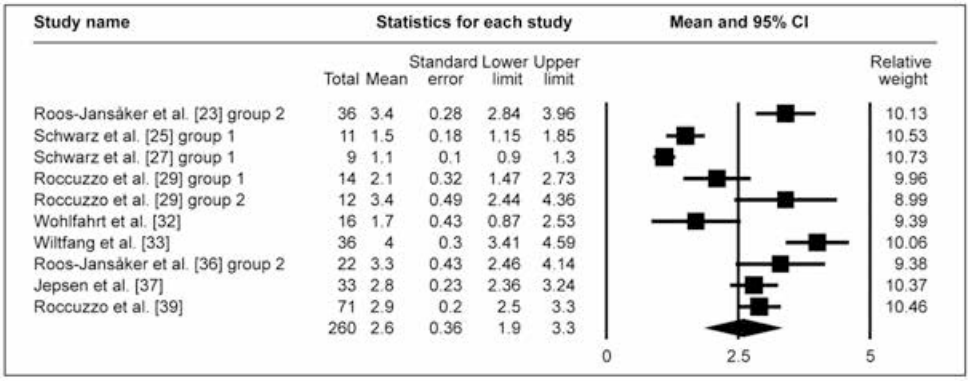

Figure 3C. Meta-analysis for probing depth change (ΔPD) without membrane coverage of the grafted area. The calculated WM was 2.6 mm (95% CI = 1.9 to 3.3 mm).

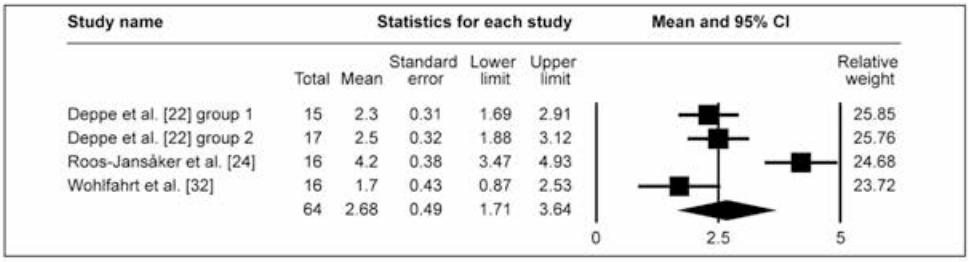

Figure 3D. Meta-analysis for probing depth change (ΔPD) in submerged peri-implant defect healing. The calculated WM was 2.68 mm (95% CI = 1.71 to 3.64 mm).

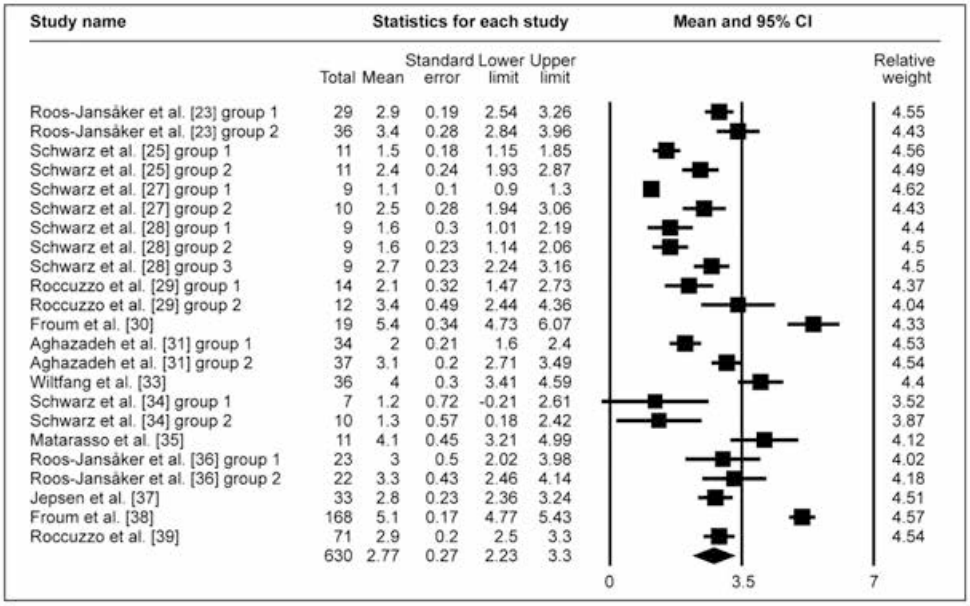

Figure 3E. Meta-analysis for probing depth change (ΔPD) in non-submerged peri-implant defect healing. The calculated WM was 2.77 mm (95% CI = 2.23 to 3.3 mm).

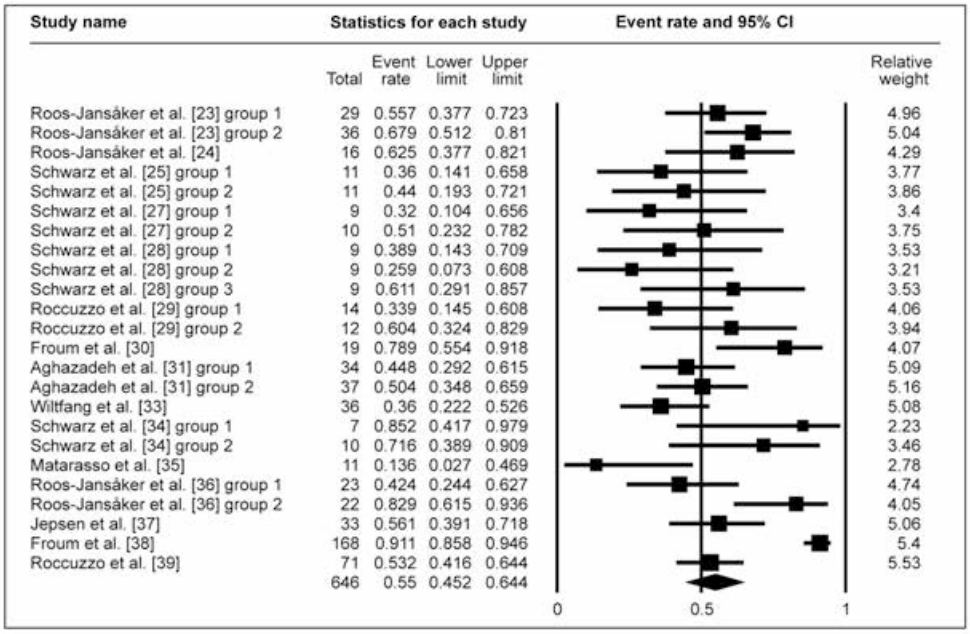

Figure 4A. Meta-analysis for bleeding on probing change (ΔBOP). The calculated WM was 55% (95% CI = 45.2% to 64.4%).

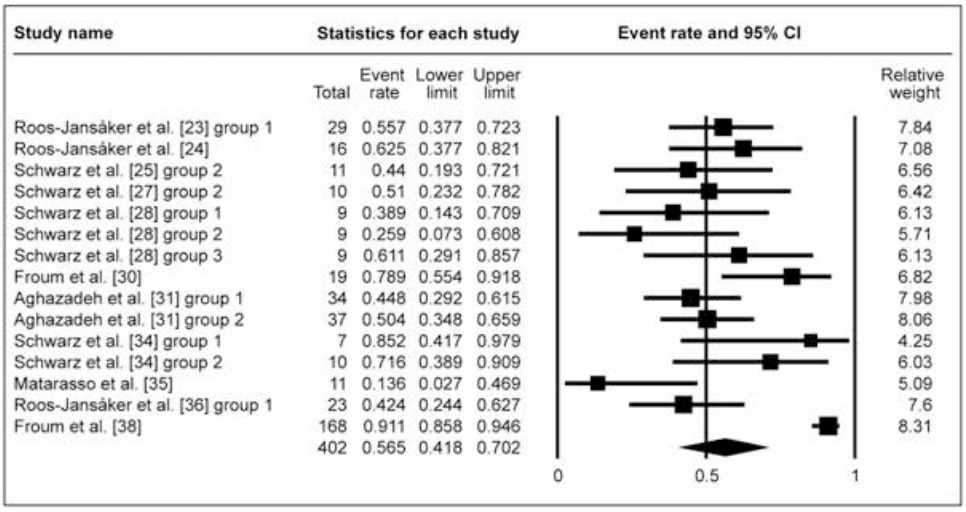

Figure 4B. Meta-analysis for bleeding on probing change (ΔBOP) with membrane coverage of the grafted area. The calculated WM was 56.5% (95% CI = 41.8% to 70.2%).

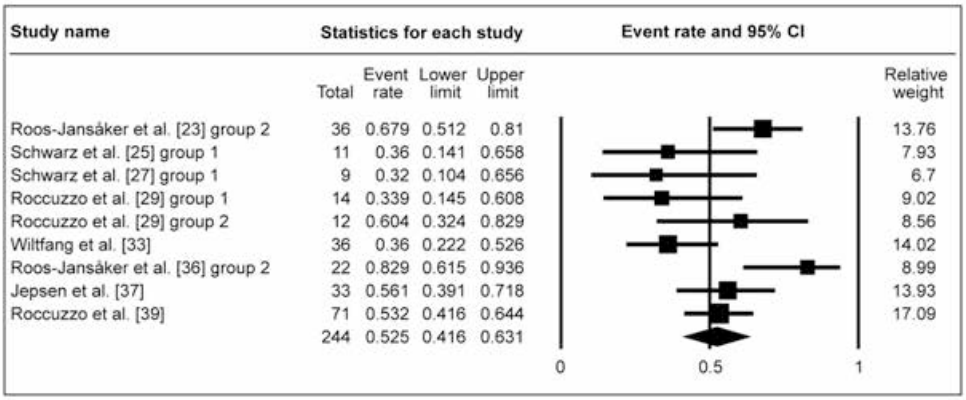

Figure 4C. Meta-analysis for bleeding on probing change (ΔBOP) without membrane coverage of the grafted area. The calculated WM was 52.5% (95% CI = 41.6% to 63.1%).

Studies, with membranes used, exhibited WM of ΔBOP 56.5% (95% CI = 41.8 to 70.2%; Figure 4B). This was similar for studies, without membranes used for graft coverage, where WM of ΔBOP was 52.5% (95% CI = 41.6 to 63.1%; Figure 4C). Due to low number of studies, investigating ΔBOP after submerged healing surgery, meta-analysis of submergence impact on ΔBOP was not conducted.

Risk of bias across studies

There were several limitations present in the current meta-analysis. Current review includes studies written in English only, which could introduce a publication bias. The included studies were of relatively short follow-up period and included relatively small numbers of patients. There were various degrees of heterogeneity in each study design, case selection, and treatment provided among studies. The absence of control groups was an important limitation. There was also too high heterogeneity of the selected studies to compare the impact of different bone grafting materials or membrane types for the final treatment outcome.

DISCUSSION

Peri-implantitis can be defined as a clinical condition characterized by an inflammatory reaction that involves the hard and soft tissue, which causes loss of supporting bone and pathological pocket formation surrounding the osseointegrated dental implants [1-18]. Several therapies options have been developed in order to manage the peri-implantitis, which could be non-surgical or surgical [6,10,47-50].

A conservative treatment option may be useful in cases without bone loss and a pocket formation limited to 3 - 4 mm. In case of evident bone loss and pocket formation over 5 mm, the surgical treatment seems to be necessary [22-39]. Surgical techniques can be divided into resective and regenerative surgery [6,50].

The resective implant treatment attempts to eliminate the aetiologic factors and maintain optimal peri-implant conditions, mainly by cleaning the surfaces of the implants; whereas regenerative therapy (using bone grafts, membranes and growth factors) aims to regenerate peri-implant bone defect and reconstruct the peri-implant unit to previously existing normal physiologic limits [6,47,49,50,66].

Romeo et al. [66] have compared the efficacy of resective surgery with that of implantoplasty. The results obtained after 3 years of therapy demonstrated that the marginal bone loss was significantly lower after implantoplasty and the surgical therapy without biomaterial results effective in case of deep peri-implantitis.

The present investigation aimed to screen what is published in the recent international literature on the overall treatment outcomes of reconstructive procedures in treating peri-implantitis. The application of bone grafting materials for peri-implant bone defect treatment was used in all the recorded studies [22-39]. The meta-analysis showed that 1.97 mm mean ΔRBL was gained after surgical regenerative treatment. The lowest bone fill (0.2 [1.8] mm) was obtained in the comparative study by Aghazadeh et al. [31] using autografts, which was similar in results of Deppe et al. [22] (0.3 [1.3] mm) and Wohlfahrt et al. [32] (0.1 [1.9] mm) study groups, where surgical non-regenerative treatment was applied. Autogenous bone, which has been often defined as the "gold standard" in bone augmentation, shows a volume loss of approximately 40% during healing time. On the other hand, synthetic bone graft substitutes show a high stability in volume, but remain nearly or completely unresorbed even several years after surgery [70]. Recently, Araujo and Lindhe [71] demonstrated, that autologous bone neither stimulate nor retard new bone formation in beagle dog extraction socket model. This raises an open dispute, if autografts, despite of their osteoinductive and osteogenic properties, still might be described as "gold standard" in situations, where slow resorption and adequate space maintaining biomaterials are desired. In contrary, regeneration of peri-implant defects with autografts mixed with bovine bovine-derived xenograft [33] or beta tricalcium phosphate [22] exhibited 2.1 (1.1) mm and 3.5 (2.4) mm peri-implant bone gain correspondingly. Decreased resorption rate and increased osteoconductivity of composite autograft mixture with synthetic or xenogenic matrials compared of autogratfs alone could influence this better outcome. However, it is important to note, that visual bone fill on the radiographs per se is barely sufficient to claim a successful long-term outcome after peri-implantitis treatment [72].

The highest ΔRBL aproximatelly 3.5 to 3.8 mm was reported in three studies (Froum et al. [30]; Wiltfang et al. [33]; Jepsen et al. [37]). Froum et al. [30] used enamel matrix derivative and platelet derived growth factor (PDGF) to enhance regenerative outcome. This might influence the increased bone fill, however well designed studies and long-term RCTs, comparing effectiveness of these bioactive materials on peri-implant bone regeneration, currently are still lacking. Wilfang el al. [33] and Jepsen et al. [37] used bovine-derived xenograft and porous titanium granules correspondingly to fill peri-implant bone defects. The above average ΔRBL, obtained in the latter two studies, should be also interpreted with caution, because both xenograft and porous titanium granules are highly radiopaque materials, and it is difficult to discern biomaterial and newly formed osseous tissue.

There were numerous surgical techniques described in the included articles of this review to regenerate the peri-implant bone defects, including various submergence protocols (e.g. submerged or non-submerged healing), polytetrafluoroethylene (PTFE), collagen, synthetic membranes or no membrane used to cover the grafted area. Submergence of the healing site was employed in four study groups of the included articles [22,24,32]. The rest study groups included in this review applied non-submerged healing. The meta-analysis and comparison between submerged and non-submerged sites provided similar clinical outcomes, having mean ΔRBL 2.17 mm and 1.91 mm alongside to the mean ΔPD 2.68 mm and 2.77 mm in submerged and non-submerged sites correspondingly.

The use of barrier membrane to cover the grafted area is often an operator dependent decision.

Barrier membranes are intended to stabilize the graft and to prevent epithelial downgrowth and fibroblast transgrowth into the grafted area, thereby favouring the population of bone cells in a bony defect. In agreement to findings in this review, Sahrmann et al. [73] concluded that guided bone regeneration using both bone graft substitute and membrane represents the major part of published surgical regenerative treatment of peri-implantitis cases. Schwarz et al. [27] stated that combination of biomaterial (bovine-derived xenograft) together with collagen membrane resulted in improved clinical outcomes compared to biomaterial (nanocrystalline hydroxyapatite) alone. However, in this study different biomaterials were used, therefore comparisons should be interpreted with caution. Another study of Schwarz et al. [28] have shown that the use of a bone graft with the additional placement of a membrane may be more efficient in specific bone lesions around implants, however well-defined crater-like defect may improve the retention of the bone graft without additional use of the barrier membrane thereby favouring the healing [27,36]. Further studies of Roos-Jansaker et al. [36,74] and systematic reviews by Figuero et al. and Chan et al. [75,76] concluded that the application of a barrier membrane is costly, time consuming, technique sensitive, related to high membrane exposure risk, and its application did not provided improved clinical outcome nor in the terms of RBL, neither PD or BOP. This is in agreement with findings of meta-analysis in this review, where mean ΔRBL was 1.86 mm versus 2.12 mm, mean ΔPD 2.88 mm versus 2.6 mm, and mean ΔBOP 56.5% versus 52.5% in case with and without membrane used for graft coverage correspondingly. These findings suggest that barrier membrane placement might be not necessary in well-contained peri-implant bone defects.

The meta-analysis revealed reduction of PD and BOP after surgical regenerative treatment of peri-implantitis in all included studies, with mean ΔPD 2.78 mm and mean ΔBOP 55%. Although surgical regenerative treatment resulted in a clinical healthier situation around treated implants, most of the included studies [23,24,28,29,31-33,35,37,39] had minimal 12 months postoperative follow-up period to meet the borderline of the inclusion criteria. At the time there is very limited number of long-term RCTs, investigating the outcomes of surgical regenerative treatment of peri-implantitis [39,48]. Nevertheless, in real clinical situations when every treatment modality should be well applied and effective to treat peri-implantis, the ethical concern is an important issue. Constantly, there were only three RCTs included in this systematic review with the longest 12 months follow-up [31,32,37]. Future years of observation are necessary to verify whether an osseous defect fill is adequate to ensure favourable long-term maintenance. A 6 months case series study published by of Schwarz et al. [40] concluded that both the application of alloplastic material (nanocrystalline hydroxyapatite) or bovine-derived xenograft covered with collagen membrane induce significant improvement in clinical parameters (probing depth, clinical attachment level) at the healing control. A continuing follow-up of the same study group in a 2-years outcomes published by Schwarz et al. [25] also underlined the successful bone filling of the peri-implant defect applying both with nanocrystalline hydroxyapatite and bovine-derived xenograft in combination with collagen membrane that provided a significant reduction of the PD and gain in clinical attachment level. However, in the 4-year follow-up [27], the combination of bovine-derived xenograft and collagen membrane were more clinically efficacious as compared to nanocrystalline hydroxyapatite alone. This difference might be influenced by different long-term physicochemical properties of the applied bone graft substitute. In this systematic review high heterogeneity among the studies regarding surgical protocols, and selection of biomaterials were found, therefore at the time no clear recommendations could be drawn, how various treatment modalities or grafting materials could influence the clinical outcomes on the long-term basis.

Limitations

Even if a comprehensive and complete investigation of the effects of surgical therapies has been performed, there were some limitations to this systematic review. Surgical regenerative treatment of peri-implantitis is a complex procedure, depending on various multiple factors, including patient general health condition, oral hygiene habits, defect configuration, implant surface characteristics, decontamination procedure, surgical technique, postoperative maintenance program, and various other factors which are not possible to fit within the frames of systematic literature review and meta-analysis.

CONCLUSIONS

Within the limits of this systematic review, surgical regenerative treatment is a predictable option in managing peri-implantitis and improving clinical parameters of peri-implant tissues. There is no fundamental advantage of membrane use for bone graft coverage or submergence of the healing site on

the final outcome of peri-implant defect regeneration. Due to the limited number of randomized clinical trials, at the time there is a lack of scientific evidence in the literature regarding the superiority of the regenerative versus non-regenerative surgical treatment. No conclusions could be drawn regarding the choice of biomaterials for peri-implant bone regeneration due to high heterogeneity among the present studies. Further well designed long-term randomized clinical trials, investigating the impact of peri-implant defect configuration, application of different grafting materials and bioactive modifiers, implant surface decontamination methods, and various surgical protocols on the final outcome of the regenerative procedure are needed.

ACKNOWLEDGMENTS AND DISCLOSURE STATEMENTS

The authors report no conflicts of interest related to this study. The authors would like to thank Irena Nedzelskiene (Clinic of Dental and Oral Pathology, Lithuanian University of Health Sciences, Kaunas, Lithuania) for her help in statistical analysis.

REFERENCE

1. Swart LC, Dreyer WP, van Zyl PP, Blignaut RJ. Early loading of mandibular implants placed immediately after extraction: a 10-year prospective study of eight patients. Int J Oral Maxillofac Implants. 2014 Nov-Dec;29(6):1388-96. [Medline: 25397802] [doi: 10.11607/jomi.3670]
2. Buser D, Bornstein MM, Weber HP, Grütter L, Schmid B, Belser UC. Early implant placement with simultaneous guided bone regeneration following single tooth extraction in the esthetic zone: A cross-sectional, retrospective study in 45 patients with a 2- to 4-year follow-up. J Periodontol 2008;79:1773–1781. [Medline: 18771381] [doi: 10.1902/jop.2008.080071]
3. Simion M, Jovanovic SA, Tinti C, Benfenati SP. Long-term evaluation of osseointegrated implants inserted at the time or after vertical ridge augmentation. A retrospective study on 123 implants with 1-5 year follow-up. Clin Oral Implants Res 2001;12:35-45. [Medline: 11168269x] [doi: 10.1034/j.1600-0501.2001.012001035.x]
4. Donati M, Ekestubbe A, Lindhe J, Wennstrom JL. Implant-supported single-tooth restorations. A 12-year prospective study. Clin Oral Implants Res. 2015 Nov 18. [Medline: 26577573] [doi: 10.1111/clr.12726]
5. Balshi TJ, Wolfinger GJ, Stein BE, Balshi SF. A long-term retrospective analysis of survival rates of implants in the mandible. Int J Oral Maxillofac Implants. 2015 Nov-Dec;30(6):1348-54. [Medline: 26574859] [doi: 10.11607/jomi.3910]
6. Lang NP, Wilson TG, Corbet EF. Biological complications with dental implants: their prevention, diagnosis and treatment. Clin Oral Implants Res. 2000;11 Suppl 1:146-55. [Medline: 11168263] [doi: 10.1034/j.1600-0501.2000.011S1146.x]
7. Mombelli A, van Oosten MA, Schurch E Jr, Lang NP. The microbiota associated with successful or failing osseointegrated titanium implants. Oral Microbiol Immunol. 1987 Dec;2(4):145-51. [Medline: 3507627] [doi: 10.1111/j.1399-302X.1987.tb00298.x]
8. Westfelt E, Rylander H, Dahlén G, Lindhe J. The effect of supragingival plaque control on the progression of advanced periodontal disease. J Clin Periodontol. 1998 Jul;25(7):536-41. [Medline: 9696252] [doi: 10.1111/j.1600-051X.1998.tb02484.x]
9. Leonhardt A, Renvert S, Dahlén G. Microbial findings at failing implants. Clin Oral Implants Res. 1999 Oct;10(5):339-45. [Medline: 10551058] [doi: 10.1034/j.1600-0501.1999.100501.x]
10. Mombelli A, Lang NP. The diagnosis and treatment of peri-implantitis. Periodontol 2000. 1998 Jun;17:63-76. [Medline: 10337314] [doi: 10.1111/j.1600-0757.1998.tb00124.x]
11. van Steenberghe D, Naert I, Jacobs R, Quirynen M. Influence of inflammatory reactions vs. occlusal loading on peri-implant marginal bone level. Adv Dent Res. 1999 Jun;13:130-5. [Medline: 11276735] [doi: 10.1177/08959374990130010201]
12. Esposito M, Thomsen P, Ericson LE, Lekholm U. Histopathologic observations on early oral implant failures. Int J Oral Maxillofac Implants. 1999 Nov-Dec;14(6):798-810. [Medline: 10612916]
13. Quirynen M, Peeters W, Naert I, Coucke W, van Steenberghe D. Peri-implant health around screw-shaped c.p. titanium machined implants in partially edentulous patients with or without ongoing periodontitis.Clin Oral Implants Res. 2001 Dec;12(6):589-94. [Medline: 11737102] [doi: 10.1034/j.1600-0501.2001.120606.x]
14. Cicciù M, Risitano G, Maiorana C, Franceschini G. Parametric analysis of the strength in the ''Toronto'' osseous-prosthesis system. Minerva Stomatol. 2009 Jan-Feb;58(1-2):9-23. [Medline: 19234433]
15. Renvert S, Lessem J, Dahlen G, Renvert H, Lindahl C. Mechanical and repeated antimicrobial therapy using a local drug delivery system in the treatment of peri implantitis: a randomized clinical trial. J Periodontol. 2008;79:836-44. [Medline: 18454662] [doi: 10.1902/jop.2008.070347]
16. Jovanovic SA. Diagnosis and treatment of peri-implant disease. Curr Opin Period 1994:194-204. [Medline: 8032461]
17. Jovanovic SA. The management of peri-implant breakdown around functioning osseointegrated dental implants. J Periodontol. 1993 Nov; 64(11 Suppl):1176-83. [Medline: 8295108] [doi: 10.1902/jop.1993.64.11s.1176]

18. Artzi Z, Tal H, Chweidan H. Bone regeneration for reintegration in peri-implant destruction. Compend Contin Educ Dent. 1998 Jan;19(1):17-20, 22-3, 26-8; quiz 30. [Medline: 9533349]
19. Moher D, Liberati A, Tetzlaff J, Altman DG; PRISMA Group. Preferred reporting items for systematic reviews and meta-analyses: the PRISMA statement. J Clin Epidemiol. 2009 Oct;62(10):1006-12. [Medline: 19631508] [doi: 10.1016/j.jclinepi.2009.06.005]
20. American Academy of Periodontology. Academy report: Peri-implant mucositis and peri-implantitis: a current understanding of their diagnoses and clinical implications. J Periodontol. 2013 Apr;84(4):436-43. [Medline: 23537178] [doi: 10.1902/jop.2013.134001]
21. Higgins JP, Altman DG, Gotzsche PC, Jüni P, Moher D, Oxman AD, Savovic J, Schulz KF, Weeks L, Sterne JA. The Cochrane Collaboration's tool for assessing risk of bias in randomised trials. BMJ 2011; 343:d5928. [Medline: 22008217] [doi: 10.1136/bmj.d5928]
22. Deppe H, Horch HH, Neff A. Conventional versus CO2 laser-assisted treatment of peri-implant defects with the concomitant use of pure-phase beta-tricalcium phosphate: a 5-year clinical report. Int J Oral Maxillofac Implants. 2007 Jan-Feb;22(1):79-86. [Medline: 17340900]
23. Roos-Jansåker AM, Renvert H, Lindahl C, Renvert S. Surgical treatment of peri-implantitis using a bone substitute with or without a resorbable membrane: a prospective cohort study. J Clin Periodontol. 2007 Jul;34(7):625-32. [Medline: 17555414] [doi: 10.1111/j.1600-051X.2007.01102.x]
24. Roos-Jansåker AM, Renvert H, Lindahl C, Renvert S. Submerged healing following surgical treatment of peri-implantitis: a case series. J Clin Periodontol. 2007 Aug;34(8):723-7. Epub 2007 May 29. [Medline: 17535286] [doi: 10.1111/j.1600-051X.2007.01098.x]
25. Schwarz F, Sculean A, Bieling K, Ferrari D, Rothamel D, Becker J. Two-year clinical results following treatment of peri-implantitis lesions using a nanocrystalline hydroxyapatite or a natural bone mineral in combination with a collagen membrane. J Clin Periodontol. 2008 Jan;35(1):80-7. [Medline: 18173402] [doi: 10.1111/j.1600-051X.2007.01168.x]
26. Romanos GE, Nentwig GH. Regenerative therapy of deep peri-implant infrabony defects after CO2 laser implant surface decontamination. Int J Periodontics Restorative Dent. 2008 Jun;28(3):245-55. [Medline: 18605600]
27. Schwarz F, Sahm N, Bieling K, Becker J. Surgical regenerative treatment of peri-implantitis lesions using a nanocrystalline hydroxyapatite or a natural bone mineral in combination with a collagen membrane: a four-year clinical follow-up report. J Clin Periodontol. 2009 Sep;36(9):807-14. [Medline: 19637997] [doi: 10.1111/j.1600-051X.2009.01443.x]
28. Schwarz F, Sahm N, Schwarz K, Becker J. Impact of defect configuration on the clinical outcome following surgical regenerative therapy of peri-implantitis. J Clin Periodontol. 2010 May;37(5):449-55. [Medline: 20374416] [doi: 10.1111/j.1600-051X.2010.01540.x]
29. Roccuzzo M, Bonino F, Bonino L, Dalmasso P. Surgical therapy of peri-implantitis lesions by means of a bovine-derived xenograft: comparative results of a prospective study on two different implant surfaces. J Clin Periodontol. 2011 Aug;38(8):738-45. [Medline: 21635278] [doi: 10.1111/j.1600-051X.2011.01742.x]
30. Froum SJ, Froum SH, Rosen PS. Successful management of peri-implantitis with a regenerative approach: a consecutive series of 51 treated implants with 3- to 7.5-year follow-up. Int J Periodontics Restorative Dent. 2012 Feb;32(1):11-20. [Medline: 22254219]
31. Aghazadeh A, Rutger Persson G, Renvert S. A single-centre randomized controlled clinical trial on the adjunct treatment of intra-bony defects with autogenous bone or a xenograft: results after 12 months. J Clin Periodontol. 2012 Jul;39(7):666-73. [Medline: 22548359] [doi: 10.1111/j.1600-051X.2012.01880.x]
32. Wohlfahrt JC, Lyngstadaas SP, Rønold HJ, Saxegaard E, Ellingsen JE, Karlsson S, Aass AM. Porous titanium granules in the surgical treatment of peri-implant osseous defects: a randomized clinical trial. Int J Oral Maxillofac Implants. 2012 Mar-Apr;27(2):401-10. [Medline: 22442781]
33. Wiltfang J, Zernial O, Behrens E, Schlegel A, Warnke PH, Becker ST. Regenerative treatment of peri-implantitis bone defects with a combination of autologous bone and a demineralized xenogenic bone graft: a series of 36 defects. Clin Implant Dent Relat Res. 2012 Jun;14(3):421-7. [Medline: 20132246] [doi: 10.1111/j.1708-8208.2009.00264.x]
34. Schwarz F, Hegewald A, John G, Sahm N, Becker J. Four-year follow-up of combined surgical therapy of advanced peri-implantitis evaluating two methods of surface decontamination. J Clin Periodontol. 2013 Oct;40(10):962-7. [Medline: 23931259] [doi: 10.1111/jcpe.12143]
35. Matarasso S, Iorio Siciliano V, Aglietta M, Andreuccetti G, Salvi GE. Clinical and radiographic outcomes of a combined resective and regenerative approach in the treatment of peri-implantitis: a prospective case series. Clin Oral Implants Res. 2014 Jul;25(7):761-7. [Medline: 23656191] [doi: 10.1111/clr.12183]
36. Roos-Jansåker AM, Persson GR, Lindahl C, Renvert S. Surgical treatment of peri-implantitis using a bone substitute with or without a resorbable membrane: a 5-year follow-up. J Clin Periodontol. 2014 Nov;41(11):1108-14. [Medline: 25195613] [doi: 10.1111/jcpe.12308]
37. Jepsen K, Jepsen S, Laine ML, Anssari Moin D, Pilloni A, Zeza B, Sanz M, Ortiz-Vigon A, Roos-Jansåker AM, Renvert S. Reconstruction of peri-implant osseous defects: a multicenter randomized trial. J Dent Res. 2016 Jan;95(1):58-66. [Medline: 26450511] [doi: 10.1177/0022034515610056]

38. Froum SJ, Froum SH, Rosen PS. A regenerative approach to the successful treatment of peri-implantitis: a consecutive series of 170 implants in 100 patients with 2- to 10-year follow-up. Int J Periodontics Restorative Dent. 2015 Nov-Dec;35(6):857-63. [Medline: 26509990] [doi: 10.11607/prd.2571]
39. Roccuzzo M, Gaudioso L, Lungo M, Dalmasso P. Surgical therapy of single peri-implantitis intrabony defects, by means of deproteinized bovine bone mineral with 10% collagen. J Clin Periodontol. 2016 Mar;43(3):311-8. [Medline: 26800389]] [doi: 10.1111/jcpe.12516]
40. Schwarz F, Bieling K, Latz T, Nuesry E, Becker J. Healing of intrabony peri-implantitis defects following application of a nanocrystalline hydroxyapatite (Ostim) or a bovine-derived xenograft (Bio-Oss) in combination with a collagen membrane (Bio-Gide). A case series. J Clin Periodontol. 2006 Jul;33(7):491-9. [Medline: 16820037] [doi: 10.1111/j.1600-051X.2006.00936.x]
41. Caccianiga G, Rey G, Baldoni M, Paiusco A. Clinical, radiographic and microbiological evaluation of high level laser therapy, a new photodynamic therapy protocol, in peri-implantitis treatment; a pilot experience. Biomed Res Int. 2016;2016:6321906. [Medline: 27379251] [doi: 10.1155/2016/6321906]
42. Mijiritsky E, Yatzkaier G, Mazor Z, Lorean A, Levin L. The use of porous titanium granules for treatment of peri-implantitis lesions: preliminary clinical and radiographic results in humans. Br Dent J. 2013 Mar;214(5):E13. [Medline: 23470415] [doi: 10.1038/sj.bdj.2013.222]
43. Schwarz F, Sahm N, Iglhaut G, Becker J. Impact of the method of surface debridement and decontamination on the clinical outcome following combined surgical therapy of peri-implantitis: a randomized controlled clinical study. J Clin Periodontol. 2011 Mar;38(3):276-84. [Medline: 21219392] [doi: 10.1111/j.1600-051X.2010.01690.x]
44. Froum SJ, Rosen PS. Reentry evaluation following treatment of peri-implantitis with a regenerative approach. Int J Periodontics Restorative Dent. 2014 Jan-Feb;34(1):47-59. [Medline: 24396840] [doi: 10.11607/prd.1904]
45. Schwarz F, Sahm N, Becker J. Combined surgical therapy of advanced peri-implantitis lesions with concomitant soft tissue volume augmentation. A case series. Clin Oral Implants Res. 2014 Jan;25(1):132-6. [Medline: 23350647] [doi: 10.1111/clr.12103]
46. Behneke A, Behneke N, d'Hoedt B. Int J Oral Maxillofac Implants. Treatment of peri-implantitis defects with autogenous bone grafts: six-month to 3-year results of a prospective study in 17 patients. 2000 Jan-Feb;15(1):125-38. [Medline: 10697947]
47. Mahato N, Wu X, Wang L. Management of peri-implantitis: a systematic review, 2010-2015. Springerplus. 2016 Feb 1;5:105. [Medline: 26877903] [doi: 10.1186/s40064-016-1735-2]
48. Esposito M, Grusovin MG, Worthington HV. Cochrane Interventions for replacing missing teeth: treatment of peri-implantitis. Database Syst Rev. 2012 Jan 18;1:CD004970. [Medline: 22258958] [doi: 10.1002/14651858.CD004970.pub5]
49. Heitz-Mayfield LJ, Mombelli A. The therapy of peri-implantitis: a systematic review. Int J Oral Maxillofac Implants. 2014;29 Suppl:325-45. [Medline: 24660207] [doi: 10.11607/jomi.2014suppl.g5.3]
50. Ramanauskaite A, Daugela P, Juodzbalys G. Treatment of peri-implantitis: Meta-analysis of findings in a systematic literature review and novel protocol proposal. Quintessence Int. 2016;47(5):379-93. [Medline: 26574611] [doi: 10.3290/j.qi.a35131]
51. Materni A. Managing an extreme peri-implantitis. Minerva Stomatol. 2013 Sep;62(9):295-305. [Medline: 24126596]
52. Slotte C, Lindfors N, Nannmark U. Surgical reconstruction of peri-implant bone defects with prehydrated and collagenated porcine bone and collagen barriers: case presentations. Clin Implant Dent Relat Res. 2013 Oct;15(5):714-23. [Medline: 22145733] [doi: 10.1111/j.1708-8208.2011.00402.x]
53. Tozum TF, Keçeli HG. Treatment of peri-implant defect with modified sandwich bone augmentation. Case report and follow-up. N Y State Dent J. 2008 Jun-Jul;74(4):52-7. [Medline: 18788182]
54. Nicoli LG, Pigossi SC, Marcantonio C, Leal Zandim-Barcelos D, Marcantonio E Jr. Surgical treatment of implants affected by periimplantitis after 15 years of loading: a case report. Implant Dent. 2016 Apr;25(2):288-92. [Medline: 26910186] [doi: 10.1097/ID.0000000000000398]
55. Lombardo G, Corrocher G, Rovera A, Pighi J, Marincola M, Lehrberg J, Nocini PF. Decontamination using a desiccant with air powder abrasion followed by biphasic calcium sulfate grafting: a new treatment for peri-implantitis. Case Rep Dent. 2015;2015:474839. [Medline: 260001789] [doi: 10.1155/2015/474839]
56. Lorenz B, Kang T. Treating peri-implantitis using a combined regenerative/resective procedure: a case report. Compend Contin Educ Dent. 2013 Apr;34(4):e57-61. [Medline: 23627486]
57. Kim JE, Kim HY, Huh JB, Lee JY, Shin SW. A two-stage surgical approach to the treatment of severe peri-implant defect: a 30-month clinical follow-up report. J Oral Implantol. 2014 Jun;40(3):299-305. [Medline: 23110578] [doi: 10.1563/AAID-JOI-D-12-00030]
58. Park JB. Treatment of peri-implantitis with deproteinised bovine bone and tetracycline: a case report. Gerodontology. 2012 Jun;29(2):145-9. [Medline: 21457295] [doi: 10.1111/j.1741-2358.2011.00470.x]
59. Azzeh MM. Er,Cr:YSGG laser-assisted surgical treatment of peri-implantitis with 1-year reentry and 18-month follow-up. J Periodontol. 2008 Oct;79(10):2000-5. [Medline: 18834257] [doi: 10.1902/jop.2008.080045]

60. Lu SY, Huang CC. Resolution of an active peri-implantitis in a chronic steroid user by bone augmentation with PepGen P-15 and a barrier membrane. J Oral Implantol. 2007;33(5):280-7. [Medline: 17987860] [doi: 10.1563/1548-1336(2007)33[280:ROAAPI]2.0.CO;2]
61. Bassi F, Poli PP, Rancitelli D, Signorino F, Maiorana C. Surgical Treatment of Peri-Implantitis: A 17-Year Follow-Up Clinical Case Report. Case Rep Dent. 2015;2015:574676. [Medline: 26064700] [doi: 10.1155/2015/574676]
62. Schwarz F, John G, Sahm N, Becker J. Combined surgical resective and regenerative therapy for advanced peri-implantitis with concomitant soft tissue volume augmentation: a case report. Int J Periodontics Restorative Dent. 2014 Jul-Aug;34(4):489-95. [Medline: 25006766] [doi: 10.11607/prd.1794]
63. Malchiodi L, Cucchi A, Ghensi P, Bondi V. A case of rapidly progressive peri-implantitis around a short sintered porous-surfaced implant. J Indiana Dent Assoc. 2009-2010 Winter;88(4):33-5. [Medline: 20415103]
64. Santos VR, Duarte PM. Surgical anti-infective mechanical therapy for peri-implantitis: a clinical report with a 12-month follow-up. Gen Dent. 2009 May-Jun;57(3):230-5; quiz 236-7. [Medline: 19819811]
65. Shabestari GO, Shayesteh YS, Khojasteh A, Alikhasi M, Moslemi N, Aminian A, Masaeli R, Eslami B, Treister NS. Implant placement in patients with oral bisphosphonate therapy: a case series. Clin Implant Dent Relat Res. 2010 Sep;12(3):175-80. [Medline: 19438964] [doi: 10.1111/j.1708-8208.2009.00150.x]
66. Romeo E, Lops D, Chiapasco M, Ghisolfi M, Vogel G. Therapy of peri-implantitis with resective surgery. A 3-year clinical trial on rough screw-shaped oral implants. Part II: radiographic outcome. Clin Oral Implant Res. 2007;18(2):179–187. [Medline: 17348882] [doi: 10.1111/j.1600-0501.2006.01318.x]
67. Lagervall M, Jansson LE. Treatment outcome in patients with peri-implantitis in a periodontal clinic: a retrospective study. J Periodontol. 2013 Oct;84(10):1365-73. [Medline: 23237584] [doi: 10.1902/jop.2012.120555]
68. Schwarz F, John G, Becker J. Reentry after combined surgical resective and regenerative therapy of advanced peri-implantitis: a retrospective analysis of five cases. Int J Periodontics Restorative Dent. 2015 Sep-Oct;35(5):647-53. [Medline: 26357694] [doi: 10.11607/prd.2320]
69. Yoshino T, Yamamoto A, Ono Y. Innovative regeneration technology to solve peri-implantitis by Er:YAG laser based on the microbiologic diagnosis: a case series. Int J Periodontics Restorative Dent. 2015 Jan-Feb;35(1):67-73. [Medline: 25734708] [doi: 10.11607/prd.2116]
70. Iezzi G, Degidi M, Scarano A, Petrone G, Piattelli A. Anorganic bone matrix retrieved 14 years after a sinus augmentation procedure: a histologic and histomorphometric evaluation. J Periodontol. 2007 Oct;78(10):2057-61. [Medline: 18062129] [doi: 10.1902/jop.2007.070062]
71. Araújo MG, Lindhe J. Socket grafting with the use of autologous bone: an experimental study in the dog. Clin Oral Implants Res. 2011 Jan;22(1):9-13. [Medline: 21091539] [doi: 10.1111/j.1600-0501.2010.01937.x]
72. Salvi GE, Lang NP. Diagnostic parameters for monitoring peri-implant conditions. Int J Oral Maxillofac Implants. 2004;19 Suppl:116-27. [Medline: 15635952]
73. Sahrmann P, Attin T, Schmidlin PR. Regenerative treatment of peri-implantitis using bone substitutes and membrane: a systematic review. Clin Implant Dent Relat Res. 2011 Mar;13(1):46-57. [Medline: 19681931] [doi: 10.1111/j.1708-8208.2009.00183.x]
74. Roos-Jansåker AM, Lindahl C, Persson GR, Renvert S. Long-term stability of surgical bone regenerative procedures of peri-implantitis lesions in a prospective case-control study over 3 years. J Clin Periodontol. 2011 Jun;38(6):590-7. [Medline: 21488935] [doi: 10.1111/j.1600-051X.2011.01729.x]
75. Figuero E, Graziani F, Sanz I, Herrera D, Sanz M. Management of peri-implant mucositis and peri-implantitis. Periodontol 2000. 2014 Oct;66(1):255-73. [Medline: 25123773] [doi: 10.1111/prd.12049]
76. Chan HL, Lin GH, Suarez F, MacEachern M, Wang HL. Surgical management of peri-implantitis: a systematic review and meta-analysis of treatment outcomes. J Periodontol. 2014 Aug;85(8):1027-41. [Medline: 24261909] [doi: 10.1902/jop.2013.130563]

To cite this article:
Daugela P, Cicciù M, Saulacic N.
Surgical Regenerative Treatments for Peri-Implantitis: Meta-analysis of Recent Findings in a Systematic Literature Review
J Oral Maxillofac Res 2016;7(3):e15
URL: http://www.ejomr.org/JOMR/archives/2016/3/e15/v7n3e15.pdf
doi: 10.5037/jomr.2016.7315

The 1st Baltic Osseointegration Academy and Lithuanian University of Health Sciences Consensus Conference 2016. Summary and Consensus Statements: Group III - Peri-Implantitis Treatment

Fernando Suárez-López del Amo[1], Ricardo Faria e Almeida[2], Marco Cicciù[3], Povilas Daugela[4], Ausra Ramanauskaite[5], Nikola Saulacic[6], Tellervo Tervonen[7,8], Hom-Lay Wang[1], Shan-Huey Yu[1]

[1]Department of Periodontics and Oral Medicine, University of Michigan, Ann Arbor Michigan, USA.
[2]Department of Oral Surgery and Periodontology, School of Dental Medicine, University of Porto, Porto, Portugal.
[3]Human Pathology Department, Messina University, Messina, Italy.
[4]Department of Oral and Maxillofacial Surgery, Kaunas University of Medicine, Lithuania.
[5]Department of Dental and Oral Pathology, Lithuanian University of Health Sciences, Lithuania.
[6]Department of Cranio-Maxillofacial Surgery, Faculty of Medicine, University of Bern, Bern, Switzerland.
[7]Department of Periodontology and Geriatric Dentistry, Unit of Oral Health Sciences, University of Oulu, Finland.
[8]Medical Research Center Oulu (MRC Oulu), University of Oulu and Oulu University Hospital, Finland.

Group Leader:
Fernando Suárez-López del Amo
Department of Periodontics and Oral Medicine
University of Michigan School of Dentistry
1011 North University Ave., Ann Arbor, MI 48109-1078
USA
Fax: 734/936-0374
E-mail: fsuarez@umich.edu

ABSTRACT

Introduction: The task of Group 3 was to review and update the existing data concerning non-surgical, surgical non-regenerative and surgical regenerative treatment of peri-implantitis. Special interest was paid to the preventive and supporting therapy in case of peri-implantitis.
Material and Methods: The main areas of interest were as follows: effect of smoking and history of periodontitis, prosthetic treatment mistakes, excess cement, overloading, general diseases influence on peri-implantitis development. The systematic review and/or meta-analysis were registered in PROSPERO, an international prospective register of systematic reviews: http://www.crd.york.ac.uk/PROSPERO/. The literature in the corresponding areas of interest was searched and reported using the PRISMA (Preferred Reporting Item for Systematic Review and Meta-Analysis) Statement: http://www.prisma-statement.org/. The method of preparation of systematic reviews of the literature based on comprehensive search strategies was discussed and standardized. The summary of the materials and methods employed by the authors in preparing the systematic review and/or meta-analysis is presented in Preface chapter.
Results: The results and conclusions of the review process are presented in the respective papers. The group's general commentaries, consensus statements, clinical recommendations and implications for research are presented in this article.

Accepted for publication: 7 September 2016
To cite this article:
Suárez-López del Amo F, Faria de Almeida R, Cicciù M, Daugela P, Ramanauskaite A, Saulacic N, Tervonen T, Wang HL, Yu SH.
The 1st Baltic Osseointegration Academy and Lithuanian University of Health Sciences Consensus Conference 2016. Summary and Consensus Statements: Group III - Peri-Implantitis Treatment
J Oral Maxillofac Res 2016;7(3):e16
URL: http://www.ejomr.org/JOMR/archives/2016/3/e16/v7n3e16.pdf
doi: 10.5037/jomr.2016.7316

RESULTS

The following reviews were prepared for publication as a result of work of Group 3:

1. The Efficacy of Supportive Peri-Implant Therapies in Preventing Peri-Implantitis and Implant Loss: a Systematic Review of the Literature (Ramanauskaite and Tervonen [1])

General commentaries

Evidence that microorganisms are essential in the aetiology of peri-implantitis, an inflammatory process in peri-implant soft tissues and alveolar bone, has been well documented. There is also strong evidence that preventive therapies targeting the removal of soft and hard microbial deposits are effective in maintaining the periodontal health of natural teeth. Likewise, there is a common consensus that peri-implant mucositis and its progression to peri-implantitis are largely preventable via patient-administered plaque control and professional intervention comprised of oral hygiene instructions and mechanical debridement. As regards the prevention of peri-implantitis and implant loss, a few studies have shown positive effects of supportive peri-implant therapies (SPTs) on the long-term success of implant treatment. Of note is that a majority of the studies were planned for purposes other than studying the effects of SPTs on peri-implant conditions. While efforts have been made to define the frequency of recall visits, it is currently recommended that supportive maintenance be established according to individual needs, based on diagnosis and risk profiling.

Consensus statement

A lack of poor adherence to SPTs results in significantly higher frequencies of implant sites with mucosal inflammation and peri-implant bone loss as well as more frequent implant loss. Implementation of regular SPTs to prevent the above complications is crucial to ensure the long-term success of implant therapy.

Clinical recommendations

In light of the microbial aetiology of peri-implant infections, SPTs targeting the removal of soft and hard microbial deposits at implant sites are needed. Individually tailored SPTs based on patient motivation and re-instruction in oral hygiene measures combined with professional mechanical debridement should be an integral part of implant therapy.

Implications for research

Prospective longitudinal studies using various treatment protocols/modes of therapies for SPT and study samples of appropriate size that enable risk profiling of individuals are needed.

2. Non-Surgical Therapy for Peri-Implant Diseases: a Systematic Review (Suárez-López del Amo et al. [2])

General commentaries

Peri-implant mucositis is characterized by an inflammatory process around a dental implant without loss of supporting bone beyond biological bone remodelling. On the other hand, peri-implantitis is characterized by both, inflammation of the surrounding peri-implant tissues and loss of supporting bone beyond initial biological bone remodelling. However, multiple interpretations of such diseases exits and there is still no agreement on how to clearly define peri-implantitis. Consequently, elaboration of an effective and predictable treatment protocol for a still not completely understood disease seems arduous if not impossible. Some studies evaluated the effect of self-performed hygiene care while more studies looked into different adjunct treatment modalities that can be performed in combination to mechanical debridement, which may be a more feasible option for treating peri-implant mucositis or peri-implantitis. Non-surgical treatments for peri-implant mucositis and peri-implantitis mostly include supramucosal/submucosal mechanical debridement in conjunction with laser, photodynamic therapy and air-abrasive devices, and results demonstrated that the most prominent change is the decreases of probing depths and the percentage of bleeding on probing. However, most of the studies fail to provide information regarding influencing local and systemic factors including implant position and implant systems/surfaces, which are significant contributing factors influencing the prevalence, severity as well as the clinical outcomes of different treatment modalities.

Consensus statement

Non-surgical treatment (mechanical debridement with or without adjunct therapy) for peri-implant

mucositis seems to be effective while modest and not-predictable outcomes are expected for peri-implantitis lesions. The absence of adequate oral hygiene care in individuals with pre-exciting mucositis may contribute to a higher incidence of peri-implantitis.

Clinical recommendations

There is currently no consensus on protocol for treating mucositis or peri-implantitis mainly due to the heterogeneous features of different implant systems, implant position and other patient related factors. Hence, no particular treatment option may be recommended at this time as well as how to manage implants with different severity of diseases extent. It has only been agreed and concluded the following:

- Non-surgical treatment seems be more effective for treating peri-implant mucositis than peri-implantitis.
- Peri-implantitis treated with non-surgical therapy result mostly in the decrease of bleeding on probing and probing depth (usually less than 1 mm).
- Self-performed hygiene care or professional maintenance program have positive effect on preventing peri-implant mucositis proceeding into peri-implantitis.

Implications for research

The greatest limitation for the studies was the varying definitions for peri-implantitis, and this may lead to the heterogeneous results of different studies. To perform a more comprehensive and unbiased evaluation of different treatment modalities, implant location (buccal/lingual, mesial/distal and apical/coronal position), implant system (implant surface, implant system) and prosthetic features (fixed appliance/removable) should be reported, as well as standardized radiographs should be applied if applicable in the studies. Also, standardized documentation of all the clinical parameters should also be achieved in future investigations.
The effectiveness of non-surgical therapy for peri-implant mucositis has been repeatedly reported, hence future investigations should focus on the local and systemic factors affecting incidence and severity of peri-implant diseases. A comprehensive understanding of such factors will lead to significant improvements in prevention and effectiveness of treatment approaches for the peri-implant diseases.

3. Surgical Non-Regenerative Treatments for Peri-Implantitis: a Systematic Review (Ramanauskaite et al. [3])

General Commentaries

The surgical non-regenerative therapy is effective in maintaining the health of peri-implant soft tissues. Few studies have shown positive effects of implantoplasty and systemic administration of antibacterial adjunct to mechanical debridement. As regards the radiographic parameters, there is a common agreement that surgical non-regenerative treatment is not predictable. Implemented surgical therapy is crucial to ensure the long-term success of surgical therapy.

Consensus statement

Based on this systematic review, it was concluded that surgical non-regenerative therapy results in significantly lower frequencies of implant sites with mucosal inflammation and arrest the progression of peri-implantitis. Due to inconsistent findings between studies, additional evidence is needed to assess the benefit of different methods of surgical non-regenerative therapy on clinical parameters and peri-implant bone level.

Clinical recommendations

Surgical non-regenerative therapy shell be established based on diagnosis and risk profiling. In light of the microbial aetiology of peri-implantis, patient motivation and instruction together with surgical therapy shell be an integral part of the peri-implantitis treatment. No specific clinical recommendation can be made as which specific method of surgical non-regenerative therapy shell be implemented.

Implications for research

Prospective longitudinal studies using various treatment protocols/modes of surgical non-regenerative therapies on the long-term with study samples of appropriate size are needed.

4. Surgical Regenerative Treatments for Peri-Implantitis: Meta-analysis of Recent Findings in a Systematic Literature Review (Daugela et al. [4])

General Commentaries

In case of evident bone loss and pocket formation

deeper than 5 mm, the surgical treatment seems to be the only effective one in managing peri-implantitis defect. Surgical regenerative treatment results in predictable improvement of peri-implant clinical and radiographic parameters, however this statement is limited and can only be based on available studies without proper control arm, as at the time there is a lack of controlled studies comparing effectiveness of surgical regenerative and non-regenerative procedures to support scientific evidence if regenerative procedures provide better outcomes.

Currently there is a lack of clear recommendation regarding choice of biomaterials for peri-implant bone regeneration due to high heterogeneity among the studies. Meanwhile, the meta-analysis of the available literature showed, that the membrane application over the bone graft as well as submergence of the implants during healing phase seems not to be fundamental in order to gain hard and soft tissue after the surgical regenerative treatment.

From the clinical point of view, surgical regenerative treatment is relevant treatment option of intrabony defect component in addition to pre- and postsurgical hygiene maintenance phases and successful implant surface decontamination. At the same time it should be emphasized, that there is no available scientific proof in the literature that regenerative procedures with the use of bone grafts and/or membranes provide superior treatment outcomes compared to non-regenerative procedures.

Consensus statement

Regenerative procedures, with the application of bone graft materials in combination or not with barrier membranes seem to give consistent results in the term of hard and soft tissues healing of the peri-implantitis defect. No conclusions can be drawn regarding the superiority among surgical regenerative or non-regenerative treatment due to the lack of scientific evidence in the literature.

Clinical recommendations

There is currently no consensus on particular protocol or selection of biomaterials in surgical regenerative treatment of peri-implantitis due to high heterogeneity and bias among investigated studies. However, several clinical recommendations could be drawn according to available data in the current literature:

- Predictable improvement of clinical parameters applying surgical regenerative treatment of peri-implantitis can be expected.
- Evaluation of systemic and local factors of the patients affected by peri-implantitis should be taken into consideration applying surgical regenerative treatment.
- Surgical regenerative treatment might be chosen for intrabony defect reconstruction, whereas non-regenerative approach and implantoplasty of the supracrestal implant component is recommended.
- Proper pre- and postsurgical hygiene maintenance phases and successful implant surface decontamination are mandatory for successful surgical regenerative procedure.
- There is no fundamental advantage of membrane use for bone graft coverage on final outcome of peri-implant defect regeneration.
- Submergence of the implants during healing period seems not to influence the final outcome of the regenerative treatment.

Implications for research

Most studies investigating surgical regenerative treatment of peri-implantitis have no proper control arm on non-regenerative treatment; therefore well designed RCT comparing long-term outcomes of surgical regenerative and non-regenerative treatment are needed. Controlled studies, investigating the impact of defect configuration, implant surface decontamination methods, application of different grafting materials, and various surgical protocols on final outcome of the regenerative procedure are also demanded.

For the future perspectives, various bioactive materials including stem cells, growth factors and other bioactive modifiers are also on the line for investigation to improve clinical outcomes of surgical regenerative treatment.

DISCLOSURE STATEMENTS

All group members were asked to sign a Panel Member Agreement (PMA). This agreement requires individuals to maintain the highest level of integrity and avoid all actual, perceived, and potential conflicts of interest. The authors reported no conflicts of interest related to this study.

REFERENCES

1. Ramanauskaite A, Tervonen T. The Efficacy of Supportive Peri-Implant Therapies in Preventing Peri-Implantitis and Implant Loss: a Systematic Review of the Literature. J Oral Maxillofac Res 2016;7(3):e12. [doi: 10.5037/jomr.2016.7312]
2. Suárez-López del Amo F, Yu SH, Wang HL. Non-Surgical Therapy for Peri-Implant Diseases: a Systematic Review. J Oral Maxillofac Res 2016;7(3):e13. [doi: 10.5037/jomr.2016.7313]
3. Ramanauskaite A, Daugela P, Faria de Almeida R, Saulacic N. Surgical Non-Regenerative Treatments for Peri-Implantitis: a Systematic Review. J Oral Maxillofac Res 2016;7(3):e14. [doi: 10.5037/jomr.2016.7314]
4. Daugela P, Cicciù M, Saulacic N. Surgical Regenerative Treatments for Peri-Implantitis: Meta-analysis of Recent Findings in a Systematic Literature Review. J Oral Maxillofac Res 2016;7(3):e15. [doi: 10.5037/jomr.2016.7315]

To cite this article:
Suárez-López del Amo F, Faria de Almeida R, Cicciù M, Daugela P, Ramanauskaite A, Saulacic N, Tervonen T, Wang HL, Yu SH.
The 1st Baltic Osseointegration Academy and Lithuanian University of Health Sciences Consensus Conference 2016. Summary and Consensus Statements: Group III - Peri-Implantitis Treatment
J Oral Maxillofac Res 2016;7(3):e16
URL: http://www.ejomr.org/JOMR/archives/2016/3/e16/v7n3e16.pdf
doi: 10.5037/jomr.2016.7316

SUMMARY

ABBREVIATIONS

CBCT	– cone beam computed tomography
µCT	– micro-computed tomography
L-PRF	– leukocyte- and platelet-rich fibrin
PRP	– platelet-rich plasma
µHA	– micro-hydroxyapatite
nHA	– nano-hydroxyapatite
Cellulose-µHA	– cellulose and micro-hydroxyapatite composite scaffold
Cellulose-nHA	– cellulose and nano-hydroxyapatite composite scaffold
IMTM	– impacted mandibular third molar
GBR	– guided bone regeneration
SEM	– scanning electron microscopy
MTT	– yellow tetrazolium salt 3-(4, 5-dimethylthiazol-2-yl)-2, 5-diphenyltetrazolium bromide) reduction assay
ALP	– alkaline phosphatase
RT-PGR	– real-time reverse transcription polymerase chain reaction
Col I	– collagen type I
BMP	– bone morphogenetic protein
Runx-2	– runt-related transcription factor-2
VOI	– volume of interest
BV	– bone volume
TV	– total volume
BV/TV	– bone volume fraction
HU	– Hounsfield unit
HI	– soft tissue healing index
VAS	– visual analog pain scale
SD	– standard deviation
M	– mean
p	– significance level

INTRODUCTION

One of today's most relevant problems in dentistry and maxillofacial surgery is the atrophy of alveolar bone and formation of bone defects related to dental diseases, oncological surgeries, trauma, or other etiological factors. Missing alveolar bone aggravates dental implant placement and impairs the chewing, speech, and facial esthetic appearance of the patient. According to the literature, more than 50% of dental implant placement surgeries require

additional bone grafting, and implant placement in the anterior maxilla requires bone grafting procedures in up to 77% of cases [1, 2].

Autogenous bone and various other bone grafting materials – including xenogeneic, allogenic, or synthetic bone scaffolds – are utilized for grafting procedures. In addition to the scaffold, adequate blood supply, osteoprogenitor cells and growth factors are mandatory for bone regeneration to occur [4]. Autogenous bone still remains the gold standard in procedures requiring bone grafting due to its osteogenicity, osteoinductivity, and osteoconductivity in addition to the fact that its use causes donor site morbidity, increased postoperative pain, prolonged healing, and – eventually, with the use of dense cortical tissue – delayed revascularization [5].

In recent years, researchers have focused on developing and investigating synthetic bone scaffolds, which may be produced from various materials: beta tricalcium phosphate, hydroxyapatite, polycaprolactone, chitosan, collagen, or cellulose. Synthetic bone grafts have several advantages – including practically unlimited scaffold size and availability, biocompatibility, and minimal risk of disease transmission [10]. On the other hand, most of the currently available synthetic (as well as allogenic or xenogeneic) bone grafts that are approved for routine clinical use are inert and serve as osteoconductive scaffolds only. In the United States of America (USA) and some other countries, growth factors – such as recombinant human bone morphogenetic proteins and recombinant human platelet-derived growth factors – were approved for clinical use as osteoinductive materials in certain bone grafting surgeries [11, 77]. However, the use of recombinant growth factors is not approved in the European Union, and numerous side effects related to the use of recombinant proteins are reported in the literature [12, 13].

Leukocyte- and platelet-rich fibrin (L-PRF) might be used in combination with osteoconductive scaffolds as an alternative to recombinant growth factors. L-PRF is natural autologous blood concentrate that is produced during the centrifugation process of whole venous blood. L-PRF consists of a solid fibrin matrix that is enmeshed with platelets, leukocytes, and various growth factors that are involved in wound healing and bone regeneration processes: platelet-derived growth factor, vascular endothelial growth factor, transforming growth factor beta, and fibroblast growth factor [14, 15]. L-PRF has been shown to stimulate the differentiation of human mesenchymal stem cells into osteoblasts [18] and the proliferation of human osteoblasts [16, 17] *in vitro*. L-PRF approval for clinical use has the same regulations as the use of other autologous tissue transplants do. In clinical settings, L-PRF might be used alone or in combination with osteoconductive scaffolds to provide osteopromotive properties and enhance clinical effectiveness.

1. AIM AND OBJECTIVES OF THE STUDY

Aim of the study

The aim of this study was to create a novel cellulose-hydroxyapatite composite scaffold for bone regeneration in bone defects, to determine the scaffold's effectiveness in bone tissue regeneration in *in vitro* and *in vivo* models, evaluate the influence of L-PRF on the bioactivity of the novel cellulose-hydroxyapatite composite scaffold in *in vivo* experiments, and determine the impact of L-PRF on soft-tissue healing and patient postoperative discomfort in a clinical study.

Objectives of the study:

1. To create porous cellulose composite scaffolds containing nano-hydroxyapatite (nHA) or micro-hydroxyapatite (μHA) and matching the principal structural, physicochemical, and biological requirements for bone tissue grafts.
2. To determine the porosity, chemical composition, crystallinity, cytotoxicity, influence on osteoblastic cells' adhesion, and functional and metabolic activity of cellulose-μHA and cellulose-nHA scaffolds *in vitro.*
3. To evaluate the biocompatibility, biodegradability, new bone formation, and cell composition within the matrix of cellulose-μHA and cellulose-nHA scaffolds according to microcomputed tomography (μCT) and histological findings in an *in vivo* New Zealand rabbit calvarial-defect model.
4. To evaluate the biocompatibility, biodegradability, new bone formation, and cell composition within the matrix of cellulose-μHA and cellulose-nHA scaffolds that are rehydrated with L-PRF and covered with L-PRF membranes, based on analyses of μCT and histological findings in an *in vivo* New Zealand rabbit calvarial-defect model.
5. To compare the effectiveness of cellulose-μHA, cellulose-nHA, and a control commercial allograft scaffold in bone defect regeneration, either in combination with L-PRF or alone, in an *in vivo* New Zealand rabbit calvarial-defect model.
6. To create and validate human impacted mandibular third molar (IMTM) impaction and extraction difficulty-degree classification.
7. To standardize study groups according to their IMTM impaction and extraction difficulty-degree classification and evaluate the influence of L-PRF on soft-tissue healing, incidence of alveolar osteitis and patient postoperative discomfort in a human IMTM extraction defect model.

2. NOVELTY OF THE STUDY

Successful bone defect regeneration in the jaws is one of the biggest challenges in modern dentistry and maxillofacial surgery practice. Most of currently the clinically available bone grafting materials of xenogeneic, allogenic, or synthetic origin are characterized as osteoconductive biomaterials only, and the use of autogenous bone is limited due to its limited availability and donor site morbidity. The possibilities of successful bone defect regeneration are highly dependent on the selection of suitable bone grafting material; therefore, the development of bioactive bone grafts to promote the effectiveness of bone regenerative procedures is in high clinical demand. In this study, new bioactive cellulose-hydroxyapatite (cellulose-HA) composite scaffolds that were enhanced with L-PRF were developed.

The experimental cellulose matrix containing nHA or μHA fillers was shown to have a porous, interconnected three-dimensional (3D) structure, which is favorable for new blood-vessel ingrowth. Biocompatibility, biodegradability, and new bone formation within the cellulose-nHA and cellulose- μHA scaffolds were confirmed *in vitro* and *in vivo*.

L-PRF was selected to enhance the bioactivity of the composite scaffolds. Most of the bioactive materials and/or modifiers that were designed for the enhancement of bone tissue regeneration are derived from synthetic origin. Currently, scientific evidence is lacking in terms of the safety and widespread clinical approval of recombinant growth factors for routine bone regenerative surgeries of the jaws. On the contrary, the clinical use of autologous L-PRF is well documented in the scientific literature and is clinically approved in most countries. Accordingly, in this study the use of L-PRF in combination with experimental cellulose-HA composite scaffolds and commercially available bone allograft was suggested to enhance bone formation. A positive influence of L-PRF on bone regeneration was confirmed *in vivo*. The effectiveness of L-PRF in the enhancement of soft-tissue healing and the diminishment of patient postoperative discomfort was confirmed in a split mouth randomized clinical trial that utilized a human IMTM defect model, with the study groups standardized according to their IMTM impaction and extraction difficulty-degree classification, as suggested by the authors.

This study expands the possibilities of continuing research on developed composite cellulose-nHA and cellulose-μHA scaffolds, seeking approval for their clinical use. From the clinical point of view, this study helps clinicians to evaluate the complex possibilities of the clinical use of L-PRF in the enhancement of soft- and hard-tissue healing.

3. MATERIALS AND METHODS

The study was performed at the Department of Maxillofacial Surgery of the Lithuanian University of Health Sciences in collaboration with the Department of Polymer Chemistry and Technology of the Kaunas University of Technology, the State Centre for Innovative Medicine, the Life Sciences Center of Biochemistry Institute of Vilnius University, the Faculty of Dental Medicine of the University of Porto, and the Department of Medicine, Surgery, and Health Sciences of the University of Trieste. The animal study protocol was approved by the Lithuanian State Food and Veterinary Service (Protocol No. G2-18; No. G2-55). The protocols of clinical studies were approved by the Lithuanian Ethical Committee of Biomedical Studies of Kaunas region, the Bioethics Center of the Lithuanian University of Health Sciences (Protocol No. BE-2-12, No. BEC-MF-01, and No. BEC-OF-367) and State Data Protection Inspectorate (Protocol No. 2R-2338).

This study consists of experimental and clinical parts.

A. Design of the experimental part of the study:
   1. The development and an *in vitro* analysis of composite cellulose scaffolds containing nHA or μHA fillers
   2. A μCT and histological analysis of composite cellulose scaffolds that contain nHA or μHA fillers, in an *in vivo* New Zealand rabbit calvarial-defect model
   3. A μCT and histological analysis of L-PRF-enhanced composite cellulose scaffolds that contain nHA or μHA fillers, in an *in vivo* New Zealand rabbit calvarial-defect model
   4. A comparison of the effectiveness of cellulose-μHA, cellulose-nHA, and a control commercial allograft scaffold – either in combination with L-PRF or alone – in bone defect regeneration in an *in vivo* New Zealand rabbit calvarial-defect model
   5. A statistical analysis

B. Design of the clinical part of the study:
   1. The creation of human IMTM impaction and extraction difficulty-degree classification
   2. A statistical analysis and the validation of IMTM impaction and extraction difficulty-degree classification
   3. An evaluation of the influence of L-PRF on soft-tissue healing, the occurrence of alveolar osteitis, and patient postoperative discomfort in a human IMTM extraction defect model, with the study groups standardized according to their IMTM impaction and extraction difficulty-degree classification
   4. A statistical analysis

3.1. Experimental *in vitro* and *in vivo* analysis

3.1.1. Development of composite cellulose scaffolds that contain nHA or µHA fillers

Cellulose acetate (Sigma-Aldrich Co., St. Louis, USA) and spherical particles (Sigma-Aldrich Co., St. Louis, USA) of nHA (average particle size 100 nm) and µHA (average particle size 20 µm) were used for the production of the composite cellulose-nHA and cellulose-µHA scaffolds, as described previously (Bryjak *et al.*, 2007; Petrauskaite *et al.*, 2013). For the preparation of the cellulose-based composite scaffolds, spherical particles of nHA or µHA were inserted within the polymer during the formation of the cellulose gel from cellulose acetate. The composites were formulated with hydroxyapatite (HA) particles comprising 50 wt%. The porous structure was formed through the use a freeze-drying technique involving an ALPHA 2-4 LSC freeze dryer (Martin Christ Gefriertrocknungsanlagen GmbH, Osterode am Harz, Germany) for 24 hours (Fig. 3.1.1.1).

Fig. 3.1.1.1. *Experimental cellulose (left), composite cellulose-µHA (middle), and cellulose-nHA (right) scaffolds.*
Cellulose-µHA – cellulose and micro-hydroxyapatite composite scaffold; cellulose-nHA – cellulose and nano-hydroxyapatite composite scaffold.

3.1.2. *In vitro* analysis of cellulose-nHA and cellulose-µHA scaffolds

In vitro analysis of cellulose-nHA and cellulose-µHA scaffolds involved characterization of the scaffolds by µCT, Fourier transform infrared spectroscopy, chemical composition determination of the scaffolds by Quantax EDS system, and X-ray diffraction. A detailed description of *in vitro* analysis methodology is provided in the published article by Daugela *et al*., 2018 [220].

3.1.3. *In vivo* analysis of cellulose-nHA and cellulose-µHA scaffolds

In vivo analysis was conducted by means of New Zealand rabbit calvarial-defect model. Developed cellulose-nHA and cellulose-µHA round constructs (8.0 mm diameter and 2.0 mm thickness) were used as experimental scaffolds. As a comparative material, a commercially available allograft cancellous block for bone regenerative applications (Maxgraft, Botiss Biomaterials GmbH, Zossen, Germany), prepared in the same manner, was used for control purposes. Scaffolds were preoperatively rehydrated either in a sterile saline solution or L-PRF exudate and were randomly distributed. Scaffolds rehydrated with L-PRF exudate were additionally covered with L-PRF membranes following implantation (Fig. 3.1.3.1). Rabbits were endorsed for the postoperative follow-up in one of the following groups: 4 or 12 weeks (n = 24).

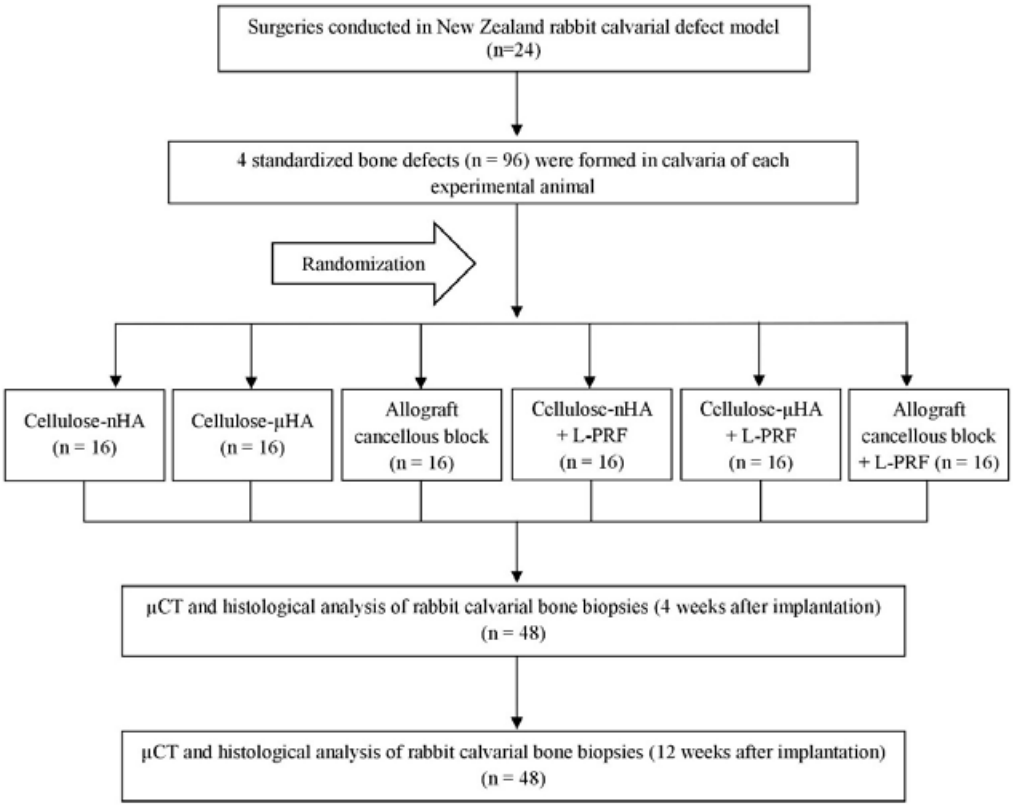

Fig. 3.1.3.1. *Flowchart of in vivo study.*
Cellulose-nHA – cellulose and nano-hydroxyapatite composite scaffold;
cellulose-µHA – cellulose and micro-hydroxyapatite composite scaffold;
L-PRF – leukocyte- and platelet-rich fibrin; µCT – micro-computed tomography.

3.1.4. L-PRF preparation

L-PRF was prepared according to the protocol, as described previously (Choukroun *et al.*, 2001) [185]. Briefly, prior to animal surgery, two 9-ml glass-coated tubes (Intra-Spin, Intra-Lock International, Boca Raton, USA) of venous blood were collected from the marginal ear vein of New Zealand rabbits. Tubes were transferred to a centrifuge (EBA 20, Andreas Hettich GmbH & Co.KG, Tuttlingen, Germany) and processed for 12 minutes at 2800 rpm to prepare L-PRF (Fig. 3.1.4.1). After preparation, L-PRF clots were transferred to a Platelet-rich fibrin (PRF) & growth factor-rich fibrin (GRF) box (Osung Mnd Co., Gimpo, Republic of Korea) for L-PRF membranes compression and the collection of L-PRF exudate, as described by Dohan Ehrenfest in 2010 [194].

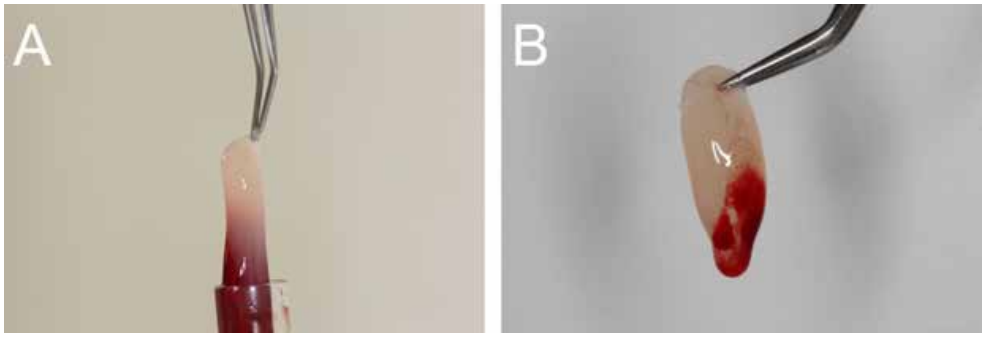

Fig. 3.1.4.1. *A – rabbit-derived L-PRF connected to red corpuscle fraction following centrifugation; B – rabbit-derived L-PRF separated from red corpuscles at the base.*
L-PRF – leukocyte- and platelet-rich fibrin.

3.1.5. *In vivo* surgical procedures

A total of twenty-four adult male New Zealand rabbits of 30–35 weeks of age and weighing 3.5–4.0 kg were acquired from a certified vendor. Animal surgical procedures were performed under the protocol, as described previously (Daugela *et al.*, 2018) [220]. Prior to the surgical procedure, the animals were premedicated with an intramuscular injection of acepromazine (0.5 mg/kg), and a subcutaneous injection of buprenorphine (0.03 mg/kg) was used for analgesia. General anesthesia was induced by intramuscular administration of ketamine hydrochloride (35 mg/kg) and xylazine hydrochloride (5 mg/kg). A trichotomy was conducted on the calvarial area, followed by the disinfection of the skin with an octenidine dihydrochloride

solution. After administration of a local injection of 4% articaine hydrochloride with epinephrine 1:100.000, for local anesthesia and bleeding control, a sagittal incision was made in the midline of the cranium, and the skin and the periosteum were reflected.

In each side of the calvaria, using a trephine drill (speed 2000 rpm), under copious irrigation with a saline solution, two standard 8.0 mm in diameter and approximately 2.0 mm in depth bone defects were made. In total, four circular defects in each animal were created, as shown in Figure 3.1.5.1. Particular care was taken to preserve dura mater during defect formation. The defects were randomly press-fitted with either saline or L-PRF exudate rehydrated scaffolds. Randomization for the selection was performed using specific software available at http://www.randomization.com. No membranes were used to cover saline-rehydrated scaffolds, as L-PRF rehydrated scaffolds were covered by the prepared L-PRF membranes (Fig. 3.1.5.2). The wound was closed in layers by suturing with a 5-0 polyglycolic acid absorbable suture material (Atramat, Internacional Farmacéutica S.A. de C.V., Mexico City, Mexico).

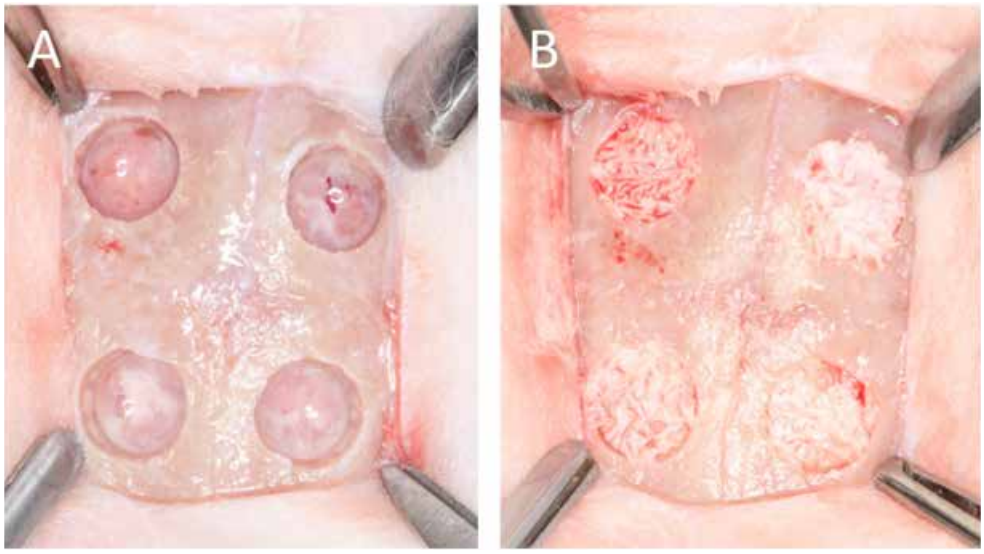

Fig. 3.1.5.1. *A – Standardized bone defects created in rabbit calvarial bone. B – Bone defects grafted with saline-rehydrated cellulose-µHA (left side defects) and cellulose-nHA scaffolds (right side defects).*
Cellulose-µHA – cellulose and micro-hydroxyapatite composite scaffold; cellulose-nHA – cellulose and nano-hydroxyapatite composite scaffold.

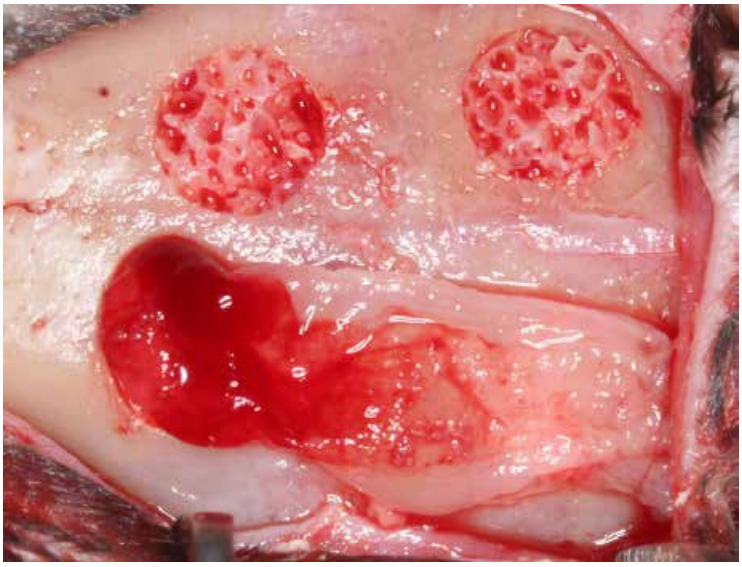

Fig. 3.1.5.2. *Top – standardized bone defects grafted with saline-rehydrated control allograft scaffold; Bottom – standardized bone defects grafted with cellulose-nHA scaffolds, rehydrated in L-PRF exudate and covered with L-PRF membrane.*

Cellulose-nHA – cellulose and nano-hydroxyapatite composite scaffold;
L-PRF – leukocyte- and platelet-rich fibrin.

Postoperative X-rays ensured the correct position of the bone grafts. During the postoperative period, animals were allowed to move freely in their cages, at a controlled temperature and light cycle. Water and food were administered *ad libitum*. An analgesic regimen with buprenorphine was maintained during the first week. No antibiotics were administered.

The animals were sacrificed 4 and 12 weeks after the surgical procedures, initially using a combination of ketamine hydrochloride (50 mg/kg) and xylazine hydrochloride (20 mg/kg) administered intramuscularly, followed by 25 mg/kg of sodium thiopental administered intravenously in the marginal ear vein 20 minutes thereafter. In order to address systemic toxicology effects, histopathological evaluation of the liver and kidney was conducted. Furthermore, the biological response of the implants within the grafted rabbit calvaria was evaluated through microtomographic and histological analysis, addressing the characterization of the bone grafts' degradation process and the disclosure of the bone formation process in the vicinity of the implanted constructs.

3.1.6. μCT analysis of *in vivo* rabbit calvarial bone biopsies

Microtomographic analyses were conducted in a commercially available desktop microtomographic unit μCT 35 (Scanco Medical AG, Bruttisellen, Switzerland), with the following parameters: voxel size of 15 μm, FOV of 30.72 mm, X-ray voltage of 70 kVp, intensity of 114 μA, and an integration time of 800 ms. Structural evaluation of the newly formed tissue was carried out using version 6.0 of the Scanco Medical software (Scanco Medical AG, Bruttisellen, Switzerland). The definition of the volume of interest (VOI) for the analysis was determined with a cylindrical contour, taking into consideration the size of the drill hole (8.0 mm in diameter) and enlarged in the vertical direction to address all the biomaterial and newly formed bone. A fixed VOI was used for all the analyses conducted on different samples. Microstructural measures included the determination of bone volume (BV), total volume (TV), and bone volume per total volume ratio (BV/TV). The computation of these structural measures has been previously detailed by Silva *et al.*, 2015 [195]. Further, an automated multi-threshold segmentation method was employed to highlight and separate the distinct mineralized phases (i.e., scaffold and bone). Briefly, each histogram was partitioned into independent zones, following the manual fixation of thresholds, based on the comparison of microtomographic images with histological images – reference thresholds for "new bone" were set at 3044 Hounsfield units (HU) and at 2033 HU for "new bone & scaffold," allowing for the segmentation and differentiation of the distinct phases within the defect, as described previously by Calvo-Guirado *et al.*, 2015 [196].

3.1.7. Statistical analysis of experimental *in vitro* and *in vivo* studies

For *in vitro* evaluation, three independent experiments were performed. Analysis of eight samples of each *in vivo* study group at each time point was performed accordingly. The data were expressed as mean ± standard deviation (SD). The sample size was estimated following power analysis computation with G*Power 3 software, following the establishment of a pilot trial for the evaluation of the metabolic activity of the cultures for 3 days *in vitro*, and the pilot results of 12-week bone volume fraction (BV/TV) analysis for *in vivo* sample size estimation was garnered. The power was set at 90% and the alpha at 0.05.

Data groups were evaluated using a one-way analysis of variance, and no significant differences in the pattern of cell behavior were found for the *in vitro* analysis. Statistical differences between the experimental *in vitro* groups were assessed through Bonferroni's method.

Analysis of *in vivo* studies was conducted by Student t-test, and one-way analysis of variance by Student–Newman–Keuls post-hoc tests was used as appropriate to determine the level of significance.

Values of $p \leq 0.05$ were considered statistically significant for both *in vitro* and *in vivo* studies.

3.2. Clinical studies

3.2.1. Impacted mandibular third molar impaction and extraction difficulty-degree classification

IMTM impaction and extraction difficulty-degree classification was suggested according to findings in the literature review, which involved factors influencing IMTM etiology, clinical anatomy, diagnostic methods, indications for IMTM extraction, surgical techniques, and possible complications and their risk factors. The literature review and suggested IMTM impaction and extraction difficulty-degree classification are described in detail in the published article by Juodzbalys and Daugela, 2013 [199].

3.2.2. Validation of impacted mandibular third molar impaction and extraction difficulty-degree classification

A clinical study was conducted to validate IMTM impaction and extraction difficulty-degree classification. The study participants were enrolled in three centers:

1. Department of Maxillofacial Surgery of the Lithuanian university of Health Sciences;
2. Department of Medicine, Surgery and Health Sciences of the University of Trieste;
3. Hesire Clinic (Cassano allo Ionio, Italy).

The author was involved in preparation of the study protocol and was a coordinator of the study process.

The study was registered at ClinicalTrials.gov (identification code: NCT02519426). All enrolled patients signed an informed consent.

The inclusion criteria were as follows:

1. Patients with an age ≥ 18 years;
2. Healthy patients (American Society of Anesthesiologists Physical Status [ASA PS] index ≤ 2);
3. Presence of CBCT and/or panoramic radiograph, accomplished no longer than 12 months prior to surgery;

4. Complete root formation of tooth No. 38 or 48;
5. Signed informed consent.

The following exclusion criteria were used:
1. Heavy smoking (>10 cigarettes / day);
2. Presence of any radiolucent lesion with a diameter larger than 1 cm at the impacted tooth level;
3. Presence of acute inflammation and/or infection in the area of interest;
4. Presence of any neoplastic lesion (benign or malignant) in contiguity with the impacted tooth;
5. Absence of the mandibular second molar;
6. Patients with congenital anomalies or systemic diseases;
7. Pharmacological treatments altering oral microbiota and/or immunologic response (e.g., corticosteroids);
8. Radiotherapy or chemotherapy in the last 24 months;
9. Patients already participating in this study with a contralateral mandibular third molar.

An expert blinded investigator performed a blind assessment of CBCTs and/or panoramic radiographs and assigned scores to each extracted tooth, according to Winter's [197], Pell and Gregory's [198], and Juodzbalys and Daugela's IMTM impaction and extraction difficulty-degree classifications [199].

Surgical procedures were performed following a standardized surgical approach, previously described by Farish and Bouloux, 2007 [200], by one expert surgeon, having at least 5 years of clinical experience, for each center. Systemic antibiotic prophylaxis (2000 mg amoxicillin or 500 mg clarithromycin in allergic patients) was administered *per os* 1 hour prior to surgery together with local antisepsis immediately before surgery (0.2% chlorhexidine 1-minute rinse).

The surgical time from flap incision to the complete tooth removal was recorded, together with the surgical technical variables of each intervention (flap design, ostectomy, coronectomy, and roots separation) and possible intraoperative complications (apex fracture, bleeding, mandibular canal penetration, damage of neighboring teeth, tooth or fragment of a tooth migration into soft tissue, and mandibular or alveolar wall fractures).

Patients were prescribed 600 mg of ibuprofen for pain control, when needed, and antiseptics (0.2% chlorhexidine 1-minute rinse twice a day for 2 weeks). Sutures were removed after 7 days and eventual postoperative complications (alveolar osteitis, surgical site infections, hematoma, and paresthesia) were recorded.

3.2.2.1. Statistical analysis

Statistical analysis was performed by using SPSS 22.0 software (International Business Machines Corp., Armonk, North Castle, New York, USA). The sample size of the study was calculated by considering the duration of the surgical procedure as the main parameter to evaluate surgical difficulty. The surgical time from a preliminary pool of 25 patients was considered by dividing them into two groups according to Juodzbalys and Daugela's cumulative score ($x \leq 9 > y$). A sample size of 52 subjects per group was calculated as being necessary to detect a mean difference of 10 minutes in the surgical time between the two groups, with an expected SD of 18 minutes. The power was set at 80% and the alpha at 0.05.

Demographic variables and clinical continuous data were expressed as mean or median ± SD. Categorical variables were processed with frequency charts and percentages. Statistical comparisons between the groups were performed by a Kruskal-Wallis test, with the level of significance at $p \leq 0.05$.

3.2.3. Evaluation of L-PRF influence on the impacted mandibular third molar socket healing

This study was conducted to evaluate L-PRF influence on IMTM socket healing, patient postoperative discomfort, and the appearance of alveolar osteitis after IMTM surgeries. The study was designed as split-mouth randomized clinical trial in patients with bilateral IMTM extractions. The study was conducted at the Department of Maxillofacial Surgery of the Lithuanian University of Health Sciences. The study was registered at ClinicalTrials.gov (identification code: NCT03357484). All enrolled patients have signed informed consent.

The detailed patient selection criteria and methodology are provided in the published article by Daugela *et al.*, 2018 [323].

4. RESULTS

4.1. Results of *in vitro* and *in vivo* studies

4.1.1. Characterization and *in vitro* analysis of composite cellulose-HA scaffolds

Cellulose-HA composite scaffolds were prepared by regenerating acetylcellulose (Sigma-Aldrich Co., St. Louis, USA) in an acetone solution,

following the embedding of nHA and μHA particles during cellulose gel formation. The porous structure was formed using a freeze-drying technique, as described previously by Petrauskaite *et al.*, 2008 [68]. The results and detailed description of composite cellulose-nHA and cellulose-μHA scaffolds *in vitro* characterization from a physicochemical and biological point of view are provided in the published article by Daugela *et al.,* 2018 [220].

4.1.2. *In vivo* analysis of composite cellulose-HA scaffolds

During the postoperative period, all animals survived and showed no signs/signals of anxiety or distress. The regions neighboring the surgical intervention healed adequately without further complications. At the predefined time points, a systematic necropsy was conducted, and no evidence of biomaterial-induced pathological alterations was identified, either locally or systemically.

The area of implantation was evaluated through microtomographic and histological evaluation. Microtomographic assessment was conducted following a segmentation procedure focused on differentiating the newly formed mineralized tissue within the defined VOI. As so, segmental thresholds were established to discern between the mineralized structure of the implanted scaffolds (light yellow) and the newly formed mineralized tissue (dark yellow) (Figs. 4.1.2.1 and 4.1.2.2). Data analysis revealed that, at 4 weeks (Fig. 4.1.2.1), within the control condition, the margins of the surgically created defect could still be identified and that minor bone formation was attained at the defect periphery, with the neoformation of thin trabecular mineral structures particularly evident in two-dimensional (2D) images. Both cellulose-μHA and cellulose-nHA scaffolds induced an improved response characterized by a higher new bone formation, with particular significance for cellulose-nHA, in which the trabecular neoformation process extended significantly into the central area of the defect, interspacing with remnants of the implanted scaffold. The addition of L-PRF to the scaffolds was found to increase the bone formation process in all experimental conditions. Significantly more mineralized tissue could be identified at the defect margins, and a more mature trabecular network of ingrown tissue was visible on both cellulose-μHA and cellulose-nHA, growing centripetally and merging with the remaining structure of the scaffold. Comparatively, a higher degree of bone ingrown within the cellulose-nHA structure was noticeable.

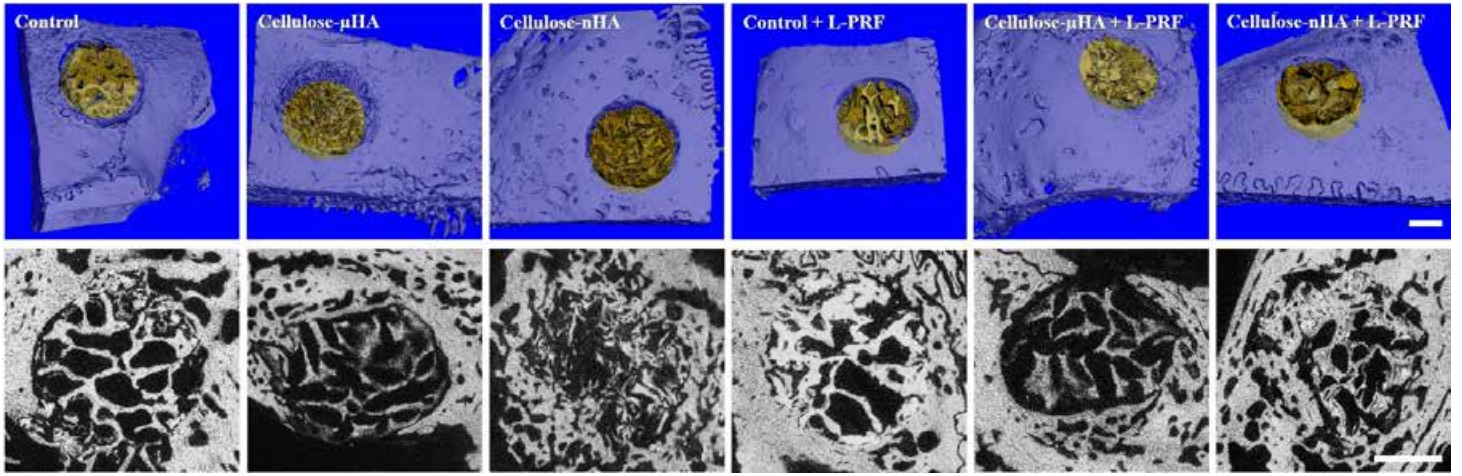

Fig. 4.1.2.1. *Representative microtomographic 3D reconstructions (top row) and 2D images (bottom row) of the control and composite cellulose scaffolds, implanted in the rabbit's calvarial bone in the absence and presence of L-PRF, for 4 weeks. Scale bar corresponds to 3 mm.*

At 12 weeks (Fig. 4.1.2.2), a higher integration of the implanted scaffolds was verified in all conditions, as compared to the 4-week time point. The addition of L-PRF induced a higher formation of mineralized tissue, with emphasis on cellulose-nHA scaffolds, in which the newly formed mineralized bone tissue encompassed the complete volume of the defect.

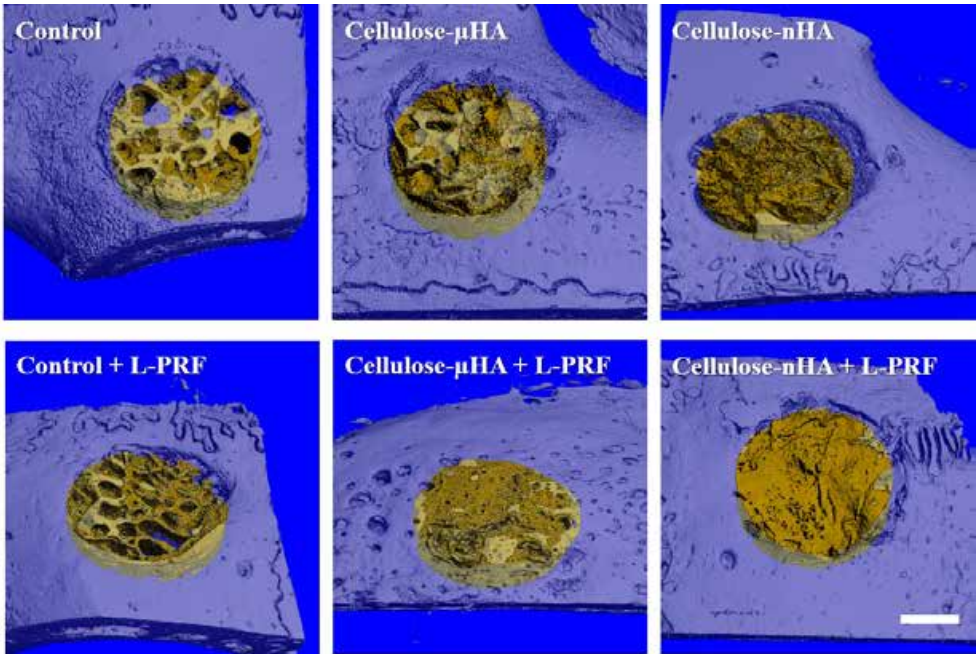

Fig. 4.1.2.2. *Representative microtomographic 3D reconstructions of the control and composite cellulose scaffolds, implanted in the rabbit's calvarial bone in the absence and presence of L-PRF, for 12 weeks. Scale bar corresponds to 3 mm.*

Quantitative analysis of the BV/TV ratio substantiated the attained results, with a higher ratio being attained at the 12-week time point ($p = 0.001$). Comparatively, cellulose-µHA and cellulose-nHA induced a higher bone formation than the control at both assayed time points (4 and 12 weeks) ($p = 0.001$), and L-PRF was found to increase the bone formation process in all experimental conditions and time points ($p < 0.05$) (Fig. 4.1.2.3).

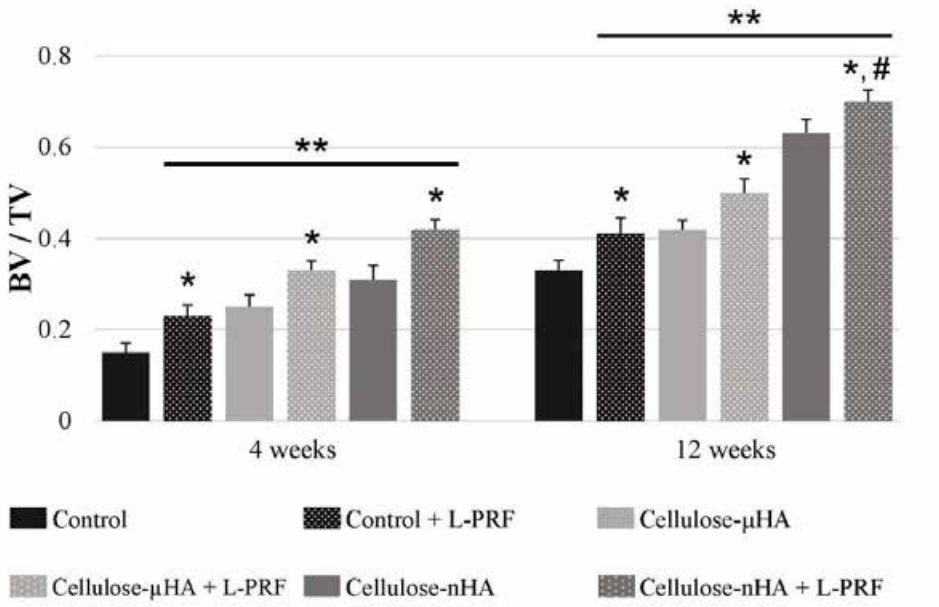

Fig. 4.1.2.3. *Bone volume / Tissue volume (BV/TV) ratio within the defined volume of interest for control and composite cellulose scaffolds, implanted in the rabbit's calvarial bone in the absence and presence of L-PRF, for 4 and 12 weeks.*

*Significantly different from respective condition without L-PRF.
**Significantly different from control, at respective time point.
#Significantly different from cellulose-µHA + L-PRF at 12 weeks.

Histological analysis was further conducted to disclose the bone-biomaterial interface and was focused on detailing the defect margin/scaffold interface. At 4 weeks (Fig. 4.1.2.4), the control scaffold presented a fibrous interconnection with minor evidence of newly formed mineralized tissue at the margins of the structure. Both cellulose-µHA and cellulose-nHA groups presented an increased integration with established bone contact with the defect margins and provided evidence for trabecular tissue ingrowth within the porous structure. The addition of L-PRF induced the integration of the scaffolds with the host bone. A direct appositional bone/scaffold interaction was verified within the control + L-PRF group, and a higher trabecular bone formation was further attained in the cellulose-µHA + L-PRF and cellulose-nHA + L-PRF groups at 4 weeks.

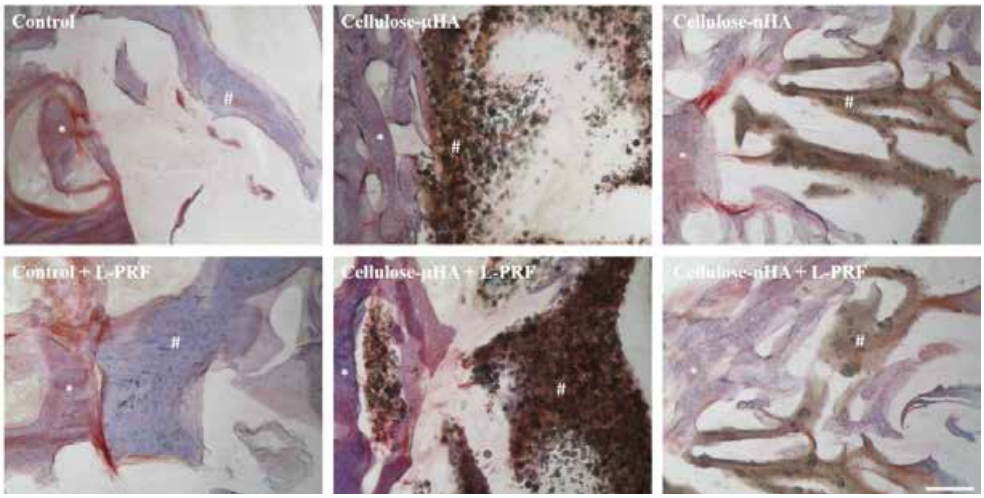

Fig. 4.1.2.4. *Representative histological sections of control and composite cellulose scaffolds, implanted in the rabbit's calvarial bone in the absence and presence of L-PRF, for 4 weeks. Scale bar corresponds to 150 µm.*
*Bone tissue. #Scaffold.

At the 12-week time point (Fig. 4.1.2.5), an increased formation of mineralized tissue was evident in all experimental situations in comparison to the respective condition at 4 weeks. In the control, an increased bone-to-scaffold interface was attained, with further evidence of new bone tissue formation at the scaffolds' edge. Both cellulose-µHA and cellulose-nHA also presented an increased bone formation with trabecular ingrown throughout the porous structure of the scaffolds. A denser mineralized structure could be identified on cellulose-nHA and further associated with a timely scaffold's degradation. The addition of L-PRF further increased the bone formation process, with increased bone trabecular formation. Comparatively, the highest bone formation was attained in association with the L-PRF-enhanced cellulose-nHA scaffold at 12 weeks.

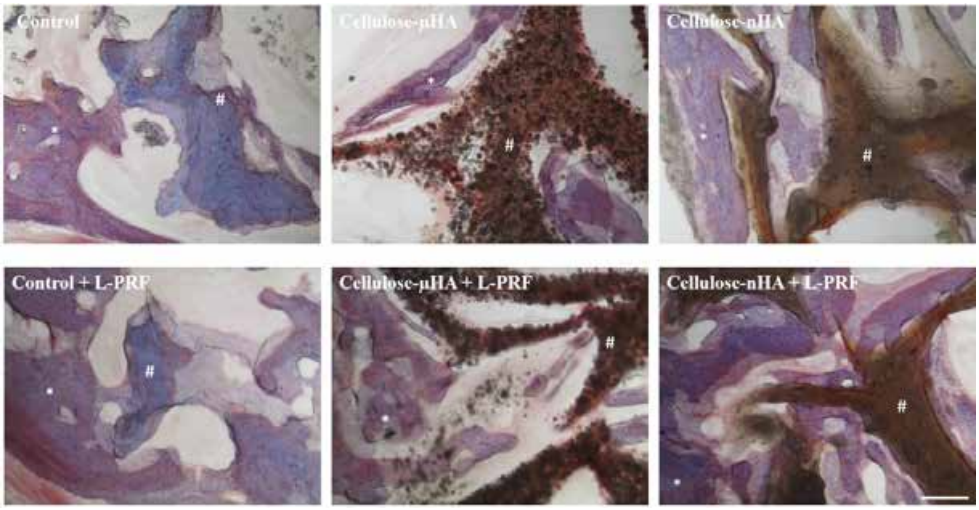

Fig. 4.1.2.5. *Representative histological sections of control and composite cellulose scaffolds, implanted in the rabbit's calvarial bone in the absence and presence of L-PRF, for 12 weeks. Scale bar corresponds to 150 µm.*
*Bone tissue. #Scaffold.

4.2. Results of clinical studies

4.2.1. Impacted mandibular third molar impaction and extraction difficulty-degree classification

IMTM impaction and extraction difficulty-degree classification was proposed, according to literature analysis, regarding important anatomical and diagnostic criteria, influencing the planning, surgical procedure, and postoperative outcomes of IMTM surgery. Classification, which was described and published in an article by Juodzbalys and Daugela, 2013 [199], is provided in Table 4.2.1.1.

IMTM impaction and extraction difficulty-degree classification is designed to have prognostic value in predicting IMTM extraction difficulty during the planning stage of the surgery, seeking to avoid possible complications. In the scientific studies on impacted IMTM, classification might be used as a tool for standardization of the study groups.

Table 4.2.1.1. *Impacted mandibular third molar impaction and extraction difficulty-degree classification.*

Position of the mandibular third molar	**Risk degree of presumptive intervention (score)**			
	Conventional (0)	**Simple (1)**	**Moderate (2)**	**Complicated (3)**
Mesio-distal position in relation to the second molar – M and the mandibular ramus – R				
Relation to the second molar – M	Crown directed at or above the equator of the second molar	Crown directed below the equator to the coronal third of the second molar root	Crown/roots directed to the middle third of the second molar root	Crown/roots directed to the apical third of the second molar root
Relation to the mandibular ramus – R	Sufficient space in the dental arch	Partially impacted in the ramus	Completely impacted in the ramus	Completely impacted in the ramus in disto-angular or horizontal position
Apico-coronal position in relation to the alveolar crest – A and the mandibular canal – C (IAN injury risk)				
Relation to the adjacent alveolar crest (from the uppermost point of the tooth) – A	Tooth is completely erupted	Partially impacted, but widest part of the crown (equator) is above the bone	Partially impacted, but widest part of the crown (equator) is below the bone	Completely encased in the bone
Relation to the mandibular canal (from the lowermost point of the tooth) – C	≥ 3 mm to the mandibular canal	< 3 mm to the mandibular canal, contacting or penetrating the canal, wall of the mandibular canal may be identified	Contacting or penetrating the mandibular canal, wall of the mandibular canal is unidentified	Roots surrounding the mandibular canal
Bucco-lingual position in relation to the mandibular lingual and buccal walls – B (LN injury risk)				
Relation to mandibular lingual and buccal walls – B	Closer to buccal wall	In the middle between lingual and buccal walls	Closer to lingual wall	Closer to lingual wall, when the tooth is partially impact-ed or completely encased in the bone (A2 or A3)
Spatial position – S				
Spatial position – S	Vertical (90°)	Mesio-angular ≤ 60°	Disto-angular ≥ 120°	Horizontal (0°) or inverted (270°)

IAN – inferior alveolar nerve; LN – lingual nerve.

4.2.2. Validation of impacted mandibular third molar impaction and extraction difficulty-degree classification

124 patients were enrolled in the study, validating the proposed IMTM impaction and extraction difficulty-degree classification. 61 males (mean age 30.5 ± 10.7) and 63 females (mean age 27.5 ± 11.3) were treated by center 1 (n = 51), center 2 (n = 50), and center 3 (n = 23). Indications for tooth extraction and postoperative complications are listed in Table 4.2.2.1 and Table 4.2.2.2, respectively.

Table 4.2.2.1. *Preoperative indications for IMTM surgery.*

Indication	Patient count
Prophylactic	61
Orthodontic	7
Chronic infection	38
Periodontal	12
Endodontic	6
Total	124

IMTM – impacted mandibular third molar.

Table 4.2.2.2. *Distribution of postoperative complications in the different centers.*

Center	Patient count	Number of complications
1	51	5
2	50	0
3	23	2
Total	124	7

All patients recovered from postoperative complications without any sequelae in a time span of 1 to 3 months. The mean duration of surgical procedures was 24.1 ± 22.2 minutes (range 1.0–120.0 minutes), with significant differences among the centers (Kruskal-Wallis test; $p = 0.001$). The mean duration of surgical procedures is provided in Table 4.2.2.3.

According to Winter's classification [197], 48 teeth were vertical, 54 were mesio-angular, 9 were horizontal, 4 were in the bucco-lingual position, and 9 were in the disto-angular position. The difference in the surgical procedure's duration among these five groups was evaluated by a Kruskal-Wallis test and did not reach statistical significance ($p > 0.05$).

Table 4.2.2.3. *Mean duration of IMTM surgical procedure among the different study centers.*

Center	Patient count	Duration of the surgery (minutes)	
		Mean ± SD	Duration range
1	51	18.7 ± 20.7*	1.0 – 120.0
2	50	28.6 ± 20.6*	2.0 – 120.0
3	23	26.4 ± 26.9	1.0 – 98.0
Total	124	24.1 ± 22.2	1.0 – 120.0

IMTM – impacted mandibular third molar; SD – standard deviation.
*Statistically significant difference among the centers, according to Mann-Whitney test.

According to Pell and Gregory's classification [198], 37 teeth were class I, 63 were class II, and 24 were class III, with different combinations of occlusal plane level (A, B, and C). The difference in duration of the surgical procedures among these three groups was evaluated by a Kruskal-Wallis test and did not reach statistical significance ($p > 0.05$).

According to Juodzbalys and Daugela's classification, the study sample was composed of three teeth with score 0, 30 teeth with score 1, 66 teeth showing score 2, and 25 teeth classified as score 3. The difference in surgical time among these four groups was evaluated by a Kruskal-Wallis test and resulted as statistically significant ($p = 0.002$) (Table 4.2.2.4).

Table 4.2.2.4. *Distribution of mean duration of IMTM surgery among different scores of IMTM impaction and extraction difficulty-degree classification.*

	Classification score								p value
	0		1		2		3		
	n	Mean ± SD	n	Mean ± SD	n	Mean ± SD	n	Mean ± SD	
Duration (minutes)	3	20.0 ± 8.7	30	13.1 ± 11.1	66	26.0 ± 23.4	25	32.8 ± 25.5	**0.002***

IMTM – impacted mandibular third molar; n – count of the patients;
SD – standard deviation; p – level of significance.
*Statistically significant difference, according to Kruskal-Wallis test.

4.2.3. Evaluation of L-PRF influence on the impacted mandibular third molar socket healing

A split-mouth randomized clinical trial was conducted to evaluate L-PRF influence on IMTM socket healing, patient postoperative discomfort, and the appearance of alveolar osteitis after IMTM surgeries. 34 patients were enrolled, and 30 patients completed the study. The results of the study are described in detail in the published article by Daugela *et al.*, 2018 [323].

CONCLUSIONS

1. Experimental cellulose-nHA and cellulose-μHA scaffolds fulfil the principal structural, physicochemical, and biological requirements for bone tissue grafts.

2. The size of hydroxyapatite particles has influence on the *in vitro* biological response to either cellulose-μHA or cellulose-nHA composite scaffolds. Cellulose-nHA scaffolds revealed superior cell adhesion, increased metabolic activity, and osteoblastic gene expression, compared with a cellulose-μHA scaffolds.

3. μCT and histological investigation of biocompatibility, biodegradability, and new bone formation revealed that cellulose-nHA scaffolds exhibited significantly higher 12-week *in vivo* formation of newly mineralized tissue compared with cellulose-μHA scaffolds and a commercially available bone allograft control.

4. μCT and histological analysis revealed that enhancement of the scaffolds with L-PRF increases new bone formation *in vivo*.

5. L-PRF-enhanced cellulose-nHA scaffolds exhibited the highest 12-week new bone formation among all investigated groups of the study.

6. Juodzbalys and Daugela's IMTM impaction and extraction difficulty-degree classification allows for predicting the duration of IMTM extraction surgery.

7. L-PRF may reduce the incidence of alveolar osteitis, improve soft-tissue healing, and reduce postoperative pain and swelling after IMTM surgical extractions.

SCIENTIFIC AND PRACTICAL RECOMMENDATIONS

According to the results of the present study, the following scientific and practical recommendations are suggested:

1. To continue research on experimental cellulose-nHA and cellulose-μHA composite scaffolds, seeking the approval for their clinical use.

2. L-PRF might be used as autologous osteopromotive biomaterial in combination with osteoconductive scaffolds for jaw bone defect regeneration.

3. IMTM impaction and extraction difficulty-degree classification might be a useful tool for clinicians in planning, risk assessment, extraction difficulty-degree prediction, and prognosis of the duration of IMTM extraction surgeries.

4. In the scientific studies on impacted IMTM, the proposed impaction and extraction difficulty-degree classification might be used as a tool for standardization of the study groups.

5. L-PRF might be used as a prophylactic measure in the prevention of alveolar osteitis, enhancement of soft-tissue healing, and diminishment of patient postoperative discomfort (pain and swelling) in the early healing period after IMTM extraction surgery.

CURRICULUM VITAE

Povilas Daugėla was born in 1986 in Jurbarkas, Lithuania.

EDUCATION

Lithuanian University of Health Sciences
Maxillofacial Surgery Department 2013 August – Pres
- Doctoral (Ph.D.) studies in dentistry

Lithuanian University of Health Sciences
Maxillofacial Surgery Department 2010 July – 2013 July
- Oral surgery residency, 3 years grades average **10** (A)

Kaunas University of Medicine
Mickeviciaus str. 9, Kaunas, Lithuania 2005 September – 2010 July
- Master's degree in Dentistry, 5 years grades average **9.93** (A)

In 2010 was awarded as the best graduate of the Faculty

Jurbarkas Antanas Giedraitis-Giedrius Gymnasium 1993–2005
- Graduation Diploma with distinction **10** (A)

SCIENTIFIC PRESENTATIONS / LECTURES

- Daugela P, Pranskunas M, Juodzbalys G, Liesiene J, Baniukaitiene O, Afonso A, Sousa Gomes P. Novel cellulose/hydroxyapatite scaffolds for bone tissue regeneration: In vitro and in vivo study. J Tissue Eng Regen Med. 2018 May;12(5): 1195–1208.
- Daugela P, Grimuta V, Sakavicius D, Jonaitis J, Juodzbalys G. Influence of leukocyte- and platelet-rich fibrin (L-PRF) on the outcomes of impacted mandibular third molar removal surgery: A split-mouth randomized clinical trial. Quintessence Int. 2018;49(5):377–388.
- Palaveniene A, Harkavenko V, Kharchenko V, Daugela P, Pranskunas M, Juodzbalys G, Babenko N, Liesiene J. Cuttlebone as a Marine-Derived Material for Preparing Bone Grafts. Mar Biotechnol (NY). 2018 Apr 3. doi: 10.1007/ s10126-018-9816-6. [Epub ahead of print].
- 9th Congress of Baltic Association for Maxillofacial and Plastic Surgery, "The Effect of L-PRF After Impacted Third Molar Teeth Extraction", Tartu, Estonia, 2017.
- Hands-on course "Advances in Implant and Prosthetic Dentistry", Kaunas, Lithuania, 2016.

- The 1st Baltic Osseointegration Academy and Lithuanian University of Health Sciences Consensus Conference, "Current Trends in Peri-Implant Bone Regeneartion", Kaunas, Lithuania, 2016.
- International Congress "Enhanced Natural Healing in Dentistry", "Platelet Concentrates: The Same, but Different", Leuven, Belgium, 2016.
- Bone and Tissue Days Vilnius, "Guided Bone Regeneration: Where Are the Limits? ", Vilnius, Lithuania, 2016.
- Suárez-López Del Amo F, Faria E Almeida R, Cicciù M, Daugela P, Ramanauskaite A, Saulacic N, Tervonen T, Wang HL, Yu SH. The 1st Baltic Osseointegration Academy and Lithuanian University of Health Sciences Consensus Conference 2016. Summary and Consensus Statements: Group III – Peri-Implantitis Treatment. J Oral Maxillofac Res. 2016 Sep 9;7(3):e16.
- Daugela P, Cicciù M, Saulacic N. Surgical Regenerative Treatments for Peri-implantitis: Meta-analysis of Recent Findings in a Systematic Literature Review. J Oral Maxillofac Res 2016;7(3):e15.
- Ramanauskaite A, Daugela P, Faria e Almeida R, Saulacic N. Surgical Non-Regenerative Treatments for Peri-Implantitis: a Systematic Review. J Oral Maxillofac Res 2016;7(3):e14.
- Lithuanian Society of Prosthodontics International Congress "Restorative Dentistry: What Could We Do Better?", "Surgeon versus prosthodontist: the importance of teamwork", Kaunas, Lithuania, 2016.
- Ramanauskaite A, Daugela P, Juodzbalys G. Treatment of peri-implantitis: Meta-analysis of findings in a systematic literature review and novel protocol proposal. Quintessence Int. 2016;47(5):379–93.
- International Congress "Immediate implant placement and stability of Peri-implant Tissues", "Novel Look at Sinus Lift Surgery", Kaunas, Lithuania, 2015.
- Hands-on course "Practical Aspects of Platelet Concentrates and Guided Bone Regeneration", Kaunas, 2014.
- BOA International Conference "Novelties in Dental Implant Practice", "New Generation Platelet Rich Fibrin", Kaunas, Lithuania, 2014.
- Third International SCOI Congress, "Novel Look at Growth Factors in Alveolar Ridge Regeneration Surgeries: Literature Review in Comparison with own Clinical Experience", Granada, Spain, 2014.
- BOA Discussion Club Conference, "Utilization of Bioactive Materials in Alveolar Ridge Preservation Surgeries: Clinical Rationale and Treatment Strategies", Kaunas, Lithuania, 2014.
- 12th ITI World Symposium, "New Generation Platelet Concentrates in Alveolar Bone Grafting Surgeries: Current Knowledge and Clinical Experience", Geneva, Switzerland, 2014.
- Venskutonis T, Daugela P, Strazdas M, Juodzbalys G. Accuracy of digital radiography and cone beam computed tomography on periapical radiolucency detection in endodontically treated teeth. J Oral Maxillofac Res. 2014 Jul 1;5(2):e1.

- Lithuanian Association of Periodontology International Congress, "Rationale and Application of Implant Treatment Protocols in Dentistry: Clinical Evaluation and Treatment Strategies", Vilnius, Lithuania, 2014.
- The Fifth International BOA Congress, "Natural Bone Regeneration Concept", Kaunas, Lithuania, 2013.
- Juodzbalys G, Daugela P. Mandibular Third Molar Impaction: Review of Literature and a Proposal of a Classification. Journal of Oral & Maxillofacial Research (JOMR). 2013;4(2):1–11.
- International Congress "Dentistry For Human Health", "Primary Alveolar Ridge Management after Tooth Extraction prior to Implantation: Clinical Evaluation and Treatment Strategies", Druskininkai, Lithuania, 2013.
- 8th Congress of Baltic Association for Maxillofacial and Plastic Surgery, "Novel Trends in Regeneration of Bone Defects after Jaw Cystectomy", Kaunas, Lithuania, 2013.
- EAO 20-Year Anniversary Meeting, "Dimensional Changes of the Periosteum in Different Gingival Biotypes and Particular Places of the Mandible", Copenhagen, Denmark, 2012.
- EAO 20-Year Anniversary Meeting, "Composite Prosthetic Components on Dental Implants: Elements Arrangement and Biomechanics", Copenhagen, Denmark, 2012.
- EAO 20-Year Anniversary Meeting, "A Novel Cellulose – Hydroxyapatite Scaffold for Bone Tissue Regeneration", Copenhagen, Denmark, 2012.
- The Fourth International BOA Congress, "Platelet Rich Concentrates – Features and Rationale for Clinical Use", Kaunas, Lithuania, 2012.
- 6th International OMFS Congress 2012, "Novel Approach to Socket Seal Surgery – The Inverted Periosteal Flap Technique", Antalya, Turkey, 2012.
- 6th International OMFS Congress 2012, "Bone Tissue Regeneration in Cellulose/Hydroxyapatite Scaffold", Antalya, Turkey, 2012.
- News and Topicalities in Dental Practice 2012, "Composite Prosthetic Components on Dental Implants: Elements Arrangement and Biomechanics", Palanga, Lithuania, 2012.
- Bone-tec 2011 Bone-Tissue-Engineering Congress, "New Look at Periosteum as a Regenerative Source for Treatment of Alveolar Bone Defects", Hannover, Germany, 2011.
- The Third International BOA Congress, "Closure of Postextraction Defects Utilizing Inverted Periosteal Flap Technique", Kaunas, Lithuania, 2011.
- News and Topicalities in Dental Practice 2011, "Covering Impacted Third Molar Extraction Sockets via Inverted Periosteal Flap Technique: Analysis of Clinical Cases", Palanga, Lithuania, 2011.
- The Second International BOA Congress New Achievements in Implant Dentistry, "Biological Properties of the Periosteum and its Handling in Alveolar Process Reconstruction", Kaunas, Lithuania, 2010.

- The Second International BOA Congress New Achievements in Implant Dentistry, "The Significance of Diagnostic Criteria on the Outcomes of Sinus Lift Surgery", Kaunas, Lithuania, 2010.
- 5th Baltic Sea Region Conference in Medical Sciences, "Prevalence and Consideration of Factors Influencing Sinus Lift Surgery", Vilnius, Lithuania, 2010.
- Annual Young Researchers Scientific Conference in Dentistry, "The Role of Oral Microorganisms in Maintenance of Oral Ecologic Balance", Kaunas, Lithuania, 2010.
- Annual Young Researchers Scientific Conference in Dentistry, "Planning of Maxillary Sinus Lift Surgery", Kaunas, Lithuania, 2010.
- Annual Young Researchers Scientific Conference in Dentistry, "The Influence of Various Disinfection Methods on Qualities of RPD Bases: Spectrometric Analysis", Kaunas, Lithuania, 2010.
- International Society for Telemedicine & eHealth Conference, "Conventional Approach for Maintaining Beneficial Balance of Oral Microflora", Kaunas, Lithuania, 2009.
- 3rd Baltic Scientific Conference in Dentistry, "A Comparative Study of 14 Dentifrices in Maintenance of Oral Bacteria Anticariogenic Balance", Vilnius, Lithuania, 2008.
- Annual Young Researchers Scientific Conference in Dentistry, "The Influence of Contemporary Toothpastes in Maintenance of Anticariogenic Balance of Oral Microflora", Kaunas, Lithuania, 2008.
- Annual Young Researchers Scientific Conference in Dentistry, "The Action of Dentifrices on Cariogenic Oral Microflora: a Comparative Study of 14 Products", Kaunas, Lithuania, 2008.
- Dentsply Competition for Nordic Dental Young Researchers, "Antibacterial Potential of Contemporary Dental Luting Cements", Copenhagen, Denmark, 2008.
- Scientific article "Antibacterial Potential of Contemporary Dental Luting Cements" (Stomatologija, Baltic Dental and Maxillofacial Journal 2008;10(1):16–21).
- Annual Young Researchers Scientific Conference, "Comparative Study of Luting Cements on Streptococcus Mutans Bacteria", Kaunas, Lithuania. 2007.

Kartą šeštadienį Jėzus atėjo į vieno fariziejų vyresniojo namus valgyti. Matydamas, kaip svečiai rinkosi pirmąsias vietas prie stalo, jis pasakė jiems palyginimą:

„Kai tave pakvies į vestuves, nesisėsk pirmoje vietoje, kad kartais nebūtų pakviesta garbingesnio už tave ir atėjęs tas, kuris tave ir jį kvietė, netartų tau: „Užleisk jam vietą!“ Tuomet tu sugėdintas turėtum sėstis į paskutinę vietą. Kai būsi pakviestas, verčiau eik ir sėskis paskutinėje vietoje, tai atėjęs šeimininkas tau pasakys: „Bičiuli, pasislink aukščiau!“ Tada tau bus garbė prieš visus svečius. Kiekvienas, kuris save aukština, bus pažemintas, o kuris save žemina, bus išaukštintas“.

LK 14, 1. 7–11

PADĖKA

Noriu padėkoti savo moksliniam vadovui profesoriui Gintarui Juodžbaliui už altruistišką mano ir kitų jaunųjų mokslininkų ugdymą, skatinimą eiti į priekį bei visapusišką pagalbą ir patarimus, rengiant disertaciją. Dėkoju LSMU Veido ir žandikaulių chirurgijos klinikos vadovui profesoriui Ričardui Kubiliui, docentui dr. Daliui Sakavičiui, gydytojui Vaidui Grimutai ir visam LSMU Veido ir žandikaulių chirurgijos klinikos kolektyvui, suteikusiems man galimybę rengti šią disertaciją, kuri yra daugelio žmonių profesionalaus darbo rezultatas. Dėkoju dr. Odetai Baniukaitienei, prof. Jolantai Liesienei ir visam KTU Polimerų chemijos ir technologijos katedros kolektyvui už įdėtą didelį darbą, kuriant ir tobulinant eksperimentinius kaulo transplantantus, dr. Pedro de Sousa Gomes už profesionalumo pamokas ir didelę pagalbą atliekant histologinius tyrimus, dr. Virginijai Bukelskienei, dr. Rasai Jarašienei ir visam VU Biochemijos instituto Gyvybės mokslų centro kolektyvui už suteiktas sąlygas gyvūnų operacijoms ir gyvūnų priežiūros pamokas, gyd. Mindaugui Pranskūnui už brolišką pagalbą, atliekant gyvūnų operacijas, ir idėjas tobulinant tyrimo protokolą, matematikei Irenai Nedzelskienei už suteiktas statistikos žinias. Džiaugiuosi ir savo darbdavių supratingumu ir kantrybe laukti, kol visą savo laiką skyriau moksliniam darbui.

Tačiau už viską labiausiai dėkoju savo šeimai, kuri visuomet palaikė ir buvo šalia tiek džiaugsmingomis, tiek ir sunkiomis gyvenimo akimirkomis.